CHAPTER 1

INTRODUCTION

1.1 GENERAL

The demand for energy has increased due to industrialization, urbanization and population growth. In order to meet the demand for energy, Renewable Energy Sources (RES) are exploited because of its advantages such as developed economic growth and sustainability etc. The generation of power from such source of energy was observed to be 21.43% as on 28th Feb 2019. However, it can rise exponentially so to meet the energy demand of the future. Further, the advancement in solar photovoltaic (PV) technology which includes the improved efficiency of solar cells, maintenance of minority carriers lifetime, minimization of optical losses and reduced cost of energy generation over last decades has attracted solar PV technology usage for generation of power. In addition, the motive behind the growing deployment of solar PV technology is diminishing the cost of photovoltaic systems given by the government of various countries. For Indian climatic conditions, the theoretical solar power has reached to around 5,000 trillion kWh/year and the daily average solar energy varied from 4-7 kWh/m^2/day where about 300 days in a year are sunny and clear. Also, the sunshine hours observed is around 1,500-2,000 hours per year which is more than the current total energy consumption. Hence, the conversion of solar energy into electricity for solar photovoltaic systems can effectively be harnessed for power generation in India [1-2].

The large-scale penetration of solar PV technology in the smart energy management system has become a challenging task. The variation in power output of solar PV system can lead to the unstable operation of the system. The fluctuations in the output subsequently lower the capacity of PV generation. Damage may arise in the stability of the utility grid and the power quality because of the imbalance between the demand and supply. Many factors are involved that affect the power generation such as climatic variations, solar insolation, ambient temperature, solar panel temperature and topographical position [3]. So, defining the output with the single model is a tedious task; therefore, in this thesis, the output is modelled based on sky-conditions namely clear sky, hazy sky, partially foggy/cloudy sky and fully foggy/cloudy sky-conditions, as such factors make a significant impact on the solar photovoltaic system power output. Simulations have been carried out for varied climatic conditions thereof, such as warm and humid, hot and dry, cold and cloudy, moderate and composite climate zone across India.

1.2 CURRENT SCENARIO OF RENEWABLE ENERGY SOURCES IN INDIA

In 2018, the highest growth rate of energy resource has met by renewable energy, which meets the quarters of the world's energy demand. The continuous growth in energy demand, depleting fossil fuels and emerging economy makes mandatory to enhance the existing potential of renewable energy for Indian power sector.

In India, as of 2005, government-funded and subsidized solar electricity production is not less than approximately 6.4 MW per year which as compared to other developing countries is more. India is ranked number one in terms of

solar electricity production per watt installed, with an solar insolation of 1,700-1,900 kWh/kWp. In 2010, 25.1 MW_p of power was added and approximately 468.30 MW_p was added in year 2011.

As on 28th February 2019, India has achieved a total grid-interactive capacity of 76,887.47 MW_p through renewable energy generation. It consists of the Wind Power capacity of 35,326.10 MW_p, Solar Power capacity of 27,099.78 MW_p, Bio Power (Biomass, Bagasse cogeneration and Waste-to-power) capacity of 9,918.54 MW_p and Small Hydro Power capacity of 4,543.05 MW_p. Target and achievement for the year 2018-19 and cumulative achievements as on 28th February 2019 are presented in Table 1.1 [4].

Table 1.1 Target and cumulative achievements of grid-interactive renewable power

Sector	**FY 2018-19**		**Cumulative Achievements as on 28.02.2019 (MW_p)**
	Target (MW_p)	**Achievement (Apr - Feb 2019) (MW_p)**	
Solar Power	11,000.00	4,634.39	27,099.78
Wind Power	4,000.00	1,031.15	35,326.10
Small Hydro Power	250.00	46.65	4,543.05
Bio Power (Biomass, Bagasse cogeneration and Waste-to-power)	352.00	416.63	9,918.54
Total	**15,602.00**	**6,128.82**	**76,887.47**

Renewable energy resources are being utilized by many for generation of power. Table 1.2 shows the target and cumulative achievements of off-grid/captive power renewable energy system source wise.

Table 1.2 Target and cumulative achievements of off-grid/captive power

Sector	**FY 2018-19**		**Cumulative Achievements as on 28.02.2019 (MW_p)**
	Target (MW_p)	**Achievement (Apr - Feb 2019) (MW_p)**	
Waste to Energy	18.00	6.58	178.73
Biomass Gassifiers	1.00	0.00	163.37
SPV Systems	200.00	171.70	843.11
Total	**219.00**	**178.28**	**1185.21**

An increase in 6.3% power generation was noticed where Wind Power contributes 46.99%, Solar Power contributes 33.71%, Small Hydro Power contributes 6.04% and Bio Power contributes a total of 13.26% only as shown in Fig. 1.1.

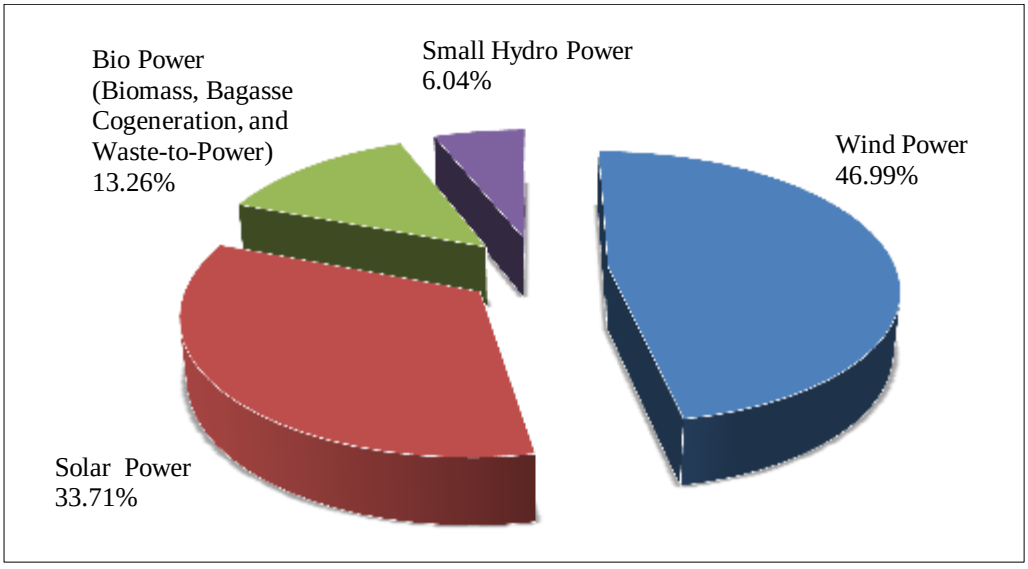

Fig. 1.1 India's RES installed capacity

As on 28th February 2019, the total installed power capacity from different sources reaches 350 GW_p approximately; in which, contribution from other sources are Coal Power shows a major contribution with 54.57%, Large Hydro Power of 12.97%, Renewable Energy Sources shows contribution of 21.43%, Gas with 7.12%, Oil shows contribution of only 0.18%, Lignite contributing to 1.79% and Nuclear contributing to 1.94% as shown in Fig. 1.2.

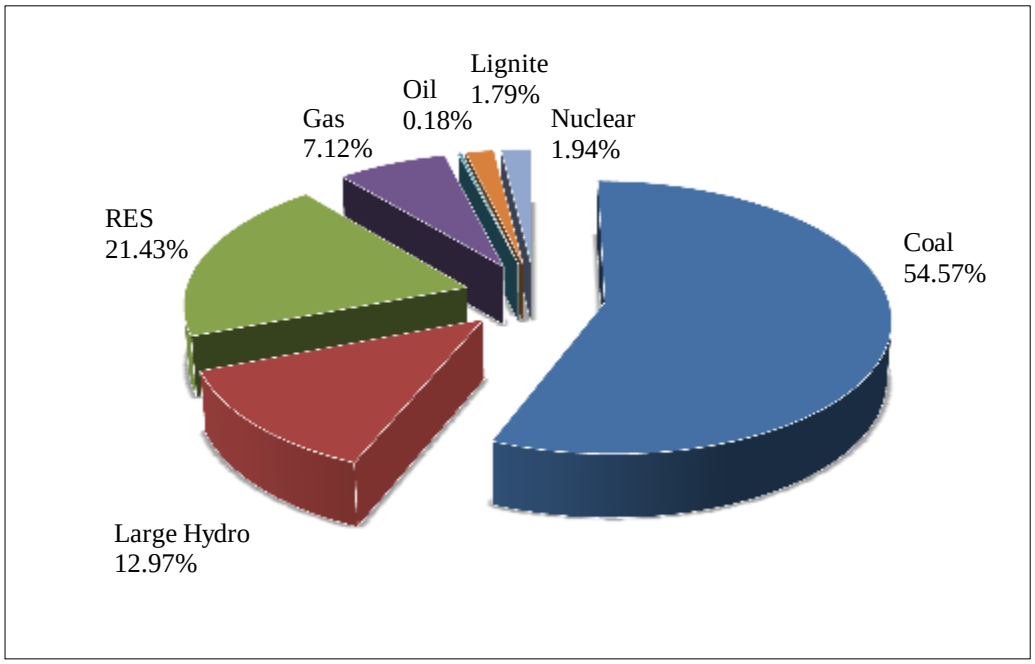

Fig. 1.2 Total installed power capacity in India as on 28th Feb 2019

In the present scenario, the total installed power capacity has reached approximately 3,50,162 MW_p as on 28th February 2019 where the Coal Power shows the major contribution of installed power capacity of 1,91,093 MW_p, Renewable Energy Source with installed power capacity of 74,082 MW_p, Gas with contribution of 24,937 MW_p, Large Hydro Power contributing with capacity of 45,399 MW_p, Lignite contributing with capacity of 6,260 MW_p, Nuclear with installed power capacity of 6,780 MW_p and Oil which shows contribution of installed power capacity of 638 MW_p only as shown in Table 1.3 [5].

Table 1.3 Total installed power capacity as on 28th Feb 2019

Source	**Total Installed Power Capacity (MW_p)**	**Percentage Share (%)**
RES	74,082	21.43%
Coal	1,91,093	54.57%
Gas	24,937	7.12%
Large Hydro	45,399	12.97%
Nuclear	6,780	1.94%
Lignite	6,260	1.79%
Oil	638	0.18%
Total	**3,50,162**	**100%**

Further, the Indian Govt. took initiatives for promoting RES electricity generation. Among these one such scheme is the Electricity Act 2003 [6-7] where the requirement of a license for stand-alone generation and distribution system in rural areas has been removed. Furthermore, National Rural Electrification Policy, 2005 and National Rural Electrification Policy, 2006 have been brought up for speeding up the process of rural electrification. The New Tariff Policy makes it mandate for purchasing a minimum percentage of energy from such sources [8-14].

1.3 INITIATIVES OF GOVERNMENT OF INDIA IN RESPECT OF RENEWABLE ENERGY

Recently, in 2016, the formation of International Solar Alliance (ISA), headquartered at National Institute of Solar Energy (NISE), Ministry of New and Renewable Energy (MNRE), in India has emerged as one of the leading

destinations for solar energy-based research and applications. More than 121 countries have participated and joined together in International Solar Alliance for exploiting the solar energy potential and thereby reducing fossil fuels dependency.

The Govt. of India has played an important role for promoting the adoption of RES by providing attractive schemes and incentives namely Generation Based Incentives (GBIs), viability gap funding, concessional finance, capital interest subsidies and fiscal incentives etc. Further, the Jawaharlal Nehru National Solar Mission (JNNSM) was launched with a target of achieving 175 GW_p of grid-interactive solar power by end of year 2022. Major initiatives were taken from the Government of India such as solar roof-top projects, solar parks, solar photovoltaic power plants, solar defence schemes and solar pumps etc. [15].

Further, an effort has been made for the expansion of the monitoring stations on high potential locations for solar PV applications. A total of 45 Indian Meteorological Department (IMD) stations undertook the measurements, but most of such locations are located either at airports or at metropolitan cities etc. Therefore, the Indian Govt. has planned for expansion of the monitoring station by installing an additional 51 Solar Radiation Resource Assessment (SRRA) stations for producing the best quality radiation data. These stations are expected to be located in areas of high potential producing the best quality data throughout the country. This project further envisages the addition of 60 meteorological stations across India and will subsequently augment the existing network of monitoring stations as shown in Fig. 1.3.

Fig. 1.3 Solar radiation resource assessment stations across India

1.4 SOLAR ENERGY POTENTIAL AND ITS UTILIZATION

There is always an increase in the demand of energy specifically electricity due to the growing population of the world. One of the major contributions in the greenhouse gas emission arises from the burning of fossil fuels which contributes to electricity production. So, there arises a need for

clean form of energy i.e. renewable energy which can contribute to the energy demand worldwide. Solar energy appears to be one of the most predictable and foreseeable forms of renewable energy which has no greenhouse gas emissions and also its natural flow is intense.

The utilization of solar energy resource for the generation of electricity especially with the solar PV technology is gaining attention and plays a major role in the global solar energy production. Since year 2000, industry based on solar PV technology has grown by around 45% per year on an average. So, after every 2-3 years, the installed global solar capacity has been doubling.

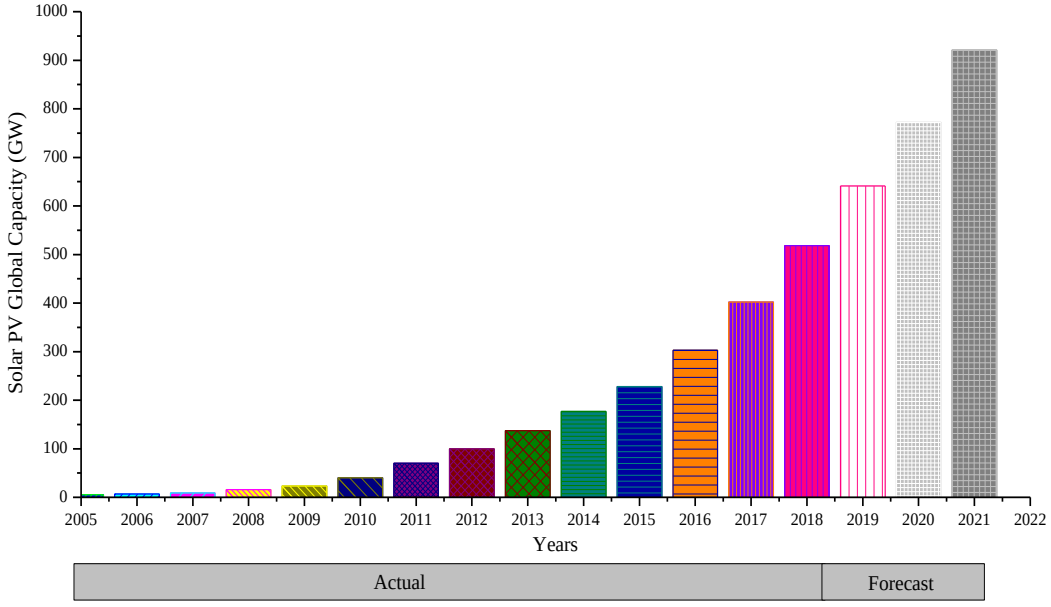

Fig. 1.4 Solar PV global capacity in GW

Most of the places on earth receives sufficient amount of sunlight to make solar photovoltaic technology a technically viable option when coupled with other forms of energy storage such as batteries or the thermal storage. Fig. 1.4 presents the solar PV global capacity from year 2005 to 2018 [16].

The effective utilization of solar energy and other renewable energy resources are considered based on the availability and capacity of source, coherency between source and a user, low cost of energy conversion and

transmission and lastly, the steady performance of a source along with ecological issues. These features along with other local conditions like location, climate and longitude have made a remarkable impact in determining the possibilities of applying solar energy and other renewable-based methods for energy conversion.

1.5 CLIMATE ZONES IN INDIA

The climatic condition of India ranges from severely cold zone with high altitude locations to extremely hot conditions. India's climatic conditions favour five different climate zones. The defined criteria for assigning location to such climate zones depend on weather condition that prevails for a period of six months or more. Based on this condition, Bansal and Minke [17] presented the climate zone by evaluating the averaged mean monthly radiation data from 233 different meteorological sites/locations and made it possible to define five distinct climatic zones across the entire country as shown in Table 1.4.

Table 1.4 Geographical features of Indian stations with distinct climate zone

Climate zone	**Station**	**Latitudinal extent (^{o}N)**	**Longitudinal extent (^{o}E)**	**Ambient temp. (^{o}C)**	**Relative humidity (%)**	**No. of clear sky days**
Composite	New Delhi, Delhi	28.61	77.2	This condition exists when six months or more do not occur in any of the below-mentioned categories.		
Hot and Dry	Jodhpur, Rajasthan	26.28	73.02	>30	< 55	>20
Warm and Humid	Chennai, Tamil Nadu	13.08	80.27	>30	>55	< 20
Moderate	Pune, Maharashtra	18.52	73.85	25-30	< 75	< 20
Cold and Cloudy	Shillong, Meghalaya	25.56	91.88	< 25	>55	< 20

1.6 MODELLING FOR SOLAR ENERGY ESTIMATION AND FORECASTING

The availability of meteorological data plays a vital role in most of the research-based applications. Because of non-availability of measured solar radiation data, the utilities are facing problem in the financial evaluation of the projects. For simulating the dynamic behaviour of solar energy systems, an accurate measurement of solar radiation data plays an important role. Further, the intelligent modelling techniques for forecasting solar energy play a significant role in the designing and the development of solar energy technologies. Wide-scale information regarding the availability of total solar radiation at the site is needed for analysis of solar energy systems.

Many sensitive measuring systems have been installed at the meteorological sites for measuring the solar radiation data and for monitoring day to day recording. But it's unfortunate that in most part of the India, the availability of weather data is scarce, so it is of prime importance and a great need to develop methodologies for weather data forecasting based on more readily available meteorological data.

1.7 PROBLEM FORMULATION

The measurement and estimation of solar energy data is a difficult task and such data are rarely available even for those stations where measurement has already been done. Further, the PV power forecasting is an important element for smart energy management system for the integration of photovoltaic into low voltage grids. In the present scenario, the utilities are developing the smart grid application across the world and the PV power forecasting is one of the key tools for a new paradigm. The forecasting of solar

energy during clear sky can be done simply with the help of mathematical and regression models; however, forecasting under the influence of hazy sky, cloudy and foggy sky conditions do not provide accurate results using these models.

In this research, an attempt has been made to establish an intelligent models for forecasting global solar energy based on sky-conditions i.e. sunny sky (type-a), hazy sky (type-b), partially foggy/cloudy sky (type-c) and fully foggy/cloudy sky (type-d) conditions and for distinct climate zones across India covering widely changing climatic conditions thereof, such as warm and humid, hot and dry, cold and cloudy, moderate and composite climate zone respectively. Simulations have been carried out based on meteorological parameters which correlates global solar energy with other available parameters namely dew-point, ambient temperature, sunshine hours, relative humidity, atmospheric pressure, dew point and wind speed. Further, the comparisons of the proposed model have been done with developed empirical models using multiple regression analysis with aid of statistical validation tests. The obtained results are simulated for solar PV system.

1.8 ORGANIZATION OF THE THESIS

This thesis comprises eight chapters; the details of which are listed below:

Chapter 1: This chapter covers a brief introduction about the current scenario of renewable energy status in India, initiatives being taken by the Government, solar energy potential and its utilization and lastly, climate zones across India. The scope of the work includes modelling techniques for solar energy estimation and forecasting.

Chapter 2: A brief literature review on mathematical and regression models for solar energy estimation is given in this chapter. Further, a comprehensive literature review on intelligent modelling techniques has been carried out and recent research on short-term PV power forecasting is also presented. Based on the detailed literature review, research gaps have been identified and presented towards the end of the chapter.

Chapter 3: In this chapter, sunshine-based models and empirical models have been developed for estimating global solar energy for five meteorological stations across India. An exercise has been carried out for selecting the most suitable model based on principal component analysis. Eight statistical indicators have been used for measuring the performance of the proposed models. Further to check for accuracy of the proposed model, a comparison has been carried out with well-established models discussed in the literature.

Chapter 4: This chapter presented a model employing fuzzy logic approach for forecasting global solar energy with aid of meteorological parameters based on sky-conditions such as sunny sky (type-a), hazy sky (type-b), partially foggy/cloudy sky (type-c) and fully foggy/cloudy sky (type-d) conditions. Simulations have been performed for distinct climatic conditions and the performance evaluation has been done by using statistical error-tests. Further, the comparison of the model has been made with the empirical model. The obtained results are implemented for short-term PV power forecasting in solar PV systems.

Chapter 5: This chapter presents the variant of Artificial Neural Network (ANN) architecture i.e. Cascade-Forward Neural Network (CFNN), Feed-Forward Neural Network (FFNN), Elman Neural Network (ENN), Generalized

Regression Neural Network (GRNN), Layered Recurrent Neural Network (LRNN), Linear Neural Network (LNN) and Radial Basis Function Neural Network (RBFNN) for modelling the system to forecast global solar energy using meteorological parameters under composite climatic conditions. Simulations have been carried out by selecting the most suitable model using evaluation indexes and further applied for different sky-conditions covering widely changing climatic conditions across India. Further, the proposed models based on sky-conditions are compared with fuzzy logic based model. The obtained results are simulated for PV power forecasting under composite climatic conditions.

Chapter 6: In this chapter, a model underlying principle of Adaptive Neural-Fuzzy Inference System (ANFIS) have been presented for forecasting global solar energy based on sky-conditions with aid of meteorological parameters and simulation have been carried out for five meteorological stations across India. Further, the developed model has been implemented for solar photovoltaic systems.

Chapter 7: This chapter includes short-term solar energy forecasting in solar PV applications. Intelligent modelling techniques have been employed and obtained results reveal that the systems may be implemented for a broad series of applications.

Chapter 8: This chapter provides a summary of conclusions which has been carried out based on the analysis of intelligent modelling techniques and its implementation for solar photovoltaic applications. Some suggestions are also presented for scope of future work in the thesis.

CHAPTER 2

LITERATURE REVIEW

2.1 INTRODUCTION

In this chapter, a brief literature survey of the previous work done has been carried out, which includes mathematical models for estimating solar energy, empirical models for estimating solar energy, fuzzy logic approach for forecasting solar energy, solar energy assessment with aid of artificial neural network and hybrid intelligent models for solar energy forecasting. Due to limited space few recent research papers have been discussed in this chapter. Based on the literature survey, the research gaps are analyzed and problems are formulated accordingly.

2.2 MATHEMATICAL MODELS FOR ESTIMATING SOLAR ENERGY

Model based on solar radiation ranges from mathematical models to hybrid intelligent models. In the past, many mathematical models namely Reference Evaluation of Solar Transmittance (REST), Modified Hottel's, Code for Physical Computation of Radiation, 2 bands (CPCR2), Reference Evaluation of Solar Transmittance, 2 bands (REST2) etc. were developed for estimation of global solar energy under cloudless-skies.

Rizwan et al. [18] proposed the REST2 and CPCR2 model for estimating solar energy. Further, in this research REST2 model uses the two-band scheme as used in CPCR2 model, which is an important parameter for estimation of solar energy. It has been concluded from this research that the

REST2 model performs better as compared to other well-established models under cloudless sky for Indian climatic conditions.

Gueymard [19] presented REST2 and CPCR2 model in the estimation of cloudless-sky illuminance, photo-synthetically active radiation and broadband irradiance. In this research, it has been observed that the REST2 model appears to perform better than the CPCR2 model for estimating illuminance, photo-synthetically active radiation and broadband irradiance.

Gueymard [20-21] proposed the performance of broadband direct irradiance model. In this work, two models i.e. the transmittance models and the bulk models were established for providing modelling of the broadband transmittances. It has been concluded from this research that the transmittance model performs better than the bulk models with aid of Linke's turbidity coefficient.

2.3 ESTIMATING SOLAR ENERGY USING REGRESSION MODELLING

The mathematical models available in the literature are found inaccurate, primarily due to extreme simplicity of parameterization; therefore, empirical models based on multiple regression analysis are presented for estimating global solar energy.

Angstrom [22] presented the first attempt for estimating global solar radiation, well-established empirical relation between sunshine hours and global solar radiation under clear sky conditions. Further, Page [23] and Prescott [24] suggested replacing clear day solar radiation with extraterrestrial solar radiation.

Kirmani et al. [25] proposed model for estimating solar energy which is based on Angstrom's model. In this work, empirical models were established based on multiple regression analysis with aid of meteorological parameters namely ambient temperature, sunshine hour, wind speed, relative humidity and rainfall. The performance of the model has been evaluated using statistical indicators. It has been concluded from this research that the correlations based on five meteorological parameters gave the best correlations.

Cenk et al. [26] proposed 105 literature models based on regression modelling for estimation of global solar energy in the Turkey region and the performance have been evaluated based on statistical validation tests. It has been concluded from this research that the cubic models are suitable from January-June period whereas quadratic models are suitable from July-December period.

Most of the previous researches available in the literature have been carried out for Middle East countries; however, very few models are available that discussed about estimating solar energy for Indian climatic conditions.

Khalil and Aly [27] proposed empirical models for estimating global solar energy using meteorological parameters such as sunshine hours, relative humidity and ambient temperature for Saudi Arabia region with aid of statistical error-tests. It has been concluded from this research that during summer, maximum value of solar energy can be obtained while this value diminishes during autumn and winter.

Awan et al. [28] proposed analysis of solar energy data and solar photovoltaic systems output across the Kingdom of Saudi Arabia. In this work, the pattern of solar resource and the solar photovoltaic system has been

compared with the country load profile. It has been observed in this research that during summer, Tabuk station performs best for the solar PV power plant as the stress can be reduced by companies during the season of the high load by cutting off the peak load in afternoon during summer season.

Teke and Yildirim [29] proposed linear, quadratic and cubic models for estimating solar energy for Eastern Mediterranean Region (EMR) with aid of meteorological data in the Turkish state metrological services. Further, comparison between monthly models and general models has been performed by using statistical error-tests. It has been observed in this research, that the use of cubic general model has been recommended for EMR.

Liu et al. [30] investigated the performance of different site-dependent models based on 15 solar radiation stations in the Tibetan Plateau and its surrounding regions. A large variation in the coefficients has been observed in this research among different site-dependent models over the Tibetan Plateau, due to the great spatial difference in elevation and the climate characteristics. It has been concluded from this research that the sunshine-based models have better performance than temperature-based models for estimating solar energy.

Ihaddadene et al. [31] proposed six empirical models namely (i) Hargreaves and Samani model, (ii) Chen model, (iii) Bristow and Campbell model, (iv) Li 1 model, (v) Li 2 model and (vi) Okonkwo model for estimating global solar energy from ambient temperature for the city of Djelfa (Algeria). It has been observed from this research, after performing the statistical analysis, that the Li 2 model perform best and has been verified for Biskra and Ghardaia.

Bahel et al. [32] proposed model based on Angstrom correlation for estimation of global solar energy. In this work, the correlations defined

between global solar energy and sunshine hours provide favourable estimates. Further, the proposed model has been compared with Rietveld's model and results obtained give better estimates than other correlations.

Abdalla [33] proposed model for measurements of global solar energy with sunshine hours, relative humidity, maximum temperature, sea level pressure and vapour pressure. It has been observed in this research that the proposed model provides an excellent agreement between the measured and estimated data and recommended to be used for the city of Bahrain.

Akinoglu and Ecevit [34] presented a quadratic model for estimating monthly average global solar radiation. In this work, the developed correlations have been compared with Rietveld, Benson et al., Ogelman et al. and recent formulation by Gopinathan model. It has been concluded from this research that the quadratic model provides better performance in terms of global applicability and should be preferred for estimation of global solar radiation when the data related to bright sunshine hours are available.

In all of the above discussed models, estimation of global solar energy have been done using meteorological parameters; however, no recent finding is reported that uses dew-point along with other known available meteorological parameters like atmospheric pressure, amount of rainfall, ambient temperature, sunshine hours, relative humidity, wind speed and cloudiness index for estimating global solar energy and for widely changing climatic conditions i.e. warm and humid, hot and dry, cold and cloudy, moderate and composite climate conditions. Hence, a clear scope exists for developing model which can measure the impact of additional meteorological parameters on global solar energy and for distinct climate zones across India.

2.4 FUZZY LOGIC APPROACH FOR SOLAR ENERGY FORECASTING

The regression models developed so far for assessing solar energy were available for clear sky-conditions; however, such models are unsuitable for estimating global solar energy during cloudy sky conditions. Presence of moisture, dust, clouds and aerosols in the lower atmospheric region causes uncertainty in the atmosphere. The reduction in extraterrestrial solar radiation occurs due to the external atmosphere which varies from 30% in a clear sky condition to 100% in a cloudy/foggy sky condition. For Indian climatic conditions where about 50-100 days are cloudy, accurately estimating global solar energy based on multiple regression analysis is a tedious task. Therefore, intelligent modelling techniques have been introduced for forecasting global solar energy.

The fuzzy logic models are introduced wherein probabilistic approaches do not give a realistic description of the phenomenon. Most of the previous researches investigated the fuzzy logic model for forecasting solar energy and its application in the field of the renewable energy system.

Sen [35] proposed a fuzzy logic based model using duration of sunshine hours for estimation of global solar energy. In this work, fuzzy logic modelling has been employed for solar energy forecasting using duration of sunshine hours. Further, the fuzzy logic algorithm has been used which has the ability to explain knowledge in a human-like manner in the form of rules with aid of linguistic variables only.

Suganthi et al. [36] presented an application of fuzzy logic modelling for renewable energy systems such as wind, solar, bio-energy, hybrid systems

and micro-grid. In this research, fuzzy logic based models has been widely used for site assessment, for solar PV system installation, optimization and Maximum Power Point Tracking (MPPT) algorithm for solar photovoltaic systems.

Saez et al. [37] proposed Energy Management System (EMS) technique in determining the generation units dispatch which is optimizer-based requiring the estimation of solar energy resources and loads. In this research, system based on forecasting techniques includes a representation of the uncertainties connected with solar energy resources and loads generating fuzzy models incorporating uncertainty representation of future predictions.

Recently, Perveen et al. [38] proposed a model based on fuzzy logic modelling in forecasting solar energy with aid of different meteorological parameters based on sky-conditions for distinct climate zones across India. It has been observed in this research that with the inclusion of dew point as a meteorological parameter the accuracy of the proposed model has significantly increased.

2.5 SOLAR ENERGY ASSESSMENT USING ANN

For complex systems with large data sets, maintaining accuracy using fuzzy logic modelling would be a tedious task. Therefore, Artificial Neural Network (ANN) based models are introduced, employing artificial intelligence techniques which can subsequently perform the structure simulation. The ANN model is ideal for modelling a non-linear, dynamic and complex system.

Kaushika et al. [39] proposed ANN model based on using diffuse, global and Direct Normal Irradiance (DNI). In this research, the algorithm includes diffuse, global and DNI estimation in a clear/sunny sky-conditions.

Further, the clearness index which corresponds to diffuse, direct and global solar energy are thereby mapped with weather data namely sunshine hour, rainfall and relative humidity in the analysis of ANN. It has been concluded from this research, that the proposed ANN model provides excellent compatibility.

Yadav and Chandel [40] proposed an ANN-based model for estimation of solar energy. It has been concluded from this research, that the ANN-based models provides more accuracy than the conventional methods after performing the review of artificial neural network based modelling techniques for identifying methods available for estimating global solar energy.

Chang et al. [41] proposed Radial Basis Function Neural Network (RBFNN) model for short-term photovoltaic (PV) power forecasting wherein 24 hour of input data at 10-min resolution have been considered for training the proposed neural network. Further, the proposed RBFNN model has been compared with other ANN-based models. It has been concluded from this research that the RBFNN model is more accurate than other models.

Jamil and Zeeshan [42] proposed ANN application for forecasting wind speed in Gujarat, India. Further, in this work, ANN model has been used to forecast wind speed with aid of data measured to train and test the given information. It has been concluded from this research that the ANN modelling techniques are better than the conventional forecasting methods.

Khosravi et al. [43] proposed three model of machine learning algorithms which has been implemented to predict wind direction, wind speed and wind turbine power. In this work, Support Vector Regression-Radial Basis Function (SVR-RBF) represents the first model, Multi-Layered Feed-Forward

Neural Network (MLFFNN) data training with distinct training algorithms represents the second model, and Adaptive Neural-Fuzzy Inference System-Particle Swarm Optimization (ANFIS-PSO) represents the third model. In this, a large data set of wind speed and direction are measured in duration of 5, 10, 30-min and 1-hour intervals efficiently used for estimating wind speed for Bushehr. It has been concluded from this research that the SVR-RBF model outperforms MLFFNN and ANFIS-PSO models.

2.6 ANFIS-BASED MODEL FOR SOLAR ENERGY FORECASTING

Detailed literature review reveals that for estimation of complex functions, an accurate analysis of a number of neurons and hidden layers with aid of ANN is a difficult task as they are large in number. Also, large training time is involved in such a neural network, which subsequently slows down the response of the system. Existing neural network model does the summation operation, however, it does not perform the operation based on the product of weighted inputs. Therefore, hybrid intelligent models are introduced for forecasting solar energy which is a fusion of artificial neural network and fuzzy logic approach for forecasting global solar energy. Many researchers have investigated the integrated features of Adaptive Neural-Fuzzy Inference System (ANFIS) in forecasting global solar energy and its application in wind power forecasting.

Kumar and Kalavathi [44] proposed ANN and ANFIS based model for predicting the PV generation. In this research, the proposed model is validated and compared with the data set of the photovoltaic power generating station. A proposed model is developed and simulated in MATLAB for evaluating the performance of the system.

Walia et al. [45] proposed the basic architecture underlying the principle of ANFIS which is implemented within the adaptive networks framework. In this research, with input and output data, the proposed architecture of ANFIS construct mapping based on human knowledge and hybrid learning algorithm. The result of simulation shows that the ANFIS based model has been used for modelling nonlinear functions.

Jang [46] have presented an ANN application for forecasting wind speed in architecture underlying the principle of ANFIS which is implemented within the framework of adaptive networks. It has been concluded from this research, that the proposed ANFIS model can construct an input-output mapping based on stipulated data pairs.

Zheng et al. [47] proposed a double stage hierarchical ANFIS approach for short-term wind power estimation in China. In this research, the ANFIS approach has two stages wherein the first ANFIS stage makes use of Numerical Weather Prediction (NWP) for forecasting wind speed at the region and the second stage models the relation between wind speed and power. Further, the influence of input data on prediction accuracy has been analyzed by dividing the input data sets into five subsets. It has been concluded from this research that the ANFIS approach resulted in significant forecasting accuracy enhancements.

A hybrid methodology for short-term power forecasting has been proposed using ANFIS by Liu et al. [48]. In this research, individual forecasting models are presented such as back-propagation neural network, least squares support vector machines and radial basis function neural network.

It has been concluded from this research that the proposed hybrid methodology based on ANFIS provides a significant improvement in accuracy.

2.7 IMPLEMENTATION OF SOLAR ENERGY FORECASTING IN SOLAR PV SYSTEMS

In the present scenario, the market for renewable energy is huge and most of the green technologies are in operation by making use of solar energy either directly or indirectly. Solar PV technology has showed a significant growth around the world as many projects are in pipeline which shares the production of electricity. Solar PV technology generate electricity directly as they make use of photovoltaic effect and directly convert the sun's energy into electricity. The electricity is then transferred to the grid as Alternating Current (AC) and with the required value of voltage.

In this research, Multi-crystalline solar PV modules and Heterojunction with Intrinsic Thin (HIT) layer solar PV modules have been employed for short-term PV power forecasting operated at Maximum Power Point Tracking (MPPT) conditions under composite climatic conditions. The solar PV power forecasting is an important element for smart grid approach which helps in optimization of the smart energy management system and has the ability to integrate the renewable power generation in an efficient manner. Since the power generating from solar energy resource is fluctuating and non-linear in nature, it becomes very difficult to estimate power output with mathematical models; therefore, intelligent approaches based on fuzzy logic, ANN and ANFIS based models have been presented for power forecasting of solar PV system employing multi-crystalline and HIT solar PV modules.

Last few years have seen tremendous growth in the field of renewable power generation especially in the field of solar energy which employs PV system comprising a number of solar cells. Its advantages include minimization of greenhouse gas emissions and simple scalability while disadvantage is that the power output diminishes due to dust, clouds and other obstructions in the atmosphere. Therefore, intelligent modelling techniques have been introduced to accurately forecast the power generation in solar PV system based on sky-conditions.

Mosa et al. [49] proposed an efficient Maximum Power Point Tracking (MPPT) of solar photovoltaic systems using Model Predictive Control (MPC) methodology which is applied to a DC to DC converter. In this research, MPC controller has been combined with Incremental Conductance (INC) method improving the speed of the controller that track incident solar energy and the result obtained in this research shows an increased photovoltaic system overall efficiency.

Mehrabankhomartash et al. [50] presented the optimal battery system in a solar photovoltaic power plant which is installed in building situated in Iran. In this research, the sizing of battery lies on financial evaluation considering the damage costs which arises because of outages which abuilding is facing in photovoltaic system life spam. In this research, the sizing of battery has been explained by the Monte-Carlo simulation method and this research confirms the advantage of the proposed approach with the conventional ones.

Chen et al. [51] presented an advanced statistical method for solar power forecasting based on artificial intelligence techniques which used power measurements and meteorological forecasts of solar irradiance, relative

humidity and temperature as input. The developed model is helpful in operational planning for transmission system operator and for PV power system operators trading in electricity market.

Mahmoudi et al. [52] proposed an MPPT method which is based on the theory of Finite Control Set-Model Predictive Control (FCS-MPC) for solar PV systems. In this research, the photovoltaic current and power data is measured from former steps to estimate power for the next step which corresponds to power converter switching configurations. It has been concluded in this research that the proposed method performs better than Perturb and Observe (P&O) method.

Shi et al. [53] proposed method for forecasting PV system power output which is based on Support Vector Machine (SVM) and weather classification for different sky conditions. In this research, a day-ahead photovoltaic power output forecasting model has been used which is based on actual power and weather forecasting data as well as SVM principle. It has been concluded from this research that the model appears to be effective and promising for grid-connected solar PV systems.

Abushaiba et al. [54] proposed an MPPT method for solar PV applications. In this research, the concept of Model predictive Control (MPC) has been used where this method treats the solar PV module as the plant and uses the behaviour of the module for maximum power point tracking conditions.

Yang et al. [55] proposed PV power forecasting in Energy management System (EMS) for distributed energy resources. In this research, weather-based hybrid method has been presented for one day ahead PV power forecasting. It

comprises classification, training and the forecasting stages. The Self-Organizing Map (SOM) and Learning Vector Quantization (LVQ) networks have been used in the classification stage which is used to classify photovoltaic power; Support Vector Regression (SVR) has been used in the training stage to train the input and output data for temperature, probability of precipitation, and solar energy. Lastly, the fuzzy inference method has been used in the forecasting stage to select a trained model for accurately forecasting solar energy. It has been concluded from this research that the proposed model provides better accuracy than the SVR and traditional ANN methods.

Riffonneau et al. [56] proposed a power management mechanism for grid-interacted PV systems so to help photovoltaic generation to grid by proposing peak shaving service in a lower cost. In this research, simulations and real condition applications have been carried out wherein peak shaving has been observed with minimal cost, but the grid power fluctuations have been minimized with photovoltaic penetration to the grid.

2.8 KNOWLEDGE GAP ANALYSIS

This section summarizes the research gaps analyzed from the literature survey discussed in the previous sections.

Empirical model for estimating global solar energy:

After carrying out a detailed literature survey on modelling techniques, it has been identified that most of the empirical models available in the literature for forecasting global solar energy were based on using meteorological parameters like duration of sunshine hours, ambient temperature, wind speed and others; however, very few literature have elucidated about using atmospheric pressure, amount of rainfall and cloudiness

index in addition to other known available meteorological parameters. Further, most of the models have been developed for Middle East countries; however, solar energy forecasting for Indian climatic conditions have been less reported in the literature.

Therefore, sunshine-based models with linear and non-linear correlations and empirical models have been established to estimate solar energy for Indian climatic conditions. Meteorological parameters include sunshine hours, global solar energy, ambient temperature, relative humidity, wind speed, atmospheric pressure, amount of rainfall and cloudiness index for distinct climate zone across India. The results obtained have been evaluated based on statistical indicators like Mean Percentage Error (MPE), Mean Bias Error (MBE), Root Mean Square Error (RMSE), t-stat method, Sum of the Square of the Relative Error (SSRE), Relative Standard Error (RSE), Correlation Coefficient (r) and Coefficient of Determination (R^2). It has been concluded based on the results obtained by statistical analysis, that the meteorological parameters considered do have a strong influence on estimating global solar energy.

Intelligent models for forecasting solar energy:

Based on the exhaustive literature review on the intelligent modelling techniques, it has been observed that the forecasting of solar energy during clear sky can be done simply with the help of mathematical and regression models; however, forecasting under the influence of cloudy sky conditions do not provide accurate results using these mathematical models.

Therefore, in the present research, an attempt has been made to develop intelligent models employing fuzzy logic approach, ANN and ANFIS

modelling for forecasting global solar energy based on variation in sky-conditions defined as clear sky (type-a), hazy sky (type-b), partially foggy/cloudy sky (type-c) and fully foggy/cloudy sky (type-d) conditions and for distinct climate zones i.e. warm and humid, hot and dry, cold and cloudy, composite and moderate climate zone. Further, the comparisons of the proposed intelligent models have been carried out with empirical models using statistical error-tests. The result obtained by employing ANFIS-based model provides more accuracy than the ANN and fuzzy logic based model.

Solar energy forecasting applications for solar PV system:

Short term solar energy forecasting models such as hourly, weekly are available in the literature but 10 minutes ahead solar energy forecasting less reported in the literature using intelligent methodologies such as fuzzy logic, ANN and ANFIS [57]. This chapter deals with the short-term solar energy forecasting in a solar PV system. In the present scenario, the bidding of power has been done on 10 minutes basis by many distribution companies. Keeping in mind aforesaid, 10 minutes ahead forecasting has been done and presented. Therefore, an intelligent approach have been developed and applied for short term solar energy forecasting problem in solar PV system under composite climatic conditions.

CHAPTER 3

EMPIRICAL MODELS FOR ESTIMATING SOLAR ENERGY

3.1 INTRODUCTION

Based on the literature review in the previous chapter, it is observed that for the development of solar devices, it is essential to develop model that can estimate solar energy based on more readily available data with reasonable accuracy. In this chapter, sunshine-based models with linear and non-linear correlations have been established to estimate solar energy for different climatic conditions. Further, empirical models have been established using multiple regression analysis that correlates global solar energy with other meteorological parameters namely relative humidity, sunshine hours, wind speed, atmospheric pressure, rainfall and cloudiness index to estimate global solar energy and applied for distinct climate zone across India. Simulations have been carried out using statistical error-tests. Further, principal component analysis has been performed to select the most suitable model based on the closeness parameter. Lastly, the comparison has been made with the well-established models available in the literature.

This chapter is based on the following published papers:

1. **Gulnar Perveen**, M. Rizwan and Nidhi Goel, "Development of empirical models for forecasting global solar energy," Proceedings of **2nd IEEE International Conference on Power Electronics, Intelligent Control and Energy Systems (ICPEICES-2018)**, October 22-24, 2018, Delhi Technological University, Delhi, India.

2. **Gulnar Perveen**, M. Rizwan and Nidhi Goel, "Correlations for forecasting global solar radiation using meteorological parameters," Proceedings of **IEEE 41st National Systems Conference (NSC) 2017 on Super-Intelligent Machines and Man,** December 1-3, pp. 49-57, 2017, Dayalbagh Educational Institute, Agra, India.

3.2 METEOROLOGICAL DATA

In this chapter, the long-term measured, 15 years averaged data have been obtained from National Institute of Solar Energy (NISE) and Indian Meteorological Department (IMD). The input parameters include sunshine duration, ambient temperature, wind speed, relative humidity, atmospheric pressure, amount of rainfall and cloudiness index whereas global solar energy is the output parameter and obtained for five meteorological sites with distinct climatic conditions across India and are presented in Table 3.1 - Table 3.5 [58].

3.3 EMPIRICAL CORRELATIONS FOR ESTIMATING SOLAR ENERGY

This chapter deals with establishing correlations using multiple regression analysis for estimating global solar energy with aid of meteorological parameters for five distinct climate zones across India. The estimated value of global solar energy H_g can be obtained on multiplication of the estimated clearness index $(\frac{H_g}{H_o})$ by H_o, where H_g represents the measured global solar energy and H_o represents an extraterrestrial solar radiation which can be calculated using standard geometric procedures and are later presented through Eq. (3.11) – Eq. (3.14). In equation with one parameter, the linear regression analysis can be obtained by Eq. (3.1) as:

$$y = a + bx, \tag{3.1}$$

Since there is increase in the number of parameters so the equation with multiple regression analysis can be obtained from Eq. (3.2) as:

$$y = a + bx_1 + cx_2 + dx_3 + ex_4 + fx_5 + \ldots + nx_n, \tag{3.2}$$

where $a,b,c,d,e,f.\ldots n$ are the regression coefficients; and x, x_1, x_2, x_3, x_4, $x_5 \ldots . x_n$ represents the correlated parameters.

Table 3.1 Meteorological data for warm and humid climate zone

Months	**Clearness Index** $\left(\frac{H_g}{H_o}\right)$	**Relative Sunshine** $\left(\frac{S}{S_o}\right)$	**Ambient Temperature (°C)**	**Relative Humidity (%)**	**Rainfall (mm)**	**Wind Speed (Km/hr)**	**Atmospheric Pressure (hPa)**	**Cloudiness Index** $\left(\frac{H_d}{H_g}\right)$
Jan	0.50	0.79	25.46	71.32	0.03	8.22	1012.84	0.44
Feb	0.54	0.84	26.61	76.29	0.09	9.06	1009.74	0.34
Mar	0.55	0.76	27.84	73.75	0.00	6.98	1008.99	0.32
Apr	0.52	0.76	30.53	71.26	0.00	8.78	1019.08	0.35
May	0.49	0.70	31.71	67.14	9.46	7.49	1033.84	0.40
Jun	0.46	0.58	30.73	64.04	0.57	8.48	1013.19	0.51
Jul	0.40	0.49	30.53	62.25	0.51	10.04	1014.78	0.79
Aug	0.41	0.38	29.07	71.30	1.55	8.85	1003.74	0.64
Sep	0.44	0.51	29.10	79.09	2.13	8.41	1014.47	0.53
Oct	0.43	0.56	27.75	80.06	1.39	6.25	1009.47	0.52
Nov	0.42	0.51	25.64	83.73	1.41	11.58	1011.95	0.59
Dec	0.41	0.63	26.09	78.13	0.31	9.49	1012.08	0.58
Avg.	0.46	0.63	28.42	73.20	1.45	8.64	1013.68	0.50

Table 3.2 Meteorological data for hot and dry climate zone

Months	**Clearness Index** $\left(\frac{H_g}{H_o}\right)$	**Relative Sunshine** $\left(\frac{S}{S_o}\right)$	**Ambient Temperature (^{o}C)**	**Relative Humidity (%)**	**Rainfall (mm)**	**Wind Speed (Km/hr)**	**Atmospheric Pressure (hPa)**	**Cloudiness Index** $\left(\frac{H_d}{H_g}\right)$
Jan	0.60	0.87	18.09	45.33	6.37	0.06	991.99	0.26
Feb	0.60	0.87	19.87	41.86	6.12	0.00	987.13	0.25
Mar	0.57	0.77	26.12	30.91	7.74	0.03	1009.11	0.29
Apr	0.52	0.78	32.91	23.98	5.70	0.02	979.69	0.35
May	0.53	0.77	34.88	35.82	8.65	0.05	978.01	0.30
Jun	0.47	0.66	33.52	45.91	14.04	0.10	974.44	0.50
Jul	0.38	0.60	31.52	60.78	14.00	0.27	974.42	0.60
Aug	0.43	0.63	31.44	62.33	5.99	0.97	976.47	0.51
Sep	0.56	0.80	29.70	59.59	6.75	0.15	980.46	0.24
Oct	0.58	0.86	28.46	42.03	4.38	0.00	993.23	0.25
Nov	0.61	0.87	22.08	42.01	3.30	0.00	988.79	0.21
Dec	0.57	0.82	18.64	48.58	3.21	0.00	991.78	0.30
Avg.	0.54	0.78	27.27	44.93	7.19	0.14	985.46	0.34

Table 3.3 Meteorological data for composite climate zone

Months	**Clearness Index** $\left(\frac{H_g}{H_o}\right)$	**Relative Sunshine** $\left(\frac{S}{S_o}\right)$	**Ambient Temperature (°C)**	**Relative Humidity (%)**	**Rainfall (mm)**	**Wind Speed (Km/hr)**	**Atmospheric Pressure (hPa)**	**Cloudiness Index** $\left(\frac{H_d}{H_g}\right)$
Jan	0.39	0.75	14.11	65.48	5.15	0.17	990.03	0.39
Feb	0.38	0.72	18.64	59.49	7.71	0.43	986.33	0.38
Mar	0.55	0.74	22.73	53.30	7.34	0.02	983.27	0.25
Apr	0.56	0.72	30.03	36.19	8.42	0.08	979.30	0.22
May	0.49	0.62	34.14	34.30	9.52	0.03	976.22	0.22
Jun	0.41	0.72	33.40	52.56	10.59	0.28	972.74	0.27
Jul	0.39	0.66	30.48	70.64	10.40	0.31	984.73	0.28
Aug	0.40	0.51	29.14	79.36	9.57	0.82	974.82	0.31
Sep	0.34	0.32	29.73	69.28	9.43	0.43	979.55	0.40
Oct	0.55	0.42	26.18	64.52	6.34	0.00	983.97	0.29
Nov	0.54	0.52	20.92	49.80	6.53	0.00	986.67	0.37
Dec	0.50	0.85	16.00	65.68	5.93	0.00	991.57	0.46
Avg.	0.46	0.63	25.46	58.38	8.08	0.21	982.43	0.32

Table 3.4 Meteorological data for moderate climate zone

Months	**Clearness Index** $\left(\frac{H_g}{H_o}\right)$	**Relative Sunshine** $\left(\frac{S}{S_o}\right)$	**Ambient Temperature (°C)**	**Relative Humidity (%)**	**Rainfall (mm)**	**Wind Speed (Km/hr)**	**Atmospheric Pressure (hPa)**	**Cloudiness Index** $\left(\frac{H_d}{H_g}\right)$
Jan	0.54	0.74	19.78	59.88	1.49	0.00	982.92	0.31
Feb	0.53	0.90	23.18	48.82	5.34	0.00	947.97	0.23
Mar	0.55	0.83	26.28	41.28	3.23	0.00	948.68	0.31
Apr	0.53	0.80	29.19	44.47	6.07	0.00	945.63	0.28
May	0.53	0.84	29.14	55.21	11.76	0.02	944.35	0.34
Jun	0.37	0.35	25.89	76.92	10.48	0.19	942.76	0.67
Jul	0.30	0.31	23.91	86.03	7.93	0.28	954.91	0.79
Aug	0.35	0.31	23.30	85.24	7.73	0.09	943.78	0.81
Sep	0.45	0.46	24.07	84.23	4.68	0.17	945.02	0.57
Oct	0.56	0.68	24.24	75.96	2.27	2.31	947.39	0.37
Nov	0.64	0.80	22.40	71.97	2.00	0.02	950.14	0.33
Dec	0.70	0.85	19.27	63.01	2.41	0.00	962.04	0.23
Avg.	0.50	0.66	24.22	66.09	5.45	0.26	948.42	0.44

Table 3.5 Meteorological data for cold and cloudy climate zone

Months	**Clearness Index** $\left(\frac{H_g}{H_o}\right)$	**Relative Sunshine** $\left(\frac{S}{S_o}\right)$	**Ambient Temperature (°C)**	**Relative Humidity (%)**	**Rainfall (mm)**	**Wind Speed (Km/hr)**	**Atmospheric Pressure (hPa)**	**Cloudiness Index** $\left(\frac{H_d}{H_g}\right)$
Jan	0.52	0.67	9.95	75.58	3.61	0.22	840.99	0.34
Feb	0.51	0.56	10.24	71.84	3.80	0.68	838.66	0.42
Mar	0.54	0.61	15.54	59.65	5.65	1.87	838.72	0.41
Apr	0.45	0.30	18.26	63.53	7.63	5.61	839.83	0.47
May	0.38	0.37	20.69	80.29	4.29	3.53	838.13	0.60
Jun	0.33	0.26	21.04	85.50	3.63	15.68	834.75	0.70
Jul	0.33	0.20	21.21	87.52	3.15	14.15	835.36	0.80
Aug	0.31	0.17	20.64	89.23	1.23	12.92	836.08	0.77
Sep	0.34	0.23	20.00	85.92	0.87	7.53	838.44	0.73
Oct	0.43	0.52	18.39	80.74	2.29	1.53	842.01	0.48
Nov	0.54	0.66	15.27	75.60	2.65	0.33	843.31	0.43
Dec	0.60	0.73	11.89	74.40	0.84	0.01	841.67	0.22
Avg.	0.44	0.44	16.93	77.48	3.30	5.34	839.00	0.53

3.4 SUNSHINE-BASED MODELS FOR ESTIMATING SOLAR ENERGY

In estimation models, the most widely used method for estimating global solar energy is Angstrom - Prescott model which is based on the correlation of the ratio of global solar energy to extraterrestrial solar radiation with ratio of relative sunshine hours. In this chapter, sunshine-based models with linear and non-linear correlations have been established and the performance is evaluated based on statistical error-tests.

Model 1: Linear model

Source – Angstrom-Prescott model [22][24]

$$\frac{H}{H_o} = a + b(\frac{S}{S_o}) \tag{3.3}$$

Model 2: Quadratic model

Source – Akinoglu and Ecevit model [34]

$$\frac{H}{H_o} = a + b(\frac{S}{S_o}) + c(\frac{S}{S_o})^2 \tag{3.4}$$

Model 3: Cubic model

Source – Bahel et al. model [32]

$$\frac{H}{H_o} = a + b(\frac{S}{S_o}) + c(\frac{S}{S_o})^2 + d(\frac{S}{S_o})^3 \tag{3.5}$$

Model 4: Linear logarithmic model

Source – Newland model [59]

$$\frac{H}{H_o} = a + b(\frac{S}{S_o}) + c\ log(\frac{S}{S_o}) \tag{3.6}$$

Model 5: Logarithmic model

Source – Ampratwum and Dorvlo model [60]

$$\frac{H}{H_o} = a + b\ log(\frac{S}{S_o}) \quad (3.7)$$

Model 6: Linear exponential model

Source – Bakirci model [61]

$$\frac{H}{H_o} = a + b(\frac{S}{S_o}) + c\ exp(\frac{S}{S_o}) \quad (3.8)$$

Model 7: Exponential model

Source – Almorox et al. model [62]

$$\frac{H}{H_o} = a + b\ exp(\frac{S}{S_o}) \quad (3.9)$$

Model 8: Exponent model

Source – Bakirci model [61]

$$\frac{H}{H_o} = a + (\frac{S}{S_o})^b \quad (3.10)$$

In Eq. (3.3) - Eq. (3.10) as shown above, *a*, *b*, *c* and *d* are the regression coefficients. The daily extraterrestrial solar radiation H_o can be expressed by Eq. (3.11) - Eq. (3.14) in the following manner as [63]:

$$H_o = \frac{24 * 3600}{\pi} G_{SC} \left(1 + 0.033 \cos\frac{360 n_{day}}{365}\right) * \left(cos\phi\ cos\delta \cos\omega_s \frac{\pi\omega_s}{180} \sin\phi\right) \quad (3.11)$$

$$\delta = 23.45 \sin\left[\frac{360}{365}(n_{day} + 284)\right] \quad (3.12)$$

$$\omega_s = \cos^{-1}(-\tan\phi\ \tan\delta) \quad (3.13)$$

S_o is calculated using Cooper's formula which is expressed as:-

$$S_o = \frac{2}{15} \cos^{-1}(-\tan\phi\ \tan\delta) \quad (3.14)$$

where G_{sc} is the solar constant and equals 1367 W/m^2, δ represents the solar declination angle, ϕ is the latitudinal extent of the site, ω_s represents the mean sunrise hour angle and n_{day} represents the number of days which is equal to 1

for 1st January and 365 for 31st December. S represents the bright sunshine hours and S_o represents the maximum daily hours of bright sunshine.

3.5 PRINCIPAL COMPONENT ANALYSIS

Principal Component Analysis (PCA) is a technique which is used for identification of a smaller number of uncorrelated variables known as principle components from a larger set of data. It is a tool used in predictive models and exploratory data analysis. The technique has been widely used to emphasize variation and capture strong patterns in a data set. It is a simple non-parametric technique for extracting information from complex and confusing data sets. Principle component analysis has been used to eliminate the number of variables or when there are too many predictors compared to number of observations or to avoid non-collinearity.

For choosing the model with best correlation, the principal component analysis has been performed. For better analysis, parameters such as correlation of coefficient (r) and coefficient of determination (R^2) are chosen as the closeness parameter. Steps for performing principal component analysis are as follows:

(a) Standardization

(b) Computation of correlation matrix

(c) Compute the eigenvectors and eigenvalues of the correlation matrix

(d) Feature vector

(e) Recast the data along the principal component axis

Consider for example warm and humid climate zone with models based on four variables correlation represented by Eq. (3.90) - Eq. (3.97). The principal component analysis have been performed on these equations based on

closeness parameters i.e. correlation coefficient (r) and coefficient of determination (R^2), the following graph has been obtained after applying PCA on above equations and shown below in Fig. 3.1.

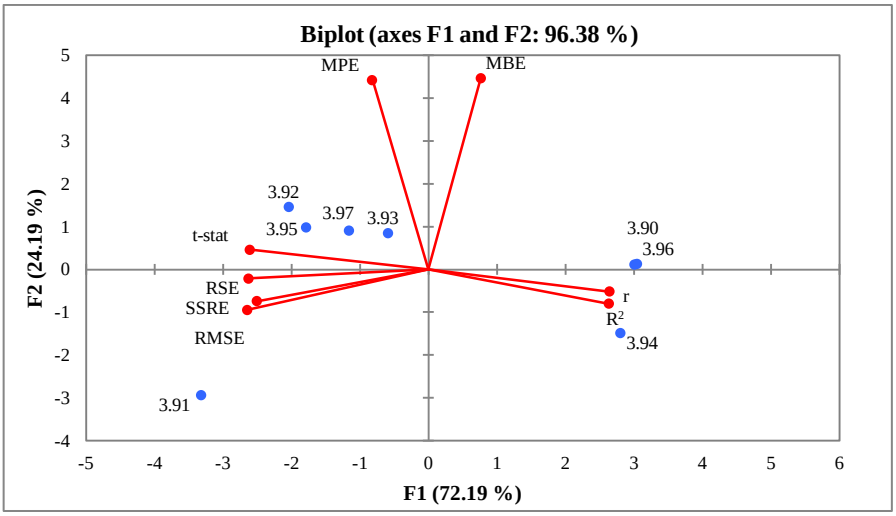

Fig. 3.1 Principal component analysis for Eq. (3.90) – Eq. (3.97)

In Fig. 3.1 as shown above, Eq. (3.94) lies in the fourth quadrant satisfying the condition and provides better analysis with (r) and (R^2) chosen as closeness parameter.

3.6 STATISTICAL PERFORMANCE EVALUATIONS

For model evaluation, different statistical evaluation indexes namely Mean Percentage Error (MPE), Relative Standard Error (RSE), Mean Bias Error (MBE), t-statistics (t-stat) method, Root Mean Square Error (RMSE), correlation coefficient (r) and the coefficient of determination (R^2) are the frequently used methods for comparison [64-75].

3.6.1 Mean Percentage Error (MPE)

It is the percentage deviation in estimated data of solar radiation from measured data of solar radiation which is given by Eq. (3.15) as shown below:

$$\text{MPE} = \sum_{i=1}^{n} \frac{E}{n} \tag{3.15}$$

where E is the absolute error and expressed as $E = \left(\frac{c_i - m_i}{m_i}\right) * 100$, n is the number of observation, c_i and m_i are the i_{th} calculated and measured values, respectively.

3.6.2 Mean Bias Error (MBE)

It gives information associated with long-term performance of the correlations on performing the comparison of the deviation between the measured and estimated values and 'zero' is its ideal value. It is expressed by Eq. (3.16) as shown below:

$$\text{MBE} = \frac{1}{n}\sum_{i=1}^{n}(c_i - m_i) \tag{3.16}$$

where n is the number of observations, c_i and m_i are the i_{th} calculated and measured values, respectively.

3.6.3 Sum of the Square of Relative Error (SSRE)

It gives the positive result of the sum of the square of relative deviation and it's value is 'zero'. It is expressed by Eq. (3.17) as shown below:

$$\text{SSRE} = \sum_{i=1}^{n}\left(\left(\frac{c_i - m_i}{m_i}\right)^2\right) \tag{3.17}$$

where n is the number of observations, c_i and m_i are the i_{th} calculated and measured values, respectively.

3.6.4 Relative Standard Error (RSE)

It gives the degree of accuracy of estimation of correlations and can be expressed by Eq. (3.18) shown below as:

$$\text{RSE} = \sqrt{\frac{SSRE}{n}} \tag{3.18}$$

where n is the number of observation.

3.6.5 Root Mean Square Error (RMSE)

It is expressed by Eq. (3.19) as shown below:

$$\text{RMSE} = \sqrt{\frac{1}{n}\sum_{i=1}^{n}(c_i - m_i)^2} \tag{3.19}$$

where n is the number of observations, c_i and m_i are the i_{th} calculated and measured values, respectively. The value of root mean square error is positive where it's ideal value is 'zero'.

3.6.6 t-stat (t-statistic) Method

In order to check for estimation of equation whether it is statistically significant, or not from the measured data, in a defined confidence level, the t-statistic can be expressed by Eq. (3.20) as:

$$\text{t-stat} = \sqrt{\left[\frac{(n-1)MBE^2}{RMSE^2 - MBE^2}\right]} \tag{3.20}$$

where n is the number of observations.

3.6.7 Coefficient of Determination (R^2)

The coefficient of determination is used to test the linear relationship between the measured and the estimated data. It can be defined by Eq. (3.21) as shown below:

$$R^2 = \frac{\sum_{i=1}^{n}(c_i - c_a)(m_i - m_a)}{\sqrt{[\sum_{i=1}^{n}(c_i - c_a)^2][\sum_{i=1}^{n}(m_i - m_a)^2]}} \tag{3.21}$$

where n is the number of observation, c_a is the average calculated values, m_a is the average measured values, c_i is the i^{th} calculated values and m_i is the i^{th} measured values.

3.7 RESULTS AND DISCUSSIONS

3.7.1 Sunshine-based Models for Estimating Global Solar Energy

In the first part of this chapter, models based on sunshine duration with linear, quadratic, cubic, linear logarithmic, logarithmic, linear exponential, exponential and exponent correlations have been established using multiple regression analysis. The regression coefficients *a, b, c* and *d* are obtained for eight models i.e. models 1-8 as shown in Eq. (3.3) - Eq. (3.10) of the sunshine-based models with aid of measured data and presented in Table 3.6 - Table 3.8 respectively for five meteorological sites representing different climatic conditions across India. MATLAB curve fitting tool has been used for obtaining the regression coefficients. From Table 3.6 - Table 3.8, the following can be briefly summarized:

(a) Warm and humid climate zone

It has been observed that for this climate zone, the dependencies are stronger for cubic term with correlation of coefficient (r = 0.80) obtained between the clearness index and relative sunshine duration.

The coefficient of determination is observed to be (R^2 = 0.65) which means 65% of the clearness index can be accounted using relative sunshine duration.

The values of the estimated global solar energy using derived correlations are compared with the measured values as shown in Fig. 3.2 (a).

Further, the relation between the clearness index and relative sunshine duration is obtained by Eq. (3.24) as:

$$\frac{H_g}{H_o} = 0.426 - 0.232\left(\frac{S}{S_o}\right) + 0.505\left(\frac{S}{S_o}\right)^2 - 0.086\left(\frac{S}{S_o}\right)^3 \quad (3.24)$$

Table 3.6 Sunshine-based models for warm and humid & hot and dry climate zone across India

Stations	Model	Eq. No.	Equations	MPE (%)	MBE (%)	RMSE (%)	r	R^2
Chennai (Warm and Humid)	Linear	3.22	$\frac{H_g}{H_o} = 0.259 + 0.321(\frac{S}{S_o})$	1.52	0.00	0.05	0.77	0.62
	Quadratic	3.23	$\frac{H_g}{H_o} = 0.289 + 0.252(\frac{S}{S_o}) + 0.041(\frac{S}{S_o})^2$	1.79	0.00	0.05	0.78	0.63
	Cubic	3.24	$\frac{H_g}{H_o} = 0.426 - 0.232(\frac{S}{S_o}) + 0.505(\frac{S}{S_o})^2 - 0.086(\frac{S}{S_o})^3$	1.79	0.00	0.04	0.80	0.65
	Linear Logarithmic	3.25	$\frac{H_g}{H_o} = 0.134 + 0.434(\frac{S}{S_o}) + 0.011 \log(\frac{S}{S_o})$	-10.35	-0.05	0.10	0.74	0.57
	Logarithmic	3.26	$\frac{H_g}{H_o} = 0.533 + 0.153 \log(\frac{S}{S_o})$	15.60	0.04	0.08	0.62	0.42
	Linear Exponential	3.27	$\frac{H_g}{H_o} = 0.243 + 0.230(\frac{S}{S_o}) + 0.037 \exp(\frac{S}{S_o})$	1.97	0.00	0.04	0.78	0.63
	Exponential	3.28	$\frac{H_g}{H_o} = 0.113 + 0.184 \exp(\frac{S}{S_o})$	2.58	0.00	0.05	0.77	0.61
	Exponent	3.29	$\frac{H_g}{H_o} = 0.556(\frac{S}{S_o})^{0.318}$	5.79	0.01	0.06	0.71	0.53
Jodhpur (Hot and Dry)	Linear	3.30	$\frac{H_g}{H_o} = 0.375 + 0.214(\frac{S}{S_o})$	-0.55	-0.01	0.05	0.51	0.33
	Quadratic	3.31	$\frac{H_g}{H_o} = 0.586 - 0.414(\frac{S}{S_o}) + 0.439(\frac{S}{S_o})^2$	-0.44	-0.01	0.04	0.60	0.41
	Cubic	3.32	$\frac{H_g}{H_o} = - 0.46 + 0.032(\frac{S}{S_o}) - 0.693(\frac{S}{S_o})^2 + 0.769(\frac{S}{S_o})^3$	1.18	0.00	0.04	0.50	0.40
	Linear Logarithmic	3.33	$\frac{H_g}{H_o} = -0.196 + 0.801(\frac{S}{S_o}) - 0.396 \log(\frac{S}{S_o})$	-7.37	-0.05	0.13	0.53	0.35
	Logarithmic	3.34	$\frac{H_g}{H_o} = 0.570 + 0.125 \log(\frac{S}{S_o})$	4.10	0.01	0.05	0.66	0.47
	Linear Exponential	3.35	$\frac{H_g}{H_o} = 0.114 - 0.673(\frac{S}{S_o}) + 0.309 \exp(\frac{S}{S_o})$	-1.51	-0.02	0.05	0.60	0.41
	Exponential	3.36	$\frac{H_g}{H_o} = 0.297 + 0.111 \exp(\frac{S}{S_o})$	-0.89	-0.01	0.05	0.52	0.34
	Exponent	3.37	$\frac{H_g}{H_o} = 0.569(\frac{S}{S_o})^{0.234}$	-1.81	-0.02	0.05	0.49	0.30

Table 3.7 Sunshine-based models for composite and moderate climate zone across India

Stations	Model	Eq. No.	Equations	MPE (%)	MBE (%)	RMSE (%)	r	R^2
Delhi (Composite)	Linear	3.38	$\frac{H_g}{H_o} = 0.367 + 0.205(\frac{S}{S_o})$	1.24	0.00	0.04	0.59	0.40
	Quadratic	3.39	$\frac{H_g}{H_o} = 0.470 - 0.117(\frac{S}{S_o}) + 0.238(\frac{S}{S_o})^2$	1.04	0.00	0.04	0.66	0.47
	Cubic	3.40	$\frac{H_g}{H_o} = 0.504 - 0.241(\frac{S}{S_o}) + 0.231(\frac{S}{S_o})^2 + 0.067(\frac{S}{S_o})^3$	1.44	0.00	0.04	0.66	0.46
	Linear Logarithmic	3.41	$\frac{H_g}{H_o} = 0.033 + 0.522(\frac{S}{S_o}) - 0.142 \log(\frac{S}{S_o})$	-19.43	-0.09	0.12	0.54	0.40
	Logarithmic	3.42	$\frac{H_g}{H_o} = 0.543 + 0.098 \log(\frac{S}{S_o})$	10.62	0.03	0.07	0.52	0.40
	Linear Exponential	3.43	$\frac{H_g}{H_o} = 0.208 - 0.282(\frac{S}{S_o}) + 0.245 \exp(\frac{S}{S_o})$	1.74	0.00	0.04	0.65	0.46
	Exponential	3.44	$\frac{H_g}{H_o} = 0.261 + 0.124 \exp(\frac{S}{S_o})$	1.61	0.00	0.04	0.61	0.40
	Exponent	3.45	$\frac{H_g}{H_o} = 0.543(\frac{S}{S_o})^{0.185}$	2.31	0.00	0.05	0.54	0.40
Pune (Moderate)	Linear	3.46	$\frac{H_g}{H_o} = 0.156 + 0.281(\frac{S}{S_o})$	3.10	0.01	0.04	0.73	0.57
	Quadratic	3.47	$\frac{H_g}{H_o} = 0.392 + 0.036(\frac{S}{S_o}) + 0.172(\frac{S}{S_o})^2$	3.65	0.01	0.04	0.71	0.53
	Cubic	3.48	$\frac{H_g}{H_o} = 0.82-0.62(\frac{S}{S_o}) + 0.52(\frac{S}{S_o})^2 - 0.6(\frac{S}{S_o})^3$	2.46	0.01	0.04	0.70	0.53
	Linear Logarithmic	3.49	$\frac{H_g}{H_o} = 0.093 + 0.506(\frac{S}{S_o}) - 0.097 \log(\frac{S}{S_o})$	5.19	0.00	0.08	0.70	0.52
	Logarithmic	3.50	$\frac{H_g}{H_o} = 0.567 + 0.193 \log(\frac{S}{S_o})$	17.69	0.06	0.08	0.65	0.45
	Linear Exponential	3.51	$\frac{H_g}{H_o} = 0.230 + 0.006(\frac{S}{S_o}) + 0.133 \exp(\frac{S}{S_o})$	3.19	0.01	0.04	0.72	0.56
	Exponential	3.52	$\frac{H_g}{H_o} = 0.119 + 0.194 \exp(\frac{S}{S_o})$	3.15	0.01	0.04	0.72	0.54
	Exponent	3.53	$\frac{H_g}{H_o} = 0.590(\frac{S}{S_o})^{0.445}$	3.16	0.01	0.04	0.72	0.54

Table 3.8 Sunshine-based models for cold and cloudy climate zone across India

Stations	Model	Eq. No.	Equations	MPE (%)	MBE (%)	RMSE (%)	r	R^2
Shillong (Cold and cloudy)	Linear	3.54	$\frac{H_g}{H_o} = 0.239 + 0.586(\frac{S}{S_o})$	1.09	-0.01	0.07	0.70	0.51
	Quadratic	3.55	$\frac{H_g}{H_o} = 0.301 + 0.187(\frac{S}{S_o}) - 0.4(\frac{S}{S_o})^2$	3.33	0.00	0.06	0.72	0.55
	Cubic	3.56	$\frac{H_g}{H_o} = 0.369 - 0.250(\frac{S}{S_o}) + 1.059(\frac{S}{S_o})^2 - 0.601(\frac{S}{S_o})^3$	3.15	0.00	0.06	0.70	0.52
	Linear Logarithmic	3.57	$\frac{H_g}{H_o} = 0.160 + 0.458(\frac{S}{S_o}) + 0.049 \log(\frac{S}{S_o})$	0.11	-0.02	0.12	0.64	0.45
	Logarithmic	3.58	$\frac{H_g}{H_o} = 0.546 + 0.145 \log(\frac{S}{S_o})$	18.88	0.06	0.10	0.64	0.44
	Linear Exponential	3.59	$\frac{H_g}{H_o} = 0.160 + 0.104(\frac{S}{S_o}) + 0.132 \exp(\frac{S}{S_o})$	4.36	0.00	0.09	0.70	0.53
	Exponential	3.60	$\frac{H_g}{H_o} = 0.061 + 0.229 \exp(\frac{S}{S_o})$	3.52	0.00	0.07	0.68	0.50
	Exponent	3.61	$\frac{H_g}{H_o} = 0.573(\frac{S}{S_o})^{0.355}$	3.76	0.00	0.07	0.70	0.52

(b) Hot and dry climate zone

It has been observed that for this climate zone, the dependencies are stronger for the logarithmic term with correlation of coefficient (r = 0.66) obtained between the clearness index and relative sunshine duration.

The coefficient of determination is observed to be (R^2 = 0.47) which means 47% of the clearness index can be accounted using relative sunshine duration.

The values of the estimated global solar energy using derived correlations are compared with the measured values as shown in Fig. 3.2 (b).

Further, the relation between the clearness index and relative sunshine duration is shown by Eq. (3.34) as:

$$\frac{H_g}{H_o} = 0.570 + 0.125 \log(\frac{S}{S_o}) \quad (3.34)$$

(c) Composite climate zone

It has been observed that for this climate zone, the dependencies are stronger for the quadratic term with correlation of coefficient r = 0.66 obtained between the clearness index and relative sunshine duration.

The coefficient of determination is observed to be R^2 = 0.47 which means 47% of the clearness index can be accounted using relative sunshine duration.

The values of the global solar energy estimated using derived correlations are compared with the measured values as shown in Fig. 3.2 (c).

Further, the relation between the clearness index and relative sunshine duration is shown by Eq. (3.39) as:

$$\frac{H_g}{H_o} = 0.470 - 0.117(\frac{S}{S_o}) + 0.238(\frac{S}{S_o})^2 \quad (3.39)$$

(d) Moderate climate zone

It has been observed that for this climate zone, the dependencies are stronger for the linear term with correlation of coefficient r = 0.73 obtained between the clearness index and relative sunshine duration.

The coefficient of determination is observed to be R^2 = 0.57 which means 57% of the clearness index can be accounted using relative sunshine duration.

The values of the estimated global solar energy using derived correlations are compared with the measured values as shown in Fig. 3.2 (d).

Further, the relation between the clearness index and relative sunshine duration is shown by Eq. (3.46) as:

$$\frac{H_g}{H_o} = 0.156 + 0.281\left(\frac{S}{S_o}\right) \quad (3.46)$$

(e) Cold and cloudy climate zone

It has been observed that for this climate zone, the dependencies are stronger for the quadratic term with correlation of coefficient r = 0.72 obtained between the clearness index and relative sunshine duration.

The coefficient of determination is observed to be R^2 = 0.55 which means 55% of the clearness index can be accounted using relative sunshine hours.

The values of the estimated global solar energy using derived correlations are compared with the measured values as shown in Fig. 3.2 (e).

Further, the relation between the clearness index and relative sunshine duration is shown by Eq. (3.55) as:

$$\frac{H_g}{H_o} = 0.301 + 0.187\left(\frac{S}{S_o}\right) - 0.4\left(\frac{S}{S_o}\right)^2 \quad (3.55)$$

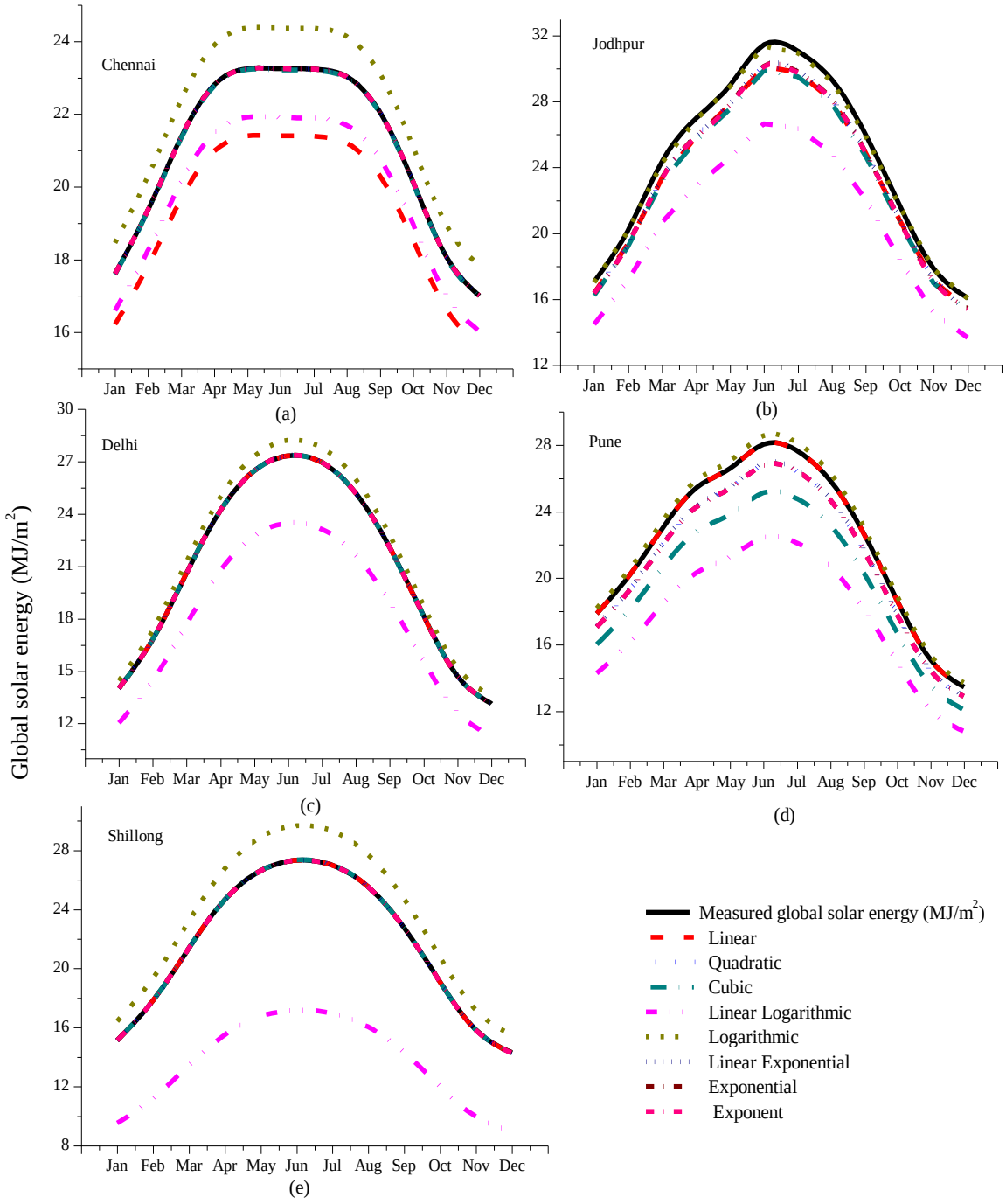

Fig. 3.2 Graphical representation of measured and estimated global solar energy for linear and non – linear sunshine based models for (a) Chennai (b) Jodhpur (c) Delhi (d) Pune and (e) Shillong

For each of the climate zone, all the developed models have distinct values of determination coefficients where the largest difference between the determination coefficients of the best and worst fit model obtained is 0.23 for warm and humid climate (Chennai), 0.17 for hot and dry climate (Jodhpur), 0.07 for composite (Delhi), 0.12 for moderate (Pune) and 0.11 for cold and cloudy climate (Shillong) zone.

It has been observed that the best fit is obtained for composite climate zone with the smallest difference between the best and worst determination coefficients of 0.07 as shown by the computed data presented in Table 3.7. Similarly, the weakest fit is obtained for warm and humid climate zone with the largest difference between the best and worst determination coefficients of 0.23 as shown by the computed data presented in Table 3.6 respectively.

3.7.2 Empirical Models for Solar Energy Estimation

In the second part of this chapter, empirical models have been established using multiple regression analysis of different parameters namely global solar energy, sunshine hours, atmospheric pressure, wind speed, rainfall, ambient temperature, relative humidity and cloudiness index for different meteorological sites in India representing widely changing climatic conditions thereof, such as warm and humid (Chennai), hot and dry (Jodhpur), cold and cloudy (Shillong), moderate (Pune) and composite (Delhi) climatic conditions. The performance of the models has been evaluated based on statistical error-tests i.e. MPE, MBE, SSRE, RSE, RMSE, t-stat, r and R^2 and are illustrated in Table 3.9 - Table 3.33.

Table 3.9 Empirical models based on one and two variables correlation along with statistical errors for warm and humid climate zone

Models	Eq. No.	Equations	MPE (%)	MBE (%)	SSRE (%)	RSE (%)	RMSE (%)	t-stat	r	R^2
Models based on one variable correlation	3.62	$\frac{H_g}{H_o} = 0.379 + 0.004(\frac{T_m}{T_o})$	0.61	0.00	0.73	0.12	0.05	23.31	0.35	0.18
	3.63	$\frac{H_g}{H_o} = -5.495 + 0.006(\frac{P_m}{P_o})$	5.51	0.02	11.23	0.30	0.14	39.13	0.21	0.07
	3.64	$\frac{H_g}{H_o} = 0.656 - 0.352(\frac{H_d}{H_g})$	-0.04	0.00	0.35	0.08	0.03	6.38	0.71	0.54
	3.65	$\frac{H_g}{H_o} = 0.532 - 0.036(\frac{RF_m}{RF_o})$	1.35	0.00	1.25	0.15	0.05	77.04	0.16	0.05
	3.66	$\frac{H_g}{H_o} = 0.636 - 0.002(\frac{RH_m}{RH_o})$	0.78	0.00	0.84	0.13	0.05	26.33	0.36	0.17
	3.67	$\frac{H_g}{H_o} = 0.259 + 0.321(\frac{S}{S_o})$	1.52	0.00	0.96	0.15	0.05	4.50	0.77	0.62
	3.68	$\frac{H_g}{H_o} = 0.540 - 0.002(\frac{WS_m}{WS_o})$	1.38	0.00	1.20	0.14	0.05	46.17	0.17	0.05
Models based on two variables correlation	3.69	$\frac{H_g}{H_o} = 0.281 + 0.217(\frac{S}{S_o}) + 0.002(\frac{T_m}{T_o})$	0.29	0.00	0.61	0.09	0.04	8.32	0.62	0.43
	3.70	$\frac{H_g}{H_o} = -3.532 + 0.225(\frac{S}{S_o}) + 0.004(\frac{P_m}{P_o})$	0.58	0.00	0.82	0.12	0.04	9.65	0.57	0.38
	3.71	$\frac{H_g}{H_o} = 0.551 + 0.107(\frac{S}{S_o}) - 0.265(\frac{H_d}{H_g})$	1.51	0.00	0.34	0.08	0.04	5.67	0.89	0.79
	3.72	$\frac{H_g}{H_o} = 0.363 + 0.220(\frac{S}{S_o}) - 0.011(\frac{RF_m}{RF_o})$	0.61	0.00	0.83	0.12	0.04	29.88	0.51	0.33
	3.73	$\frac{H_g}{H_o} = 0.436 + 0.195(\frac{S}{S_o}) - 0.001(\frac{RH_m}{RH_o})$	0.45	0.00	0.72	0.11	0.04	17.19	0.55	0.38
	3.74	$\frac{H_g}{H_o} = 0.368 + 0.230(\frac{S}{S_o}) - 0.002(\frac{WS_m}{WS_o})$	0.48	0.00	0.66	0.11	0.04	24.82	0.54	0.36

Table 3.10 Empirical models based on three variables correlation along with statistical errors for warm and humid climate zone

Models	Eq. No.	Equations	MPE (%)	MBE (%)	SSRE (%)	RSE (%)	RMSE (%)	t-stat	r	R^2
Models based on three variables correlation	3.75	$\frac{H_g}{H_o} = 0.683 + 0.063(\frac{S}{S_o}) + 0.0001(\frac{P_m}{P_o}) - 0.332(\frac{H_d}{H_g})$	2.95	0.01	0.81	0.13	0.04	3.06	0.90	0.80
	3.76	$\frac{H_g}{H_o} = -1.813 + 0.282(\frac{S}{S_o}) - 0.001(\frac{P_m}{P_o}) + 0.002(\frac{RH_m}{RH_o})$	2.24	0.00	1.07	0.15	0.05	4.53	0.77	0.63
	3.77	$\frac{H_g}{H_o} = -3.163 + 0.283(\frac{S}{S_o}) + 0.0001(\frac{WS_m}{WS_0}) + 0.003(\frac{P_m}{P_o})$	2.19	0.00	1.12	0.15	0.04	3.82	0.81	0.66
	3.78	$\frac{H_g}{H_o} = -2.854 + 0.277(\frac{S}{S_o}) + 0.006(\frac{T_m}{T_o}) + 0.003(\frac{P_m}{P_o})$	2.13	0.00	0.95	0.14	0.05	4.44	0.79	0.65
	3.79	$\frac{H_g}{H_o} = 0.435 + 0.054(\frac{S}{S_o}) + 0.006(\frac{T_m}{T_o}) - 0.336(\frac{H_d}{H_g})$	1.35	0.00	0.62	0.11	0.03	2.46	0.90	0.82
	3.80	$\frac{H_g}{H_o} = 0.184 + 0.272(\frac{S}{S_o}) + 0.006(\frac{T_m}{T_o}) - 0.001(\frac{RH_m}{RH_o})$	2.67	0.00	1.68	0.18	0.05	4.31	0.79	0.64
	3.81	$\frac{H_g}{H_o} = 0.131 + 0.286(\frac{S}{S_o}) + 0.006(\frac{T_m}{T_o}) - 0.006(\frac{RF_m}{RF_o})$	2.68	0.00	1.54	0.18	0.05	4.47	0.79	0.64
	3.82	$\frac{H_g}{H_o} = 0.120 + 0.273(\frac{S}{S_o}) + 0.006(\frac{T_m}{T_o}) - 0.008(\frac{WS_m}{WS_0})$	4.09	0.01	3.08	0.24	0.07	6.67	0.70	0.56
	3.83	$\frac{H_g}{H_o} = 0.671 + 0.055(\frac{S}{S_o}) - 0.001(\frac{RH_m}{RH_o}) - 0.342(\frac{H_d}{H_g})$	1.34	0.00	0.56	0.11	0.03	2.56	0.90	0.81
	3.84	$\frac{H_g}{H_o} = 0.433 + 0.274(\frac{S}{S_o}) - 0.002(\frac{RH_m}{RH_o}) - 0.001(\frac{WS_m}{WS_0})$	2.60	0.00	1.69	0.18	0.05	3.86	0.81	0.66
	3.85	$\frac{H_g}{H_o} = -1.836 + 0.295(\frac{S}{S_o}) - 0.012(\frac{RF_m}{RF_o}) + 0.002(\frac{P_m}{P_o})$	2.19	0.00	1.06	0.15	0.05	4.60	0.78	0.64
	3.86	$\frac{H_g}{H_o} = 0.592 + 0.066(\frac{S}{S_o}) - 0.003(\frac{RF_m}{RF_o}) - 0.340(\frac{H_d}{H_g})$	1.32	0.00	0.55	0.11	0.03	2.47	0.90	0.82
	3.87	$\frac{H_g}{H_o} = 0.362 + 0.3(\frac{S}{S_o}) - 0.001(\frac{RF_m}{RF_o}) - 0.008(\frac{RH_m}{RH_o})$	2.62	0.00	1.49	0.17	0.05	4.57	0.77	0.63
	3.88	$\frac{H_g}{H_o} = 0.284 + 0.29(\frac{S}{S_o}) + 0.0001(\frac{RF_m}{RF_o}) - 0.011(\frac{WS_m}{WS_0})$	2.39	0.00	1.41	0.17	0.04	3.71	0.82	0.67
	3.89	$\frac{H_g}{H_o} = 0.573 + 0.060(\frac{S}{S_o}) + 0.003(\frac{WS_m}{WS_0}) - 0.341(\frac{H_d}{H_g})$	1.41	0.00	0.67	0.12	0.03	2.47	0.90	0.82

Table 3.11 Empirical models based on four variables correlation along with statistical errors for warm and humid climate zone

Models	Eq. No.	Equations	MPE (%)	MBE (%)	SSRE (%)	RSE (%)	RMSE (%)	t-stat	r	R^2
Models based on four variables correlation	3.90	$\frac{H_g}{H_o} = 0.467 + 0.054\left(\frac{S}{S_o}\right) + 0.004\left(\frac{T_m}{T_o}\right) + 0.003\left(\frac{WS_m}{WS_0}\right) - 0.329\left(\frac{H_d}{H_g}\right)$	1.31	0.00	0.61	0.11	0.03	2.36	0.91	0.83
	3.91	$\frac{H_g}{H_o} = 0.236 + 0.276\left(\frac{S}{S_o}\right) + 0.004\left(\frac{T_m}{T_o}\right) - 0.001\left(\frac{RH_m}{RH_o}\right) - 0.008\left(\frac{RF_m}{RF_o}\right)$	0.29	-0.01	1.64	0.18	0.05	4.16	0.79	0.66
	3.92	$\frac{H_g}{H_o} = -1.644 + 0.285\left(\frac{S}{S_o}\right) - 0.001\left(\frac{RH_m}{RH_o}\right) - 0.007\left(\frac{RF_m}{RF_o}\right) + 0.002\left(\frac{P_m}{P_o}\right)$	2.39	0.00	1.03	0.15	0.05	4.38	0.79	0.65
	3.93	$\frac{H_g}{H_o} = -1.528 + 0.268\left(\frac{S}{S_o}\right) - 0.001\left(\frac{RH_m}{RH_o}\right) - 0.001\left(\frac{WS_m}{WS_0}\right) + 0.002\left(\frac{P_m}{P_o}\right)$	1.97	0.00	0.90	0.14	0.04	3.61	0.82	0.69
	3.94	$\frac{H_g}{H_o} = 0.530 + 0.048\left(\frac{S}{S_o}\right) + 0.004\left(\frac{T_m}{T_o}\right) - 0.001\left(\frac{RF_m}{RF_o}\right) - 0.330\left(\frac{H_d}{H_g}\right)$	0.48	0.00	0.54	0.11	0.04	2.50	0.91	0.82
	3.95	$\frac{H_g}{H_o} = 0.204 + 0.256\left(\frac{S}{S_o}\right) + 0.006\left(\frac{T_m}{T_o}\right) - 0.001\left(\frac{RH_m}{RH_o}\right) + 0.0001\left(\frac{WS_m}{WS_0}\right)$	2.38	0.00	1.47	0.17	0.04	3.62	0.82	0.69
	3.96	$\frac{H_g}{H_o} = 0.620 + 0.055\left(\frac{S}{S_o}\right) - 0.001\left(\frac{RH_m}{RH_o}\right) + 0.003\left(\frac{WS_m}{WS_0}\right) - 0.338\left(\frac{H_d}{H_g}\right)$	1.29	0.00	0.54	0.11	0.03	2.40	0.91	0.82
	3.97	$\frac{H_g}{H_o} = 0.448 + 0.273\left(\frac{S}{S_o}\right) - 0.002\left(\frac{RH_m}{RH_o}\right) - 0.002\left(\frac{WS_m}{WS_0}\right) - 0.005\left(\frac{RF_m}{RF_o}\right)$	2.21	0.00	1.21	0.16	0.04	3.55	0.83	0.69

Table 3.12 Empirical models based on five variables correlation along with statistical errors for warm and humid climate zone

Models	Eq. No.	Equations	MPE (%)	MBE (%)	SSRE (%)	RSE (%)	RMSE (%)	t-stat	r	R^2
Models based on five variables correlation	3.98	$\frac{H_g}{H_o} = 0.44 + 0.074(\frac{S}{S_o}) + 0.004(\frac{T_m}{T_o}) - 0.001(\frac{RF_m}{RF_o}) + 0.01(\frac{P_m}{P_o}) - 0.3(\frac{H_d}{H_g})$	0.89	0.00	0.30	0.08	0.03	2.13	0.92	0.86
	3.99	$\frac{H_g}{H_o} = 0.163 + 0.070(\frac{S}{S_o}) + 0.005(\frac{T_m}{T_o}) + 0.001(\frac{RH_m}{RH_o}) + 0.001(\frac{P_m}{P_o}) - 0.3(\frac{H_d}{H_g})$	0.99	0.00	0.34	0.09	0.03	2.27	0.92	0.84
	3.100	$\frac{H_g}{H_o} = -3.2 + 0.25(\frac{S}{S_o}) + 0.007(\frac{T_m}{T_o}) + 0.0001(\frac{RH_m}{RH_o}) + 0.0001(\frac{WS_m}{WS_0}) + 0.003(\frac{P_m}{P_o})$	1.85	0.00	0.75	0.13	0.04	3.40	0.84	0.71
	3.101	$\frac{H_g}{H_o} = -2 + 0.275(\frac{S}{S_o}) + 0.005(\frac{T_m}{T_o}) + 0.0001(\frac{WS_m}{WS_0}) - 0.008(\frac{RF_m}{RF_o}) + 0.002(\frac{P_m}{P_o})$	1.62	0.00	0.63	0.12	0.04	3.27	0.84	0.73
	3.102	$\frac{H_g}{H_o} = 0.548+0.066(\frac{S}{S_o}) + 0.003(\frac{T_m}{T_o}) + 0.003(\frac{WS_m}{WS_0}) + 0.0001(\frac{P_m}{P_o}) - 0.307(\frac{H_d}{H_g})$	0.98	0.00	0.34	0.09	0.03	2.23	0.92	0.84
	3.103	$\frac{H_g}{H_o} = 0.508 + 0.05(\frac{S}{S_o}) + 0.003(\frac{T_m}{T_o}) + 0.003(\frac{RH_m}{RH_o}) + 0.0001(\frac{WS_m}{WS_0}) - 0.333(\frac{H_d}{H_g})$	1.40	0.00	0.54	0.11	0.03	2.42	0.91	0.83
	3.104	$\frac{H_g}{H_o} = 0.28 + 0.25(\frac{S}{S_o}) + 0.005(\frac{T_m}{T_o}) - 0.001(\frac{RH_m}{RH_o}) + 0.0001(\frac{WS_m}{WS_0}) - 0.004(\frac{RF_m}{RF_o})$	2.06	0.00	1.11	0.15	0.04	3.34	0.84	0.72
	3.105	$\frac{H_g}{H_o} = 0.564 + 0.059(\frac{S}{S_o}) + 0.003(\frac{T_m}{T_o}) - 0.001(\frac{RH_m}{RH_o}) - 0.001(\frac{RF_m}{RF_o}) - 0.323(\frac{H_d}{H_g})$	1.12	0.00	0.43	0.10	0.03	2.21	0.92	0.85

Table 3.13 Empirical models based on six and seven variables correlation along with statistical errors for warm and humid climate zone

Models	Eq. No.	Equations	MPE (%)	MBE (%)	SSRE (%)	RSE (%)	RMSE (%)	t-stat	r	R^2
Models based on six variables correlation	3.106	$\frac{H_g}{H_o}$ = -0.823 + 0.261$(\frac{S}{S_o})$ + 0.005$(\frac{T_m}{T_o})$ - 0.001$(\frac{RH_m}{RH_o})$ - 0.001$(\frac{WS_m}{WS_0})$ - 0.003$(\frac{RF_m}{RF_o})$ + 0.001$(\frac{P_m}{P_o})$	1.53	0.00	0.57	0.11	0.04	3.13	0.86	0.74
	3.107	$\frac{H_g}{H_o}$ = 0.627 + 0.076$(\frac{S}{S_o})$ + 0.004$(\frac{T_m}{T_o})$ + 0.0001$(\frac{RH_m}{RH_o})$ + 0.0001$(\frac{RF_m}{RF_o})$ + 0.0001$(\frac{P_m}{P_o})$ - 0.296$(\frac{H_d}{H_g})$	0.86	0.00	0.28	0.08	0.03	2.09	0.93	0.86
	3.108	$\frac{H_g}{H_o}$ = 0.938 + 0.073$(\frac{S}{S_o})$ + 0.002$(\frac{T_m}{T_o})$ + 0.003$(\frac{WS_m}{WS_0})$ + 0.001$(\frac{RF_m}{RF_o})$ + 0.0001$(\frac{P_m}{P_o})$ - 0.304$(\frac{H_d}{H_g})$	0.86	0.00	0.28	0.08	0.03	2.07	0.93	0.86
	3.109	$\frac{H_g}{H_o}$ = 0.558 + 0.054$(\frac{S}{S_o})$ + 0.002$(\frac{T_m}{T_o})$ + 0.0001$(\frac{RH_m}{RH_o})$+ 0.003$(\frac{WS_m}{WS_0})$ + 0.0001$(\frac{RF_m}{RF_o})$ - 0.325$(\frac{H_d}{H_g})$	1.10	0.00	0.43	0.10	0.03	2.16	0.92	0.85
Models based on seven variables correlation	3.110	$\frac{H_g}{H_o}$ = 0.945 + 0.072$(\frac{S}{S_o})$ + 0.003$(\frac{T_m}{T_o})$ + 0.0001$(\frac{RH_m}{RH_o})$ + 0.003$(\frac{WS_m}{WS_0})$ + 0.001$(\frac{RF_m}{RF_o})$ + 0.0001$(\frac{P_m}{P_o})$ - 0.300$(\frac{H_d}{H_g})$	1.93	0.00	0.56	0.11	0.04	2.55	0.93	0.87

From Table 3.9 - Table 3.13, the following can be briefly summarized:

(a) Warm and humid climate zone

Correlation based on seven variables has been observed to be the most suitable model on the basis of closeness parameters with correlation of coefficient (r = 0.93) obtained between the clearness index and relative sunshine duration, wind speed, ambient temperature, relative humidity, atmospheric pressure, amount of rainfall, cloudiness index.

The coefficient of determination has been observed to be (R^2 = 0.87) which mean 87% of the clearness index can be accounted by sunshine hours, ambient temperature, relative humidity, wind speed, amount of rainfall, atmospheric pressure and cloudiness index.

The relation between the parameters namely clearness index, relative sunshine duration, ambient temperature, relative humidity, wind speed, amount of rainfall, atmospheric pressure and cloudiness index is given by Eq. (3.110) expressed as:

$$\frac{H_g}{H_o} = 0.945 + 0.072\left(\frac{S}{S_o}\right) + 0.003\left(\frac{T_m}{T_o}\right) + 0.0001\left(\frac{RH_m}{RH_o}\right) +$$

$$0.003\left(\frac{WS_m}{WS_0}\right) + 0.001\left(\frac{RF_m}{RF_o}\right) + 0.0001\left(\frac{P_m}{P_o}\right) - 0.300\left(\frac{H_d}{H_g}\right) \quad (3.110)$$

Further, the estimated data values of global solar energy using the derived correlation have been compared with the measured data values as shown in Fig. 3.3(a).

Table 3.14 Empirical models based on one and two variables correlation along with statistical errors for hot and dry climate zone

Models	Eq. No.	Equations	MPE (%)	MBE (%)	SSRE (%)	RSE (%)	RMSE (%)	t-stat	r	R^2
Models based on one variable correlation	3.111	$\frac{H_g}{H_o} = 0.379 + 0.004\left(\frac{T_m}{T_o}\right)$	0.61	0.00	0.73	0.12	0.05	23.31	0.35	0.18
	3.112	$\frac{H_g}{H_o} = -5.495 + 0.006\left(\frac{P_m}{P_o}\right)$	5.51	0.02	11.23	0.30	0.14	39.13	0.21	0.07
	3.113	$\frac{H_g}{H_o} = 0.656 - 0.352\left(\frac{H_d}{H_g}\right)$	-0.04	0.00	0.35	0.08	0.03	6.38	0.71	0.54
	3.114	$\frac{H_g}{H_o} = 0.532 - 0.036\left(\frac{RF_m}{RF_o}\right)$	1.35	0.00	1.25	0.15	0.05	77.04	0.16	0.05
	3.115	$\frac{H_g}{H_o} = 0.636 - 0.002\left(\frac{RH_m}{RH_o}\right)$	0.78	0.00	0.84	0.13	0.05	26.33	0.36	0.17
	3.116	$\frac{H_g}{H_o} = 0.540 - 0.002\left(\frac{WS_m}{WS_0}\right)$	1.38	0.00	1.20	0.14	0.05	46.17	0.17	0.05
	3.117	$\frac{H_g}{H_o} = 0\ .375 + 0.214\left(\frac{S}{S_o}\right)$	-0.55	-0.01	0.85	0.12	0.05	8.67	0.51	0.33
Models based on two variables correlation	3.118	$\frac{H_g}{H_o} = 0.281 + 0.217\left(\frac{S}{S_o}\right) + 0.002\left(\frac{T_m}{T_o}\right)$	0.29	0.00	0.61	0.09	0.04	8.32	0.62	0.43
	3.119	$\frac{H_g}{H_o} = -3.532 + 0.225\left(\frac{S}{S_o}\right) + 0.004\left(\frac{P_m}{P_o}\right)$	0.58	0.00	0.82	0.12	0.04	9.65	0.57	0.38
	3.120	$\frac{H_g}{H_o} = 0.587 + 0.069\left(\frac{S}{S_o}\right) - 0.307\left(\frac{H_d}{H_g}\right)$	-0.08	0.00	0.34	0.08	0.03	5.67	0.70	0.55
	3.121	$\frac{H_g}{H_o} = 0.363 + 0.220\left(\frac{S}{S_o}\right) - 0.011\left(\frac{RF_m}{RF_o}\right)$	0.61	0.00	0.83	0.12	0.04	29.88	0.51	0.33
	3.122	$\frac{H_g}{H_o} = 0.436 + 0.195\left(\frac{S}{S_o}\right) - 0.001\left(\frac{RH_m}{RH_o}\right)$	0.45	0.00	0.72	0.11	0.04	17.19	0.55	0.38
	3.123	$\frac{H_g}{H_o} = 0.368 + 0.230\left(\frac{S}{S_o}\right) - 0.002\left(\frac{WS_m}{WS_0}\right)$	0.48	0.00	0.66	0.11	0.04	24.82	0.54	0.36

Table 3.15 Empirical models based on three variables correlation along with statistical errors for hot and dry climate zone

Models	Eq. No.	Equations	MPE (%)	MBE (%)	SSRE (%)	RSE (%)	RMSE (%)	t-stat	r	R^2
Models based on three variables correlation	3.124	$\frac{H_g}{H_o}$ = -1.797 + 0.055$(\frac{S}{S_o})$ + 0.002$(\frac{P_m}{P_o})$ - 0.306$(\frac{H_d}{H_g})$	-0.12	0.00	0.33	0.08	0.03	4.64	0.77	0.61
	3.125	$\frac{H_g}{H_o}$ = -3.093 + 0.192$(\frac{S}{S_o})$ - 0.001$(\frac{P_m}{P_o})$ + 0.004$(\frac{RH_m}{RH_o})$	0.42	0.00	0.70	0.11	0.04	8.76	0.60	0.41
	3.126	$\frac{H_g}{H_o}$ = -3.428 + 0.231$(\frac{S}{S_o})$ - 0.002$(\frac{WS_m}{WS_0})$ + 0.004$(\frac{P_m}{P_o})$	-0.35	-0.01	0.68	0.11	0.04	8.29	0.60	0.40
	3.127	$\frac{H_g}{H_o}$= -2.941 + 0.206$(\frac{S}{S_o})$ + 0.003$(\frac{T_m}{T_o})$ + 0.003$(\frac{P_m}{P_o})$	0.24	0.00	0.59	0.10	0.04	7.31	0.65	0.46
	3.128	$\frac{H_g}{H_o}$ = 0.541 + 0.073$(\frac{S}{S_o})$ + 0.001$(\frac{T_m}{T_o})$ - 0.293$(\frac{H_d}{H_g})$	-0.14	0.00	0.30	0.08	0.03	4.85	0.77	0.62
	3.129	$\frac{H_g}{H_o}$ = 0.363 + 0.204$(\frac{S}{S_o})$ + 0.001$(\frac{T_m}{T_o})$ - 0.001$(\frac{RH_m}{RH_o})$	0.25	0.00	0.59	0.10	0.04	7.43	0.65	0.46
	3.130	$\frac{H_g}{H_o}$ = 0.289 + 0.208$(\frac{S}{S_o})$ + 0.002$(\frac{T_m}{T_o})$ - 0.012$(\frac{RF_m}{RF_o})$	0.27	0.00	0.60	0.10	0.04	8.20	0.63	0.44
	3.131	$\frac{H_g}{H_o}$ = 0.312 + 0.218$(\frac{S}{S_o})$ + 0.001$(\frac{T_m}{T_o})$ - 0.002$(\frac{WS_m}{WS_0})$	0.19	0.00	0.48	0.10	0.04	7.80	0.64	0.45
	3.132	$\frac{H_g}{H_o}$ = 0.630 + 0.056$(\frac{S}{S_o})$ - 0.001$(\frac{RH_m}{RH_o})$ - 0.306$(\frac{H_d}{H_g})$	-0.18	0.00	0.29	0.07	0.03	5.49	0.75	0.60
	3.133	$\frac{H_g}{H_o}$ = 0.459 + 0.196$(\frac{S}{S_o})$ - 0.001$(\frac{RH_m}{RH_o})$ - 0.002$(\frac{WS_m}{WS_0})$	0.29	0.00	0.53	0.10	0.04	16.05	0.58	0.40
	3.134	$\frac{H_g}{H_o}$ = -3.445 + 0.219$(\frac{S}{S_o})$ - 0.009$(\frac{RF_m}{RF_o})$ + 0.004$(\frac{P_m}{P_o})$	0.57	0.00	0.82	0.11	0.04	9.59	0.57	0.38
	3.135	$\frac{H_g}{H_o}$ = 0.606 + 0.051$(\frac{S}{S_o})$ - 0.014$(\frac{RF_m}{RF_o})$ - 0.315$(\frac{H_d}{H_g})$	-0.11	0.00	0.32	0.08	0.03	5.68	0.75	0.59
	3.136	$\frac{H_g}{H_o}$ = 0.442 + 0.192$(\frac{S}{S_o})$ - 0.001$(\frac{RF_m}{RF_o})$ + 0.002$(\frac{RH_m}{RH_o})$	0.43	0.00	0.70	0.11	0.04	17.04	0.56	0.38
	3.137	$\frac{H_g}{H_o}$ = 0.374 + 0.226$(\frac{S}{S_o})$ - 0.002$(\frac{RF_m}{RF_o})$ - 0.005$(\frac{WS_m}{WS_0})$	0.45	0.00	0.63	0.08	0.04	24.68	0.55	0.37
	3.138	$\frac{H_g}{H_o}$ = 0.591 + 0.070$(\frac{S}{S_o})$ - 0.001$(\frac{WS_m}{WS_0})$ - 0.310$(\frac{H_d}{H_g})$	-0.10	0.00	0.32	0.08	0.03	5.62	0.75	0.59

Table 3.16 Empirical models based on four variables correlation along with statistical errors for hot and dry climate zone

Models	Eq. No.	Equations	MPE (%)	MBE (%)	SSRE (%)	RSE (%)	RMSE (%)	t-stat	r	R^2
Models based on four variables correlation	3.139	$\frac{H_g}{H_o} = 0.543 + 0.067\left(\frac{S}{S_o}\right) + 0.001\left(\frac{T_m}{T_o}\right) + 0.0001\left(\frac{WS_m}{WS_0}\right) - 0.305\left(\frac{H_d}{H_g}\right)$	-0.13	0.00	0.30	0.08	0.03	4.76	0.77	0.62
	3.140	$\frac{H_g}{H_o} = 0.362 + 0.201\left(\frac{S}{S_o}\right) + 0.01\left(\frac{T_m}{T_o}\right) - 0.001\left(\frac{RH_m}{RH_o}\right) - 0.004\left(\frac{RF_m}{RF_o}\right)$	0.24	0.00	0.58	0.10	0.04	7.29	0.65	0.47
	3.141	$\frac{H_g}{H_o} = -2.223 + 0.195\left(\frac{S}{S_o}\right) - 0.001\left(\frac{RH_m}{RH_o}\right) + 0.0001\left(\frac{RF_m}{RF_o}\right) + 0.003\left(\frac{P_m}{P_o}\right)$	0.42	-0.01	0.74	0.11	0.04	9.15	0.58	0.38
	3.142	$\frac{H_g}{H_o} = -2.967 + 0.195\left(\frac{S}{S_o}\right) - 0.001\left(\frac{RH_m}{RH_o}\right) + 0.0001\left(\frac{WS_m}{WS_0}\right) + 0.003\left(\frac{P_m}{P_o}\right)$	7.10	0.02	3.69	0.17	0.06	7.67	0.60	0.40
	3.143	$\frac{H_g}{H_o} = 0.684 + 0.060\left(\frac{S}{S_o}\right) - 0.002\left(\frac{T_m}{T_o}\right) - 0.001\left(\frac{RH_m}{RH_o}\right) - 0.305\left(\frac{H_d}{H_g}\right)$	-0.19	0.00	0.28	0.06	0.03	4.52	0.78	0.63
	3.144	$\frac{H_g}{H_o} = 0.466 + 0.207\left(\frac{S}{S_o}\right) - 0.002\left(\frac{T_m}{T_o}\right) - 0.001\left(\frac{RH_m}{RH_o}\right) - 0.001\left(\frac{WS_m}{WS_0}\right)$	0.15	0.00	0.46	0.09	0.04	5.81	0.66	0.48
	3.145	$\frac{H_g}{H_o} = 0.637 + 0.057\left(\frac{S}{S_o}\right) - 0.001\left(\frac{RH_m}{RH_o}\right) - 0.001\left(\frac{WS_m}{WS_0}\right) - 0.304\left(\frac{H_d}{H_g}\right)$	-0.20	0.00	0.27	0.07	0.03	5.31	0.76	0.61
	3.146	$\frac{H_g}{H_o} = 0.464 + 0.194\left(\frac{S}{S_o}\right) - 0.001\left(\frac{RH_m}{RH_o}\right) - 0.002\left(\frac{WS_m}{WS_0}\right) + 0.003\left(\frac{RF_m}{RF_o}\right)$	0.26	0.00	0.51	0.10	0.04	15.88	0.59	0.41

Table 3.17 Empirical models based on five variables correlation along with statistical errors for hot and dry climate zone

Models	Eq. No.	Equations	MPE (%)	MBE (%)	SSRE (%)	RSE (%)	RMSE (%)	t-stat	r	R^2
Models based on five variables correlation	3.147	$\frac{H_g}{H_o}$ = -1.289 + 0.042$(\frac{S}{S_o})$ + 0.001$(\frac{T_m}{T_o})$ - 0.013$(\frac{RF_m}{RF_o})$ + 0.002$(\frac{P_m}{P_o})$ - 0.291$(\frac{H_d}{H_g})$	-0.20	0.00	0.28	0.07	0.03	4.22	0.79	0.65
	3.148	$\frac{H_g}{H_o}$ = -1.2 + 0.049$(\frac{S}{S_o})$ - 0.001$(\frac{T_m}{T_o})$ - 0.001$(\frac{RH_m}{RH_o})$ + 0.002$(\frac{P_m}{P_o})$ - 0.296$(\frac{H_d}{H_g})$	-0.21	0.00	0.28	0.07	0.03	4.11	0.80	0.65
	3.149	$\frac{H_g}{H_o}$ = -2.16 + 0.18$(\frac{S}{S_o})$ + 0.0001$(\frac{T_m}{T_o})$ - 0.001$(\frac{RH_m}{RH_o})$ - 0.002$(\frac{WS_m}{WS_0})$ + 0.003$(\frac{P_m}{P_o})$	0.10	-0.01	0.48	0.09	0.04	6.33	0.69	0.49
	3.150	$\frac{H_g}{H_o}$ = -2.269 + 0.207$(\frac{S}{S_o})$ + 0.002$(\frac{T_m}{T_o})$ - 0.002$(\frac{WS_m}{WS_0})$ - 0.009$(\frac{RF_m}{RF_o})$ + 0.003$(\frac{P_m}{P_o})$	0.13	0.00	0.44	0.09	0.04	6.55	0.68	0.49
	3.151	$\frac{H_g}{H_o}$ = -1.78 + 0.051$(\frac{S}{S_o})$ + 0.001$(\frac{T_m}{T_o})$ + 0.0001$(\frac{WS_m}{WS_0})$ + 0.002$(\frac{P_m}{P_o})$ - 0.299$(\frac{H_d}{H_g})$	-0.19	0.00	0.29	0.07	0.03	4.24	0.79	0.64
	3.152	$\frac{H_g}{H_o}$ = 0.712 + 0.057$(\frac{S}{S_o})$ - 0.002$(\frac{T_m}{T_o})$ - 0.001$(\frac{RH_m}{RH_o})$ + 0.0001$(\frac{WS_m}{WS_0})$ - 0.310$(\frac{H_d}{H_g})$	-0.21	0.00	0.27	0.07	0.03	4.44	0.78	0.64
	3.153	$\frac{H_g}{H_o}$ = 0.469 + 0.203$(\frac{S}{S_o})$ - 0.002$(\frac{T_m}{T_o})$ - 0.001$(\frac{RH_m}{RH_o})$ - 0.002$(\frac{WS_m}{WS_0})$ - 0.003$(\frac{RF_m}{RF_o})$	0.13	0.00	0.44	0.09	0.04	6.83	0.67	0.49
	3.154	$\frac{H_g}{H_o}$ = 0.677 + 0.085$(\frac{S}{S_o})$ - 0.002$(\frac{T_m}{T_o})$ - 0.001$(\frac{RH_m}{RH_o})$ - 0.011$(\frac{RF_m}{RF_o})$ - 0.301$(\frac{H_d}{H_g})$	-0.19	0.00	0.28	0.08	0.03	4.46	0.78	0.64

Table 3.18 Empirical models based on six and seven variables correlation along with statistical errors for hot and dry climate zone

Models	**Eq. No.**	**Equations**	**MPE (%)**	**MBE (%)**	**SSRE (%)**	**RSE (%)**	**RMSE (%)**	**t-stat**	**r**	**R^2**
Models based on six variables correlation	3.155	$\frac{H_g}{H_o}$ = -2.364 + 0.194$(\frac{S}{S_o})$ + 0.0001$(\frac{T_m}{T_o})$ - 0.001$(\frac{RH_m}{RH_o})$ - 0.002$(\frac{WS_m}{WS_0})$ - 0.005$(\frac{RF_m}{RF_o})$ + 0.003$(\frac{P_m}{P_o})$	0.10	0.00	0.43	0.09	0.04	5.96	0.70	0.52
	3.156	$\frac{H_g}{H_o}$ = -1.087 + 0.036$(\frac{S}{S_o})$ - 0.001$(\frac{T_m}{T_o})$ - 0.001$(\frac{RH_m}{RH_o})$ - 0.011$(\frac{RF_m}{RF_o})$ + 0.002$(\frac{P_m}{P_o})$ - 0.299$(\frac{H_d}{H_g})$	-0.22	0.00	0.27	0.07	0.03	4.07	0.80	0.66
	3.157	$\frac{H_g}{H_o}$ = -1.510 + 0.038$(\frac{S}{S_o})$ + 0.001$(\frac{T_m}{T_o})$ + 0.0001$(\frac{WS_m}{WS_0})$ - 0.013$(\frac{RF_m}{RF_o})$ + 0.002$(\frac{P_m}{P_o})$ - 0.302$(\frac{H_d}{H_g})$	-0.21	0.00	0.28	0.07	0.03	4.17	0.79	0.65
	3.158	$\frac{H_g}{H_o}$ = 0.734 + 0.043$(\frac{S}{S_o})$ - 0.003$(\frac{T_m}{T_o})$ - 0.001$(\frac{RH_m}{RH_o})$ + 0.0001$(\frac{WS_m}{WS_0})$ - 0.011$(\frac{RF_m}{RF_o})$ - 0.316$(\frac{H_d}{H_g})$	-0.22	0.00	0.27	0.07	0.03	4.39	0.79	0.65
Models based on seven variables correlation	3.159	$\frac{H_g}{H_o}$ = -1.087 + 0.034$(\frac{S}{S_o})$ - 0.002$(\frac{T_m}{T_o})$ - 0.001$(\frac{RH_m}{RH_o})$ - 0.001$(\frac{WS_m}{WS_0})$ - 0.011$(\frac{RF_m}{RF_o})$ + 0.002$(\frac{P_m}{P_o})$ - 0.305$(\frac{H_d}{H_g})$	-0.36	-0.01	0.28	0.08	0.03	3.77	0.79	0.64

From Table 3.14 - Table 3.18, the following can be briefly summarized:

(b) Hot and dry climate zone

Correlation based on seven variables has been observed to be the most suitable model on the basis of closeness parameters with correlation of coefficient (r = 0.79) obtained between the clearness index and relative sunshine duration, wind speed, ambient temperature, relative humidity, atmospheric pressure, amount of rainfall, cloudiness index.

The coefficient of determination has been observed to be (R^2 = 0.64) which mean 64% of the clearness index can be accounted by sunshine hours, ambient temperature, relative humidity, wind speed, amount of rainfall, atmospheric pressure and cloudiness index.

The relation between the parameters namely clearness index, relative sunshine duration, ambient temperature, relative humidity, wind speed, amount of rainfall, atmospheric pressure and cloudiness index is given by Eq. (3.159) expressed as:

$$\frac{H_g}{H_o} = -1.087 + 0.034\left(\frac{S}{S_o}\right) - 0.002\left(\frac{T_m}{T_o}\right) - 0.001\left(\frac{RH_m}{RH_o}\right) -$$

$$0.001\left(\frac{WS_m}{WS_0}\right) - 0.011\left(\frac{RF_m}{RF_o}\right) + 0.002\left(\frac{P_m}{P_o}\right) - 0.305\left(\frac{H_d}{H_g}\right) \quad (3.159)$$

Further, the estimated data values of global solar energy using the derived correlation have been compared with the measured data values as shown in Fig. 3.3(b).

Table 3.19 Empirical models based on one and two variables correlation along with statistical errors for composite climate zone

Models	Eq. No.	Equations	MPE (%)	MBE (%)	SSRE (%)	RSE (%)	RMSE (%)	t-stat	r	R^2
Models based on one variable correlation	3.160	$\frac{H_g}{H_o} = 0.360 + 0.003(\frac{T_m}{T_o})$	1.67	0.00	0.58	0.13	0.05	31.70	0.30	0.13
	3.161	$\frac{H_g}{H_o} = 1.501 - 0.001(\frac{P_m}{P_o})$	1.98	0.00	0.73	0.14	0.06	31.48	0.26	0.09
	3.162	$\frac{H_g}{H_o} = 0.670 - 0.405(\frac{H_d}{H_g})$	0.67	0.00	0.23	0.08	0.03	4.28	0.78	0.62
	3.163	$\frac{H_g}{H_o} = 0.491 - 0.053(\frac{RF_m}{RF_o})$	1.67	0.00	0.60	0.13	0.05	24.80	0.39	0.21
	3.164	$\frac{H_g}{H_o} = 0.692 - 0.003(\frac{RH_m}{RH_o})$	1.43	0.00	0.47	0.12	0.05	14.42	0.46	0.25
	3.165	$\frac{H_g}{H_o} = 0.487 + 0.001(\frac{WS_m}{WS_0})$	1.80	0.00	0.63	0.13	0.06	38.18	0.27	0.11
	3.166	$\frac{H_g}{H_o} = 0.367 + 0.205(\frac{S}{S_o})$	1.24	0.00	0.46	0.08	0.04	7.86	0.59	0.40
Models based on two variables correlation	3.167	$\frac{H_g}{H_o} = 25.4855 + 0.307(\frac{S}{S_o}) + 0.23(\frac{T_m}{T_o})$	0.48	0.76	0.00	0.36	0.10	0.04	0.20	0.62
	3.168	$\frac{H_g}{H_o} = 1.580 + 0.18(\frac{S}{S_o}) - 0.001(\frac{P_m}{P_o})$	0.90	0.00	0.30	0.09	0.04	7.10	0.63	0.43
	3.169	$\frac{H_g}{H_o} = 0.4597 + 0.625(\frac{S}{S_o}) + 0.055(\frac{H_d}{H_g})$	0.49	0.59	0.00	0.19	0.07	0.03	0.63	0.81
	3.170	$\frac{H_g}{H_o} = 0.397 + 0.176(\frac{S}{S_o}) - 0.028(\frac{RF_m}{RF_o})$	0.87	0.00	0.29	0.09	0.04	7.77	0.62	0.43
	3.171	$\frac{H_g}{H_o} = 0.483 + 0.155(\frac{S}{S_o}) - 0.001(\frac{RH_m}{RH_o})$	0.88	0.00	0.29	0.09	0.04	7.67	0.63	0.44
	3.172	$\frac{H_g}{H_o} = 0.391 + 0.177(\frac{S}{S_o}) + 0.001(\frac{WS_m}{WS_0})$	0.84	0.00	0.26	0.09	0.04	7.65	0.60	0.45

Table 3.20 Empirical models based on three variables correlation along with statistical errors for composite climate zone

Models	Eq. No.	Equations	MPE (%)	MBE (%)	SSRE (%)	RSE (%)	RMSE (%)	t-stat	r	R^2
Models based on three variables correlation	3.173	$\frac{H_g}{H_o} = 0.527 + 0.131\left(\frac{S}{S_o}\right) + 0.0001\left(\frac{P_m}{P_o}\right) - 0.278\left(\frac{H_d}{H_g}\right)$	0.58	0.00	0.18	0.08	0.03	4.76	0.76	0.59
	3.174	$\frac{H_g}{H_o} = 0.590 + 0.153\left(\frac{S}{S_o}\right) - 0.001\left(\frac{P_m}{P_o}\right) + 0.001\left(\frac{RH_m}{RH_o}\right)$	0.84	0.00	0.27	0.09	0.04	6.35	0.67	0.48
	3.175	$\frac{H_g}{H_o} = 1.615 + 0.172\left(\frac{S}{S_o}\right) + 0.001\left(\frac{WS_m}{WS_0}\right) - 0.001\left(\frac{P_m}{P_o}\right)$	0.80	0.00	0.26	0.09	0.04	6.42	0.66	0.47
	3.176	$\frac{H_g}{H_o} = 2.312 + 0.177\left(\frac{S}{S_o}\right) - 0.002\left(\frac{T_m}{T_o}\right) - 0.002\left(\frac{P_m}{P_o}\right)$	0.86	0.00	0.28	0.09	0.04	6.21	0.67	0.47
	3.177	$\frac{H_g}{H_o} = 0.589 + 0.138\left(\frac{S}{S_o}\right) - 0.004\left(\frac{T_m}{T_o}\right) - 0.301\left(\frac{H_d}{H_g}\right)$	0.56	0.00	0.18	0.07	0.03	4.21	0.77	0.61
	3.178	$\frac{H_g}{H_o} = 0.584 + 0.157\left(\frac{S}{S_o}\right) - 0.004\left(\frac{T_m}{T_o}\right) - 0.002\left(\frac{RH_m}{RH_o}\right)$	0.81	0.00	0.26	0.09	0.04	6.03	0.69	0.50
	3.179	$\frac{H_g}{H_o} = 0.449 + 0.174\left(\frac{S}{S_o}\right) + 0.003\left(\frac{T_m}{T_o}\right) - 0.027\left(\frac{RF_m}{RF_o}\right)$	0.83	0.00	0.27	0.09	0.04	6.50	0.66	0.47
	3.180	$\frac{H_g}{H_o} = 0.432 + 0.131\left(\frac{S}{S_o}\right) - 0.002\left(\frac{T_m}{T_o}\right) - 0.001\left(\frac{WS_m}{WS_0}\right)$	-3.32	-0.02	0.56	0.12	0.06	11.07	0.57	0.39
	3.181	$\frac{H_g}{H_o} = 0.547 + 0.116\left(\frac{S}{S_o}\right) - 0.001\left(\frac{RH_m}{RH_o}\right) - 0.263\left(\frac{H_d}{H_g}\right)$	0.78	0.00	0.19	0.08	0.04	6.40	0.72	0.56
	3.182	$\frac{H_g}{H_o} = 0.485 + 0.148\left(\frac{S}{S_o}\right) - 0.001\left(\frac{RH_m}{RH_o}\right) + 0.001\left(\frac{WS_m}{WS_0}\right)$	0.78	0.00	0.25	0.09	0.04	6.62	0.67	0.48
	3.183	$\frac{H_g}{H_o} = 1.672 + 0.172\left(\frac{S}{S_o}\right) - 0.023\left(\frac{RF_m}{RF_o}\right) - 0.001\left(\frac{P_m}{P_o}\right)$	0.82	0.00	0.27	0.09	0.04	6.44	0.67	0.47
	3.184	$\frac{H_g}{H_o} = 0.498 + 0.131\left(\frac{S}{S_o}\right) - 0.020\left(\frac{RF_m}{RF_o}\right) - 0.258\left(\frac{H_d}{H_g}\right)$	0.57	0.00	0.18	0.08	0.03	5.09	0.74	0.58
	3.185	$\frac{H_g}{H_o} = 0.476 + 0.150\left(\frac{S}{S_o}\right) - 0.001\left(\frac{RF_m}{RF_o}\right) - 0.024\left(\frac{RH_m}{RH_o}\right)$	0.82	0.00	0.27	0.09	0.04	7.14	0.65	0.46
	3.186	$\frac{H_g}{H_o} = 0.398 + 0.168\left(\frac{S}{S_o}\right) + 0.001\left(\frac{RF_m}{RF_o}\right) - 0.024\left(\frac{WS_m}{WS_0}\right)$	0.77	0.00	0.25	0.09	0.04	6.96	0.65	0.47
	3.187	$\frac{H_g}{H_o} = 0.492 + 0.114\left(\frac{S}{S_o}\right) + 0.001\left(\frac{WS_m}{WS_0}\right) - 0.262\left(\frac{H_d}{H_g}\right)$	-1.70	-0.01	0.37	0.09	0.04	5.55	0.71	0.54

Table 3.21 Empirical models based on four variables correlation along with statistical errors for composite climate zone

Models	Eq. No.	Equations	MPE (%)	MBE (%)	SSRE (%)	RSE (%)	RMSE (%)	t-stat	r	R^2
Models based on four variables correlation	3.188	$\frac{H_g}{H_o} = 0.586 + 0.136\left(\frac{S}{S_o}\right) - 0.004\left(\frac{T_m}{T_o}\right) + 0.0001\left(\frac{WS_m}{WS_0}\right) - 0.284\left(\frac{H_d}{H_g}\right)$	0.51	0.00	0.16	0.07	0.03	4.33	0.78	0.62
	3.189	$\frac{H_g}{H_o} = 0.593 + 0.159\left(\frac{S}{S_o}\right) - 0.005\left(\frac{T_m}{T_o}\right) - 0.002\left(\frac{RH_m}{RH_o}\right) - 0.031\left(\frac{RF_m}{RF_o}\right)$	0.76	0.00	0.25	0.09	0.04	5.72	0.71	0.55
	3.190	$\frac{H_g}{H_o} = -0.038 + 0.159\left(\frac{S}{S_o}\right) - 0.001\left(\frac{RH_m}{RH_o}\right) - 0.023\left(\frac{RF_m}{RF_o}\right) + 0.001\left(\frac{P_m}{P_o}\right)$	0.78	0.00	0.26	0.09	0.04	6.00	0.69	0.50
	3.191	$\frac{H_g}{H_o} = 0.725 + 0.148\left(\frac{S}{S_o}\right) - 0.001\left(\frac{RH_m}{RH_o}\right) + 0.001\left(\frac{WS_m}{WS_0}\right) + 0.0001\left(\frac{P_m}{P_o}\right)$	0.74	0.00	0.24	0.08	0.04	5.71	0.70	0.51
	3.192	$\frac{H_g}{H_o} = 0.723 + 0.121\left(\frac{S}{S_o}\right) - 0.006\left(\frac{T_m}{T_o}\right) - 0.001\left(\frac{RH_m}{RH_o}\right) - 0.282\left(\frac{H_d}{H_g}\right)$	0.52	0.00	0.17	0.07	0.03	3.96	0.80	0.65
	3.193	$\frac{H_g}{H_o} = 0.611 + 0.160\left(\frac{S}{S_o}\right) - 0.005\left(\frac{T_m}{T_o}\right) - 0.002\left(\frac{RH_m}{RH_o}\right) + 0.0001\left(\frac{WS_m}{WS_0}\right)$	3.12	0.01	0.50	0.10	0.04	5.84	0.71	0.52
	3.194	$\frac{H_g}{H_o} = 0.549 + 0.113\left(\frac{S}{S_o}\right) - 0.001\left(\frac{RH_m}{RH_o}\right) + 0.001\left(\frac{WS_m}{WS_0}\right) - 0.249\left(\frac{H_d}{H_g}\right)$	0.65	0.00	0.17	0.07	0.03	4.61	0.77	0.62
	3.195	$\frac{H_g}{H_o} = 0.479 + 0.144\left(\frac{S}{S_o}\right) - 0.001\left(\frac{RH_m}{RH_o}\right) + 0.001\left(\frac{WS_m}{WS_0}\right) - 0.026\left(\frac{RF_m}{RF_o}\right)$	0.54	0.00	0.24	0.09	0.04	6.69	0.68	0.49

Table 3.22 Empirical models based on five variables correlation along with statistical errors for composite climate zone

Models	Eq. No.	Equations	MPE (%)	MBE (%)	SSRE (%)	RSE (%)	RMSE (%)	t-stat	r	R^2
Models based on five variables correlation	3.196	$\frac{H_g}{H_o}$ =1.421 + 0.141$(\frac{S}{S_o})$ - 0.005$(\frac{T_m}{T_o})$ - 0.014$(\frac{RF_m}{RF_o})$ + 0.0001$(\frac{P_m}{P_o})$ - 0.27$(\frac{H_d}{H_g})$	0.50	0.00	0.16	0.07	0.03	3.89	0.81	0.66
	3.197	$\frac{H_g}{H_o}$ = 0.733 + 0.127$(\frac{S}{S_o})$ - 0.006$(\frac{T_m}{T_o})$ - 0.001$(\frac{RH_m}{RH_o})$ + 0.0001$(\frac{P_m}{P_o})$ - 0.287$(\frac{H_d}{H_g})$	0.49	0.00	0.16	0.07	0.03	3.79	0.81	0.67
	3.198	$\frac{H_g}{H_o}$ = 0.5 + 0.16$(\frac{S}{S_o})$ - 0.004$(\frac{T_m}{T_o})$ -0.001$(\frac{RH_m}{RH_o})$ + 0.0001$(\frac{WS_m}{WS_0})$ + 0.0001$(\frac{P_m}{P_o})$	-0.4	-0.01	0.26	0.09	0.04	4.67	0.72	0.55
	3.199	$\frac{H_g}{H_o}$ = 2.546 + 0.176$(\frac{S}{S_o})$ - 0.003$(\frac{T_m}{T_o})$ + 0.0001$(\frac{WS_m}{WS_0})$ - 0.026$(\frac{RF_m}{RF_o})$ - 0.002$(\frac{P_m}{P_o})$	0.69	0.00	0.22	0.08	0.04	5.30	0.72	0.54
	3.200	$\frac{H_g}{H_o}$ = 1.558 + 0.144$(\frac{S}{S_o})$ - 0.004$(\frac{T_m}{T_o})$ + 0.0001$(\frac{WS_m}{WS_0})$ - 0.001$(\frac{P_m}{P_o})$ - 0.294$(\frac{H_d}{H_g})$	0.49	0.00	0.16	0.07	0.03	3.94	0.80	0.65
	3.201	$\frac{H_g}{H_o}$ = 0.74 + 0.127$(\frac{S}{S_o})$ - 0.007$(\frac{T_m}{T_o})$ - 0.001$(\frac{RH_m}{RH_o})$ + 0.0001$(\frac{WS_m}{WS_0})$ - 0.268$(\frac{H_d}{H_g})$	0.47	0.00	0.15	0.13	0.03	3.82	0.81	0.67
	3.202	$\frac{H_g}{H_o}$ = 0.61 + 0.155$(\frac{S}{S_o})$ - 0.005$(\frac{T_m}{T_o})$ - 0.002$(\frac{RH_m}{RH_o})$ + 0.0001$(\frac{WS_m}{WS_0})$ - 0.031$(\frac{RF_m}{RF_o})$	0.69	0.00	0.22	0.08	0.04	5.24	0.73	0.55
	3.203	$\frac{H_g}{H_o}$ = 0.743 + 0.122$(\frac{S}{S_o})$ - 0.007$(\frac{T_m}{T_o})$ - 0.001$(\frac{RH_m}{RH_o})$ - 0.027$(\frac{RF_m}{RF_o})$ - 0.269$(\frac{H_d}{H_g})$	0.49	0.00	0.16	0.07	0.03	3.81	0.81	0.67

Table 3.23 Empirical models based on six and seven variables correlation along with statistical errors for composite climate zone

Models	Eq. No.	Equations	MPE (%)	MBE (%)	SSRE (%)	RSE (%)	RMSE (%)	t-stat	r	R^2
Models based on six variables correlation	3.204	$\frac{H_g}{H_o} = 1.370 + 0.155(\frac{S}{S_o}) - 0.004(\frac{T_m}{T_o}) - 0.002(\frac{RH_m}{RH_o}) + 0.0001(\frac{WS_m}{WS_0}) - 0.030(\frac{RF_m}{RF_o}) - 0.001(\frac{P_m}{P_o})$	0.65	0.00	0.21	0.08	0.04	4.80	0.75	0.58
	3.205	$\frac{H_g}{H_o} = 0.735 + 0.12(\frac{S}{S_o}) - 0.006(\frac{T_m}{T_o}) - 0.001(\frac{RH_m}{RH_o}) - 0.030(\frac{RF_m}{RF_o}) + 0.0001(\frac{P_m}{P_o}) - 0.274(\frac{H_d}{H_g})$	0.46	0.00	0.15	0.07	0.03	3.64	0.82	0.69
	3.206	$\frac{H_g}{H_o} = 1.920 + 0.140(\frac{S}{S_o}) - 0.005(\frac{T_m}{T_o}) + 0.0001(\frac{WS_m}{WS_0}) - 0.022(\frac{RF_m}{RF_o}) - 0.001(\frac{P_m}{P_o}) - 0.283(\frac{H_d}{H_g})$	0.45	0.00	0.15	0.07	0.03	3.72	0.82	0.68
	3.207	$\frac{H_g}{H_o} = 1.171 + 0.123(\frac{S}{S_o}) - 0.007(\frac{T_m}{T_o}) - 0.001(\frac{RH_m}{RH_o}) + 0.0001(\frac{WS_m}{WS_0}) - 0.029(\frac{RF_m}{RF_o}) - 0.261(\frac{H_d}{H_g})$	0.45	0.00	0.15	0.07	0.03	3.68	0.82	0.68
Models based on seven variables correlation	3.208	$\frac{H_g}{H_o} = 1.008 + 0.123(\frac{S}{S_o}) - 0.006(\frac{T_m}{T_o}) - 0.001(\frac{RH_m}{RH_o}) + 0.0001(\frac{WS_m}{WS_0}) - 0.028(\frac{RF_m}{RF_o}) + 0.0001(\frac{P_m}{P_o}) - 0.264(\frac{H_d}{H_g})$	0.42	0.00	0.14	0.07	0.03	3.48	0.83	0.71

From Table 3.19 - Table 3.23, the following can be briefly summarized:

(c) Composite climate zone

Correlation based on seven variables has been observed to be the most suitable model on the basis of closeness parameters with correlation of coefficient (r = 0.83) obtained between the clearness index and relative sunshine duration, wind speed, ambient temperature, relative humidity, atmospheric pressure, amount of rainfall, cloudiness index.

The coefficient of determination has been observed to be R^2 = 0.71 which mean 71% of the clearness index can be accounted by sunshine hours, ambient temperature, relative humidity, wind speed, amount of rainfall, atmospheric pressure and cloudiness index.

The relation between the parameters namely clearness index, relative sunshine duration, ambient temperature, relative humidity, wind speed, amount of rainfall, atmospheric pressure and cloudiness index is given by Eq. (3.208) expressed as:

$$\frac{H_g}{H_o} = 1.008 + 0.123\left(\frac{S}{S_o}\right) - 0.006\left(\frac{T_m}{T_o}\right) - 0.001\left(\frac{RH_m}{RH_o}\right) +$$

$$0.0001\left(\frac{WS_m}{WS_0}\right) - 0.028\left(\frac{RF_m}{RF_o}\right) + 0.0001\left(\frac{P_m}{P_o}\right) - 0.264\left(\frac{H_d}{H_g}\right) \quad (3.208)$$

Further, the estimated data values of global solar energy using the derived correlation have been compared with the measured data values as shown in Fig. 3.3(c).

Table 3.24 Empirical models based on one and two variables correlation along with statistical errors for moderate climate zone

Models	Eq. No.	Equations	MPE (%)	MBE (%)	SSRE (%)	RSE (%)	RMSE (%)	t-stat	r	R^2
Models based on one variable correlation	3.209	$\frac{H_g}{H_o} = 0.469 + 0.001(\frac{T_m}{T_o})$	1.90	-0.02	3.25	0.24	0.09	47.45	0.23	0.07
	3.210	$\frac{H_g}{H_o} = -1.954 + 0.003(\frac{P_m}{P_o})$	9.04	0.00	7.27	0.32	0.11	273.9	0.19	0.05
	3.211	$\frac{H_g}{H_o} = 0.591 - 0.324(\frac{H_d}{H_g})$	1.46	-0.02	2.85	0.22	0.08	27.28	0.47	0.30
	3.212	$\frac{H_g}{H_o} = 0.487 + 0.034(\frac{RF_m}{RF_o})$	2.27	-0.02	3.59	0.25	0.09	51.46	0.14	0.03
	3.213	$\frac{H_g}{H_o} = 0.611 - 0.002(\frac{RH_m}{RH_o})$	2.07	-0.02	3.42	0.25	0.09	37.80	0.25	0.09
	3.214	$\frac{H_g}{H_o} = 0.479 + 0.005(\frac{WS_m}{WS_0})$	1.97	-0.02	3.27	0.25	0.09	51.51	0.21	0.06
	3.215	$\frac{H_g}{H_o} = 0.156 + 0.281(\frac{S}{S_o})$	3.10	0.01	0.75	0.12	0.04	6.97	0.71	0.53
Models based on two variables correlation	3.216	$\frac{H_g}{H_o} = 0.160 + 0.268(\frac{S}{S_o}) + 0.005(\frac{T_m}{T_o})$	-0.15	-0.03	2.29	0.19	0.08	31.3	0.53	0.35
	3.217	$\frac{H_g}{H_o} = -0.011 + 0.292(\frac{S}{S_o}) + 0.0001(\frac{P_m}{P_o})$	-0.07	-0.03	2.43	0.19	0.08	9.80	0.56	0.36
	3.218	$\frac{H_g}{H_o} = 0.426 + 0.159(\frac{S}{S_o}) - 0.178(\frac{H_d}{H_g})$	-0.29	-0.03	2.17	0.18	0.07	19.8	0.58	0.41
	3.219	$\frac{H_g}{H_o} = 0.267 + 0.282(\frac{S}{S_o}) - 0.003(\frac{RF_m}{RF_o})$	0.06	-0.02	2.74	0.20	0.08	16.5	0.50	0.32
	3.220	$\frac{H_g}{H_o} = 0.369 + 0.249(\frac{S}{S_o}) - 0.001(\frac{RH_m}{RH_o})$	-0.01	-0.02	2.43	0.19	0.08	13.6	0.53	0.36
	3.221	$\frac{H_g}{H_o} = 0.273 + 0.277(\frac{S}{S_o}) + 0.003(\frac{WS_m}{WS_0})$	-0.07	-0.03	2.41	0.19	0.08	15.9	0.52	0.34

Table 3.25 Empirical models based on three variables correlation along with statistical errors for moderate climate zone

Models	Eq. No.	Equations	MPE (%)	MBE (%)	SSRE (%)	RSE (%)	RMSE (%)	t-stat	r	R^2
Models based on three variables correlation	3.222	$\frac{H_g}{H_o} = 0.439 + 0.222\left(\frac{S}{S_o}\right) + 0.0001\left(\frac{P_m}{P_o}\right) - 0.358\left(\frac{H_d}{H_g}\right)$	1.03	0.00	0.42	0.08	0.03	3.04	0.87	0.75
	3.223	$\frac{H_g}{H_o} = -0.435 + 0.377\left(\frac{S}{S_o}\right) - 0.002\left(\frac{P_m}{P_o}\right) + 0.001\left(\frac{RH_m}{RH_o}\right)$	1.26	0.00	0.52	0.09	0.03	4.43	0.77	0.61
	3.224	$\frac{H_g}{H_o} = 0.276 + 0.422\left(\frac{S}{S_o}\right) + 0.004\left(\frac{WS_m}{WS_0}\right) + 0.0001\left(\frac{P_m}{P_o}\right)$	1.17	0.00	0.61	0.10	0.04	4.91	0.75	0.59
	3.225	$\frac{H_g}{H_o} = -0.731 + 0.407\left(\frac{S}{S_o}\right) + 0.002\left(\frac{T_m}{T_o}\right) + 0.001\left(\frac{P_m}{P_o}\right)$	0.99	0.00	0.42	0.09	0.03	4.19	0.79	0.64
	3.226	$\frac{H_g}{H_o} = 0.467 + 0.214\left(\frac{S}{S_o}\right) + 0.001\left(\frac{T_m}{T_o}\right) - 0.340\left(\frac{H_d}{H_g}\right)$	0.61	0.00	0.24	0.07	0.03	3.01	0.87	0.76
	3.227	$\frac{H_g}{H_o} = 0.211 + 0.369\left(\frac{S}{S_o}\right) + 0.003\left(\frac{T_m}{T_o}\right) - 0.001\left(\frac{RH_m}{RH_o}\right)$	0.37	0.00	0.88	0.10	0.04	3.65	0.75	0.64
	3.228	$\frac{H_g}{H_o} = 0.180 + 0.375\left(\frac{S}{S_o}\right) + 0.003\left(\frac{T_m}{T_o}\right) - 0.010\left(\frac{RF_m}{RF_o}\right)$	4.28	0.01	2.12	0.14	0.04	5.52	0.74	0.59
	3.229	$\frac{H_g}{H_o} = 0.158 + 0.397\left(\frac{S}{S_o}\right) + 0.003\left(\frac{T_m}{T_o}\right) - 0.004\left(\frac{WS_m}{WS_0}\right)$	1.02	0.00	0.43	0.09	0.03	4.23	0.79	0.63
	3.230	$\frac{H_g}{H_o} = 0.561 + 0.194\left(\frac{S}{S_o}\right) - 0.001\left(\frac{RH_m}{RH_o}\right) - 0.288\left(\frac{H_d}{H_g}\right)$	0.64	0.00	0.32	0.08	0.03	3.67	0.82	0.69
	3.231	$\frac{H_g}{H_o} = 0.390 + 0.375\left(\frac{S}{S_o}\right) - 0.002\left(\frac{RH_m}{RH_o}\right) + 0.002\left(\frac{WS_m}{WS_0}\right)$	1.31	0.00	0.55	0.09	0.03	4.46	0.76	0.61
	3.232	$\frac{H_g}{H_o} = -0.836 + 0.427\left(\frac{S}{S_o}\right) + 0.002\left(\frac{RF_m}{RF_o}\right) + 0.001\left(\frac{P_m}{P_o}\right)$	0.71	0.00	0.27	0.08	0.03	4.77	0.76	0.60
	3.233	$\frac{H_g}{H_o} = 0.502 + 0.216\left(\frac{S}{S_o}\right) + 0.001\left(\frac{RF_m}{RF_o}\right) - 0.353\left(\frac{H_d}{H_g}\right)$	0.41	0.00	0.14	0.06	0.03	3.01	0.87	0.76
	3.234	$\frac{H_g}{H_o} = 0.395 + 0.3\left(\frac{S}{S_o}\right) + 0.380\left(\frac{RF_m}{RF_o}\right) - 0.002\left(\frac{RH_m}{RH_o}\right)$	0.49	0.00	0.31	0.08	0.04	4.18	0.77	0.61
	3.235	$\frac{H_g}{H_o} = 0.219 + 0.415\left(\frac{S}{S_o}\right) + 0.004\left(\frac{RF_m}{RF_o}\right) + 0.004\left(\frac{WS_m}{WS_0}\right)$	0.73	0.00	0.29	0.08	0.03	4.78	0.76	0.60
	3.236	$\frac{H_g}{H_o} = 0.502 + 0.203\left(\frac{S}{S_o}\right) + 0.004\left(\frac{WS_m}{WS_0}\right) - 0.358\left(\frac{H_d}{H_g}\right)$	0.67	0.00	0.31	0.07	0.03	3.07	0.86	0.75

Table 3.26 Empirical models based on four variables correlation along with statistical errors for moderate climate zone

Models	Eq. No.	Equations	MPE (%)	MBE (%)	SSRE (%)	RSE (%)	RMSE (%)	t-stat	r	R^2
Models based on four variables correlation	3.237	$\frac{H_g}{H_o} = 0.457 + 0.2\left(\frac{S}{S_o}\right) + 0.001\left(\frac{T_m}{T_o}\right) + 0.004\left(\frac{WS_m}{WS_0}\right) - 0.343\left(\frac{H_d}{H_g}\right)$	0.58	0.00	0.24	0.07	0.03	2.90	0.87	0.77
	3.238	$\frac{H_g}{H_o} = 0.353 + 0.37\left(\frac{S}{S_o}\right) - 0.001\left(\frac{T_m}{T_o}\right) - 0.001\left(\frac{RH_m}{RH_o}\right) + 0.004\left(\frac{RF_m}{RF_o}\right)$	0.58	0.00	0.22	0.07	0.03	3.67	0.82	0.69
	3.239	$\frac{H_g}{H_o} = -0.697 + 0.381\left(\frac{S}{S_o}\right) - 0.002\left(\frac{RH_m}{RH_o}\right) + 0.020\left(\frac{RF_m}{RF_o}\right) + 0.001\left(\frac{P_m}{P_o}\right)$	0.61	0.00	0.24	0.08	0.03	4.14	0.79	0.65
	3.240	$\frac{H_g}{H_o} = 0.125 + 0.370\left(\frac{S}{S_o}\right) - 0.002\left(\frac{RH_m}{RH_o}\right) + 0.002\left(\frac{WS_m}{WS_0}\right) + 0.0001\left(\frac{P_m}{P_o}\right)$	1.25	0.00	0.52	0.09	0.03	4.29	0.77	0.62
	3.241	$\frac{H_g}{H_o} = 0.544 + 0.181\left(\frac{S}{S_o}\right) + 0.001\left(\frac{T_m}{T_o}\right) - 0.001\left(\frac{RH_m}{RH_o}\right) - 0.335\left(\frac{H_d}{H_g}\right)$	0.57	0.00	0.23	0.07	0.03	2.71	0.89	0.79
	3.242	$\frac{H_g}{H_o} = 0.253 + 0.36\left(\frac{S}{S_o}\right) + 0.002\left(\frac{T_m}{T_o}\right) - 0.001\left(\frac{RH_m}{RH_o}\right) + 0.003\left(\frac{WS_m}{WS_0}\right)$	0.94	0.00	0.40	0.08	0.03	3.79	0.81	0.67
	3.243	$\frac{H_g}{H_o} = 0.586 + 0.168\left(\frac{S}{S_o}\right) - 0.001\left(\frac{RH_m}{RH_o}\right) + 0.003\left(\frac{WS_m}{WS_0}\right) - 0.252\left(\frac{H_d}{H_g}\right)$	-1.7	-0.02	0.51	0.09	0.04	2.86	0.86	0.75
	3.244	$\frac{H_g}{H_o} = 0.385 + 0.374\left(\frac{S}{S_o}\right) - 0.002\left(\frac{RH_m}{RH_o}\right) + 0.003\left(\frac{WS_m}{WS_0}\right) + 0.022\left(\frac{RF_m}{RF_o}\right)$	0.49	0.00	0.30	0.08	0.03	4.09	0.78	0.62

Table 3.27 Empirical models based on five variables correlation along with statistical errors for moderate climate zone

Models	Eq. No.	Equations	MPE (%)	MBE (%)	SSRE (%)	RSE (%)	RMSE (%)	t-stat	r	R^2
Models based on five variables correlation	3.245	$\frac{H_g}{H_o} = 0.390 + 0.222\left(\frac{S}{S_o}\right) - 0.001\left(\frac{T_m}{T_o}\right) + 0.001\left(\frac{RF_m}{RF_o}\right) + 0.0001\left(\frac{P_m}{P_o}\right) - 0.339\left(\frac{H_d}{H_g}\right)$	0.35	0.00	0.12	0.06	0.02	2.74	0.89	0.79
	3.246	$\frac{H_g}{H_o} = 0.541 + 0.176\left(\frac{S}{S_o}\right) + 0.001\left(\frac{T_m}{T_o}\right) - 0.001\left(\frac{RH_m}{RH_o}\right) + 0.0001\left(\frac{P_m}{P_o}\right) - 0.339\left(\frac{H_d}{H_g}\right)$	0.54	0.00	0.22	0.06	0.02	2.61	0.88	0.80
	3.247	$\frac{H_g}{H_o} = -1.03 + 0.35\left(\frac{S}{S_o}\right) + 0.004\left(\frac{T_m}{T_o}\right) - 0.001\left(\frac{RH_m}{RH_o}\right) + 0.002\left(\frac{WS_m}{WS_0}\right) + 0.001\left(\frac{P_m}{P_o}\right)$	0.95	0.00	0.41	0.09	0.03	3.39	0.84	0.71
	3.248	$\frac{H_g}{H_o} = -0.5 + 0.3\left(\frac{S}{S_o}\right) + 0.0001\left(\frac{T_m}{T_o}\right) + 0.004\left(\frac{WS_m}{WS_0}\right) + 0.002\left(\frac{RF_m}{RF_o}\right) + 0.001\left(\frac{P_m}{P_o}\right)$	0.62	0.00	0.23	0.07	0.03	3.82	0.81	0.68
	3.249	$\frac{H_g}{H_o} = 1.083 + 0.199\left(\frac{S}{S_o}\right) + 0.002\left(\frac{T_m}{T_o}\right) + 0.003\left(\frac{WS_m}{WS_0}\right) - 0.001\left(\frac{P_m}{P_o}\right) - 0.342\left(\frac{H_d}{H_g}\right)$	0.08	0.00	0.23	0.07	0.03	2.80	0.88	0.78
	3.250	$\frac{H_g}{H_o} = 0.498 + 0.165\left(\frac{S}{S_o}\right) + 0.002\left(\frac{T_m}{T_o}\right) - 0.001\left(\frac{RH_m}{RH_o}\right) + 0.003\left(\frac{WS_m}{WS_0}\right) - 0.343\left(\frac{H_d}{H_g}\right)$	0.32	0.00	0.30	0.07	0.03	2.55	0.87	0.77
	3.251	$\frac{H_g}{H_o} = 0.368 + 0.36\left(\frac{S}{S_o}\right) - 0.001\left(\frac{T_m}{T_o}\right) - 0.001\left(\frac{RH_m}{RH_o}\right) + 0.003\left(\frac{WS_m}{WS_0}\right) + 0.006\left(\frac{RF_m}{RF_o}\right)$	3.75	0.02	0.61	0.10	0.05	5.33	0.80	0.67
	3.252	$\frac{H_g}{H_o} = 0.589 + 0.185\left(\frac{S}{S_o}\right) - 0.001\left(\frac{T_m}{T_o}\right) - 0.001\left(\frac{RH_m}{RH_o}\right) + 0.002\left(\frac{RF_m}{RF_o}\right) - 0.333\left(\frac{H_d}{H_g}\right)$	0.34	0.00	0.12	0.05	0.02	2.57	0.90	0.81

Table 3.28 Empirical models based on six and seven variables correlation along with statistical errors for moderate climate zone

Models	Eq. No.	Equations	MPE (%)	MBE (%)	SSRE (%)	RSE (%)	RMSE (%)	t-stat	r	R^2
Models based on six variables correlation	3.253	$\frac{H_g}{H_o}$ = -1.188 + 0.359$(\frac{S}{S_o})$ - 0.001$(\frac{T_m}{T_o})$ - 0.001$(\frac{RH_m}{RH_o})$ + 0.003$(\frac{WS_m}{WS_0})$ + 0.005$(\frac{RF_m}{RF_o})$ + 0.002$(\frac{P_m}{P_o})$	0.53	0.00	0.21	0.07	0.03	3.46	0.84	0.71
	3.254	$\frac{H_g}{H_o}$ = 0.258 + 0.183$(\frac{S}{S_o})$ + 0.0001$(\frac{T_m}{T_o})$ - 0.001$(\frac{RH_m}{RH_o})$ + 0.003$(\frac{RF_m}{RF_o})$ + 0.0001$(\frac{P_m}{P_o})$ - 0.336$(\frac{H_d}{H_g})$	0.31	0.00	0.11	0.05	0.02	2.47	0.90	0.82
	3.255	$\frac{H_g}{H_o}$ = 0.9 + 0.21$(\frac{S}{S_o})$ + 0.0001$(\frac{T_m}{T_o})$ + 0.004$(\frac{WS_m}{WS_0})$ + 0.002$(\frac{RF_m}{RF_o})$ + 0.0001$(\frac{P_m}{P_o})$ - 0.340$(\frac{H_d}{H_g})$	0.33	0.00	0.12	0.05	0.02	2.64	0.89	0.80
	3.256	$\frac{H_g}{H_o}$ = 0.545 + 0.17$(\frac{S}{S_o})$ + 0.0001$(\frac{T_m}{T_o})$ - 0.001$(\frac{RH_m}{RH_o})$ + 0.003$(\frac{WS_m}{WS_0})$ + 0.003$(\frac{RF_m}{RF_o})$ - 0.339$(\frac{H_d}{H_g})$	0.32	0.00	0.12	0.05	0.02	2.46	0.90	0.82
Models based on seven variables correlation	3.257	$\frac{H_g}{H_o}$ = 0.447 + 0.17$(\frac{S}{S_o})$ + 0.0001$(\frac{T_m}{T_o})$ - 0.001$(\frac{RH_m}{RH_o})$ + 0.003$(\frac{WS_m}{WS_0})$ + 0.004$(\frac{RF_m}{RF_o})$ + 0.0001$(\frac{P_m}{P_o})$ - 0.340$(\frac{H_d}{H_g})$	0.25	0.02	4.78	0.05	0.05	4.80	0.90	0.81

From Table 3.24 - Table 3.28, the following can be briefly summarized:

(d) Moderate climate zone

Correlation based on seven variables has been observed to be the most suitable model on the basis of closeness parameters with correlation of coefficient (r = 0.90) obtained between the clearness index and relative sunshine duration, wind speed, ambient temperature, relative humidity, atmospheric pressure, amount of rainfall, cloudiness index.

The coefficient of determination has been observed to be R^2 = 0.81 which mean 81% of the clearness index can be accounted by sunshine hours, ambient temperature, relative humidity, wind speed, amount of rainfall, atmospheric pressure and cloudiness index.

The relation between the parameters namely clearness index, relative sunshine duration, ambient temperature, relative humidity, wind speed, amount of rainfall, atmospheric pressure and cloudiness index is given by Eq. (3.257) expressed as:

$$\frac{H_g}{H_o} = 0.447 + 0.17\left(\frac{S}{S_o}\right) + 0.0001\left(\frac{T_m}{T_o}\right) - 0.001\left(\frac{RH_m}{RH_o}\right) +$$

$$0.003\left(\frac{WS_m}{WS_0}\right) + 0.004\left(\frac{RF_m}{RF_o}\right) + 0.0001\left(\frac{P_m}{P_o}\right) - 0.340\left(\frac{H_d}{H_g}\right) \quad (3.257)$$

Further, the estimated data values of global solar energy using the derived correlation have been compared with the measured data values as shown in Fig. 3.3(d).

Table 3.29 Empirical models based on one and two variables correlation along with statistical errors for cold and cloudy climate zone

Models	Eq. No.	Equations	MPE (%)	MBE (%)	SSRE (%)	RSE (%)	RMSE (%)	t-stat	r	R^2
Models based on one variable correlation	3.258	$\frac{H_g}{H_o}$ = -0.121 + 0.032$(\frac{T_m}{T_o})$	6.77	0.00	3.08	0.30	0.09	17.23	0.41	0.21
	3.259	$\frac{H_g}{H_o}$ = 4.069 + 0.005$(\frac{P_m}{P_o})$	9.77	0.00	6.37	0.41	0.10	52.24	0.19	0.06
	3.260	$\frac{H_g}{H_o}$ = 0.729 - 0.563$(\frac{H_d}{H_g})$	4.75	0.00	2.44	0.25	0.07	8.43	0.70	0.77
	3.261	$\frac{H_g}{H_o}$ = 0.453 - 0.007$(\frac{RF_m}{RF_o})$	8.33	0.00	4.83	0.35	0.10	32.65	0.30	0.13
	3.262	$\frac{H_g}{H_o}$ = 1.059 - 0.008$(\frac{RH_m}{RH_o})$	5.86	0.00	2.76	0.28	0.08	7.89	0.58	0.36
	3.263	$\frac{H_g}{H_o}$ = 0.396 + 0.013$(\frac{WS_m}{WS_0})$	8.78	0.00	5.59	0.39	0.10	110.60	0.22	0.09
	3.264	$\frac{H_g}{H_o}$ = 0.239 + 0.586$(\frac{S}{S_o})$	1.09	-0.01	1.73	0.20	0.07	12.52	0.67	0.49
Models based on two variables correlation	3.265	$\frac{H_g}{H_o}$ = 0.097 + 0.364$(\frac{S}{S_o})$ + 0.009$(\frac{T_m}{T_o})$	2.59	0.00	0.94	0.16	0.06	5.96	0.72	0.55
	3.266	$\frac{H_g}{H_o}$ = -2.025 + 0.375$(\frac{S}{S_o})$ + 0.003$(\frac{P_m}{P_o})$	3.47	0.00	1.47	0.18	0.07	5.98	0.69	0.51
	3.267	$\frac{H_g}{H_o}$ = 0.480 + 0.245$(\frac{S}{S_o})$ - 0.296$(\frac{H_d}{H_g})$	2.00	0.00	0.76	0.15	0.05	4.41	0.78	0.62
	3.268	$\frac{H_g}{H_o}$ = 0.257 + 0.372$(\frac{S}{S_o})$ + 0.001$(\frac{RF_m}{RF_o})$	3.29	0.00	1.34	0.18	0.07	6.05	0.70	0.52
	3.269	$\frac{H_g}{H_o}$ = 0.404 + 0.339$(\frac{S}{S_o})$ - 0.002$(\frac{RH_m}{RH_o})$	0.69	-0.01	1.09	0.17	0.06	5.60	0.73	0.56
	3.270	$\frac{H_g}{H_o}$ = 0.230 + 0.376$(\frac{S}{S_o})$ + 0.005$(\frac{WS_m}{WS_0})$	2.51	0.00	0.96	0.16	0.06	5.57	0.72	0.55

Table 3.30 Empirical models based on three variables correlation along with statistical errors for cold and cloudy climate zone

Models	Eq. No.	Equations	MPE (%)	MBE (%)	SSRE (%)	RSE (%)	RMSE (%)	t-stat	r	R^2
Models based on three variables correlation	3.271	$\frac{H_g}{H_o}$ = -1.645 + 0.246$(\frac{S}{S_o})$ + 0.003$(\frac{P_m}{P_o})$ - 0.287$(\frac{H_d}{H_g})$	1.92	0.00	0.71	0.14	0.05	4.21	0.79	0.64
	3.272	$\frac{H_g}{H_o}$ = -0.429 + 0.336$(\frac{S}{S_o})$ - 0.002$(\frac{P_m}{P_o})$ + 0.001$(\frac{RH_m}{RH_o})$	2.37	0.00	0.86	0.15	0.06	4.85	0.75	0.59
	3.273	$\frac{H_g}{H_o}$ = -1.734 + 0.375$(\frac{S}{S_o})$ + 0.005$(\frac{WS_m}{WS_0})$ + 0.002$(\frac{P_m}{P_o})$	2.52	0.00	0.92	0.16	0.06	5.23	0.74	0.57
	3.274	$\frac{H_g}{H_o}$ = -3.537 + 0.366$(\frac{S}{S_o})$ + 0.008$(\frac{T_m}{T_o})$ + 0.004$(\frac{P_m}{P_o})$	2.50	0.00	0.89	0.16	0.06	5.26	0.74	0.57
	3.275	$\frac{H_g}{H_o}$ = 0.412 + 0.253$(\frac{S}{S_o})$ + 0.003$(\frac{T_m}{T_o})$ - 0.270$(\frac{H_d}{H_g})$	1.84	0.00	0.66	0.13	0.05	4.25	0.79	0.64
	3.276	$\frac{H_g}{H_o}$ = 0.459 + 0.342$(\frac{S}{S_o})$ + 0.001$(\frac{T_m}{T_o})$ - 0.002$(\frac{RH_m}{RH_o})$	2.33	0.00	0.81	0.15	0.06	4.95	0.75	0.59
	3.277	$\frac{H_g}{H_o}$ = 0.122 + 0.363$(\frac{S}{S_o})$ + 0.008$(\frac{T_m}{T_o})$ + 0.001$(\frac{RF_m}{RF_o})$	2.47	0.00	0.91	0.16	0.06	5.40	0.73	0.57
	3.278	$\frac{H_g}{H_o}$ = 0.103 + 0.363$(\frac{S}{S_o})$ + 0.007$(\frac{T_m}{T_o})$ + 0.004$(\frac{WS_m}{WS_0})$	2.24	0.00	0.76	0.15	0.06	5.19	0.74	0.58
	3.279	$\frac{H_g}{H_o}$ = 0.605 + 0.221$(\frac{S}{S_o})$ - 0.002$(\frac{RH_m}{RH_o})$ - 0.226$(\frac{H_d}{H_g})$	1.87	0.00	0.66	0.14	0.05	4.11	0.79	0.65
	3.280	$\frac{H_g}{H_o}$ = 0.430 + 0.338$(\frac{S}{S_o})$ - 0.002$(\frac{RH_m}{RH_o})$ + 0.002$(\frac{WS_m}{WS_0})$	2.29	0.00	0.82	0.15	0.06	4.80	0.76	0.61
	3.281	$\frac{H_g}{H_o}$ = -2.620 + 0.371$(\frac{S}{S_o})$ + 0.0001$(\frac{RF_m}{RF_o})$ + 0.003$(\frac{P_m}{P_o})$	3.22	0.00	1.31	0.17	0.06	5.61	0.68	0.54
	3.282	$\frac{H_g}{H_o}$ = 0.465 + 0.248$(\frac{S}{S_o})$ + 0.001$(\frac{RF_m}{RF_o})$ - 0.279$(\frac{H_d}{H_g})$	1.90	0.00	0.72	0.14	0.05	4.22	0.79	0.64
	3.283	$\frac{H_g}{H_o}$ = 0.445 + 0.336$(\frac{S}{S_o})$ - 0.002$(\frac{RF_m}{RF_o})$ + 0.002$(\frac{RH_m}{RH_o})$	2.36	0.00	0.93	0.16	0.06	4.88	0.75	0.59
	3.284	$\frac{H_g}{H_o}$ = 0.228 + 0.374$(\frac{S}{S_o})$ + 0.005$(\frac{RF_m}{RF_o})$ + 0.002$(\frac{WS_m}{WS_0})$	2.50	0.00	0.93	0.16	0.06	5.21	0.74	0.57
	3.285	$\frac{H_g}{H_o}$ = 0.459 + 0.263$(\frac{S}{S_o})$ + 0.004$(\frac{WS_m}{WS_0})$ - 0.280$(\frac{H_d}{H_g})$	2.85	0.00	0.74	0.15	0.06	4.02	0.79	0.64

Table 3.31 Empirical models based on four variables correlation along with statistical errors for cold and cloudy climate zone

Models	Eq. No.	Equations	MPE (%)	MBE (%)	SSRE (%)	RSE (%)	RMSE (%)	t-stat	r	R^2
Models based on four variables correlation	3.286	$\frac{H_g}{H_o} = 0.390 + 0.247\left(\frac{S}{S_o}\right) + 0.004\left(\frac{T_m}{T_o}\right) + 0.004\left(\frac{WS_m}{WS_0}\right) - 0.263\left(\frac{H_d}{H_g}\right)$	2.23	0.00	0.62	0.14	0.05	4.00	0.80	0.66
	3.287	$\frac{H_g}{H_o} = 0.492 + 0.342\left(\frac{S}{S_o}\right) - 0.001\left(\frac{T_m}{T_o}\right) - 0.002\left(\frac{RH_m}{RH_o}\right) + 0.001\left(\frac{RF_m}{RF_o}\right)$	2.21	0.00	0.83	0.15	0.06	4.65	0.77	0.61
	3.288	$\frac{H_g}{H_o} = -0.688 + 0.337\left(\frac{S}{S_o}\right) - 0.002\left(\frac{RH_m}{RH_o}\right) + 0.001\left(\frac{RF_m}{RF_o}\right) + 0.001\left(\frac{P_m}{P_o}\right)$	2.96	0.00	0.91	0.16	0.06	4.66	0.77	0.61
	3.289	$\frac{H_g}{H_o} = -0.473 + 0.340\left(\frac{S}{S_o}\right) - 0.002\left(\frac{RH_m}{RH_o}\right) + 0.003\left(\frac{WS_m}{WS_0}\right) + 0.001\left(\frac{P_m}{P_o}\right)$	2.20	0.00	0.77	0.15	0.06	4.49	0.77	0.62
	3.290	$\frac{H_g}{H_o} = 0.682 + 0.239\left(\frac{S}{S_o}\right) - 0.002\left(\frac{T_m}{T_o}\right) - 0.002\left(\frac{RH_m}{RH_o}\right) - 0.258\left(\frac{H_d}{H_g}\right)$	2.07	0.00	0.61	0.14	0.05	3.93	0.81	0.67
	3.291	$\frac{H_g}{H_o} = 0.429 + 0.343\left(\frac{S}{S_o}\right) + 0.001\left(\frac{T_m}{T_o}\right) - 0.002\left(\frac{RH_m}{RH_o}\right) + 0.002\left(\frac{WS_m}{WS_0}\right)$	2.12	0.00	0.71	0.15	0.06	4.58	0.77	0.61
	3.292	$\frac{H_g}{H_o} = 0.587 + 0.221\left(\frac{S}{S_o}\right) - 0.002\left(\frac{RH_m}{RH_o}\right) + 0.003\left(\frac{WS_m}{WS_0}\right) - 0.263\left(\frac{H_d}{H_g}\right)$	1.75	0.00	0.62	0.14	0.05	3.82	0.81	0.67
	3.293	$\frac{H_g}{H_o} = 0.420 + 0.341\left(\frac{S}{S_o}\right) - 0.002\left(\frac{RH_m}{RH_o}\right) + 0.003\left(\frac{WS_m}{WS_0}\right) + 0.002\left(\frac{RF_m}{RF_o}\right)$	2.21	0.00	0.84	0.15	0.06	4.62	0.77	0.61

Table 3.32 Empirical models based on five variables correlation along with statistical errors for cold and cloudy climate zone

Models	Eq. No.	Equations	MPE (%)	MBE (%)	SSRE (%)	RSE (%)	RMSE (%)	t-stat	r	R^2
Models based on five variables correlation	3.294	$\frac{H_g}{H_o}$ = -2.59 + 0.252$(\frac{S}{S_o})$ + 0.002$(\frac{T_m}{T_o})$ + 0.0001$(\frac{RF_m}{RF_o})$ + 0.004$(\frac{P_m}{P_o})$ - 0.268$(\frac{H_d}{H_g})$	-1.43	-0.01	0.86	0.14	0.06	3.56	0.81	0.67
	3.295	$\frac{H_g}{H_o}$ = -0.394 + 0.244$(\frac{S}{S_o})$ - 0.004$(\frac{T_m}{T_o})$ - 0.002$(\frac{RH_m}{RH_o})$ + 0.001$(\frac{P_m}{P_o})$ - 0.256$(\frac{H_d}{H_g})$	5.85	0.02	1.30	0.13	0.06	4.27	0.81	0.67
	3.296	$\frac{H_g}{H_o}$ = 0.19 + 0.34$(\frac{S}{S_o})$ - 0.001$(\frac{T_m}{T_o})$ - 0.002$(\frac{RH_m}{RH_o})$ + 0.003$(\frac{WS_m}{WS_0})$ + 0.0001$(\frac{P_m}{P_o})$	5.77	0.01	1.21	0.18	0.07	4.88	0.78	0.62
	3.297	$\frac{H_g}{H_o}$ = -2.75 + 0.36$(\frac{S}{S_o})$ + 0.006$(\frac{T_m}{T_o})$ + 0.005$(\frac{WS_m}{WS_0})$ + 0.0001$(\frac{RF_m}{RF_o})$ +0.003$(\frac{P_m}{P_o})$	-1.25	-0.01	1.39	0.18	0.08	4.46	0.76	0.59
	3.298	$\frac{H_g}{H_o}$ = -1.861 + 0.248$(\frac{S}{S_o})$ + 0.002$(\frac{T_m}{T_o})$ + 0.004$(\frac{WS_m}{WS_0})$ + 0.003$(\frac{P_m}{P_o})$ - 0.256$(\frac{H_d}{H_g})$	1.72	0.00	0.57	0.13	0.05	3.75	0.81	0.68
	3.299	$\frac{H_g}{H_o}$ = 0.651 + 0.234$(\frac{S}{S_o})$ - 0.001$(\frac{T_m}{T_o})$ - 0.002$(\frac{RH_m}{RH_o})$ + 0.003$(\frac{WS_m}{WS_0})$ - 0.256$(\frac{H_d}{H_g})$	1.61	0.00	0.54	0.13	0.05	3.67	0.82	0.68
	3.300	$\frac{H_g}{H_o}$ = 0.46 + 0.34$(\frac{S}{S_o})$ + 0.0001$(\frac{T_m}{T_o})$ - 0.002$(\frac{RH_m}{RH_o})$ + 0.002$(\frac{WS_m}{WS_0})$ + 0.001$(\frac{RF_m}{RF_o})$	1.94	0.00	0.72	0.14	0.05	4.37	0.78	0.63
	3.301	$\frac{H_g}{H_o}$ = 0.7 + 0.24$(\frac{S}{S_o})$ - 0.003$(\frac{T_m}{T_o})$ - 0.002$(\frac{RH_m}{RH_o})$ + 0.0001$(\frac{RF_m}{RF_o})$ - 0.253$(\frac{H_d}{H_g})$	1.65	0.00	0.57	0.13	0.05	3.69	0.82	0.68

Table 3.33 Empirical models based on six and seven variables correlation along with statistical errors for cold and cloudy climate zone

Models	Eq. No.	Equations	MPE (%)	MBE (%)	SSRE (%)	RSE (%)	RMSE (%)	t-stat	r	R^2
Models based on six variables correlation	3.302	$\frac{H_g}{H_o}$ = -0.495 + 0.35$(\frac{S}{S_o})$ - 0.003$(\frac{T_m}{T_o})$ - 0.002$(\frac{RH_m}{RH_o})$ + 0.003$(\frac{WS_m}{WS_0})$+ 0.001$(\frac{RF_m}{RF_o})$ + 0.001$(\frac{P_m}{P_o})$	1.99	0.00	0.71	0.14	0.05	4.24	0.79	0.64
	3.303	$\frac{H_g}{H_o}$ = -0.718 + 0.246$(\frac{S}{S_o})$ - 0.004$(\frac{T_m}{T_o})$ - 0.002$(\frac{RH_m}{RH_o})$ + 0.0001$(\frac{RF_m}{RF_o})$ + 0.0001$(\frac{P_m}{P_o})$ + 0.002$(\frac{H_d}{H_g})$	1.62	0.00	0.56	0.13	0.05	3.57	0.83	0.69
	3.304	$\frac{H_g}{H_o}$ = -2.175 + 0.246$(\frac{S}{S_o})$ + 0.002$(\frac{T_m}{T_o})$ + 0.004$(\frac{WS_m}{WS_0})$ + 0.0001$(\frac{RF_m}{RF_o})$ + 0.003$(\frac{P_m}{P_o})$ - 0.257$(\frac{H_d}{H_g})$	3.50	0.01	0.70	0.21	0.05	4.13	0.82	0.69
	3.305	$\frac{H_g}{H_o}$ = 0.675 + 0.219$(\frac{S}{S_o})$ - 0.002$(\frac{T_m}{T_o})$ - 0.002$(\frac{RH_m}{RH_o})$ + 0.002$(\frac{WS_m}{WS_0})$ + 0.0001$(\frac{RF_m}{RF_o})$ - 0.255$(\frac{H_d}{H_g})$	-0.19	-0.01	0.58	0.13	0.05	3.50	0.82	0.69
Models based on seven variables correlation	3.306	$\frac{H_g}{H_o}$ = -0.547 + 0.241$(\frac{S}{S_o})$ - 0.004$(\frac{T_m}{T_o})$ - 0.002$(\frac{RH_m}{RH_o})$ + 0.003$(\frac{WS_m}{WS_0})$ + 0.0001$(\frac{RF_m}{RF_o})$ + 0.001$(\frac{P_m}{P_o})$ - 0.256$(\frac{H_d}{H_g})$	1.50	0.00	0.50	0.12	0.05	3.42	0.84	0.71

From Table 3.29 - Table 3.33, the following can be briefly summarized:

(e) Cold and cloudy climate zone

Correlation based on seven variables has been observed to be the most suitable model on the basis of closeness parameters with correlation of coefficient (r = 0.84) obtained between the clearness index and relative sunshine duration, wind speed, ambient temperature, relative humidity, atmospheric pressure, amount of rainfall, cloudiness index.

The coefficient of determination has been observed to be (R^2 = 0.71) which mean 71% of the clearness index can be accounted by sunshine hours, ambient temperature, relative humidity, wind speed, amount of rainfall, atmospheric pressure and cloudiness index.

The relation between the parameters namely clearness index, relative sunshine duration, ambient temperature, relative humidity, wind speed, amount of rainfall, atmospheric pressure and cloudiness index is given by Eq. (3.306) expressed as:

$$\frac{H_g}{H_o} = -0.547 + 0.241\left(\frac{S}{S_o}\right) - 0.004\left(\frac{T_m}{T_o}\right) - 0.002\left(\frac{RH_m}{RH_o}\right) +$$

$$0.003\left(\frac{WS_m}{WS_0}\right) + 0.0001\left(\frac{RF_m}{RF_o}\right) + 0.001\left(\frac{P_m}{P_o}\right) - 0.256\left(\frac{H_d}{H_g}\right) \quad (3.306)$$

Further, the estimated data values of global solar energy using the derived correlation have been compared with the measured data values as shown in Fig. 3.3(e).

The developed models have been further processed based on principal component analysis to obtain the correlation with highest correlation coefficients using one, two, three, four, five and six variables correlation and the performance of the models have been evaluated based on statistical error-tests and are illustrated in Table 3.34 - Table 3.36.

Table 3.34 Empirical correlations alongwith statistical errors for warm and humid & hot and dry climate zone across India

Climate Zone	Eq. No.	Models/Equations	MPE (%)	MBE (%)	RMSE (%)	r	R^2
Chennai (Warm and humid)	3.67	$\frac{H_g}{H_o} = 0.259 + 0.321(\frac{S}{S_o})$	1.52	0.00	0.05	0.77	0.62
	3.71	$\frac{H_g}{H_o} = 0.551 + 0.107(\frac{S}{S_o}) - 0.265(\frac{H_d}{H_g})$	1.51	0.00	0.04	0.89	0.79
	3.75	$\frac{H_g}{H_o} = 0.683 + 0.063(\frac{S}{S_o}) + 0.0001(\frac{P_m}{P_o}) - 0.332(\frac{H_d}{H_g})$	2.95	0.01	0.04	0.89	0.80
	3.94	$\frac{H_g}{H_o} = 0.530 + 0.048(\frac{S}{S_o}) + 0.004(\frac{T_m}{T_o}) - 0.001(\frac{RH_m}{RH_o}) - 0.330(\frac{H_d}{H_g})$	0.48	0.00	0.04	0.91	0.82
	3.103	$\frac{H_g}{H_o} = 0.508 + 0.05(\frac{S}{S_o}) + 0.003(\frac{T_m}{T_o}) + 0.003(\frac{RH_m}{RH_o}) + 0.0001(\frac{WS_m}{WS_0}) - 0.333(\frac{H_d}{H_g})$	1.40	0.00	0.03	0.91	0.83
	3.108	$\frac{H_g}{H_o} = 0.938 + 0.073(\frac{S}{S_o}) + 0.002(\frac{T_m}{T_o}) + 0.003(\frac{WS_m}{WS_0}) + 0.001(\frac{RF_m}{RF_o}) + 0.0001(\frac{P_m}{P_o}) - 0.304(\frac{H_d}{H_g})$	0.86	0.00	0.03	0.93	0.86
	3.110	$\frac{H_g}{H_o} = 0.945 + 0.072(\frac{S}{S_o}) + 0.003(\frac{T_m}{T_o}) + 0.0001(\frac{RH_m}{RH_o}) + 0.003(\frac{WS_m}{WS_0}) + 0.001(\frac{RF_m}{RF_o}) + 0.0001(\frac{P_m}{P_o}) - 0.300(\frac{H_d}{H_g})$	1.93	0.00	0.04	0.93	0.87
Jodhpur (Hot and dry)	3.113	$\frac{H_g}{H_o} = 0.656 - 0.352(\frac{H_d}{H_g})$	-0.04	0.00	0.03	0.71	0.54
	3.120	$\frac{H_g}{H_o} = 0.587 + 0.069(\frac{S}{S_o}) - 0.307(\frac{H_d}{H_g})$	-0.08	0.00	0.03	0.70	0.55
	3.128	$\frac{H_g}{H_o} = 0.541 + 0.073(\frac{S}{S_o}) + 0.001(\frac{T_m}{T_o}) - 0.293(\frac{H_d}{H_g})$	-0.14	0.00	0.03	0.77	0.62
	3.139	$\frac{H_g}{H_o} = 0.543 + 0.067(\frac{S}{S_o}) + 0.001(\frac{T_m}{T_o}) + 0.0001(\frac{WS_m}{WS_0}) - 0.305(\frac{H_d}{H_g})$	-0.13	0.00	0.03	0.77	0.62
	3.151	$\frac{H_g}{H_o} = -1.78 + 0.051(\frac{S}{S_o}) + 0.001(\frac{T_m}{T_o}) + 0.0001(\frac{WS_m}{WS_0}) + 0.002(\frac{P_m}{P_o}) - 0.299(\frac{H_d}{H_g})$	-0.19	0.00	0.03	0.79	0.64
	3.156	$\frac{H_g}{H_o} = -1.087 + 0.036(\frac{S}{S_o}) - 0.001(\frac{T_m}{T_o}) - 0.001(\frac{RH_m}{RH_o}) - 0.011(\frac{RF_m}{RF_o}) + 0.002(\frac{P_m}{P_o}) - 0.299(\frac{H_d}{H_g})$	-0.22	0.00	0.03	0.80	0.66
	3.159	$\frac{H_g}{H_o} = -1.087 + 0.034(\frac{S}{S_o}) - 0.002(\frac{T_m}{T_o}) - 0.001(\frac{RH_m}{RH_o}) - 0.001(\frac{WS_m}{WS_0}) - 0.011(\frac{RF_m}{RF_o}) + 0.002(\frac{P_m}{P_o}) - 0.305(\frac{H_d}{H_g})$	-0.36	-0.01	0.03	0.79	0.64

Table 3.35 Empirical correlations along with statistical errors for composite and moderate climate zone across India

Climate Zone	Eq. No.	Models/Equations	MPE (%)	MBE (%)	RMSE (%)	r	R^2
Delhi (Composite)	3.162	$\frac{H_g}{H_o} = 0.670 - 0.405\left(\frac{H_d}{H_g}\right)$	0.67	0.00	0.03	0.78	0.62
	3.169	$\frac{H_g}{H_o} = 0.4597 + 0.625\left(\frac{S}{S_o}\right) + 0.055\left(\frac{H_d}{H_g}\right)$	0.49	0.59	0.07	0.63	0.81
	3.177	$\frac{H_g}{H_o} = 0.589 + 0.138\left(\frac{S}{S_o}\right) - 0.004\left(\frac{T_m}{T_o}\right) - 0.301\left(\frac{H_d}{H_g}\right)$	0.56	0.00	0.03	0.77	0.61
	3.192	$\frac{H_g}{H_o} = 0.723 + 0.121\left(\frac{S}{S_o}\right) - 0.006\left(\frac{T_m}{T_o}\right) - 0.001\left(\frac{RH_m}{RH_o}\right) - 0.282\left(\frac{H_d}{H_g}\right)$	0.52	0.00	0.03	0.80	0.65
	3.201	$\frac{H_g}{H_o} = 0.74 + 0.127\left(\frac{S}{S_o}\right) - 0.007\left(\frac{T_m}{T_o}\right) - 0.001\left(\frac{RH_m}{RH_o}\right) + 0.0001\left(\frac{WS_m}{WS_0}\right) - 0.268\left(\frac{H_d}{H_g}\right)$	0.47	0.00	0.03	0.81	0.67
	3.205	$\frac{H_g}{H_o} = 0.73+0.120\left(\frac{S}{S_o}\right)-0.006\left(\frac{T_m}{T_o}\right)-0.001\left(\frac{RH_m}{RH_o}\right)-0.030\left(\frac{RF_m}{RF_o}\right)+0.0001\left(\frac{P_m}{P_o}\right) - 0.274\left(\frac{H_d}{H_g}\right)$	0.46	0.00	0.03	0.82	0.69
	3.208	$\frac{H_g}{H_o} = 1.008 + 0.123\left(\frac{S}{S_o}\right) - 0.006\left(\frac{T_m}{T_o}\right) - 0.001\left(\frac{RH_m}{RH_o}\right) + 0.0001\left(\frac{WS_m}{WS_0}\right) - 0.028\left(\frac{RF_m}{RF_o}\right) + 0.0001\left(\frac{P_m}{P_o}\right) - 0.264\left(\frac{H_d}{H_g}\right)$	0.42	0.00	0.03	0.83	0.71
Pune (Moderate)	3.215	$\frac{H_g}{H_o} = 0.156 + 0.281\left(\frac{S}{S_o}\right)$	3.10	0.01	0.04	0.71	0.53
	3.218	$\frac{H_g}{H_o} = 0.426 + 0.159\left(\frac{S}{S_o}\right) - 0.178\left(\frac{H_d}{H_g}\right)$	-0.29	-0.03	0.07	0.58	0.41
	3.222	$\frac{H_g}{H_o} = 0.439 + 0.222\left(\frac{S}{S_o}\right) + 0.0001\left(\frac{P_m}{P_o}\right) - 0.358\left(\frac{H_d}{H_g}\right)$	1.03	0.00	0.03	0.87	0.75
	3.243	$\frac{H_g}{H_o} = 0.586 + 0.168\left(\frac{S}{S_o}\right) - 0.001\left(\frac{RH_m}{RH_o}\right) + 0.003\left(\frac{WS_m}{WS_0}\right) - 0.252\left(\frac{H_d}{H_g}\right)$	-1.71	-0.02	0.04	0.86	0.75
	3.252	$\frac{H_g}{H_o} = 0.589 + 0.185\left(\frac{S}{S_o}\right) - 0.001\left(\frac{T_m}{T_o}\right) - 0.001\left(\frac{RH_m}{RH_o}\right) + 0.002\left(\frac{RF_m}{RF_o}\right) - 0.33\left(\frac{H_d}{H_g}\right)$	0.34	0.00	0.02	0.90	0.81
	3.255	$\frac{H_g}{H_o} = 0.9+0.21\left(\frac{S}{S_o}\right)+0.0001\left(\frac{T_m}{T_o}\right)+0.004\left(\frac{WS_m}{WS_0}\right)+0.002\left(\frac{RF_m}{RF_o}\right)+0.0001\left(\frac{P_m}{P_o}\right)-0.34\left(\frac{H_d}{H_g}\right)$	0.33	0.00	0.02	0.89	0.80
	3.257	$\frac{H_g}{H_o} = 0.447 + 0.17\left(\frac{S}{S_o}\right) + 0.0001\left(\frac{T_m}{T_o}\right) - 0.001\left(\frac{RH_m}{RH_o}\right) + 0.003\left(\frac{WS_m}{WS_0}\right) + 0.004\left(\frac{RF_m}{RF_o}\right) + 0.0001\left(\frac{P_m}{P_o}\right) - 0.34\left(\frac{H_d}{H_g}\right)$	0.25	0.02	0.05	0.90	0.81

Table 3.36 Empirical correlations along with statistical errors for cold and cloudy climate zone across India

Climate Zone	Eq. No.	Models/Equations	MPE (%)	MBE (%)	RMSE (%)	r	R^2
Shillong (Cold and cloudy)	3.260	$\frac{H_g}{H_o} = 0.729 - 0.563\left(\frac{H_d}{H_g}\right)$	4.75	0.00	0.07	0.70	0.77
	3.269	$\frac{H_g}{H_o} = 0.404 + 0.339\left(\frac{S}{S_o}\right) - 0.002\left(\frac{RH_m}{RH_o}\right)$	0.69	-0.01	0.06	0.73	0.56
	3.279	$\frac{H_g}{H_o} = 0.605 + 0.221\left(\frac{S}{S_o}\right) - 0.002\left(\frac{RH_m}{RH_o}\right) - 0.226\left(\frac{H_d}{H_g}\right)$	1.87	0.00	0.05	0.79	0.65
	3.286	$\frac{H_g}{H_o} = 0.390 + 0.247\left(\frac{S}{S_o}\right) + 0.004\left(\frac{T_m}{T_o}\right) + 0.004\left(\frac{WS_m}{WS_0}\right) - 0.263\left(\frac{H_d}{H_g}\right)$	2.23	0.00	0.05	0.80	0.66
	3.299	$\frac{H_g}{H_o} = 0.651 + 0.234\left(\frac{S}{S_o}\right) - 0.001\left(\frac{T_m}{T_o}\right) - 0.002\left(\frac{RH_m}{RH_o}\right) + 0.003\left(\frac{WS_m}{WS_0}\right) - 0.256\left(\frac{H_d}{H_g}\right)$	1.61	0.00	0.05	0.82	0.68
	3.303	$\frac{H_g}{H_o} = -0.718 + 0.246\left(\frac{S}{S_o}\right) - 0.004\left(\frac{T_m}{T_o}\right) - 0.002\left(\frac{RH_m}{RH_o}\right) + 0.0001\left(\frac{RF_m}{RF_o}\right) + 0.0001\left(\frac{P_m}{P_o}\right) + 0.002\left(\frac{H_d}{H_g}\right)$	1.62	0.00	0.05	0.83	0.69
	3.306	$\frac{H_g}{H_o} = -0.547 + 0.241\left(\frac{S}{S_o}\right) - 0.004\left(\frac{T_m}{T_o}\right) - 0.002\left(\frac{RH_m}{RH_o}\right) + 0.003\left(\frac{WS_m}{WS_0}\right) + 0.0001\left(\frac{RF_m}{RF_o}\right) + 0.001\left(\frac{P_m}{P_o}\right) - 0.256\left(\frac{H_d}{H_g}\right)$	1.50	0.00	0.05	0.84	0.71

It has been concluded from Table 3.34 - 3.36 that the correlations based on seven variables provides accurate model with highest values of (r) and (R^2) for each of the climate zones across the entire country. Further, the graphical representation has been shown in Fig. 3.3 for distinct climate zone.

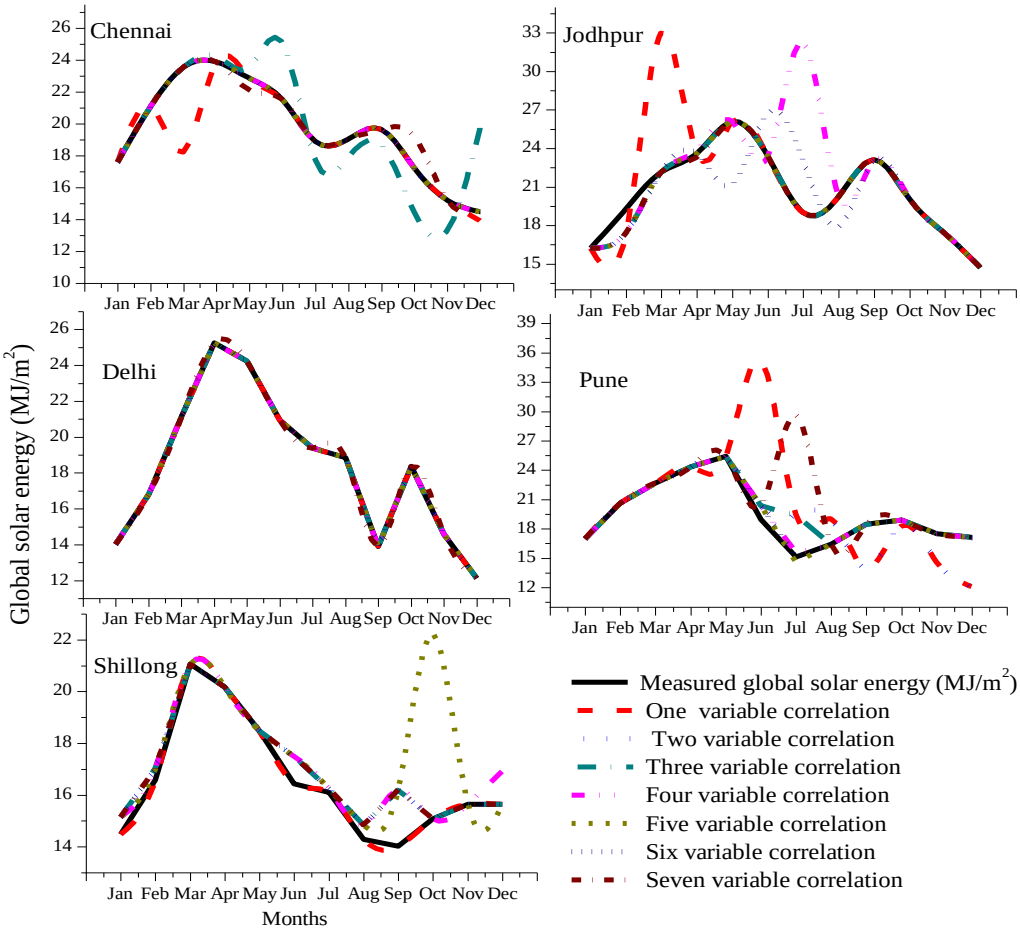

Fig. 3.3 Graphical representation of measured and estimated global solar energy for empirical models (a) Chennai (b) Jodhpur (c) Delhi (d) Pune and (e) Shillong

It has been observed from Fig. 3.3 that for composite climate zone, an excellent match has been noticed between the measured and estimated data.

3.8 COMPARISON OF PROPOSED MODEL WITH OTHER MODELS

The proposed model is further compared with other well-established models available in the literature and is presented in Table 3.37.

Table 3.37 Comparison with other well-established models

Models	**Eq. No.**	**Equations/Models**	**MPE (%)**	**MBE (%)**	**RMSE (%)**
Proposed Model	3.110	$\frac{H_g}{H_o} = 0.945 + 0.072(\frac{S}{S_o}) + 0.003(\frac{T_m}{T_o}) + 0.0001(\frac{RH_m}{RH_o}) + 0.003(\frac{WS_m}{WS_0}) + 0.001(\frac{RF_m}{RF_o}) + 0.0001(\frac{P_m}{P_o}) - 0.300(\frac{H_d}{H_g})$	1.93	0.00	0.04
	3.159	$\frac{H_g}{H_o} = -1.087 + 0.034(\frac{S}{S_o}) - 0.002(\frac{T_m}{T_o}) - 0.001(\frac{RH_m}{RH_o}) - 0.001(\frac{WS_m}{WS_0}) - 0.011(\frac{RF_m}{RF_o}) + 0.002(\frac{P_m}{P_o}) - 0.305(\frac{H_d}{H_g})$	-0.36	-0.01	0.03
	3.208	$\frac{H_g}{H_o} = 1.008 + 0.123(\frac{S}{S_o}) - 0.006(\frac{T_m}{T_o}) - 0.001(\frac{RH_m}{RH_o}) + 0.0001(\frac{WS_m}{WS_0}) - 0.028(\frac{RF_m}{RF_o}) + 0.0001(\frac{P_m}{P_o}) - 0.264(\frac{H_d}{H_g})$	0.42	0.00	0.03
	3.257	$\frac{H_g}{H_o} = 0.447 + 0.17(\frac{S}{S_o}) + 0.0001(\frac{T_m}{T_o}) - 0.001(\frac{RH_m}{RH_o}) + 0.003(\frac{WS_m}{WS_0}) + 0.004(\frac{RF_m}{RF_o}) + 0.0001(\frac{P_m}{P_o}) - 0.340(\frac{H_d}{H_g})$	0.25	0.02	0.05
	3.306	$\frac{H_g}{H_o} = -0.547 + 0.241(\frac{S}{S_o}) - 0.004(\frac{T_m}{T_o}) - 0.002(\frac{RH_m}{RH_o}) + 0.003(\frac{WS_m}{WS_0}) + 0.0001(\frac{RF_m}{RF_o}) + 0.001(\frac{P_m}{P_o}) - 0.256(\frac{H_d}{H_g})$	1.50	0.00	0.05
Angstrom- Prescott Model	3.307	$\frac{H_g}{H_o} = 0.0801 + 0.709(\frac{S}{S_o})$	96.06	15.62	16.54
Rietveld Model	3.308	$\frac{H_g}{H_o} = 0.18 + 0.62(\frac{S}{S_o})$	35.71	4.80	5.21
Page Model	3.309	$\frac{H_g}{H_o} = 0.23 + 0.48(\frac{S}{S_o})$	25.90	3.32	3.52
Akinoglu and Ecevit Model	3.310	$\frac{H_g}{H_o} = 0.145 + 0.845(\frac{S}{S_o}) - 0.28(\frac{S}{S_o})^2$	32.47	4.15	4.36
Bahel Model	3.311	$\frac{H_g}{H_o} = 0.16 + 0.87(\frac{S}{S_o}) - 0.16(\frac{S}{S_o})^2 + 0.34(\frac{S}{S_o})^3$	-53.24	-6.51	7.69
Newland Model	3.312	$\frac{H_g}{H_o} = 0.34 - 0.4(\frac{S}{S_o}) + 0.17 \log(\frac{S}{S_o})$	88.87	16.72	18.54
Abdalla Model	3.313	$\frac{H_g}{H_o} = 0.5289 + 0.459(\frac{S}{S_o}) + 0.004073(\frac{T_m}{T_o}) - 0.006481(\frac{RH_m}{RH_o})$	-93.19	-14.40	15.40

The results of statistical error-tests reveal that the proposed model is accurate as compared to other models with mean percentage error of 1.93% for warm and humid climate (Chennai), 0.36% for hot and dry climate (Jodhpur), 0.42% for composite climate (Delhi), 0.25% for moderate climate (Pune) and 1.50% for cold and cloudy climate zone (Shillong). The obtained results indicate a good agreement between the measured and estimated data in comparison to other well-established models.

3.9 CONCLUSION

In the present work, 40 sunshine-based models with linear and non-linear correlations have been established using sunshine hour as a meteorological parameter for five meteorological stations that represents distinct climate zone across India. It has been concluded from the obtained results that the weakest fit is achieved for warm and humid climate zone with the largest difference between the best and worst determination coefficients and the best fit is obtained for composite climatic zone with the smallest difference between the best and worst determination coefficients.

Further, in this work, 245 empirical models have been established correlating global solar energy with other parameters namely sunshine hours, relative humidity, ambient temperature, wind speed, atmospheric pressure, amount of rainfall and cloudiness index using multiple regression analysis for five weather stations across India. The regression and correlation coefficients for each model has been calculated and presented. The developed models have been further processed based on principal component analysis to obtain the correlation with highest correlation coefficients. The performance of the models has been evaluated using statistical error-tests. It has been concluded

from the statistical analysis that the correlations which incorporate seven variables has emerged to be accurate and shows a good agreement between measured and estimated data making it useful for estimating solar energy in each climate zones across the country. Further, the proposed model have been compared with well-established model available in the literature and the results of statistical error-tests reveal that the models presented are accurate and have reasonable estimation errors. It has been concluded from statistical analysis that the meteorological parameters considered made a strong influence on estimating global solar energy. Also, the geographical parameters tend to effect global solar energy and have a strong influence on it. Therefore, in this research, the models being proposed could be successfully used for estimating global solar energy in distinct climate zone across India and elsewhere with similar climatic conditions.

CHAPTER 4

FUZZY LOGIC APPROACH FOR ASSESSING SOLAR ENERGY

4.1 INTRODUCTION

This chapter presents a model employing fuzzy logic approach to forecast global solar energy based on sky-conditions namely sunny sky (type-a), hazy sky (type-b), partially foggy/cloudy sky (type-c) and fully foggy/cloudy sky (type-d) conditions. Meteorological parameters include dew-point along with other available parameters namely duration of sunshine hours, wind speed, global solar energy, relative humidity and ambient temperature. Simulations have been carried out for distinct climate zone across India such as composite (Delhi), warm and humid (Chennai), hot and dry (Jodhpur), cold and cloudy (Shillong) and moderate (Pune) climate zone. Also, the comparison of the proposed model has been made with the empirical models using statistical indicators for each of the climate zones across the country. Further, the developed model has been implemented for solar photovoltaic system under composite climatic conditions.

This chapter is based on the following published papers:

1. **Gulnar Perveen**, M. Rizwan and Nidhi Goel, "Intelligent model for solar energy forecasting and its implementation for solar photovoltaic applications," **Journal of Renewable and Sustainable Energy, AIP,** Vol. 10, No. 6, Article ID. 063702, pp. 1-23, 2018. ISSN No. 1941-7012, Impact factor: 1.337, SCI Expanded.

2. **Gulnar Perveen**, M. Rizwan and Nidhi Goel, "Fuzzy logic modelling and its solar thermal applications," Proceedings of **2nd IEEE International Conference on Power Electronics, Intelligent Control and Energy Systems (ICPEICES-2018)**, October 22-24, 2018, Delhi Technological University, Delhi, India.

4.2 SOLAR ENERGY FORECASTING AND ITS NECESSITY

Solar energy is one of the most important parameter for solar energy based research and applications but the measuring equipment's are unavailable in most of the meteorological sites because of the high cost of instruments and limited spatial coverage. Therefore, forecasting global solar energy is essential for these stations where measurements have not been done with aid of meteorological parameters.

Most of the grid-interactive solar PV plants are built using photovoltaic technology. However, because of variation in sky-conditions, the system output is stochastic and non-deterministic. Therefore, accurately forecasting global solar energy is essential in different sky-condition as the power output of the solar system has been greatly influenced by the presence of environmental factors such as dust, moisture, cloud and atmospheric temperature differences. Most of the previous researches provided a forecasting tool for estimating PV power output with reasonable accuracy. Some of them were based on Markov chain, Auto Regressive (AR) and Auto Regressive Moving Average (ARMA). However, such non-deterministic model shows inaccuracy and relatively observed with large errors because they are based on probability estimation. Moreover, global solar energy forecasting using these models is a tedious task as it depends on the mathematical formulation. These drawbacks can be overcome by using intelligent models for forecasting global solar energy. In many previous researches, intelligent modelling techniques have been discussed such as fuzzy logic modelling which is applied to meteorology [76]. Many deals with meteorological estimations such as atmospheric circulation pattern by fuzzy c-mean, micro-grid planning on fuzzy interval modes, fuzzy classification

of clouds [77-85]. Many models based on fuzzy logic techniques have been proposed using meteorological parameters namely ambient temperature and cloudiness index for forecasting global solar energy [86-87]. Most of the models discussed in the literature were confined to clear sky-conditions; however, very few literature is available that discussed about modelling based on different sky conditions such as sunny/clear, hazy, foggy and cloudy sky-conditions for estimating global solar energy by using fuzzy logic based model.

This chapter aims to develop model based on sky-conditions using intelligent modelling techniques to forecast global solar energy which is classified as sunny and clear sky (type-a), hazy sky (type-b), partially foggy/cloudy sky (type-c) and fully foggy/cloudy sky (type-d) conditions by using meteorological parameters for five weather stations representing different climatic conditions across India. The performance of the model has been measured with aid of statistical error-tests. Further, the results obtained by employing fuzzy logic modelling have been used for 210 W_p Heterojunction with Intrinsic Thick (HIT) layer solar photovoltaic (PV) modules in forecasting power of the solar PV system at Maximum Power Point Tracking (MPPT) conditions. Lastly, comparative analysis has been made with regression models to verify for the accuracy and supremacy of the proposed model.

4.3 METEOROLOGICAL DATA

4.3.1 Compilation and Normalization/Scaling of Data

In this chapter, the recorded hourly averaged data (2006-2016) have been obtained from Indian Meteorological Department (IMD), National Institute of Solar Energy (NISE) and in collaboration with National Institute of Wind Energy (NIWE) and are presented in Table 4.1 - Table 4.5 [88].

Table 4.1 Measured and scaled data for composite climate zone

Months	Sunshine hours (hrs)		H_g (MJ/m^2)		Relative Humidity (%)		Ambient Temp. (^oC)		Wind Speed (m/s)		Dew Point (^oC)	
	Measured	Scaled	Measured	Scaled	Measured	Scaled	Measured	Scaled	Measured	Scaled	Measured	Scaled
January	7.854	0.665	15.406	0.342	63.990	0.461	16.061	0.452	3.200	0.308	7.585	0.520
February	7.936	0.594	30.206	0.610	59.940	0.448	21.551	0.667	3.835	0.420	9.067	0.379
March	7.338	0.715	37.413	0.478	40.996	0.497	26.793	0.439	3.982	0.359	11.481	0.686
April	9.220	0.718	40.810	0.671	21.083	0.510	34.213	0.551	4.187	0.469	10.837	0.396
May	8.848	0.645	36.325	0.590	34.658	0.433	35.076	0.591	4.276	0.406	15.296	0.598
June	7.604	0.577	32.239	0.630	47.960	0.552	34.916	0.477	4.111	0.433	21.934	0.550
July	4.740	0.375	24.584	0.529	78.492	0.531	30.317	0.508	2.995	0.504	25.920	0.623
August	5.934	0.524	28.998	0.554	81.261	0.427	29.801	0.532	3.552	0.500	26.092	0.571
September	6.683	0.550	34.356	0.655	61.926	0.323	31.235	0.631	3.080	0.394	22.766	0.408
October	9.329	0.713	31.284	0.651	43.948	0.342	29.867	0.548	3.156	0.441	15.409	0.387
November	7.197	0.547	25.436	0.601	40.824	0.259	24.263	0.708	2.932	0.398	8.881	0.375
December	5.807	0.597	23.105	0.719	61.105	0.417	19.211	0.588	2.784	0.384	10.089	0.411

Table 4.2 Measured and scaled data for warm and humid climate zone

Months	Sunshine hours (hrs)		H_g (MJ/m^2)		Relative Humidity (%)		Ambient Temp. (^oC)		Wind Speed (m/s)		Dew Point (^oC)	
	Measured	Scaled	Measured	Scaled	Measured	Scaled	Measured	Scaled	Measured	Scaled	Measured	Scaled
January	8.939	0.701	36.723	0.627	66.306	0.459	27.605	0.653	4.429	0.417	16.658	0.657
February	9.745	0.768	42.053	0.542	68.185	0.571	28.801	0.535	4.581	0.487	21.796	0.724
March	9.048	0.660	42.904	0.785	68.902	0.483	29.660	0.717	5.552	0.468	23.517	0.615
April	9.370	0.610	45.108	0.420	70.923	0.546	31.212	0.734	7.452	0.479	25.548	0.683
May	8.826	0.626	38.886	0.704	58.133	0.568	32.210	0.686	6.152	0.573	20.613	0.701
June	7.607	0.642	31.346	0.536	50.155	0.542	31.505	0.609	5.207	0.427	15.379	0.510
July	6.768	0.554	34.562	0.563	64.267	0.552	31.148	0.515	5.402	0.429	22.659	0.718
August	5.235	0.535	33.742	0.632	61.215	0.453	31.504	0.593	5.326	0.571	16.880	0.640
September	6.160	0.582	32.469	0.592	68.075	0.443	30.529	0.612	4.587	0.535	21.678	0.705
October	6.942	0.598	35.381	0.661	61.848	0.413	30.606	0.665	4.148	0.456	18.109	0.616
November	6.778	0.607	34.611	0.623	67.610	0.502	28.215	0.729	4.937	0.453	17.324	0.646
December	7.295	0.624	29.994	0.677	74.825	0.501	26.883	0.721	5.676	0.209	17.882	0.646

Table 4.3 Measured and scaled data for hot and dry climate zone

Months	Sunshine hours (hrs)		H_g (MJ/m^2)		Relative Humidity (%)		Ambient Temp. (^oC)		Wind Speed (m/s)		Dew Point (^oC)	
	Measured	Scaled	Measured	Scaled	Measured	Scaled	Measured	Scaled	Measured	Scaled	Measured	Scaled
January	9.226	0.683	29.401	0.706	52.680	0.396	21.874	0.542	2.961	0.409	11.113	0.516
February	9.714	0.694	25.876	0.580	43.371	0.321	23.289	0.400	3.675	0.407	10.492	0.275
March	9.120	0.649	41.565	0.657	43.781	0.420	29.297	0.561	3.811	0.461	14.227	0.508
April	9.867	0.114	45.527	0.663	39.967	0.463	33.304	0.389	4.512	0.422	10.266	0.455
May	11.207	0.720	44.668	0.664	54.048	0.448	36.172	0.448	6.640	0.451	21.585	0.656
June	8.937	0.682	42.398	0.630	66.533	0.553	35.373	0.416	6.937	0.395	28.830	0.550
July	8.039	0.645	34.383	0.554	51.791	0.510	31.722	0.649	5.319	0.562	22.048	0.564
August	8.097	0.675	29.267	0.593	38.743	0.413	29.120	0.572	4.350	0.469	16.688	0.540
September	9.727	0.669	43.056	0.640	74.121	0.662	31.146	0.430	4.634	0.496	24.035	0.652
October	9.790	0.794	38.689	0.732	61.764	0.482	30.185	0.575	3.458	0.440	21.277	0.594
November	9.323	0.774	34.811	0.595	33.593	0.321	26.310	0.508	2.606	0.404	2.727	0.367
December	8.503	0.352	33.146	0.542	36.781	0.432	23.842	0.605	2.838	0.405	7.274	0.523

Table 4.4 Measured and scaled data for cold and cloudy climate zone

Months	Sunshine hours (hrs)		H_g (MJ/m^2)		Relative Humidity (%)		Ambient Temp. (^oC)		Wind Speed (m/s)		Dew Point (^oC)	
	Measured	Scaled	Measured	Scaled	Measured	Scaled	Measured	Scaled	Measured	Scaled	Measured	Scaled
January	7.463	0.633	25.668	0.662	60.397	0.425	18.845	0.593	2.783	0.519	10.361	0.674
February	6.488	0.567	31.894	0.658	54.030	0.500	22.126	0.473	3.233	0.394	12.160	0.423
March	7.216	0.635	34.109	0.638	50.563	0.399	25.340	0.503	3.685	0.517	13.693	0.508
April	3.790	0.317	32.930	0.598	66.778	0.506	25.771	0.505	4.086	0.361	18.787	0.512
May	4.842	0.483	33.664	0.523	74.971	0.547	27.203	0.537	4.348	0.362	22.311	0.533
June	4.180	0.492	31.453	0.665	79.623	0.290	28.139	0.723	6.208	0.533	24.263	0.607
July	3.245	0.403	14.122	0.469	82.342	0.572	27.193	0.422	3.195	0.303	23.839	0.668
August	2.505	0.439	22.089	0.556	84.819	0.520	27.043	0.573	3.981	0.451	24.304	0.610
September	3.287	0.394	19.580	0.527	82.378	0.522	27.148	0.432	2.719	0.380	23.795	0.650
October	5.871	0.557	22.366	0.461	71.681	0.498	26.310	0.446	2.015	0.337	20.755	0.538
November	7.057	0.632	19.460	0.468	63.465	0.507	23.759	0.433	1.783	0.274	16.345	0.497
December	7.600	0.630	20.430	0.560	61.230	0.560	21.350	0.500	2.560	0.450	17.250	0.520

Table 4.5 Measured and scaled data for moderate climate zone

Months	Sunshine hours (hrs)		H_g (MJ/m^2)		Relative Humidity (%)		Ambient Temp. (^oC)		Wind Speed (m/s)		Dew Point (^oC)	
	Measured	Scaled	Measured	Scaled	Measured	Scaled	Measured	Scaled	Measured	Scaled	Measured	Scaled
January	9.497	0.529	21.431	0.454	43.378	0.376	22.907	0.558	2.424	0.332	9.007	0.394
February	10.214	0.730	19.437	0.607	40.726	0.493	27.010	0.560	2.833	0.450	11.500	0.494
March	9.900	0.695	27.621	0.456	38.978	0.523	29.078	0.489	2.980	0.434	13.768	0.483
April	9.970	0.650	25.986	0.624	39.984	0.405	30.728	0.511	3.143	0.401	16.281	0.462
May	10.832	0.720	22.087	0.590	48.620	0.596	30.473	0.498	4.316	0.498	18.937	0.546
June	5.070	0.502	18.694	0.540	68.874	0.564	26.741	0.516	4.247	0.475	20.564	0.545
July	4.271	0.283	16.304	0.514	80.475	0.527	24.557	0.448	4.170	0.386	20.928	0.396
August	4.003	0.437	17.319	0.576	77.787	0.459	24.703	0.537	4.768	0.429	20.549	0.585
September	5.567	0.530	17.249	0.461	73.359	0.538	25.010	0.407	3.790	0.419	19.761	0.498
October	7.668	0.590	10.901	0.467	65.409	0.459	24.631	0.608	2.248	0.364	18.086	0.510
November	8.460	0.607	13.812	0.442	53.745	0.620	21.823	0.458	2.143	0.466	11.449	0.301
December	8.739	0.698	25.561	0.479	43.514	0.514	24.589	0.615	2.699	0.306	10.854	0.403

The data has been obtained at meteorological location/sites for parameters like global solar energy, sunshine hours, ambient temperature, wind speed, dew-point and relative humidity. The normalization/scaling of the input parameters has been done for avoiding convergence issues which are defined in 0.1 - 0.9 range and expressed by Eq. (4.1) for five meteorological sites across India.

$$L_s = \left[\left(\left(\frac{(X_{max} - X_{min})}{(L_{max} - L_{min})}\right)*(L - L_{min})\right) + X_{min}\right] \quad (4.1)$$

where

L = measured data

L_s = scaled data

L_{max} = highest value of relevant set of data

L_{min} = lowest value of relevant set of data

X_{max} = maximum limit of normalized range

X_{min} = minimum limit of normalized range

4.3.2 Classification of Sky-Conditions

The models based on sky-conditions can be classified as follows [87]:

(a) Clear/sunny sky (type-a)

If the sunshine hour is equivalent to or greater than 9 hour, and diffuse solar energy is lower than or equivalent to 25% of global solar energy.

(b) Hazy sky (type-b)

If the sunshine hour is between 7-9 hour and diffuse solar energy is lower than 50% or greater than 25% of global solar energy.

(c) Partially foggy/cloudy sky (type-c)

If the sunshine hour is between 5-7 hour and the diffuse solar energy is lower than 75% or greater than 50% of global solar energy.

(d) Fully foggy/cloudy sky (type-d)

If the sunshine hour is lower than 5 hour and the diffuse solar energy is greater than 75% of global solar energy.

4.4 DEVELOPMENT OF FUZZY LOGIC BASED MODEL FOR FORECASTING SOLAR ENERGY

The fuzzy logic based model has been employed for forecasting global solar energy with aid of meteorological parameters in different sky conditions and for distinct climate zones across India. The model has been developed with input parameters namely sunshine duration, relative humidity, wind speed, ambient temperature, dew point, latitude, longitude and altitude for forecasting global solar energy and shown below in Fig. 4.1. The results obtained are then defuzzified to get the forecasted output.

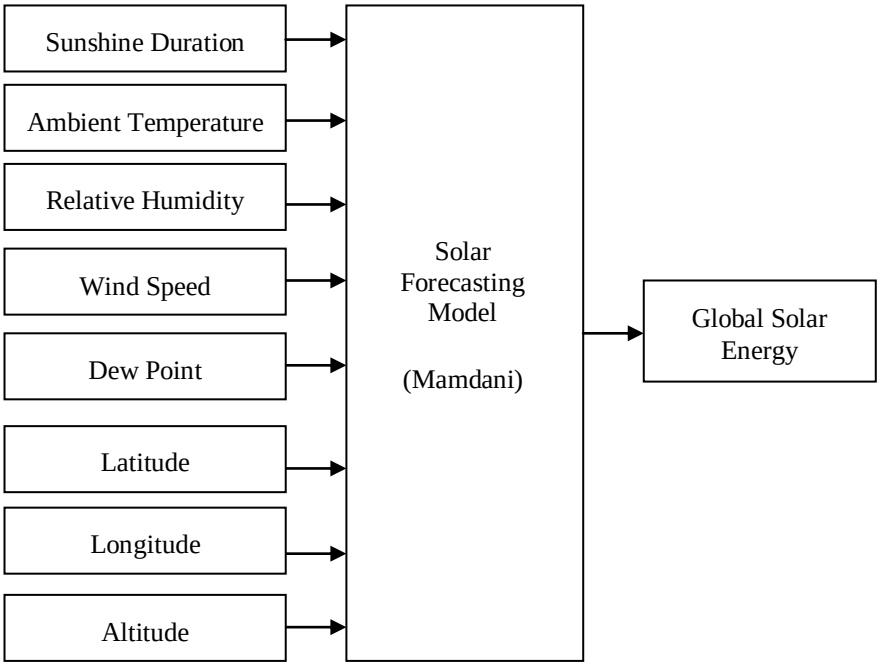

Fig. 4.1 Fuzzy logic based model for forecasting global solar energy

4.4.1 Fuzzy Sets

The theory of fuzzy logic has been introduced by Prof. Lotfi Zadeh in 1965 at University of California. Since, then it has been successfully implemented in many engineering applications. The concept of fuzzy logic lies in truth values between 0 and 1 i.e. between completely true and completely false. In conditions where mathematical models do not give practical descriptions of the models, approach based on fuzzy logic is being used for many applications.

Let A and B be two sets of universal set Y. The union between two sets is denoted by A∪B and represents all the elements in the universe belonging to set A, set B or both sets A and B. The intersection of two sets is denoted by A∩B and represents all the elements in the universe belonging to both set as A and B. Here, characteristic function μ_p of a subset of universal set Y lies in the two element sets {0,1} and $\mu_p(Y) = 1$, if YεP otherwise it's value is zero. The value of the fuzzy set P lies in the interval {0,1}. Now, μ_p is defined as the membership function and $\mu_p(Y)$ is the grade of membership function of yεY in P.

Consider fuzzy subsets A and B with membership function as μ_A and μ_B. The union and intersection can be defined as follows:

$$\text{Union: } \mu_{A\cup B}(Y) = \max [\mu_A(Y), \mu_B(Y)]$$

$$\text{Intersection: } \mu_{A\cap B}(Y) = \min [\mu_A(Y), \mu_B(Y)]$$

4.4.2 Fuzzy Inference System

A fuzzy inference system defines a mechanism for evaluating fuzzy system for calculating output from input data sets and is represented by input and output linguistic variables along with fuzzy IF-THEN rule base defined by

rule editor and rule viewer as shown in Fig. 4.2. It consists of fuzzification, fuzzy rules evaluation and defuzzification.

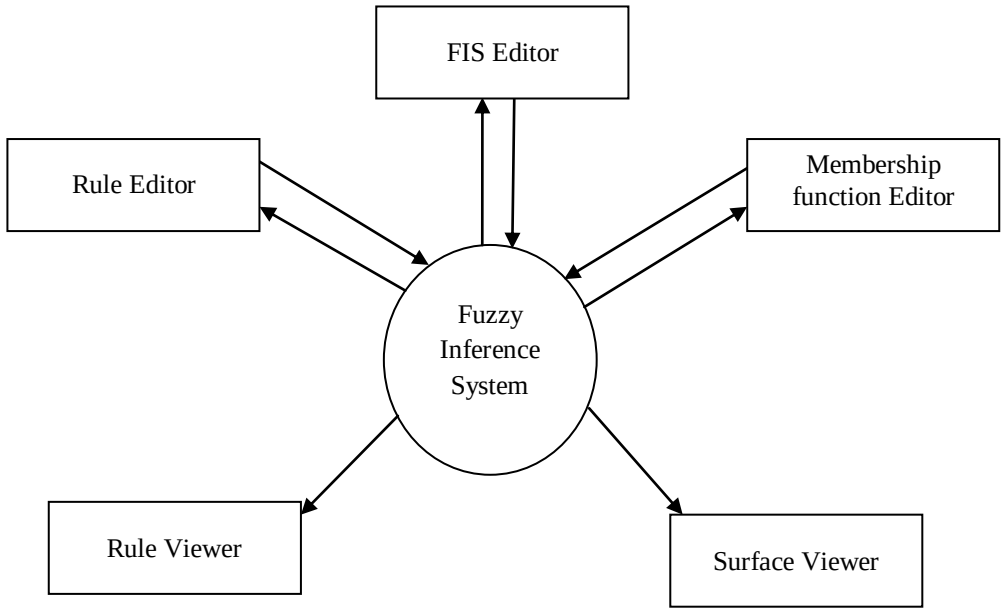

Fig. 4.2 Block diagram of fuzzy inference system

4.4.3 Fuzzy Membership Function

The model based on fuzzy logic approach for forecasting global solar energy has been established and simulated in MATLAB where the developed model comprises set of rules being made for qualitative descriptions. In the proposed model based on fuzzy logic approach, three variables are defined namely low, medium and high. The assignment of the membership function is the key task. In this, five membership functions are described with fuzzy terms namely Very Low (VL), Low-Medium/Low (LM/L), Medium-High/Medium (MH/M), High-High/High (HH/H) and Very High (VH) which lies in 0.1 - 0.9 range and fuzzy inference system defined a set of rules for forecasting global solar energy. Fig. 4.3 - Fig. 4.4 presents the fuzzy membership function for parameters namely wind speed and sunshine duration respectively.

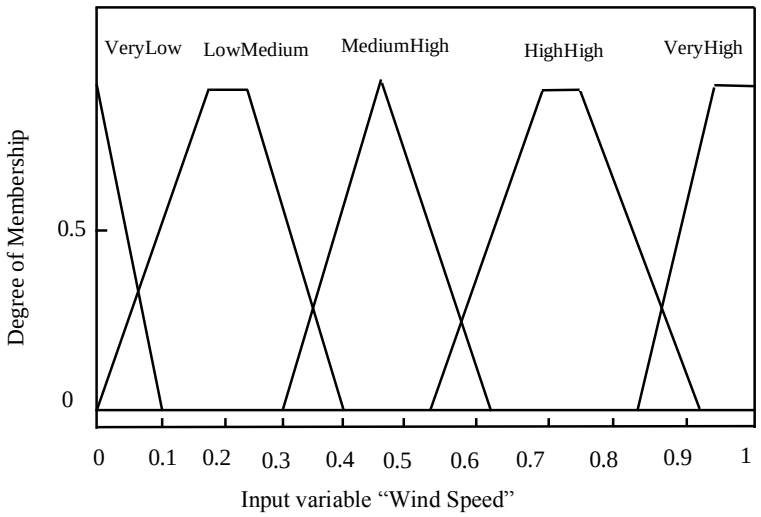

Fig. 4.3 Fuzzy membership functions for wind speed

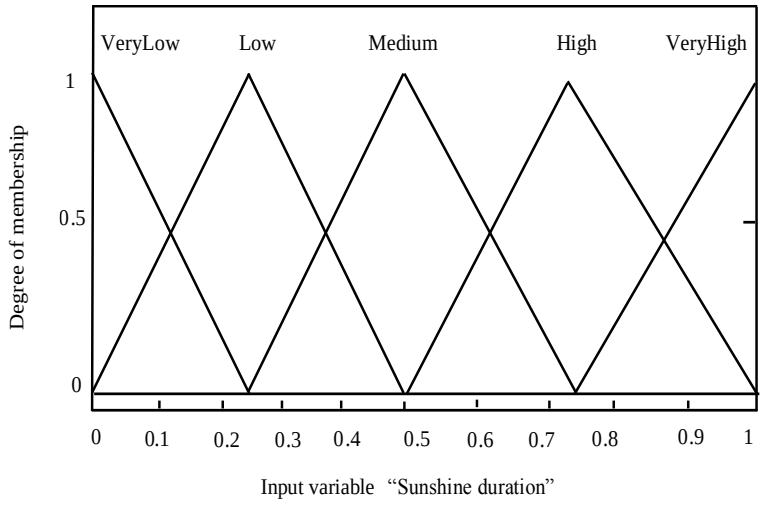

Fig. 4.4 Fuzzy membership functions for sunshine duration

4.4.4 Fuzzy Rules

The MATLAB fuzzy logic toolbox has been used for implementing the defined fuzzy rules which are fired in fuzzy systems with aid of fuzzy inference system.

The design of fuzzy system refers to the development of mechanisms for fuzzy information processing and decision making capability within a digital platform and soft computing environment.

The fuzzy inference algorithm implements IF-THEN rules or statements which are used to formulate the condition statement comprising fuzzy logic. A fuzzy rule base has IF-THEN components where the IF part is denoted as an antecedent and the THEN part is denoted as a consequent. The basic structure of fuzzy IF-THEN rule is expressed as:

IF <antecedent> THEN <consequent>

Here, a set of multiple-antecedent fuzzy rules have been defined for forecasting global solar energy where the input includes sunshine duration, wind speed, ambient temperature, relative humidity, dew-point and the output is global solar energy as shown in Table 4.6.

Further, the fuzzy rule base simulated in MATLAB for the month of January for warm and humid climate zone (Chennai) have been shown in Fig. 4.5. Similar analysis has been carried out for remaining period i.e. from February to December and for other climate zones i.e. hot and dry (Jodhpur), cold and cloudy (Shillong), moderate (Pune) and composite (Delhi) climate zone respectively.

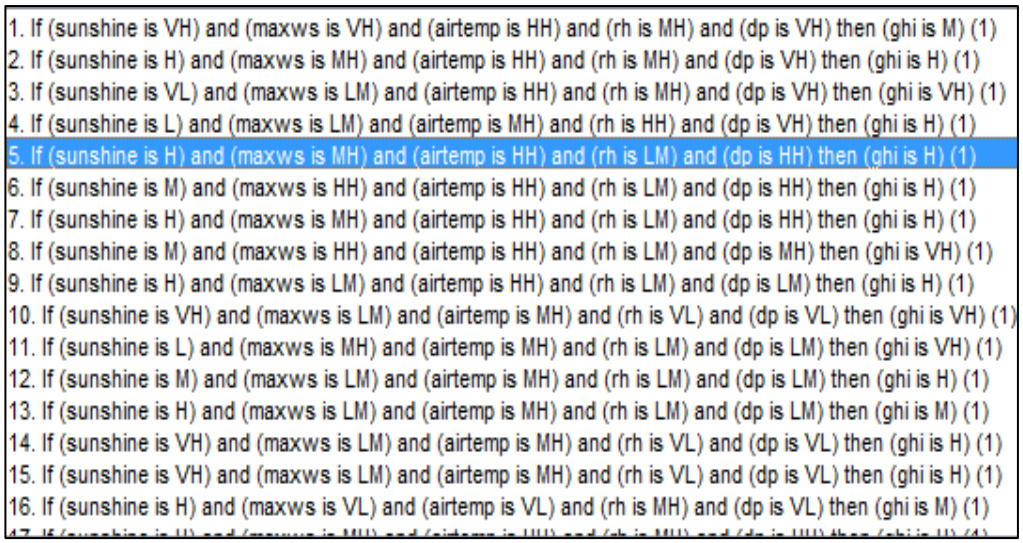

Fig. 4.5 Fuzzy rule base simulated in MATLAB

Table 4.6 Fuzzy rule base defined for the month of January for warm and humid climate zone

No. of days in month	Inputs					Output
	Sunshine hours	Wind Speed	Ambient Temperature	Relative Humidity	Dew Point	Global Solar Energy
1	VH	VH	HH	MH	VH	M
2	H	MH	HH	MH	VH	H
3	VL	LM	HH	MH	VH	VH
4	L	LM	MH	HH	VH	H
5	H	MH	HH	LM	HH	H
6	M	HH	HH	LM	HH	H
7	H	MH	HH	LM	HH	H
8	M	HH	HH	LM	MH	VH
9	H	LM	HH	LM	LH	H
10	VH	LM	MH	VL	VL	VH
11	L	MH	MH	LM	LH	VH
12	M	LM	MH	LM	LH	H
13	H	LM	MH	LM	LH	M
14	H	LM	MH	LM	LH	M
15	VH	LM	MH	VL	VL	H
16	H	VL	VL	MH	VL	M
17	H	MH	HH	MH	HH	H
18	H	LM	HH	LM	HH	H
19	VH	MH	HH	MH	VH	M
20	VH	MH	HH	VH	VH	L
21	H	LM	VH	MH	VH	M
22	M	MH	HH	VH	VH	VL
23	H	HH	MH	VH	VH	L
24	H	VH	HH	HH	VH	M
25	H	MH	HH	MH	VH	H
26	VH	LM	HH	MH	VH	H
27	VH	LM	MH	MH	HH	H
28	VH	VL	HH	MH	HH	H
29	VH	LM	VH	MH	VH	H
30	VH	LM	VH	MH	VH	H
31	VH	LM	VH	MH	VH	H

4.4.5 Fuzzy Editor Viewer

The fuzzy editor viewer in MATLAB has been used for viewing output. Further, Fig. 4.6 shows output corresponding to 5th rule in an editor viewer of MATLAB.

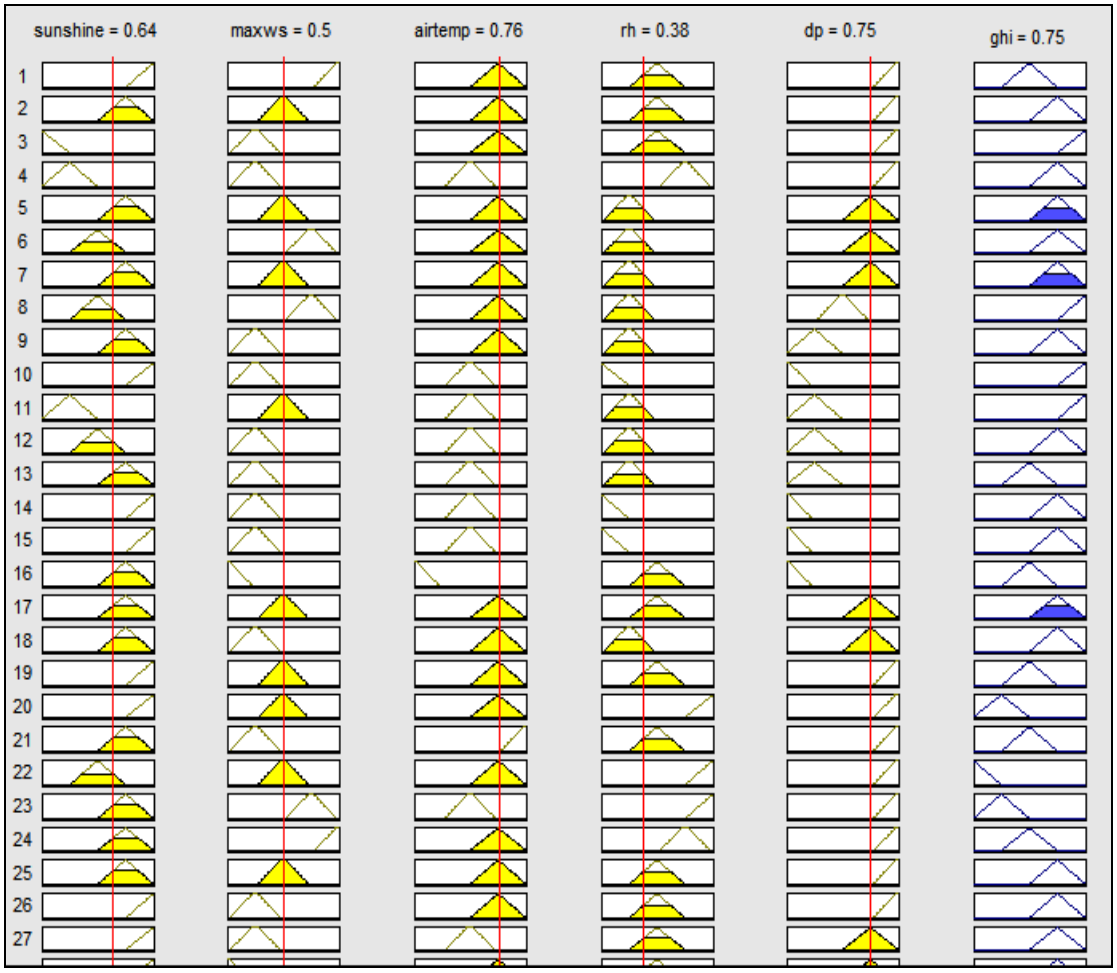

Fig. 4.6 Fuzzy editor viewer corresponding to 5th rule in MATLAB

4.5 RESULTS AND DISCUSSIONS

In this chapter, models based on sky-conditions such as clear sky (type-a), hazy sky (type-b), partially foggy/cloudy sky (type-c) and fully foggy/cloudy sky (type-d) employing fuzzy logic approach has been developed and presented for forecasting global solar energy with aid of meteorological parameters namely dew-point along with other known available parameters namely wind speed, duration of sunshine hours, global solar energy, ambient temperature and relative

humidity. A comparative analysis has been carried out between the measured and the forecasted data for five meteorological sites which represents different climatic conditions such as warm and humid, hot and dry, cold and cloudy, composite and moderate climate zone based on statistical indicators as shown in Table 4.7 from which, the following can be briefly summarized:-

4.5.1 Clear/Sunny Sky (Type-a)

The fuzzy logic based model has been employed for forecasting global solar energy, wherein for this sky-condition, the minimum value of mean percentage error is observed to be 1.23% and obtained for hot and dry climatic conditions (Jodhpur) as shown by the calculated data presented in Table 4.7.

The minimum error has been obtained for this climate climate zone beacause Jodhpur climatic conditions are hot and dry with relative humidity varying from 33 - 74% as shown by the measured data presented in Table 4.3, which is generally low, because of low water surface bodies and vegetation.

For this sky condition, the sky is generally clear with a large amount of solar insolation at day time since the surrounded atmospheric region gets heated up very fast. It has been also observed that the average sunshine hour is approximately 12.36 hrs, which is comparatively high as compared to other meteorological sites as shown by the computed data presented in Table 4.7. At night time also, there is a clear sky, therefore, the heat absorbed by the surface at day time gets dissipated in upper atmospheric region fast. Hence, at night time, the ambient temperature is low which makes the atmospheric surface much cooler.

Jodhpur is well famous as the ‘Sun City’ for clear/sunny sky-conditions prevailing throughout the year.

Table 4.7 Fuzzy logic based model for forecasting global solar energy for distinct climate zone

Climate Zone	Sky Conditions	H_g (MJ/m^2)		Sunshine hours (hrs)	MPE (%)	MBE (%)
		Measured	Fuzzy			
New Delhi (Composite)	Clear/Sunny Sky	29.96	30.20	9.30	1.94	0.24
	Hazy Sky	29.71	29.76	8.09	0.22	0.05
	Partially Foggy/Cloudy Sky	23.93	23.88	6.30	1.96	-0.05
	Fully Foggy/Cloudy Sky	23.13	22.54	0.30	-2.56	-0.59
Chennai (Warm and Humid)	Clear/Sunny Sky	38.60	36.80	10.28	-4.32	-1.80
	Hazy Sky	32.98	36.49	8.58	6.82	0.07
	Partially Foggy/Cloudy Sky	37.93	37.50	6.61	-0.80	-0.43
	Fully Foggy/Cloudy Sky	34.79	35.73	2.26	5.79	0.94
Jodhpur (Hot and Dry)	Clear/Sunny Sky	38.63	37.81	12.36	-1.23	-0.82
	Hazy Sky	36.93	36.35	8.67	1.39	-0.57
	Partially Foggy/Cloudy Sky	35.35	31.72	6.63	-7.90	-3.63
	Fully Foggy/Cloudy Sky	36.56	38.58	2.84	4.39	2.02
Shillong (Cold and Cloudy)	Clear/Sunny Sky	31.30	30.12	9.546	-2.74	-1.18
	Hazy Sky	24.48	25.45	7.256	5.77	0.97
	Partially Foggy/Cloudy Sky	26.25	26.25	4.443	9.05	-0.002
	Fully Foggy/Cloudy Sky	32.68	32.41	1.200	0.36	-0.30
Pune (Moderate)	Clear/Sunny Sky	20.25	20.61	10.12	4.75	0.28
	Hazy Sky	19.70	19.68	8.46	0.89	0.26
	Partially Foggy/Cloudy Sky	18.89	18.94	6.08	1.78	0.04
	Fully Foggy/Cloudy Sky	16.42	16.01	2.85	-0.89	-0.41

4.5.2 Hazy Sky (Type-b)

For this sky-condition, by employing fuzzy logic based model, the minimum value of mean percentage error is observed to be 0.22% and has been obtained for composite climatic conditions (Delhi) as shown by the computed data presented in Table 4.7. This is due to the reason that relative humidity is high which varies 35 - 61% in dry periods and 64 - 81% in wet periods as shown by the measured data presented in Table 4.1. It has been also observed that during monsoon the solar insolation intensity is low and during summer the solar intensity is high as the average sunshine hour measured is 8.09 hrs, as shown by the computed data presented in Table 4.7, which when compared to Jodhpur station is comparatively lesser.

For this sky condition, the sky is generally dull and overcast in monsoon and becomes hazy during summer.

4.5.3 Partially Foggy/Cloudy sky (Type-c)

For this sky-condition, by employing fuzzy logic based model, the minimum value of mean percentage error is observed to be 0.80% and has been obtained for warm and humid climatic conditions (Chennai) as shown by the computed data presented in Table 4.7. The reason behind is that diffuse solar energy is high due to cloud cover and because of presence of clouds the heat dissipation from the earth's surface to the sky during the night is least. Hence, during summer, the sky is partially cloudy as variation in ambient temperature is from 30-35^{o}C during the day and 25-30^{o}C during the night. The variation in maximum ambient temperature is from 25-30^{o}C in day time and 20-25^{o}C in night time during the winter season. It has been observed for this climate zone

that the relative humidity varies from 58-74% in a year, which is generally high as shown by the measured data presented in Table 4.2 and the averaged sunshine hours are 6.61 hrs only.

4.5.4 Fully Foggy/Cloudy Sky (Type-d)

For this sky-condition, by employing fuzzy logic based model, the minimum value of mean percentage error is observed to be 0.36% and has been obtained for cold and cloudy climatic conditions (Shillong) as shown by the computed data presented in Table 4.7.

This is due to the reason that during winter, the solar insolation is quite low due to the presence of diffuse solar energy which makes winters extremely cold. The summers are comparatively quite pleasant as the variation in maximum air temperature lies between 25 - 30^{o}C during day time and 17 - 27^{o}C during night time whereas the winters are comparatively chilly.

It has been also observed from the measured data presented in Table 4.4, that the variation in relative humidity is from 50 - 85% which is generally high. For this climate zone, the sky is generally cloudy and overcast throughout the year except for short summer where the daily measured bright sunshine hour availability is 1.20 hrs only as shown by the data presented in Table 4.7.

Further, the graphical analysis of comparison of the measured and forecasted data by employing fuzzy logic based for different sky-conditions and for distinct climate zone across India has been shown in Fig. 4.7 - Fig. 4.11 respectively.

For composite climate zone (Delhi), as shown in Fig. 4.7(b), the hazy sky model perform better than other models as the forecasted data is almost same as that of the measured data.

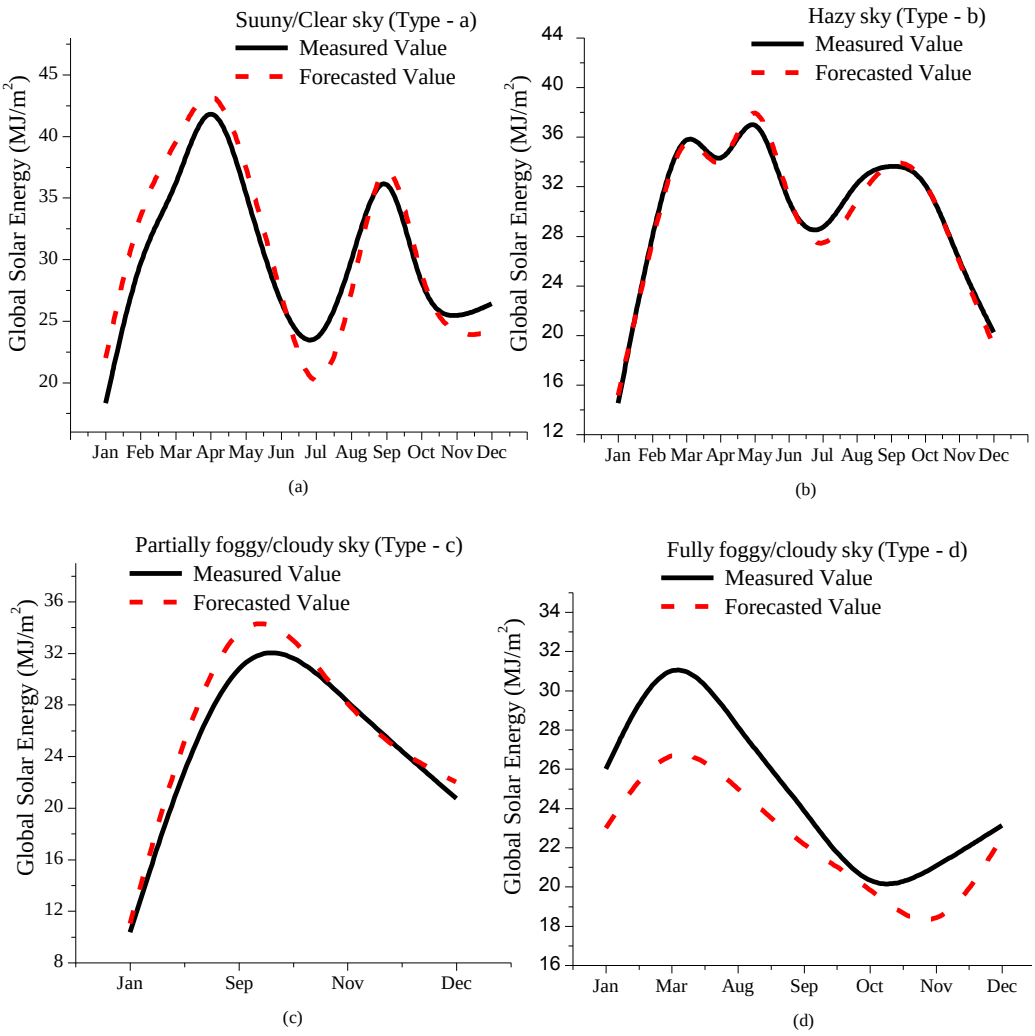

Fig. 4.7 Graphical analysis of the measured and forecasted H_g for composite climatic conditions

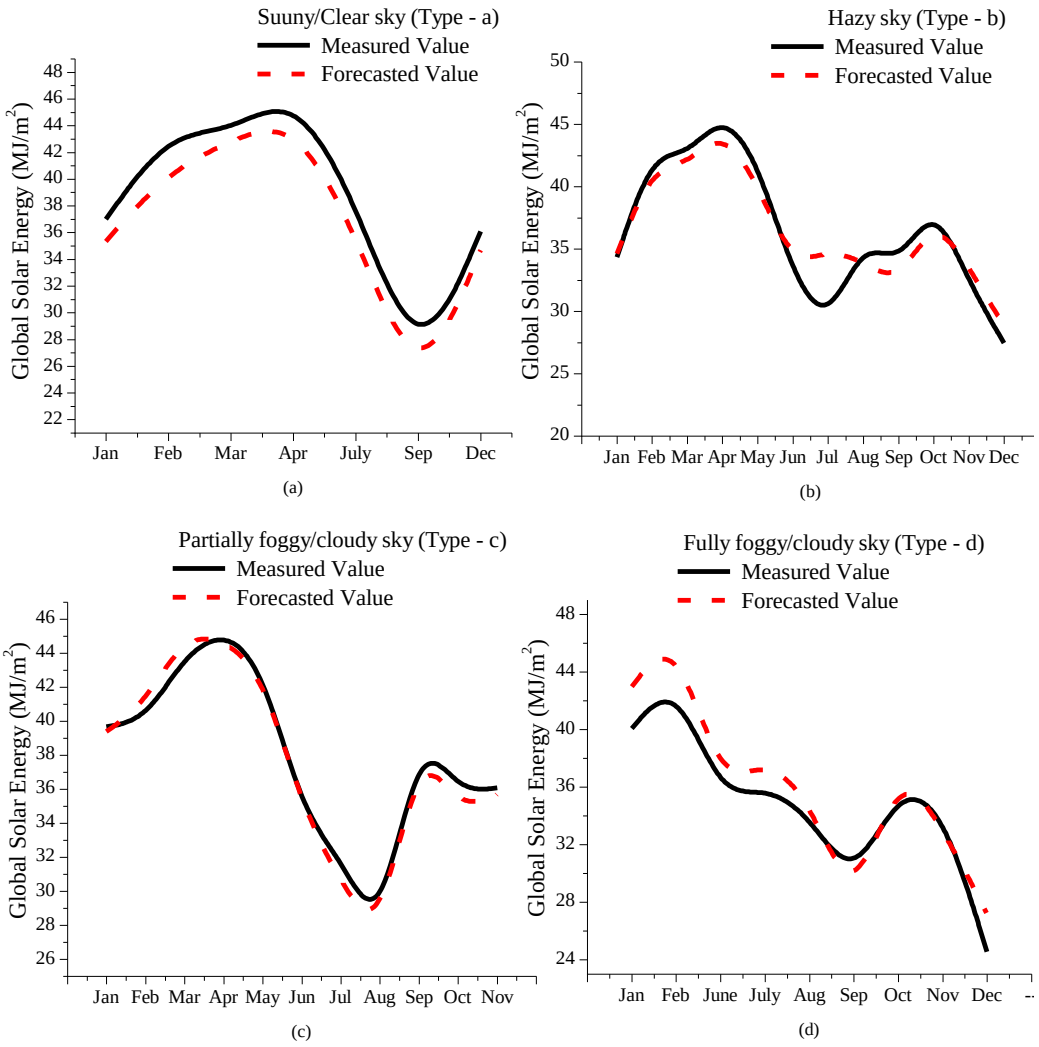

Fig. 4.8 Graphical analysis of the measured and forecasted H_g for warm and humid climatic conditions

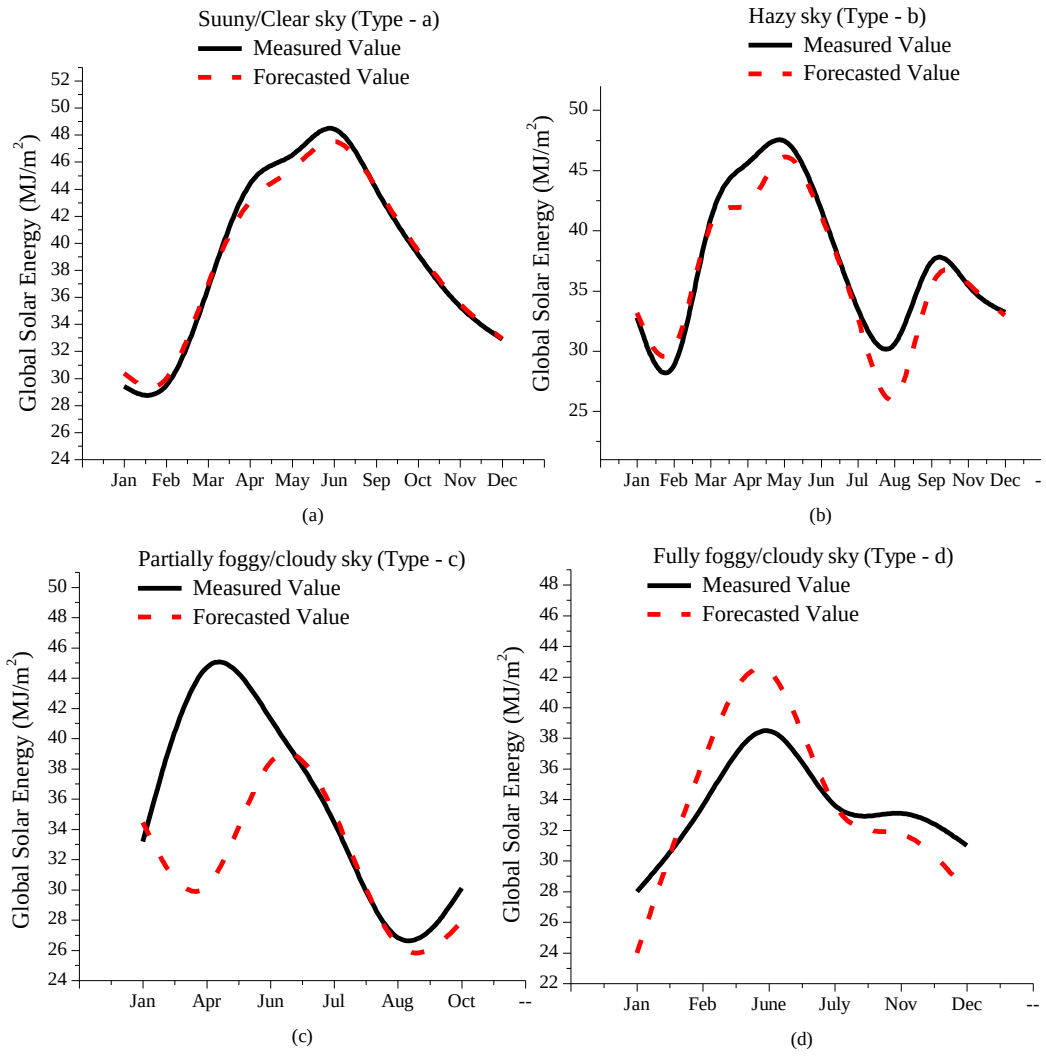

Fig. 4.9 Graphical analysis of the measured and forecasted H_g for hot and dry climatic conditions

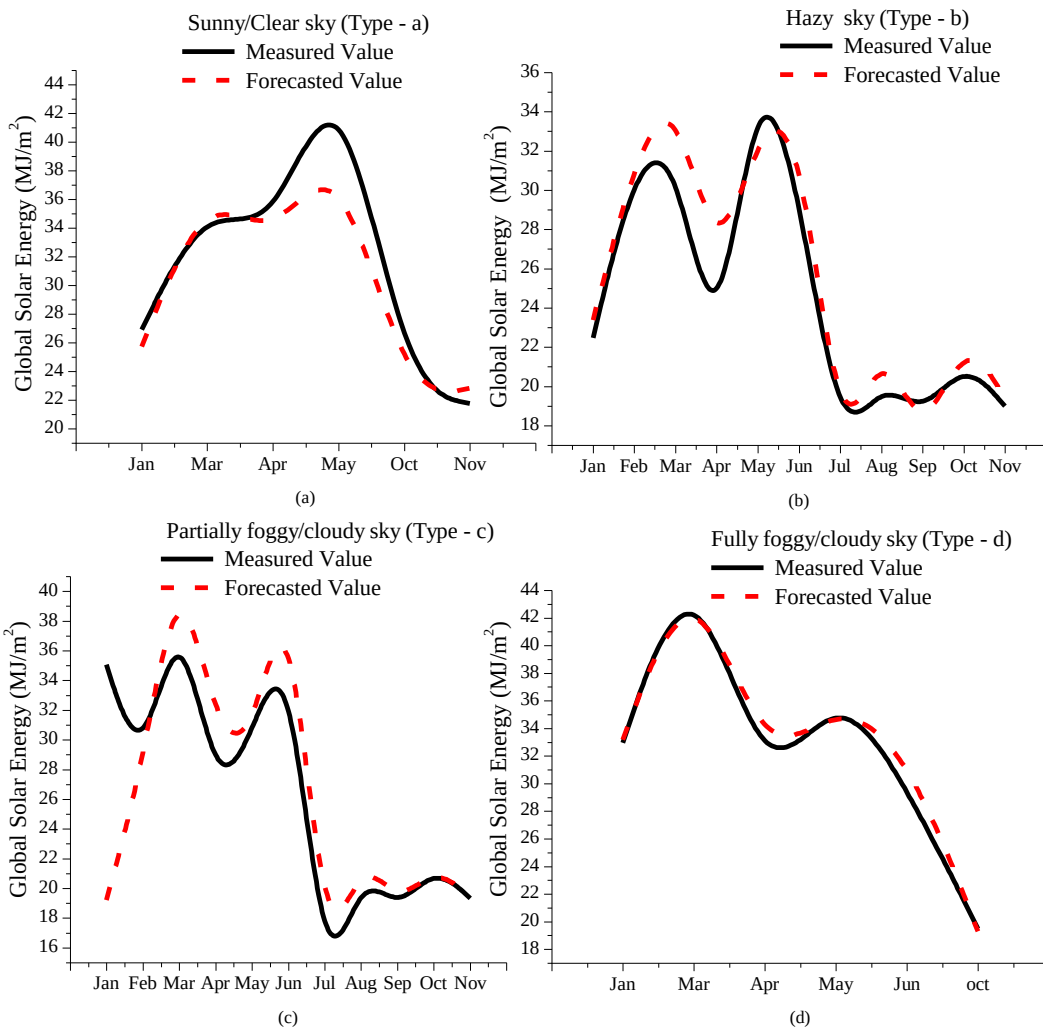

Fig. 4.10 Graphical analysis of the measured and forecasted H_g for cold and cloudy climatic conditions

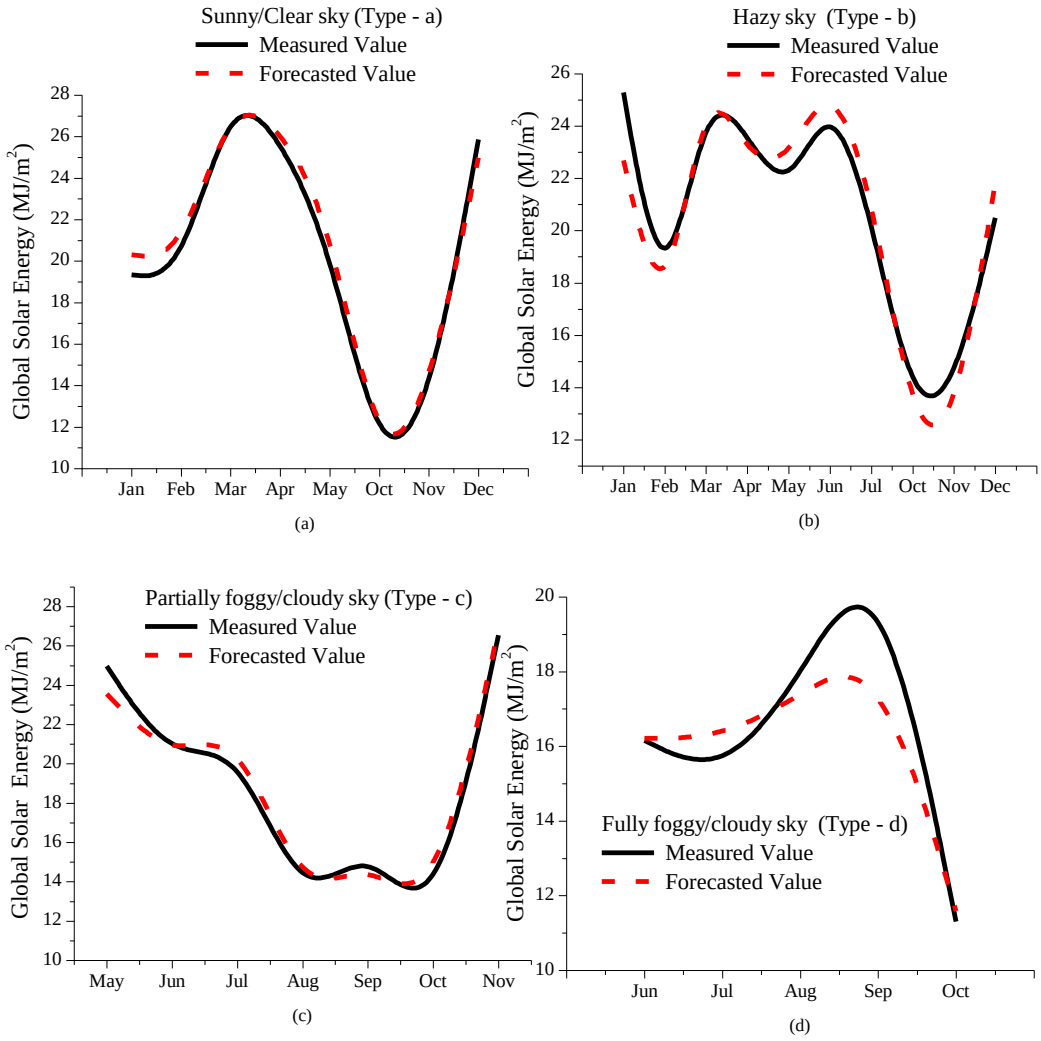

Fig. 4.11 Graphical analysis of the measured and forecasted H_g for moderate climatic conditions

For hot and dry climate zone (Jodhpur), as shown in Fig. 4.9(a), sunny/clear sky model perform better than other models as the forecasted data is almost same as that of the measured data.

Similarly, for warm and humid climatic zone (Chennai), as shown in Fig. 4.8(c), partially foggy/cloudy sky model perform better than other models as the forecasted data is almost same as that of the measured data.

Also, for cold and cloudy climate zone (Shillong), as shown in Fig. 4.10(d), fully foggy/cloudy sky model perform better than other models as the forecasted data is almost same as that of the measured data.

4.6 APPLICATION OF SOLAR ENERGY FORECASTING IN SOLAR PV SYSTEM

The power generation in solar PV system is dependent on certain factors namely cell temperature, solar irradiance and the topographical position. In this chapter, HIT solar PV module of 210 W_p power output is selected whose performance specifications are listed in Table A.2 of Appendix A and operated at MPPT conditions. Since, the power generation has been greatly affected by solar irradiance and ambient temperature, therefore, such parameters are taken into consideration. The data which includes solar irradiance, cell temperature and PV power has been obtained and arranged within 1 hour. During the summer season, the availability of sunshine hours is from morning 6:00 A.M. to 18:00 P.M. in the evening, the data are collected on daily basis with the availability of solar irradiance. Similarly, during winter season, the variation is from morning 8:00 A.M. to evening 17:00 P.M. Fuzzy logic methodology has been employed for forecasting power output in solar PV system. The fuzzy inference system includes input parameter like solar irradiance, ambient

temperature and weather descriptions, follows fuzzification, rule evaluation and lastly, results has been defuzzified for PV power forecasting.

Based on Standard Test Condition (STC) conditions, and influenced by parameters namely solar irradiance and cell temperature, the solar PV power generation can be expressed by using Eq. (4.2) – Eq. (4.3) as:

$$P_{PV} = \left[P_{PV,STC} * \frac{G_T}{1000} * \ [1 - \gamma * (T_j - \ 25)]\right] * N_{PVs} \ * \ N_{PVp} \tag{4.2}$$

$$\text{and } T_j = \ T_m + \frac{G_T}{800} * (N_{OCT} \text{ - } 20) \tag{4.3}$$

where $P_{PV,STC}$ represents the rated power output of solar PV system of single array at Maximum Power Point (MPP), P_{PV} is the solar PV array power output at MPP, G_T is solar irradiance at STC in W/m^2, N_{PVS} represents the series PV arrays, γ is temperature parameter at Maximum Power Point (MPP), N_{PVP} represents the parallel PV arrays, T_m is ambient temperature in ^{o}C, T_j is the temperature of the solar panel in ^{o}C and N_{OCT} is a constant.

The solar PV power output can be forecasted by using fuzzy logic based model as shown below in Fig. 4.12.

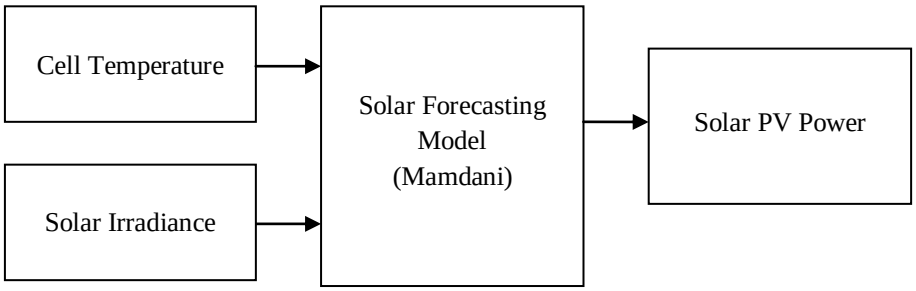

Fig. 4.12 Fuzzy logic based model for PV power forecasting

In this, 210 W_p HIT solar PV modules have been chosen and operated at MPPT conditions. The input parameters include solar irradiance, cell temperature and sky information obtained from NISE and power is the output parameter. The forecasted PV power has been obtained by employing fuzzy logic methodology and is illustrated in Table 4.8 for composite climate zone.

Table 4.8 Forecasted power in solar PV system under composite climatic conditions

Month	**V_{oc} (V)**	**I_{sc} (A)**	**Solar Irradiance (W/m^2)**	**Cell Temperature (^oC)**	**Power (W)**		**MPE (%)**
					Measured	**Forecasted**	
January	81.47	0.42	361.15	28.14	20.80	19.79	-0.0064
February	82.03	0.61	461.52	35.69	30.15	30.02	0.0060
March	83.64	0.62	548.24	40.12	31.56	31.25	0.0100
April	79.62	0.60	575.12	42.53	30.23	32.56	0.1500
May	77.35	0.59	559.67	46.22	31.05	35.19	0.1938
June	76.92	0.55	537.17	45.24	26.20	26.00	0.0166
July	76.66	0.05	537.81	48.28	24.45	25.72	0.0023
August	76.90	0.47	428.80	53.27	22.33	22.59	0.0308
September	77.78	0.50	437.51	51.62	23.80	23.99	0.0378
October	78.74	0.63	466.57	53.21	29.92	29.40	-0.0090
November	78.48	0.44	369.82	45.08	20.85	20.65	-0.0173
December	80.66	0.47	370.84	43.36	25.53	32.57	0.2827
Average	79.19	0.50	471.18	44.40	26.41	27.48	**0.0581**

The result obtained in Table 4.8 reveals that the mean percentage error obtained for solar PV system averaged month-wise is 0.0581% by using fuzzy logic based model which is observed within the permissible error limit.

Further, it is to be noted that for the winter season (January), the mean percentage error is 0.0064%; for the rainy season (May), the mean percentage error obtained is 0.1938% which is comparatively large because of the large uncertainties associated with the data and mean percentage error for summer season (June) is 0.0166%.

4.7 FUZZY LOGIC APPROACH FOR SHORT-TERM PV POWER FORECASTING

Further, the variation in sky-condition has influenced the forecasting pattern of solar energy. Sunny/clear sky (type-a), hazy sky (type-b), partially foggy/cloudy sky (type-c) and fully foggy/cloudy (type-d) sky-conditions have been considered. The performance evaluation of the models has been done using statistical error-tests and obtained results are illustrated in Table 4.9.

From Table 4.9, it has been observed that for composite climatic conditions, the hazy-sky model provide better results with mean percentage error of 0.0031%, followed by the sunny-sky model, partially foggy/cloudy sky model and fully foggy/cloudy sky model with mean percentage error of 0.0741%, 0.0072% and 0.0077%, respectively.

After the detailed analysis, the average forecasting errors of the proposed model are 0.023% in mean percentage error for the sample photovoltaic installation.

Table 4.9 Short-term PV power forecasting using fuzzy logic approach under composite climatic conditions

Sky-Conditions	Time (hr)	Solar Irradiance (W/m^2)	Cell Temp. (^oC)	Power (W)		MPE (%)
				Measured	Forecasted	
Sunny/Clear Sky (Type-a)	7:00	140.93	34.11	7.00	7.03	0.0036
	8:00	273.76	40.55	15.00	15.00	-0.0002
	9:00	486.12	48.14	30.33	30.34	0.1749
	10:00	625.25	52.23	41.67	41.66	0.1210
	11:00	783.13	57.79	54.17	54.18	0.1271
	12:00	875.34	62.86	60.50	60.50	0.0702
	13:00	888.95	64.69	61.17	61.18	-0.0060
	14:00	744.96	63.91	42.00	42.00	-0.3153
	15:00	726.73	61.55	46.33	46.33	0.3563
	16:00	549.15	58.04	31.50	31.51	-0.3178
	17:00	361.60	52.72	19.33	19.33	-0.4892
	18:00	204.59	48.83	9.80	9.80	-0.6141
	Avg.	**555.04**	**53.79**	**34.90**	**34.90**	**-0.0741**
Hazy Sky (Type-b)	10:00	123.10	40.83	7.00	7.12	0.0218
	11:00	146.12	44.49	9.67	9.70	0.0040
	12:00	307.56	43.56	24.17	24.20	0.0031
	13:00	519.54	52.55	45.50	45.46	-0.0008
	14:00	467.65	42.40	37.33	37.40	0.0018
	15:00	313.06	49.36	21.50	21.50	0.0003
	16:00	185.35	41.05	10.20	10.09	-0.0082
	Avg.	**294.62**	**44.89**	**22.20**	**22.21**	**0.0031**
Partially foggy/cloudy Sky (Type-c)	8:00	134.08	45.79	10.25	10.26	0.0024
	9:00	179.69	47.49	13.00	12.99	-0.0021
	10:00	355.98	52.07	30.33	30.14	-0.0063
	11:00	463.45	55.57	40.17	40.78	0.0130
	12:00	547.32	58.38	44.67	44.39	-0.0117
	13:00	519.74	59.96	33.00	31.40	-0.0372
	14:00	492.69	55.52	41.00	40.93	-0.0001
	15:00	647.10	61.30	52.00	51.69	-0.0105
	16:00	562.02	59.64	34.67	35.16	0.0094
	17:00	299.99	50.88	18.17	18.22	0.0049
	18:00	235.30	50.73	12.83	12.65	-0.0158
	19:00	156.43	47.99	6.50	7.23	0.1405
	Avg.	**382.82**	**53.78**	**28.05**	**27.99**	**0.0072**
Fully foggy/cloudy Sky (Type-d)	9:00	170.77	19.08	10.67	10.75	0.0120
	10:00	74.87	19.02	10.67	10.62	-0.0030
	11:00	96.49	23.29	9.00	8.72	-0.0042
	12:00	41.20	18.50	8.00	8.10	0.0105
	13:00	140.77	18.57	10.33	10.46	0.0500
	14:00	87.31	18.59	11.17	11.14	0.0067
	15:00	164.25	17.86	11.00	10.83	-0.0183
	Avg.	**110.81**	**19.27**	**10.12**	**10.09**	**0.0077**

Further, the graph presented in Fig. 4.13 shows the variation in the measured and the forecasted data for different sky-conditions.

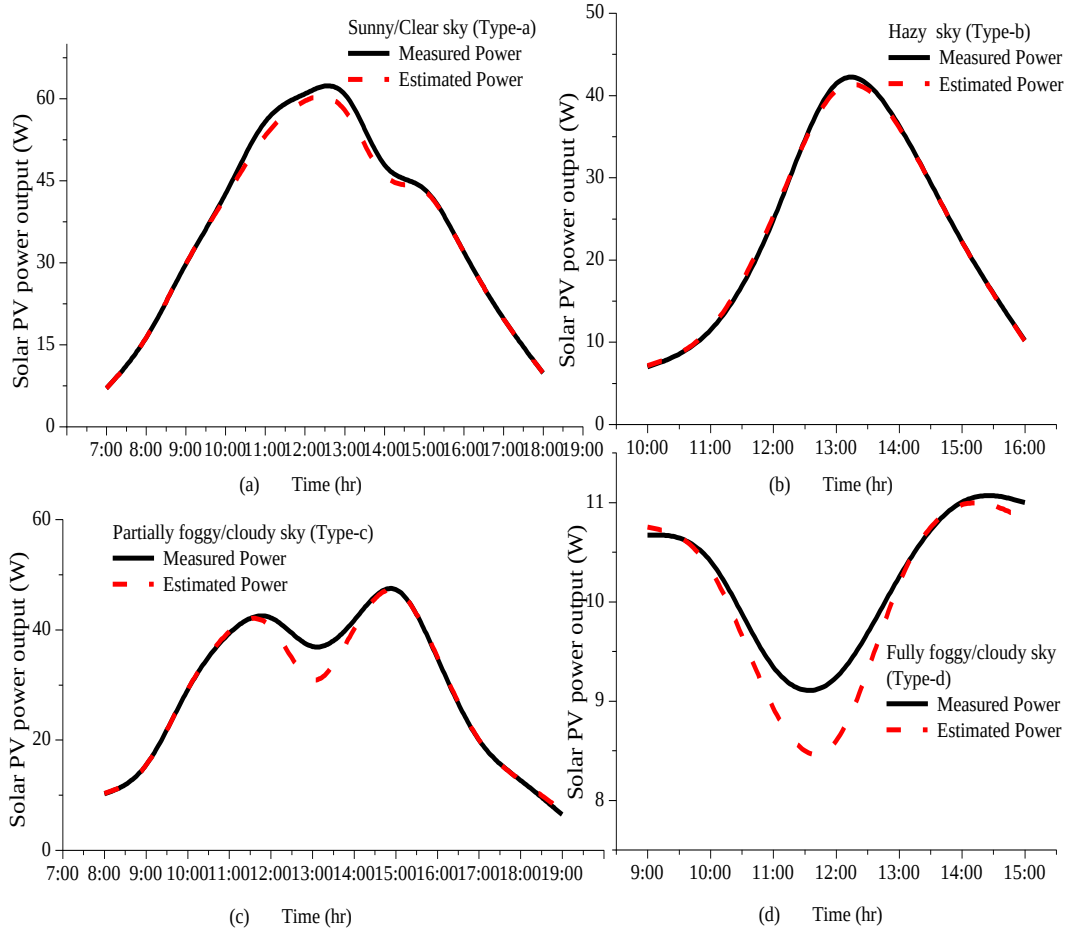

Fig. 4.13 Graphical analysis of short-term PV power forecasting under composite climatic conditions

Normally, the day considered here is the different combination of sunny, hazy, partially foggy/cloudy and fully foggy/cloudy sky-conditions periods considered during the day time. For the sunny/clear day, Fig. 4.13(a) shows the graphical analysis between the measured and forecasted data variation based on fuzzy logic modelling. For this sky-condition, as compared to temperature factor, a factor of time is important which majorly influenced the solar energy and the time considered is from 7:00 A.M. to 18:00 P.M. in the

evening and the day averaged mean percentage error is observed to be 0.0741% as shown by the measured data presented in Table 4.9.

For hazy sky-condition, Fig. 4.13(b) shows the graphical analysis between measured and forecasted data based on fuzzy logic modelling. For this sky-condition, sun rays will get blocked as the factor of temperature affect solar energy in comparison to a factor of time and the time considered is from morning 10.00 A.M. to 16.00 P.M. in the evening and the day averaged mean percentage error is observed to be 0.0031% for this sky-condition. The maximum value of solar irradiance is 519.54 W/m^2 as shown by the measured data presented in Table 4.9.

In partially foggy/cloudy sky-condition, Fig. 4.13(c) represents the graphical analysis between the measured and the forecasted data based on fuzzy logic modelling. For this sky-condition, the sunshine is partly absorbed by the PV and partly by the cloud. Solar energy is correlated with both the factor of temperature and time, and the considered time period is from morning 8:00 A.M. to 19:00 P.M. in the evening. The day average mean percentage error is observed to be 0.0072% as shown by the measured data presented in Table 4.9.

For fully foggy/cloudy day, Fig. 4.13(d) shows the graphical analysis between the measured and forecasted data based on fuzzy logic modelling. The maximum value of solar irradiance is 164.25 W/m^2 and the time considered is from morning 9:00 A.M. to 15:00 P.M. in the evening. In this, the sun rays will get fully blocked by the presence of cloud and both the factor of time and temperature will affect solar irradiance. The day averaged mean percentage

error is observed to be 0.0077% as shown by the measured data presented in Table 4.9.

In addition, the industrial requirements have been satisfied as the short-term PV power forecasting mean percentage error is less than 20%. However, for each of the sky-model, the mean percentage error fluctuates, and the variation in mean percentage error between the measured and forecasted data in distinct sky-conditions during day time is presented below in Fig. 4.14.

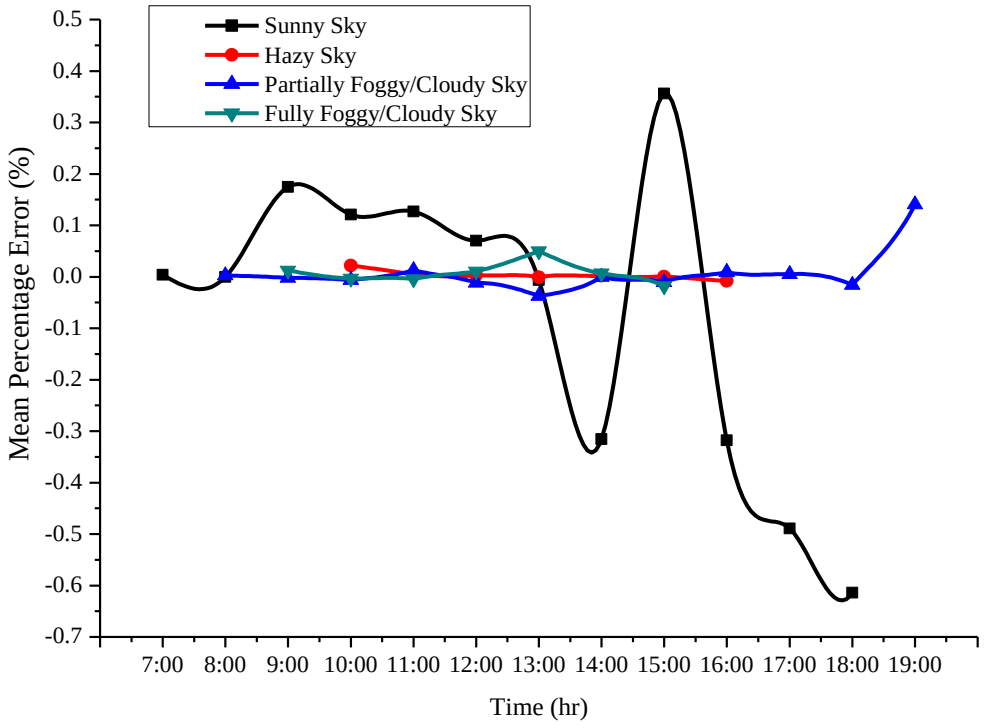

Fig. 4.14 Mean percentage error of four forecasting sky-based models

The variations in the error are highest for the sunny/clear sky model in comparison to other models and the reason behind is that the intensity of solar radiation is relatively large as compared to other models. It has been observed that out of the four models, especially the hazy-sky model as shown in Fig. 4.13(b) perform well in forecasting power of a solar PV system for composite climatic conditions.

4.8 COMPARISON OF FUZZY LOGIC BASED MODEL WITH EMPIRICAL MODELS

The developed model based on fuzzy logic approach has been compared with empirical models for widely changing climatic conditions across India and are reported in Table 4.10. The performance of models has been evaluated by using statistical error-tests.

Table 4.10 Comparison of proposed fuzzy logic based model with regression model

Station	Measured H_g (MJ/m^2)	Fuzzy		Regression	
		H_g (MJ/m^2)	MPE (%)	H_g (MJ/m^2)	MPE (%)
Delhi (Composite)	18.27	18.28	0.41	18.29	0.70
Chennai (Warm and Humid)	19.53	19.51	0.37	19.59	2.25
Jodhpur (Hot and Dry)	20.41	20.44	0.02	20.27	0.41
Shillong (Cold and Cloudy)	16.45	16.49	0.68	16.88	1.94
Pune (Moderate)	19.36	19.33	0.06	19.86	2.40

The results of simulation reveal that the fuzzy logic based model is accurate and has less value of mean percentage error for all meteorological stations across India as compared to regression models. So comparison result shows that the model developed by implementing fuzzy logic modelling provides accuracy and is convenient as compared to empirical models using multiple regression analysis.

4.9 CONCLUSION

In this chapter, model employing fuzzy logic approach based on sky-conditions have been developed and presented for global solar energy forecasting for five meteorological sites/locations representing distinct climate zones across India. The meteorological parameters namely dew-point has been considered along with other known available parameters namely sunshine duration, ambient temperature, relative humidity, wind speed and global solar energy. It has been concluded from the obtained results that the sunny/clear sky (type-a) model favours hot and dry climate zone (Jodhpur), hazy sky (type-b) model favours composite climate zone (Delhi), partially foggy/cloudy sky (type-c) model favours warm and humid climate zone (Chennai) and fully foggy/cloudy sky (type-d) model favours cold and cloudy climate zone (Shillong), respectively.

Further, the fuzzy logic based model has been implemented for solar photovoltaic applications and model based on sky-conditions employing fuzzy logic methodology have been presented for one-hour ahead PV power forecasting of solar PV system based upon the principle of fuzzy inference system and the characteristics of sky-condition classification. The results of correlation analysis shows that the forecasting errors of the proposed model are within the permissible error limit for the solar photovoltaic installation. It has been concluded from the obtained results that under composite climatic conditions, the hazy-sky model outperforms other models as the measured data closely matches the forecasted data followed by the sunny sky model, partially foggy/cloudy sky model and fully foggy/cloudy sky model. The fuzzy logic

approach favour results for the application of the sky-based model in forecasting PV power output of solar PV system.

Lastly, the developed model have been compared with the empirical models and the numerical results reveal that the proposed fuzzy logic based model achieves better accuracy and is convenient than the empirical models using multiple regression analysis.

CHAPTER 5

SOLAR ENERGY FORECASTING USING ANN-BASED MODEL

5.1 INTRODUCTION

In the previous chapter, the solar energy forecasting is performed using fuzzy logic methodology. This chapter is focussed on the variants of Artificial Neural Network (ANN) model i.e. Cascade-Forward Neural Network (CFNN), Feed-Forward Neural Network (FFNN), Generalized Regression Neural Network (GRNN), Elman Neural Network (ENN), Layered Recurrent Neural Network (LRNN), Linear Neural Network (LNN) and Radial Basis Function Neural Network (RBFNN) for modelling the system in forecasting global solar energy under composite climatic conditions using meteorological parameters. Simulations have been carried out by selecting the most suitable model based on evaluation indexes and further applied for sky-condition defined as sunny, hazy, partially and fully foggy/cloudy sky conditions and for distinct climatic zone across India. The developed model has been implemented for solar PV applications. Lastly, a comparison has been made with fuzzy logic based model to check for accuracy and supremacy of the proposed ANN model.

This chapter is partially based on the following published papers:

1. **Gulnar Perveen**, M. Rizwan and Nidhi Goel, "Comparison of intelligent modelling techniques for solar energy forecasting and its application in solar photovoltaic systems," **IET Energy Systems Integration**, Vol. 1, No. 1, pp. 34-51, 2019. ISSN No. 2516-8401(Online).

2. **Gulnar Perveen**, M. Rizwan and Nidhi Goel, "ANN modelling for estimating global solar energy and its implementation in Solar Thermal Systems," Proceedings of **International Conference on Renewable Energy and Sustainable Climate (Solaris 2019)**, Feb 07-09, 2019, Jamia Millia Islamia, Delhi, India.

Lot of research has been carried out across the globe for forecasting solar energy using ANN [89-91]. These models have been used in a broad series of applications which include optimum estimation and forecasting; least square optimization of numerical weather prediction; clustering and classification technique [92-94]. Further, several previous researchers have worked towards the accuracy in power forecasting of the solar PV system and wind speed forecasting. Recently, solar PV technology has been growing rapidly due to the benefits of solar energy which is available in abundance and is a clean form of energy.

Numerous factors influence the generation of power in a solar PV system namely solar irradiance, cell temperature, efficiency and sky-conditions. Because of the inconsistency in solar radiation and factors affecting environment such as sky-conditions, the power generation in a solar PV system is a stochastic process, which not only affects the stability of the system but the working capital and maintenance costs as well. So, to advance the solar PV system stability, accurately forecasting global solar energy is needed taking into consideration the influence of sky-conditions, since the accuracy of the solar PV system has been greatly affected by the external environmental factors such as clouds, moisture, dust and atmospheric temperature differences. The power forecasting can help a manufacturer's device some operational strategies or policies in a way that can achieve better management [95-106].

This chapter aims to establish different ANN models in forecasting global solar energy using meteorological parameters namely dew-point, sunshine duration, wind speed, global solar energy, relative humidity and ambient temperature under composite climatic conditions. Cascade-forward

back propagation, feed-forward back propagation, generalized regression, elman back-propagation, layered recurrent, linear layer and radial basis function neural network model have been developed for modelling the system using neural network toolbox of MATLAB. Simulations have been done by carrying out a comparative analysis of different ANN models and selecting the most suitable model based on statistical indicators and further employed for five meteorological stations across India that represents distinct climate zones such as hot and dry, cold and cloudy, warm and humid, moderate and composite climate zone. Simulations are based on sky-conditions namely sunny/clear sky (type-a), hazy sky (type-b), partially foggy/cloudy sky (type-c) and fully foggy/cloudy sky (type-d) conditions. The obtained results can be further extended in forecasting the power of a solar PV system for different sky-conditions under composite climatic conditions. Lastly, comparisons have been done with fuzzy logic based model using statistical error-tests to check for accuracy and supremacy of the artificial neural network model.

5.2 COLLECTION AND SCALING OF METEOROLOGICAL DATA

The 15 years averaged data have been obtained from National Institute of Solar Energy (NISE) and Indian Meteorological Department (IMD) for meteorological parameters namely sunshine hours, dew-point, global solar energy, relative humidity, ambient temperature and wind speed. Further, the normalization/scaling of the parameters have been done in 0.1 - 0.9 range and expressed by Eq. (5.1). The data have been obtained for five meteorological sites across India and are presented in Table 5.1 - Table 5.6.

Table 5.1 Measured and scaled data for composite climatic conditions

Months	Sunshine hours (hrs)		H_g (MJ/m^2)		Relative Humidity (%)		Ambient Temp. (^oC)		Wind Speed (m/s)		Dew Point (^oC)	
	Measured	Scaled	Measured	Scaled	Measured	Scaled	Measured	Scaled	Measured	Scaled	Measured	Scaled
January	7.719	0.65	13.985	0.428	65.487	0.381	14.119	0.475	5.153	0.42	4.60	0.446
February	7.936	0.594	16.788	0.449	59.643	0.496	18.581	0.557	7.848	0.28	4.90	0.448
March	7.406	0.722	21.118	0.682	53.297	0.409	22.730	0.361	7.344	0.422	5.62	0.479
April	9.22	0.718	25.214	0.609	36.188	0.456	30.027	0.538	8.417	0.350	5.72	0.433
May	8.848	0.645	24.227	0.561	34.297	0.355	34.138	0.656	9.516	0.409	8.559	0.539
June	7.133	0.599	20.912	0.638	52.560	0.383	33.399	0.530	10.589	0.458	16.14	0.491
July	4.587	0.431	19.381	0.414	70.637	0.61	30.48	0.422	10.395	0.508	24.60	0.629
August	5.552	0.531	18.802	0.538	79.359	0.429	29.14	0.599	9.57	0.379	26.06	0.609
September	6.683	0.550	13.851	0.534	69.278	0.377	29.728	0.516	9.428	0.562	24.49	0.654
October	9.329	0.713	18.334	0.542	64.519	0.534	26.179	0.492	6.339	0.371	12.43	0.629
November	7.197	0.547	14.562	0.341	49.800	0.437	20.921	0.622	6.531	0.484	7.06	0.553
December	5.261	0.595	12.124	0.574	65.683	0.484	15.995	0.468	5.933	0.444	3.33	0.366

Table 5.2 Measured and scaled data for warm and humid climatic conditions

Months	Sunshine hours (hrs)		H_g (MJ/m^2)		Relative Humidity (%)		Ambient Temp. (^oC)		Wind Speed (m/s)		Dew Point (^oC)	
	Measured	Scaled	Measured	Scaled	Measured	Scaled	Measured	Scaled	Measured	Scaled	Measured	Scaled
January	8.94	0.701	17.64	0.524	71.32	0.515	25.46	0.223	8.22	0.432	20.33	0.467
February	9.75	0.866	21.07	0.899	76.29	0.549	26.61	0.788	9.06	0.451	21.13	0.519
March	9.05	0.882	23.53	0.594	73.75	0.318	27.84	0.799	6.98	0.503	20.77	0.540
April	9.37	0.61	23.86	0.472	71.26	0.412	30.53	0.475	8.78	0.420	23.07	0.468
May	8.83	0.626	22.87	0.753	67.14	0.452	31.71	0.506	7.49	0.583	24.49	0.498
June	7.35	0.64	21.51	0.683	64.04	0.532	30.73	0.539	8.48	0.569	24.65	0.433
July	6.18	0.534	18.87	0.661	62.25	0.465	30.53	0.649	10.04	0.455	22.74	0.501
August	4.78	0.511	19.04	0.583	71.30	0.504	29.07	0.554	8.85	0.491	24.52	0.490
September	6.16	0.582	19.66	0.596	79.09	0.542	29.10	0.216	8.41	0.442	24.63	0.436
October	6.52	0.622	17.28	0.633	80.06	0.461	27.75	0.595	6.25	0.415	24.20	0.694
November	5.81	0.547	15.13	0.566	83.73	0.467	25.64	0.519	11.58	0.461	22.71	0.577
December	7.07	0.638	13.89	0.527	78.13	0.527	26.09	0.272	9.49	0.50	21.16	0.482

Table 5.3 Measured and scaled data for hot and dry climatic conditions

Months	Sunshine hours (hrs)		H_g (MJ/m^2)		Relative Humidity (%)		Ambient Temp. (^oC)		Wind Speed (m/s)		Dew Point (^oC)	
	Measured	Scaled	Measured	Scaled	Measured	Scaled	Measured	Scaled	Measured	Scaled	Measured	Scaled
January	9.226	0.683	16.244	0.598	45.327	0.396	18.095	0.462	6.371	0.504	2.23	0.523
February	9.714	0.694	19.311	0.485	41.857	0.41	19.867	0.535	6.116	0.376	4.37	0.48
March	9.142	0.653	22.059	0.490	30.913	0.442	26.115	0.463	7.742	0.408	4.68	0.485
April	9.867	0.633	23.554	0.656	23.975	0.379	32.910	0.618	5.696	0.349	6.71	0.435
May	10.219	0.759	26.062	0.644	35.823	0.428	34.877	0.479	8.653	0.461	9.64	0.521
June	8.937	0.682	23.354	0.587	45.914	0.573	33.520	0.553	14.038	0.555	19.38	0.678
July	8.039	0.645	19.055	0.618	60.780	0.426	31.518	0.533	13.996	0.540	25.07	0.511
August	8.097	0.675	20.157	0.716	62.331	0.422	31.445	0.471	5.988	0.462	25.39	0.499
September	9.727	0.669	23.084	0.534	59.593	0.474	29.702	0.515	6.746	0.470	23.34	0.512
October	9.790	0.794	19.978	0.522	42.026	0.503	28.457	0.511	4.375	0.414	15.29	0.626
November	9.323	0.774	17.342	0.474	42.008	0.474	22.078	0.475	3.30	0.351	9.56	0.451
December	8.503	0.809	14.671	0.317	48.582	0.554	18.639	0.570	3.214	0.362	7.82	0.538

Table 5.4 Measured and scaled data for moderate climatic conditions

Months	Sunshine hours (hrs)		H_g (MJ/m^2)		Relative Humidity (%)		Ambient Temp. (^oC)		Wind Speed (m/s)		Dew Point (^oC)	
	Measured	Scaled	Measured	Scaled	Measured	Scaled	Measured	Scaled	Measured	Scaled	Measured	Scaled
January	9.497	0.529	16.998	0.607	59.887	0.49	19.781	0.464	1.493	0.504	11.58	0.494
February	10.214	0.730	20.640	0.588	48.815	0.437	23.179	0.423	5.343	0.201	12.59	0.496
March	9.9	0.695	22.667	0.60	41.278	0.459	26.277	0.492	3.234	0.344	5.08	0.303
April	9.97	0.650	24.342	0.641	44.469	0.588	29.192	0.598	6.066	0.486	10.73	0.571
May	10.832	0.720	25.393	0.612	55.212	0.608	29.138	0.406	11.756	0.521	18.39	0.525
June	4.753	0.484	18.937	0.60	76.922	0.407	25.889	0.643	10.475	0.469	22.38	0.482
July	4.271	0.283	15.119	0.503	86.028	0.523	23.913	0.544	7.931	0.304	21.78	0.546
August	4.003	0.437	16.453	0.433	85.245	0.522	23.298	0.555	7.734	0.523	21.87	0.533
September	5.567	0.530	18.404	0.535	84.233	0.555	24.07	0.388	4.675	0.518	21.58	0.575
October	7.668	0.590	18.785	0.534	75.960	0.615	24.237	0.552	2.274	0.304	20.06	0.60
November	8.460	0.607	17.527	0.469	71.969	0.404	22.401	0.484	2.00	0.450	18.12	0.418
December	8.739	0.734	17.109	0.721	63.012	0.405	19.274	0.502	2.407	0.503	16.33	0.653

Table 5.5 Measured and scaled data for cold and cloudy climatic conditions

Months	Sunshine hours (hrs)		H_g (MJ/m^2)		Relative Humidity (%)		Ambient Temp. (^oC)		Wind Speed (m/s)		Dew Point (^oC)	
	Measured	Scaled	Measured	Scaled	Measured	Scaled	Measured	Scaled	Measured	Scaled	Measured	Scaled
January	7.055	0.72	14.437	0.637	75.581	0.426	9.948	0.635	3.613	0.363	6.42	0.475
February	6.264	0.606	16.575	0.511	71.839	0.529	10.242	0.551	3.804	0.404	6.36	0.495
March	7.216	0.635	21.004	0.588	59.645	0.470	15.544	0.450	5.645	0.386	9.38	0.523
April	3.79	0.352	19.967	0.541	63.533	0.523	18.258	0.501	7.633	0.476	15.24	0.646
May	4.842	0.483	18.429	0.428	80.29	0.523	20.694	0.576	4.290	0.363	18.19	0.658
June	3.487	0.453	16.416	0.593	85.50	0.568	21.04	0.600	3.633	0.351	20.80	0.536
July	2.706	0.358	16.064	0.611	87.516	0.535	21.206	0.599	3.145	0.380	21.58	0.458
August	2.158	0.414	14.253	0.520	89.226	0.560	20.642	0.519	1.226	0.189	21.23	0.49
September	2.747	0.356	13.982	0.432	85.917	0.483	20.002	0.471	0.867	0.331	20.05	0.64
October	5.871	0.557	15.004	0.464	80.742	0.654	18.39	0.603	2.290	0.466	17.79	0.467
November	7.057	0.632	15.643	0.546	75.60	0.525	15.273	0.393	2.650	0.336	12.53	0.441
December	7.597	0.638	15.632	0.634	74.403	0.593	11.889	0.344	0.839	0.268	10.04	0.527

The normalization of the data has been obtained by using Eq. (5.1) as:

$$L_s = \left[\left(\left(\frac{(X_{max} - X_{min})}{(L_{max} - L_{min})}\right)*(L - L_{min})\right) + X_{min}\right] \quad (5.1)$$

where

L = measured data

L_s = scaled/normalized data

L_{max} = maximum value of relevant set of data

L_{min} = minimum value of relevant set of data

X_{max} = maximum limit of normalized range

X_{min} = minimum limit of normalized range

5.3 ARCHITECTURE OF ARTIFICIAL NEURAL NETWORK

Model based on artificial intelligence techniques i.e. Artificial Neural Network (ANN) is designed in such a way that the variables at the output are calculated from variables at the input side by the composition of basic connections and functions. The architecture has an input layer of nine inputs, a hidden layer with tan-sigmoid function 'tansig' and an output layer as shown in Fig. 5.1. MATLAB neural network toolbox has been used for implementing a neural network algorithm. For training the network, Levenberg-Marquardt training algorithms have been used and can be defined by using 'TRAINLM' command in MATLAB as shown in Fig. 5.2. The output is modelled by using Eq. (5.2) as:

$$y = \sum_{j=1}^{n}(w_{ij}x_{ij} + \theta_i) \quad (5.2)$$

where x_{ij} is the j_{th} neuron incoming signal (at the input layer), θ_i is the bias of i neuron and w_{ij} is the connection weight directed from j neuron to i neuron (at the hidden layer).

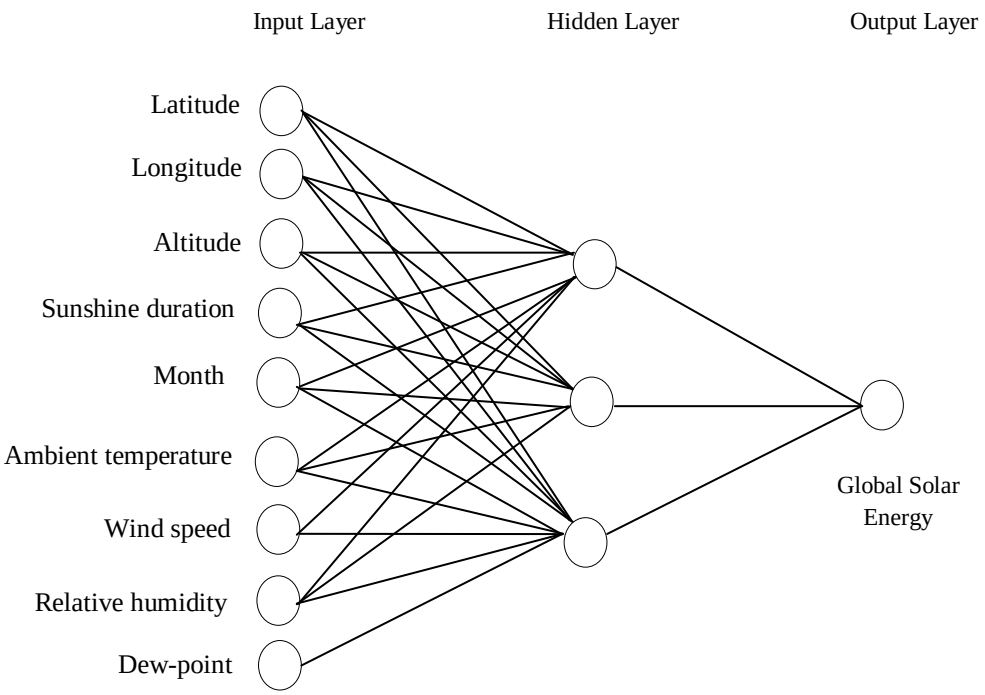

Fig. 5.1 ANN architecture used for forecasting global solar energy

In this chapter, cascade-forward back-propagation, feed-forward back-propagation, elman back-propagation, generalized regression, layered recurrent, linear layer and radial basis function neural network architecture have been designed and simulated in MATLAB. The following can be briefly outlined for ANN model:-

(a) Normalization and scaling of the input and target data has been done, and the range varies from 0 to 1.

(b) Creation of a neural network.

(c) Training and simulation of the neural network.

(d) Generation of the output data.

(e) De-normalize the output data.

(f) Comparing the obtained data with target data. Performance can be evaluated by use of evaluation indexes.

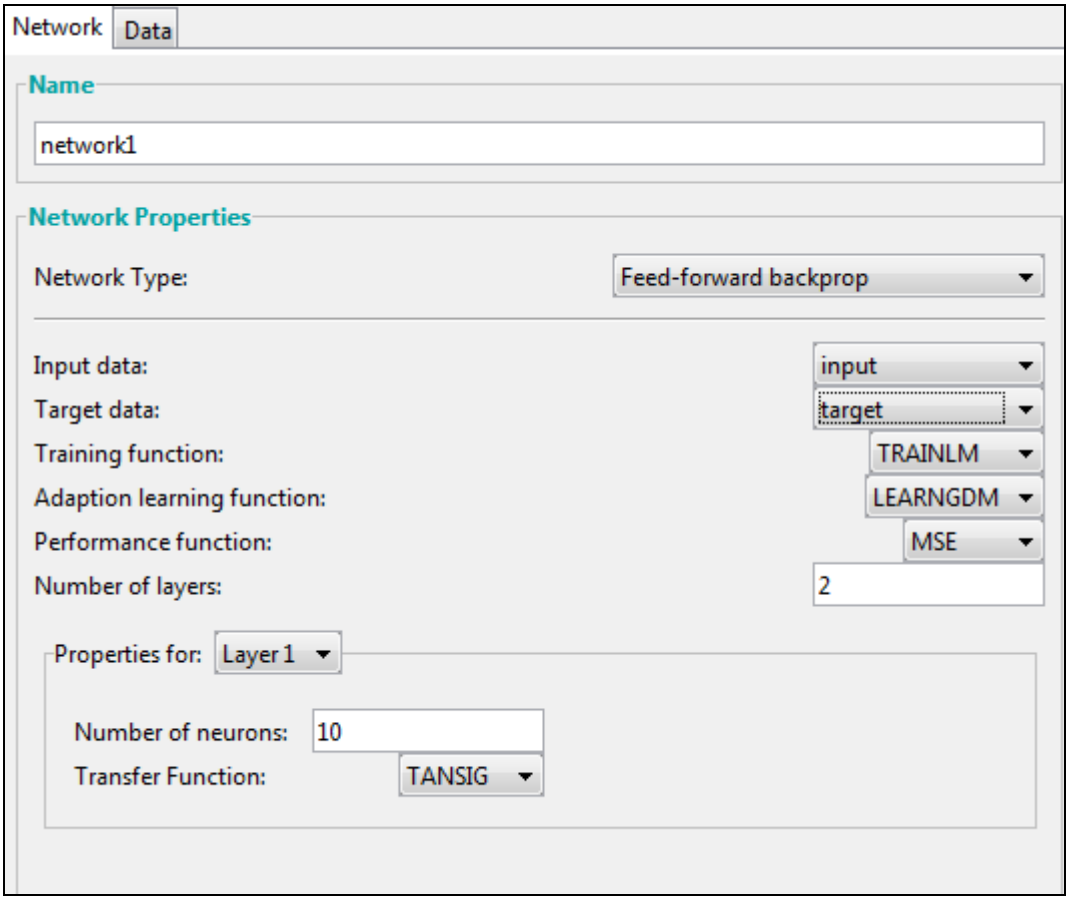

Fig. 5.2 MATLAB neural network toolbox

The variants of ANN architectures are discussed below as:

5.3.1 Feed-Forward Neural Network (FFNN)

The feed-forward neural network comprises series of layers where the first layer connects the inputs to the network and every subsequent layer connects with the previous layer. The network output is obtained in the final layer. These networks are used for input-output mapping. Feed-forward neural network with neurons in the hidden layer can fit any input to output mapping problem.

5.3.2 Cascade-Forward Neural Network (CFNN)

The cascade-forward neural networks are related and same as that of the feed-forward networks but such network creates connection its previous layer

to the subsequent layers. Similar to feed-forward neural networks, a two or more layer cascade network can have finite input to output relationship.

5.3.3 Elman Neural Network (ENN)

These are feed-forward networks with the layered recurrent connection additions with tap delays. Elman networks with one or more hidden layers can learn any dynamic input to output relationship with enough number of neurons in the hidden layers. However, these networks make use of simple calculations at the cost of less reliable learning which results in a trade-off of reduced training calculations, but the risk of poorer accuracy.

5.3.4 Generalized Regression Neural Network (GRNN)

These networks are used for function approximation. To fit the data closely, a spread smaller than the typical distance between input vectors has been used. To fit the data more smoothly, a larger spread has been used.

5.3.5 Layered Recurrent Neural Network (LRNN)

The layered recurrent neural network is same as that of the time and distributed delay neural networks with finite input responses. Layer recurrent networks with two and more layers can estimate dynamic output from past inputs with enough hidden neurons and recurrent layer delays.

5.3.6 Linear Neural Network (LNN)

Linear layers can be trained to model static and dynamic linear systems, given a low learning rate to be stable.

5.3.7 Radial Basis Function Neural Network (RBFNN)

It is used for function approximation and pattern classification problems

which can easily design a radial basis function neural network with zero error.

5.4 EVALUATION INDEXES

For validation of the models, evaluation indexes have been used and are defined as [107]:

5.4.1 Mean Absolute Percentage Error (MAPE)

It is described as summing up the absolute error in each period divided by the measured values and then averaging the fixed percentages and the relationship is given by Eq. (5.3) as:

$$\text{MAPE}_{\%} = \frac{1}{n}\sum_{i=1}^{n}\left|\frac{E}{m_i}\right| * 100 \tag{5.3}$$

where n is the number of observation, $E = (m_i - e_i)$ is the absolute error, m_i and e_i are the i_{th} measured and forecasted data values, respectively.

5.4.2 Normalized Mean Absolute Error (NMAE)

It is described by the following given Eq. (5.4) and can be expressed as:

$$\text{NMAE}_{\%} = \frac{1}{n}\sum_{i=1}^{n}\left|\frac{E}{\max(m_i)}\right| * 100 \tag{5.4}$$

where n is the number of observation, E is the absolute error, m_i and e_i are the i_{th} measured and forecasted data, respectively. Since the measured data changes significantly in a day i.e. from sunrise to sunset, so for the sake of fair comparison, the normalized mean absolute error have been preferred.

5.4.3 Normalized Root Mean Square Error (nRMSE)

It is described by the following given Eq. (5.5) and expressed as:

$$\text{nRMSE}_{\%} = \frac{\sqrt{\frac{1}{n}\sum_{i=1}^{n}|E|^2}}{\max(m_i)} * 100 \tag{5.5}$$

where $E = (m_i - e_i)$ is the absolute error, n is the number of observation, m_i and e_i are the i_{th} measured and forecasted data values, respectively. This definition of error is normalized over the maximum hourly measured data. It measures the mean magnitude of the absolute error.

5.5 RESULTS AND DISCUSSIONS

5.5.1 Modeling Variants of ANN Architectures

In the first part of this chapter, the variants of the artificial neural network architecture have been developed which include cascade-forward, feed-forward, elman back-propagation, generalized regression, layered recurrent, linear layer and radial basis function neural network under composite climatic conditions. It comprises an input layer, hidden layer with 'tansig' tangent sigmoid transfer function and 'purelin' linear transfer function in the output layer. Levenberg-Marquardt training algorithm was found to give a good prediction. For validation of the models, evaluation indexes have been used and are presented in Table 5.6.

From Table 5.6, it is learned that among the different artificial neural network architecture investigated, the radial basis function neural network model gave the most accurate result as compared to other models with averaged mean absolute percentage error (MAPE) of 0.001%, normalized mean absolute error (NMAE) of 0.017% and normalized root mean square error (nRMSE) of 0.092% when the simulation is performed between the measured and forecasted data.

Table 5.6 Variants of ANN architectures along with evaluation indexes under composite climatic conditions

Month	Measured H_g (MJ/m^2)	Performance Measures	ANN Architecture						
			Cascade-forward backdrop	Elman backdrop	Feed-forward	Generalized regression	Layer recurrent	Linear layer (train)	Radial basis
Jan	13.98	Estimated H_g (MJ/m^2)	13.98	13.98	13.99	13.91	13.93	13.95	13.95
		MAPE (%)	0.03	0.02	0.02	0.26	0.04	0.02	0.01
		NMAE (%)	0.76	0.45	0.49	6.21	0.93	0.50	0.20
		nRMSE (%)	1.04	0.79	0.80	7.90	1.78	1.17	1.11
Feb	16.79	Estimated H_g (MJ/m^2)	16.76	16.80	16.90	16.76	16.82	16.79	16.79
		MAPE (%)	0.04	0.02	0.08	0.31	0.02	0.00	0.00
		NMAE (%)	0.78	0.47	1.52	6.70	0.42	0.00	0.00
		nRMSE (%)	1.26	0.94	2.02	8.50	0.63	0.00	0.00
Mar	21.12	Estimated H_g (MJ/m^2)	21.08	21.16	21.13	21.30	21.10	21.12	21.12
		MAPE (%)	0.04	0.02	0.04	0.27	0.02	0.04	0.00
		NMAE (%)	1.07	0.51	1.02	7.22	0.62	1.19	0.00
		nRMSE (%)	1.89	0.76	1.26	9.64	1.40	1.47	0.00
Apr	25.12	Estimated H_g (MJ/m^2)	25.31	25.15	25.15	25.26	25.21	25.22	25.21
		MAPE (%)	0.03	0.02	0.02	0.20	0.01	0.00	0.00
		NMAE (%)	0.81	0.45	0.58	5.42	0.17	0.10	0.00
		nRMSE (%)	1.39	0.83	1.28	6.71	0.34	0.12	0.00
May	24.23	Estimated H_g (MJ/m^2)	24.2	24.24	24.25	24.28	24.25	24.23	24.23
		MAPE (%)	0.02	0.01	0.01	0.18	0.03	0.01	0.00
		NMAE (%)	0.49	0.33	0.29	5.08	0.70	0.37	0.00
		nRMSE (%)	0.69	0.44	0.86	5.69	0.98	0.46	0.00
Jun	20.91	Estimated H_g (MJ/m^2)	20.8	20.91	20.93	21.17	20.86	20.91	20.91
		MAPE (%)	0.08	0.04	0.02	0.36	0.02	0.00	0.00
		NMAE (%)	1.90	0.92	0.45	8.95	0.49	0.00	0.00
		nRMSE (%)	2.57	1.23	0.76	11.86	0.93	0.00	0.00
Jul	19.38	Estimated H_g (MJ/m^2)	19.48	19.36	19.34	19.31	19.32	19.38	19.38
		MAPE (%)	0.04	0.04	0.04	0.47	0.04	0.04	0.00
		NMAE (%)	0.97	0.92	0.77	10.24	0.89	0.79	0.00
		nRMSE (%)	1.58	1.18	1.21	12.13	1.17	0.97	0.00

Table 5.6 Variants of ANN architectures along with evaluation indexes under composite climatic conditions (contd….)

Month	Measured H_g (MJ/m^2)	Performance Measures	ANN Architecture						
			Cascade-forward backdrop	Elman backdrop	Feed-forward	Generalized regression	Layer recurrent	Linear layer (train)	Radial basis
Aug	18.80	Estimated H_g (MJ/m^2)	18.94	18.75	18.84	18.95	18.78	18.80	18.80
		MAPE (%)	0.12	0.04	0.05	0.54	0.03	0.01	0.00
		NMAE (%)	2.44	0.74	0.14	12.21	0.74	0.18	0.00
		nRMSE (%)	2.91	1.30	0.05	13.89	1.11	0.22	0.00
Sep	13.85	Estimated H_g (MJ/m^2)	13.87	13.86	13.85	13.83	13.85	13.85	13.85
		MAPE (%)	0.03	0.01	0.01	0.24	0.01	0.00	0.00
		NMAE (%)	0.86	0.15	0.26	5.94	0.22	0.11	0.00
		nRMSE (%)	1.07	0.34	0.39	7.69	0.32	0.14	0.00
Oct	18.33	Estimated H_g (MJ/m^2)	18.40	18.31	18.34	18.36	18.33	18.33	18.33
		MAPE (%)	0.03	0.01	0.02	0.21	0.01	0.01	0.00
		NMAE (%)	0.82	0.32	0.53	5.58	0.24	0.32	0.00
		nRMSE (%)	1.14	0.58	0.72	6.72	0.61	0.47	0.00
Nov	14.56	Estimated H_g (MJ/m^2)	14.59	14.56	14.57	14.59	14.57	14.56	14.56
		MAPE (%)	0.03	0.01	0.01	0.21	0.01	0.02	0.00
		NMAE (%)	0.68	0.12	0.13	5.04	0.26	0.55	0.00
		nRMSE (%)	1.63	0.19	0.19	6.38	0.70	0.71	0.00
Dec	12.12	Estimated H_g (MJ/m^2)	12.26	12.20	12.15	12.21	12.13	12.13	12.12
		MAPE (%)	0.06	0.03	0.08	0.37	0.03	0.03	0.00
		NMAE (%)	1.48	0.79	1.95	9.17	0.84	0.66	0.00
		nRMSE (%)	2.12	2.29	2.41	11.04	1.29	0.80	0.00
Avg.	18.27	Estimated H_g (MJ/m^2)	18.31	18.27	18.29	18.33	18.26	18.27	18.27
		MAPE (%)	0.05	0.02	0.03	0.30	0.02	0.02	0.001
		NMAE (%)	1.09	0.51	0.68	7.31	0.54	0.40	0.017
		nRMSE (%)	1.61	0.91	1.00	9.01	0.94	0.54	0.092

5.5.2 Forecasting Solar Energy Employing the RBFNN and FFNN Model

In the second part of this chapter, by employing Radial Basis Function Neural Network (RBFNN) model, simulations have been carried out based on sky-conditions i.e. sunny sky (type-a), hazy sky (type-b), partially foggy/cloudy sky (type-c) and fully foggy/cloudy sky (type-d) conditions and applied for different meteorological stations with distinct climate zone across India and are presented in Table 5.7.

Further, it is evident from Table 5.7 that the RBFNN model is far accurate and precise with Mean Absolute Percentage Error (MAPE) of 0.00646%, Normalized Mean Absolute Error (NMAE) of 0.0049% and normalized Root Mean Square Error (nRMSE) of 0.078% which shows that the error is within the permissible error limits. Similarly, the Feed-Forward Neural Network (FFNN) model is chosen at random for comparing the results with the RBFNN model. The obtained results have been further simulated based on sky-conditions and for distinct climate zone across India and are presented in Table 5.8. From Table 5.7 and Table 5.8, the following can be briefly summarized:-

(a) Clear/Sunny sky (type-a)

For sunny/clear sky-condition, it has been observed from the computed data presented in Table 5.8 which employs the FFNN model, the minimum value of MAPE obtained is 0.44%, NMAE is 0.40% and nRMSE is 0.70%, whereas, in case of RBFNN model, the minimum value of MAPE obtained is 1.1×10^{-8} %, NMAE is 1×10^{-8} % and nRMSE is 0.01363% as shown by the computed data presented in Table 5.7 by simulating the measured and forecasted data.

Table 5.7 Forecasted global solar energy employing the RBFNN model based on sky-conditions for distinct climate zones across India

Climate Zone	**Sky-Conditions**	**Global Solar Energy H_g (MJ/m^2)**		**MAPE (%)**	**NMAE (%)**	**nRMSE (%)**
		Measured	**Fuzzy**			
New Delhi (Composite)	Clear/Sunny Sky	20.58	20.58	0.000008062	0.000007276	0.023162273
	Hazy Sky	18.12	18.10	0.000000012	0.000000010	0.014784684
	Partially Foggy/Cloudy Sky	12.51	12.51	0.000000023	0.000000017	0.015340431
	Fully Foggy/Cloudy Sky	11.37	11.30	0.000000041	0.000000018	0.019464528
Chennai (Warm and Humid)	Clear/Sunny Sky	23.62	23.62	0.000000014	0.0000000137	0.0130413684
	Hazy Sky	21.04	21.04	0.000000025	0.0000000222	0.0664993013
	Partially Foggy/Cloudy Sky	18.40	18.40	0.000000013	0.0000000009	0.0214053710
	Fully Foggy/Cloudy Sky	11.88	11.88	0.000000032	0.0000000140	0.0218700869
Jodhpur (Hot and Dry)	Clear/Sunny Sky	21.76	21.76	0.000000011	0.000000010	0.013635427
	Hazy Sky	19.79	19.80	0.000000015	0.000000014	0.015340431
	Partially Foggy/Cloudy Sky	18.16	18.16	0.000000018	0.000000014	0.016476619
	Fully Foggy/Cloudy Sky	15.75	15.78	0.000000007	0.000000003	0.004467361
Shillong (Cold and Cloudy)	Clear/Sunny Sky	22.85	22.85	0.009598276	0.008828894	0.088976002
	Hazy Sky	19.25	19.25	0.006468338	0.004964164	0.078564044
	Partially Foggy/Cloudy Sky	15.93	15.93	0.000000025	0.000000016	0.019464087
	Fully Foggy/Cloudy Sky	11.22	11.22	0.0000000001	0.0000000001	0.0000000001
Pune (Moderate)	Clear/Sunny Sky	21.49	21.52	0.000000018	0.000000007	0.012756144
	Hazy Sky	20.41	20.42	0.000005699	0.000005086	0.024854072
	Partially Foggy/Cloudy Sky	18.71	18.71	0.000054524	0.000037123	0.014467972
	Fully Foggy/Cloudy Sky	13.73	13.73	0.000000038	0.000000020	0.020648805

Table 5.8 Forecasted global solar energy employing the FFNN model based on sky-conditions for distinct climate zone across India

Climate Zone	**Sky-Conditions**	**Global Solar Energy H_g (MJ/m^2)**		**MAPE (%)**	**NMAE (%)**	**nRMSE (%)**
		Measured	**Fuzzy**			
New Delhi (Composite)	Clear/Sunny Sky	20.54	20.55	0.9098539	0.8237889	1.2491250
	Hazy Sky	18.12	18.14	0.6061892	0.5101836	1.0993097
	Partially Foggy/Cloudy Sky	12.51	12.51	1.6099966	1.1410815	2.0724769
	Fully Foggy/Cloudy Sky	11.37	11.31	2.2029587	0.9092731	1.5296920
Chennai (Warm and Humid)	Clear/Sunny Sky	23.41	22.77	3.0888259	2.7558138	1.3601598
	Hazy Sky	21.11	21.07	1.2512550	1.0771491	1.3079257
	Partially Foggy/Cloudy Sky	18.37	18.25	0.7914716	0.6094748	0.9984168
	Fully Foggy/Cloudy Sky	11.95	12.21	2.8557605	1.5777821	1.6175690
Jodhpur (Hot and Dry)	Clear/Sunny Sky	21.76	21.81	0.4471779	0.4079172	0.7088581
	Hazy Sky	19.79	19.68	0.8232167	0.6524025	1.2857318
	Partially Foggy/Cloudy Sky	18.16	18.25	1.0856531	0.7390095	1.5030082
	Fully Foggy/Cloudy Sky	15.75	15.54	0.0162731	0.0107279	0.0107279
Shillong (Cold and Cloudy)	Clear/Sunny Sky	22.92	22.85	0.5298038	0.4953913	0.9758976
	Hazy Sky	19.25	19.25	0.8151853	0.6580462	1.2527437
	Partially Foggy/Cloudy Sky	16.28	16.24	1.9176360	1.3166599	1.6443384
	Fully Foggy/Cloudy Sky	11.62	11.63	0.0162731	0.0107279	0.0205869
Pune (Moderate)	Clear/Sunny Sky	21.49	21.48	0.6985575	0.6432756	1.2194507
	Hazy Sky	20.42	20.31	0.8042275	0.6318676	1.1171241
	Partially Foggy/Cloudy Sky	18.71	18.90	1.8603160	1.4328736	1.4152323
	Fully Foggy/Cloudy Sky	13.73	13.75	1.6115142	0.7257172	1.3800854

The error for the Radial Basis Function Neural Network (RBFNN) model is comparatively less and reduced than the Feed-Forward Neural Network (FFNN) model. Also, in both of the developed model i.e. the RBFNN and FFNN model, the error is observed to be minimum for Jodhpur station. This is due to the reason that the Jodhpur climatic conditions are hot and dry which prevail sunny weather throughout the year, with high variation in ambient temperature. During summer, the ambient temperature varies from 30-35^{o}C whereas, during winter, it varies from 5 - 25^{o}C; so, the variation is high of the value of 10^{o}C as illustrated in Table 5.3.

Jodhpur climate is extreme, with high solar insolation during day time because of which the surrounding region got heated up very quickly and at night time also there is a clear sky because of which the heat absorbed by atmosphere got dissipated to the upper atmospheric region. The climate of Jodhpur is defined as hot and dry with sandy ground conditions as the relative humidity varies from 24 - 62% due to water surface bodies. In such climatic conditions, the design criteria should be for increasing power generation from solar energy technology based photovoltaic system.

(b) Hazy sky (type-b)

For hazy sky-condition, it has been observed from the computed data presented in Table 5.8 which employs the FFNN model, the minimum value of MAPE obtained is 0.60%, NMAE is 0.51% and nRMSE is 1.09%, whereas, in case of RBFNN model, the minimum value of MAPE obtained is 1.2 x 10^{-8} %, NMAE is 1 x 10^{-8} % and nRMSE is 0.014% as shown by the computed data presented in Table 5.7 by simulating the measured and forecasted data.

The error for the RBFNN model is comparatively less and reduced than FFNN model. Also, in both of the developed model, the error is observed to be minimum for Delhi station that falls under composite climate zone.

The contributing factor for this sky-condition is the variation in relative humidity from 30 - 40% during dry days to 60 - 80% during wet days. The presence of high value of relative humidity is one of the main reasons that categorize Delhi under the composite climate zone and not under hot and dry climate zone as shown by the measured data presented in Table 5.1. Also, during the summer season, the solar insolation is high and in monsoon season the solar insolation is low with predominant diffuse radiation.

The sky is clear in winter; overcast and dull in monsoon season; and often hazy in the summer season.

(c) Partially foggy/cloudy sky (type-c)

For this sky-condition, it has been observed from the computed data presented in Table 5.8 which employs the FFNN model, the minimum value of MAPE obtained is 0.79%, NMAE is 0.60% and nRMSE is 0.99%, whereas, in case of RBFNN model, the minimum value of MAPE obtained is 1.3×10^{-8} %, NMAE is 9×10^{-10} % and nRMSE is 0.0214%, by simulating the measured and forecasted data respectively.

The error for the RBFNN model is comparatively less and reduced than FFNN model. Also, in both of the developed models, the error is observed to be the minimum for Chennai station that falls under warm and humid climate zone.

The reason behind is that for this sky-conditions, the sky is partially cloudy as diffuse radiation is very intense during clear days and the dissipated

heat from the surface of the earth is generally marginal during the night because of the presence of clouds. Hence, ambient temperature variation is quite low. One of the main characteristics of this climate zone is the high amount of relative humidity that varies from 70-90% throughout the year. In summer, the temperature can go as high as 30-35^{o}C during the day whereas, in winter, the maximum temperature is between 20-25^{o}C during day time as as shown by the measured data presented in Table 5.2.

(d) Fully foggy/cloudy sky (type-d)

For this sky-condition, it has been observed from the data presented in Table 5.8 which employs the FFNN model, the minimum value of MAPE obtained is 0.016%, NMAE is 0.010% and nRMSE is 0.020%; whereas, in case of RBFNN model, the minimum value of MAPE obtained is 1.0 x 10^{-10} %, NMAE is 1.0 x 10^{-10} % and nRMSE is 1.0 x 10^{-10} % as shown by the computed data presented in Table 5.7 by simulating the measured and forecasted data.

The error for the RBFNN model is comparatively less and reduced than the FFNN model. Also, in both of the developed models, the error is found to be the minimum for Shillong that falls under cold and cloudy climate zone.

This is due to the reason that the intensity of solar radiation is low during winter due to the presence of high amount of diffuse solar radiation which makes extremely cold winters. During summer, the ambient temperature varies between 20-25^{o}C and 10-15^{o}C during winter. The variation in humidity is high of the range 70-90% as shown by the measured data presented in Table 5.5. The sky for this climate zone is overcast and cloudy all throughout the year except during short summer.

Further, the graphical representation showing a comparison of the measured data and forecasted data obtained by employing the RBFNN model and FFNN model have been shown in Fig. 5.3 - Fig. 5.7 based on sky-conditions and further simulated for distinct climatic conditions across India.

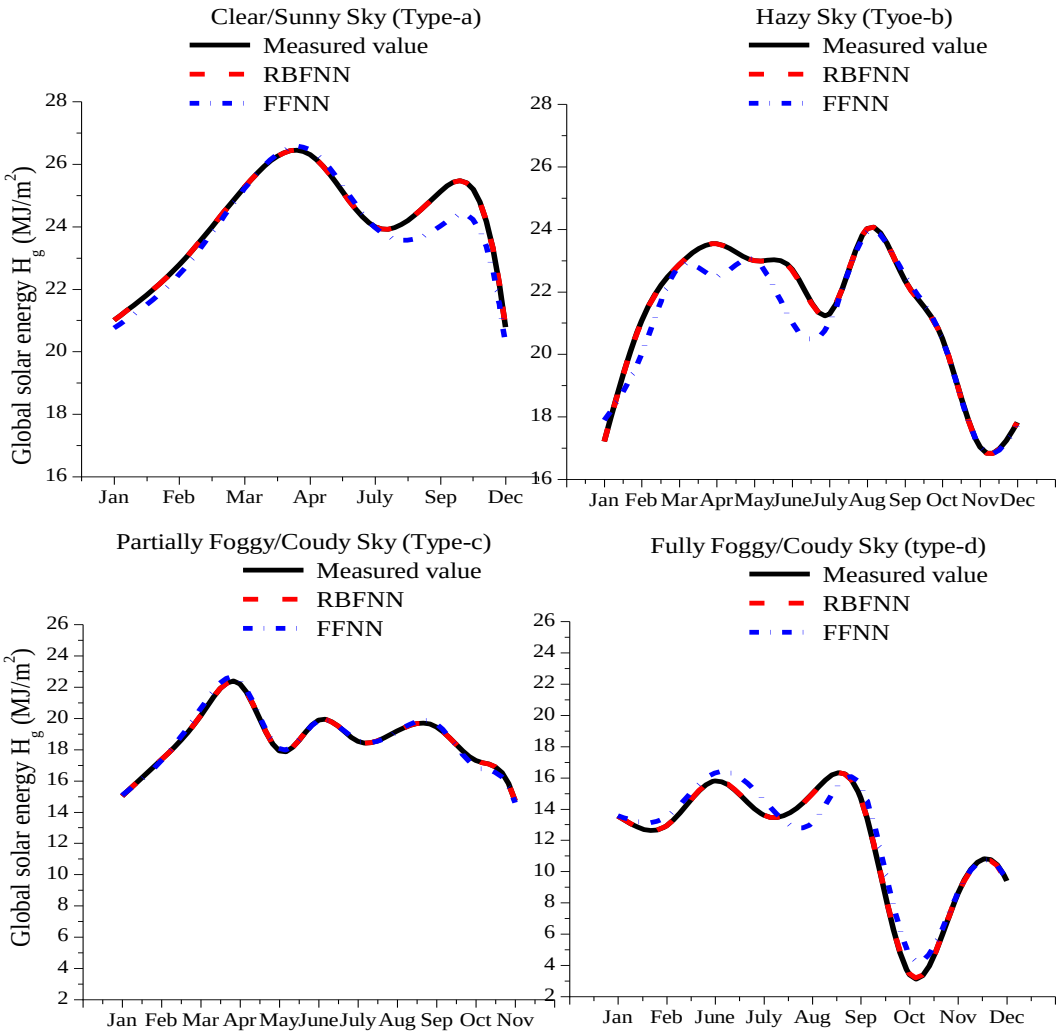

Fig. 5.3 Graphical representation of measured and forecasted global solar energy employing the RBFNN and FFNN model for warm and humid climate zone

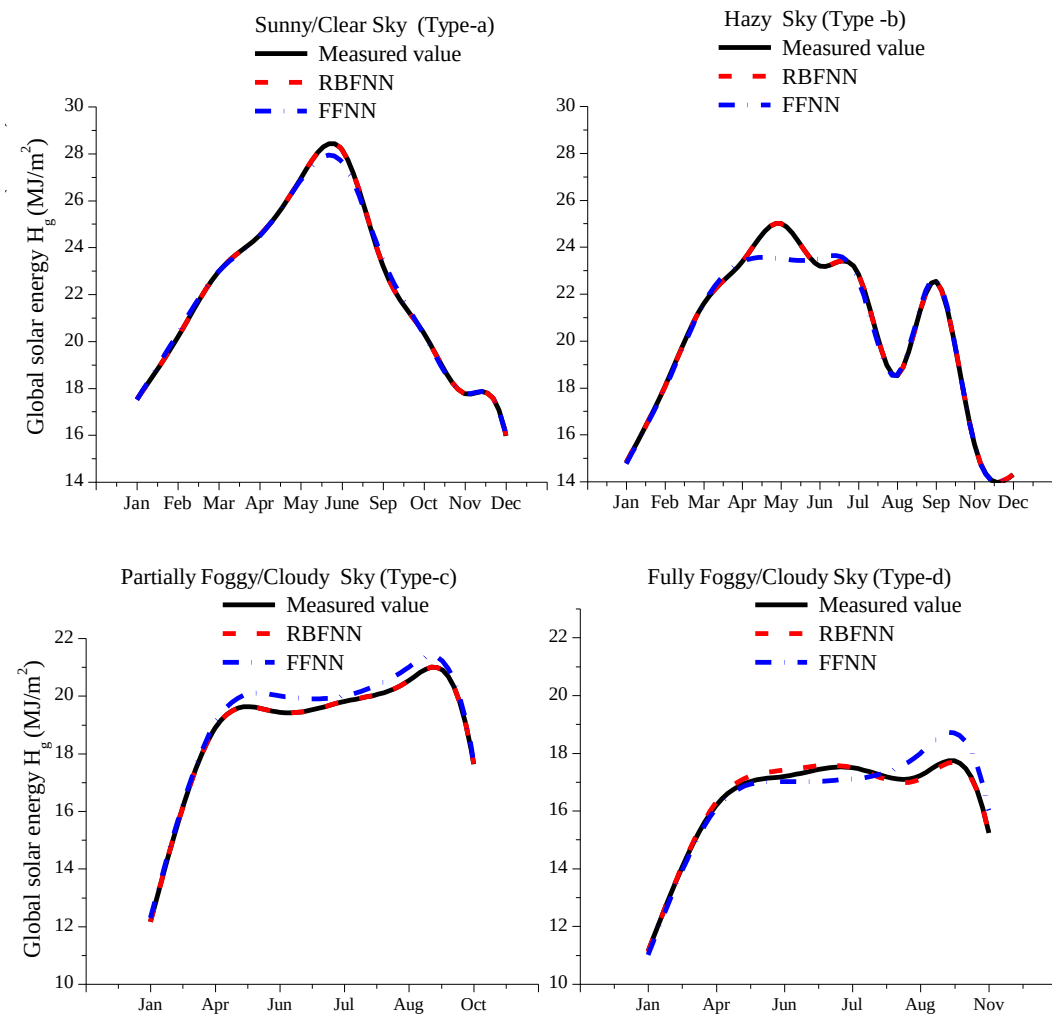

Fig. 5.4 Graphical representation of measured and forecasted global solar energy employing the RBFNN and FFNN model for hot and dry climate zone

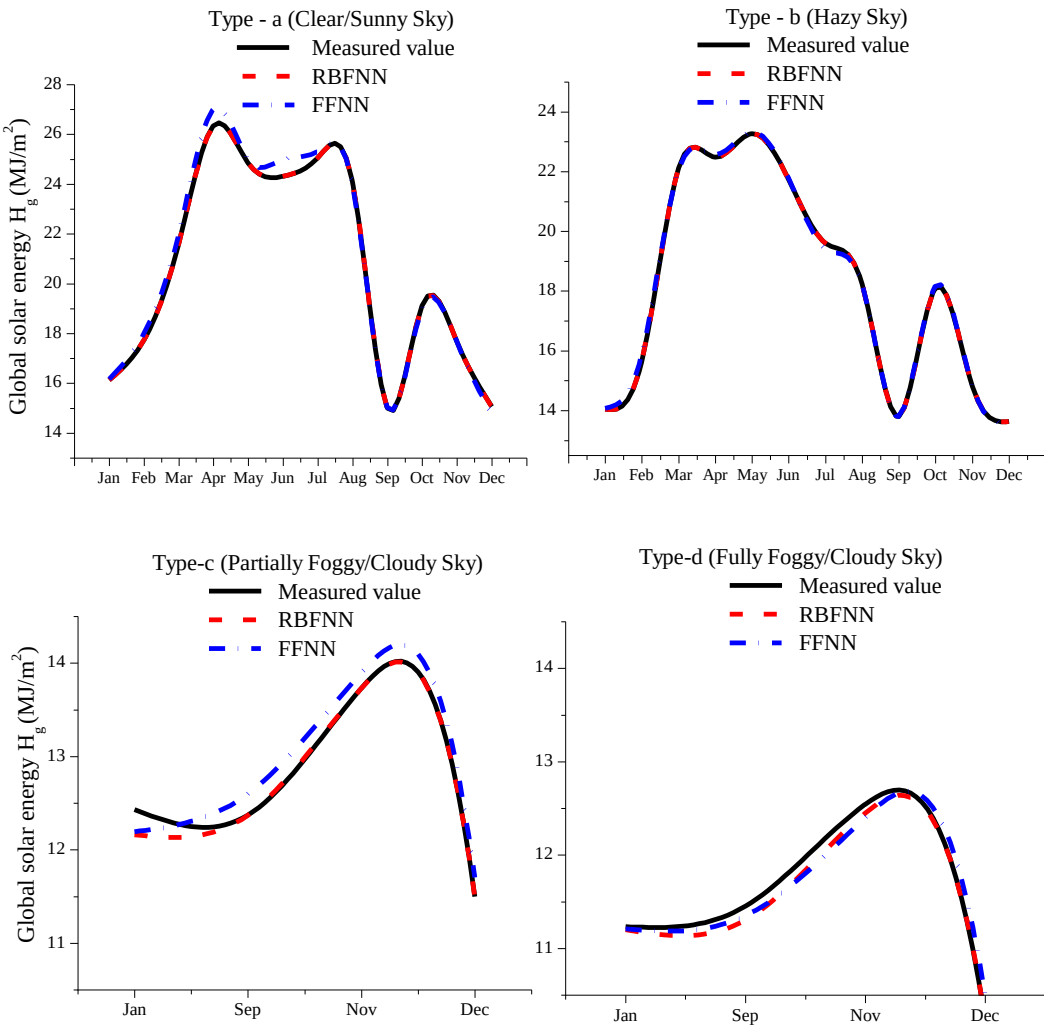

Fig. 5.5 Graphical representation of measured and forecasted global solar energy employing the RBFNN and FFNN model for composite climate zone

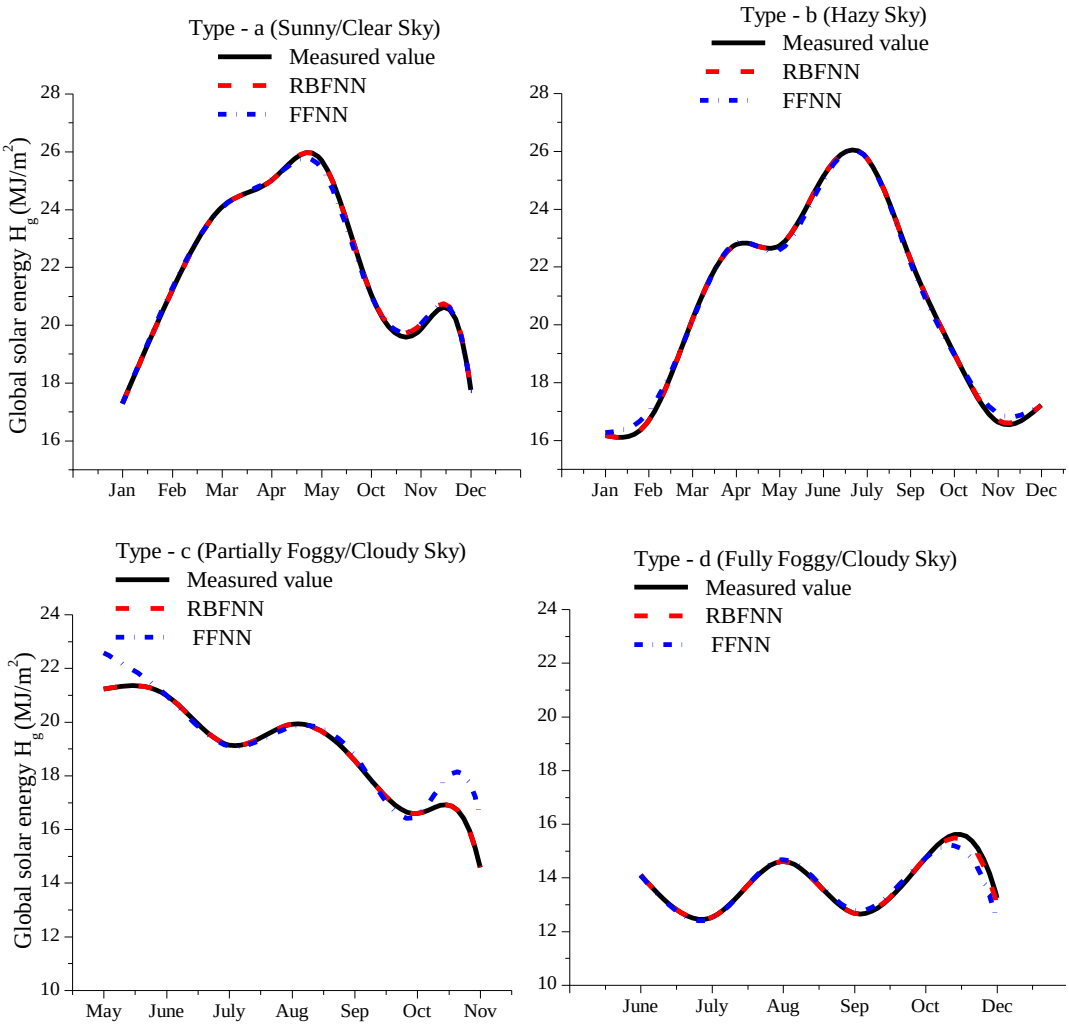

Fig. 5.6 Graphical representation of measured and forecasted global solar energy employing the RBFNN and FFNN model for moderate climate zone

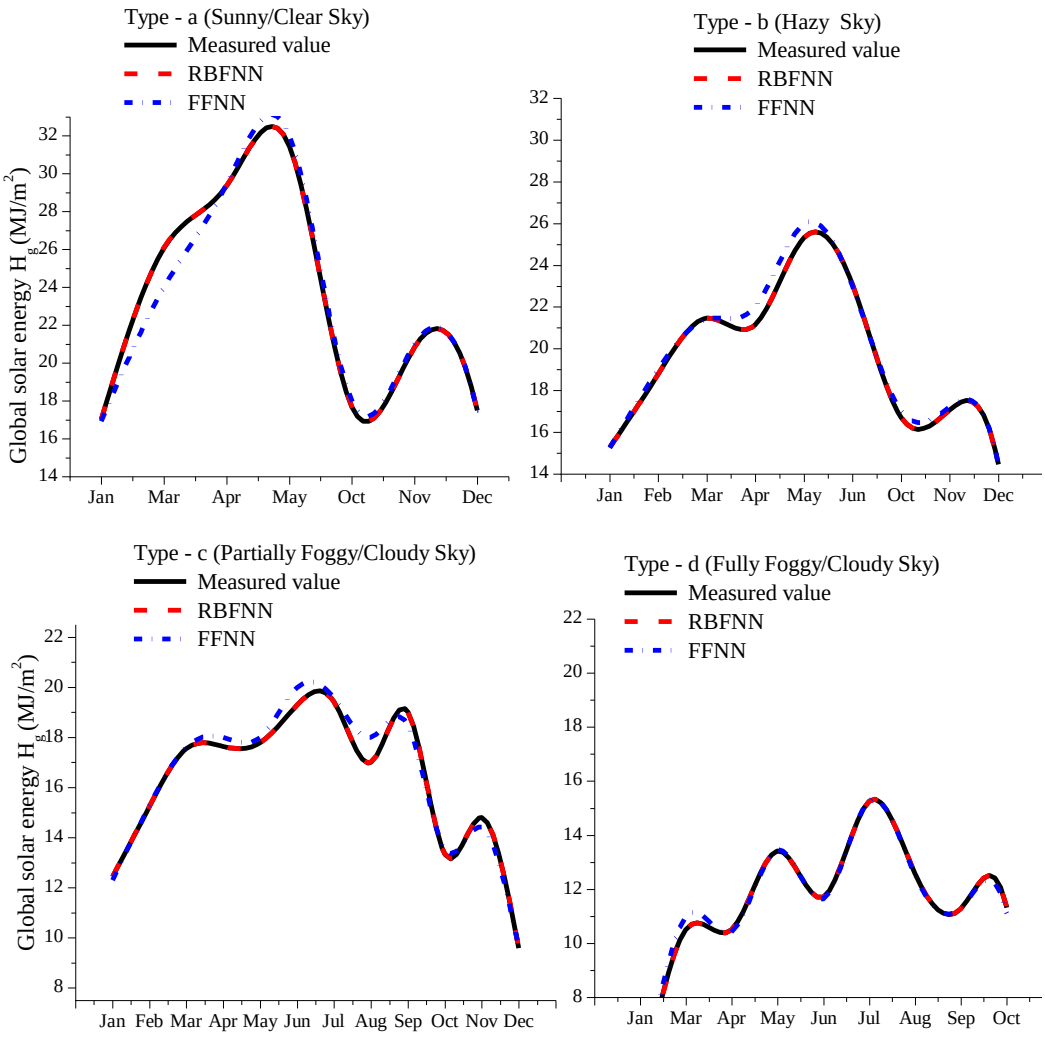

Fig. 5.7 Graphical representation of measured and forecasted global solar energy employing the RBFNN and FFNN model for cold and cloudy climate zone

From Fig. 5.3 - Fig. 5.7, it is evident that the RBFNN model i.e. the red dashed line (– – –) exactly follows the black solid line (———) which represents the measured data where in case of the FFNN model i.e. the blue dash dot line (-·-·-·-) shows some deviation with the measured data. Therefore, it has been observed that the radial-basis function neural network model outperforms feed-forward neural network model.

5.6 IMPLEMENTATION IN SOLAR PV SYSTEM

Forecasting of power is essential for planning the operation of solar PV systems. So, obtained results are further exploited for simulating with input parameters namely solar insolation, and cell temperature by employing ANN model for forecasting power in solar PV system using Heterojunction with Intrinsic Thin Layer (HIT) solar PV module of 210 W_p operated at maximum power point conditions, the performance specification are listed in Table A.2 of Appendix A. The ANN model employing radial basis function neural network have been implemented in forecasting power of a solar photovoltaic system and are presented in Table 5.9 under composite climatic conditions.

It has been observed from Table 5.9, that by employing the RBFNN model, the month-wise average mean absolute percentage error is 0.007% which is obtained by comparing the measured data with forecasted data in a solar PV system employing 210 W_p HIT solar PV module, which is within the permissible error limit. Also, the month-wise average normalized mean absolute error is 0.092% and normalized root mean square error observed is 0.109% respectively.

Table 5.9 Forecasted power in a solar PV system employing the RBFNN model under composite climatic conditions

Month	H_g (W/m^2)	I_{sc} (A)	V_{oc} (V)	Cell Temperature (^oC)	Power (W)		MAPE (%)	NMAE (%)	nRMSE (%)
					Measured	ANN			
Jan	361.15	0.42	81.47	28.14	20.65	20.61	0.007	0.120	0.140
Feb	461.52	0.61	82.03	35.69	29.89	29.87	0.002	0.040	0.049
Mar	548.24	0.62	83.64	40.12	31.56	30.61	0.006	0.030	0.025
April	575.12	0.60	79.62	42.53	30.23	30.26	0.005	0.018	0.031
May	559.67	0.59	77.35	46.22	30.53	30.53	0.002	0.022	0.028
June	537.17	0.55	76.92	45.24	26.14	26.14	0.008	0.193	0.217
July	537.81	0.05	76.66	48.28	25.68	25.71	0.020	0.167	0.199
Aug	428.80	0.47	76.90	53.27	22.13	22.13	0.001	0.027	0.031
Sep	437.51	0.50	77.78	51.62	23.68	23.68	0.016	0.236	0.288
Oct	466.57	0.63	78.74	53.21	29.91	29.90	0.001	0.016	0.019
Nov	369.82	0.44	78.48	45.08	21.20	21.23	0.014	0.205	0.257
Dec	370.84	0.47	80.66	43.36	25.60	25.61	0.004	0.023	0.029
Avg.	471.18	0.50	79.19	44.40	26.43	26.36	0.007	0.092	0.109

5.7 ANN MODEL FOR SHORT-TERM SOLAR ENERGY FORECASTING

Further, the generation of power in a solar photovoltaic system depends more on the changes in climatic conditions. Therefore, in the present work, different sky-conditions have been considered for forecasting power under composite climatic conditions and evaluation indexes have been used to validate the performance of models and shown in Fig. 5.8 – Fig. 5.11.

5.7.1 Sunny/Clear Sky (Type-a)

1st June 2016 was observed as a sunny day as the diffuse solar energy is lower than 25% of global solar energy and the sunshine duration is equal to or more than 9 hours. As shown in Fig. 5.8, the forecasted bell-shaped power curve on hourly basis was accurately following the measured power employing the ANN methodology and the considered duration is of 24 hours.

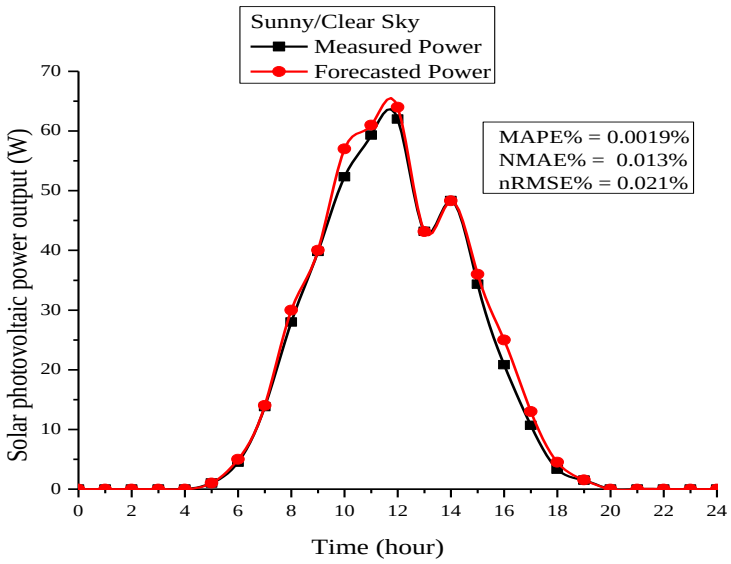

Fig. 5.8 Forecasted power in a solar photovoltaic system for a sunny day - 1st June 2016 with evaluation indexes

It has been observed that the sunny sky model gives the maximum power output of 16.92 W with MAPE of 0.0019%, NMAE of 0.013% and

nRMSE of 0.021%. In this sky-condition, time factor majorly affects the solar radiation than the factor of temperature.

5.7.2 Hazy Sky (Type-b)

Similarly, 26th December 2016 was observed as a hazy day as the diffuse solar energy is lower than 50% of global solar energy and the sunshine duration is between 7-9 hours. In this sky-condition as well, the forecasted bell-shaped power curve on hourly was accurately following the measured power employing the proposed artificial neural network methodology as illustrated in Fig. 5.9 and the considered duration is of 24 hours.

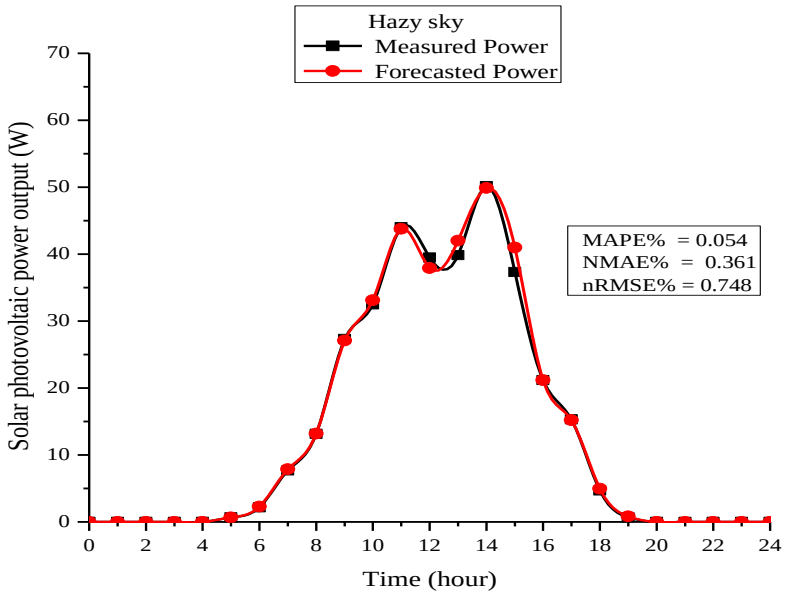

Fig. 5.9 Forecasted power in a solar photovoltaic system for the hazy day - 26th December 2016 with evaluation indexes

For hazy sky model, the forecasted power is comparatively smaller than the sunny sky model with a maximum power output of 13.44 W, MAPE of 0.054%, NMAE of 0.361% and nRMSE of 0.7488%. In a hazy sky day, the sun rays will get blocked and here a factor of temperature majorly affects the solar insolation as compared to a factor of time, which is not the same as incase of sunny sky day.

5.7.3 Partially Foggy/Cloudy Sky (Type-c)

Similarly, 3rd August 2016 was observed as a partially foggy/cloudy sky as the diffuse solar energy is lower than 75% of global solar energy and the sunshine durationis between 5-7 hours. In this sky-condition, the power curve is biased during noon with a maximum power output of only 6.42 W, MAPE of 0.024%, NMAE of 0.087% and nRMSE of 0.204% as shown in Fig. 5.10.

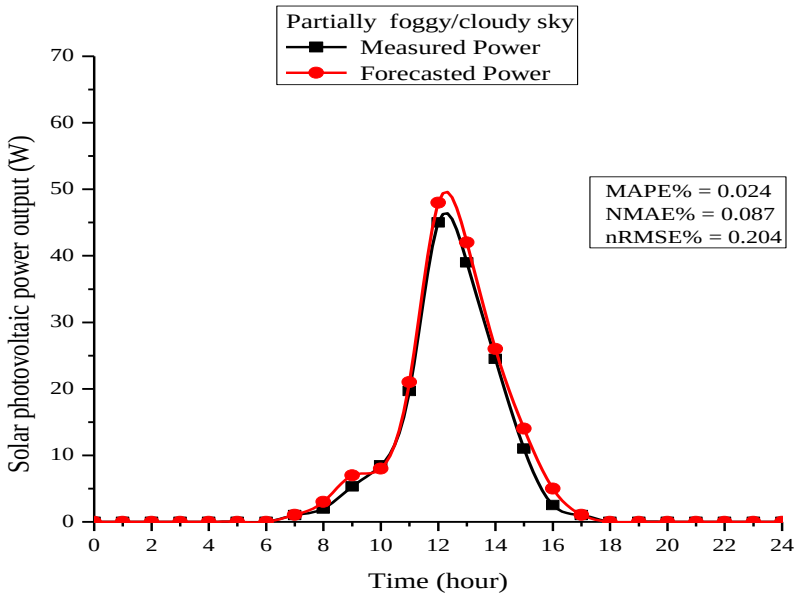

Fig. 5.10 Forecasted power in a solar PV system for the partially foggy/cloudy day - 3rd August 2016 with evaluation indexes

The considered duration is of 24 hours and for this model, the sun rays are partially absorbed by the solar photovoltaic system and partially by the cloud cover and both the factor of time and temperature affects the solar radiation.

5.7.4 Fully Foggy/Cloudy Sky (Type-d)

Similarly, 3rd January 2016 was observed as a fully foggy/cloudy sky as the diffuse solar energy is greater than 75% of global solar energy and the sunshine duration is lower than 5 hours. For this sky-condition, the power

curve is biased during noon hours with a maximum power output of 2.97 W, mean absolute percentage error of 0.109%, the normalized mean absolute error of 0.716% and normalized root mean square error of 1.58% as represented by the measured and forecasted data shown in Fig. 5.11 employing artificial neural network methodology and the considered duration is of 24 hours. In this model, the sun rays will get fully blocked by the presence of cloud, and both the factor of time and temperature will affect the solar radiation.

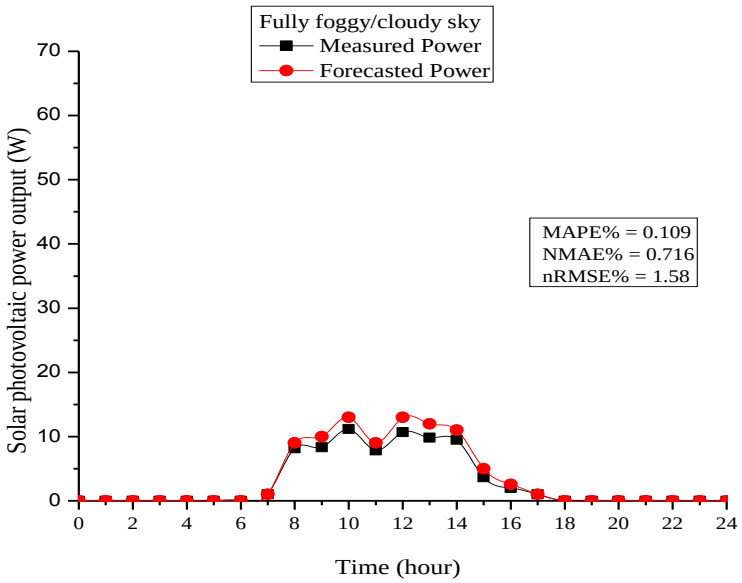

Fig. 5.11 Forecasted power in a solar PV system for fully foggy/cloudy day - 3rd January 2016 with evaluation indexes

5.8 COMPARISON OF ANN MODELS WITH FUZZY LOGIC BASED MODEL

A comparative analysis has been carried out between the ANN model employing radial basis function neural network and fuzzy logic based model in forecasting global solar energy for different sky-conditions and the performance has been measured based on evaluation indexes and are presented in Table 5.10.

Table 5.10 Comparative analysis of ANN model with fuzzy logic based model for distinct climate zone across India

Climate Zone	**Sky-Conditions**	**Global Solar Energy H_g (MJ/m^2)**			**MPE (%)**	
		Measured	**Fuzzy**	**ANN**	**Fuzzy**	**ANN**
New Delhi (Composite)	Clear/Sunny Sky	20.57	20.2	20.58	-2.32	-0.03
	Hazy Sky	18.12	18.5	18.14	0.03	0.14
	Partially Foggy/Cloudy Sky	12.51	12.8	12.51	2.24	0.16
	Fully Foggy/Cloudy Sky	7.48	10.1	8.13	35.1	8.63
Chennai (Warm and Humid)	Clear/Sunny Sky	23.60	22.3	23.30	-5.83	-1.31
	Hazy Sky	21.11	20.8	21.10	-1.08	-0.03
	Partially Foggy/Cloudy Sky	18.33	18.9	18.37	0.10	0.02
	Fully Foggy/Cloudy Sky	11.88	12.1	12.22	3.27	2.14
Jodhpur (Hot and Dry)	Clear/Sunny Sky	21.76	21.7	21.73	-0.31	-0.05
	Hazy Sky	19.99	20.1	19.86	0.68	-0.51
	Partially Foggy/Cloudy Sky	18.08	18	18.16	-0.34	0.21
	Fully Foggy/Cloudy Sky	16.63	19.2	16.62	13.6	0.11
Shillong (Cold and Cloudy)	Clear/Sunny Sky	22.85	22.7	22.78	-0.95	-0.25
	Hazy Sky	19.25	19.3	19.25	0.51	0.02
	Partially Foggy/Cloudy Sky	16.09	16.5	16.06	2.94	-0.16
	Fully Foggy/Cloudy Sky	11.22	11.6	11.23	1.30	0.46
Pune (Moderate)	Clear/Sunny Sky	21.49	21.5	21.48	-0.06	-0.05
	Hazy Sky	20.41	20.2	20.44	-0.57	0.25
	Partially Foggy/Cloudy Sky	18.71	18.9	19.18	1.16	0.90
	Fully Foggy/Cloudy Sky	13.73	13.8	13.75	4.95	0.30

On comparing the obtained results, the error in case of proposed ANN model employing radial basis function neural network is comparatively less and reduced as compared to fuzzy logic based model for each of the climate zone across the entire country which means that it provides better accuracy.

5.9 CONCLUSION

In this chapter, the variants of ANN architectures i.e. cascade-forward, feed-forward, elman back-propagation, generalized regression, layered recurrent, linear layer and radial basis function neural network architecture have been developed and presented for modelling the system in forecasting global solar energy using meteorological parameters under composite climatic conditions. It has been concluded from the obtained results that the radial basis function neural network model has emerged to provide a better prediction with minimum error as compared to other models based on evaluation indexes.

Further, simulations have been performed for forecasting global solar energy employing radial basis function neural network model based on sky-conditions i.e. sunny sky (type-a), hazy sky (type-b), partially foggy/cloudy sky (type-c) and fully foggy/cloudy sky (type-d) condition and obtained results have been compared with feed-forward neural network model and further applied for distinct climate zone across India.

It has been concluded that by employing radial basis function neural network, the obtained results are precise and accurate in each of the climate zone across the entire country.

Obtained results are further exploited to forecast solar PV system power based on sky-conditions which employ 210 W_p HIT solar PV modules operated at MPPT conditions for composite climatic conditions.

It has been concluded from the results that for composite climatic conditions, the hazy-sky model outperforms other models as the measured data matches the forecasted data followed by the sunny-sky model, partially foggy/cloudy sky model and fully foggy/cloudy sky model. The result reveals that the model may be implemented for a broad series of applications.

Lastly, the comparison of the proposed ANN model has been made with fuzzy logic based model and the obtained results after statistical analysis reveals the accuracy and supremacy of the proposed ANN model as compared to fuzzy logic based model.

CHAPTER 6

HYBRID INTELLIGENT MODEL FOR FORECASTING SOLAR ENERGY

6.1 INTRODUCTION

In the previous chapters modelling based on Artificial Neural Network (ANN) and fuzzy logic were used for forecasting solar energy. This chapter presents the hybrid intelligent models for forecasting global solar energy using meteorological parameters. In this, a model underlying the principle of Adaptive Neural-Fuzzy Inference System (ANFIS) architecture has been presented, which provides a basis of Fuzzy Inference System (FIS) implemented within the framework of adaptive networks. Simulations have been carried out based on sky-conditions such as sunny sky (type-a), hazy sky (type-b), partially foggy/cloudy sky (type-c) and fully foggy/cloudy (type-d) sky-conditions and for distinct climate zone i.e. warm and humid, hot and dry, cold and cloudy, moderate and composite climate across India. Further, the obtained results have been implemented for solar PV system based on sky-conditions such as sunny, hazy, partially and fully foggy/cloudy sky-conditions under composite climatic conditions. Lastly, a comparison of the proposed model has been carried out with variants of artificial neural network model and fuzzy logic based model for validation of the results.

This chapter is partially based on the following published papers:

1. **Gulnar Perveen**, M. Rizwan and Nidhi Goel, "Comparison of intelligent modelling techniques for solar energy forecasting and its application in solar PV systems," **IET Energy Systems Integration**, Vol. 1, No.1, pp. 34-51, 2019. ISSN No. 2516-8401 (Online).

For modelling complex systems, an accurate analysis of a number of hidden layers with aid of artificial neural network is a difficult task. Therefore, to overcome these drawbacks, a hybrid intelligent model has been proposed which integrate the concept of Fuzzy Inference System (FIS) and Artificial Neural Network (ANN) in forecasting global solar energy. Recently, the ANFIS based model has attracted many researchers in various scientific fields due to the growing need of an intelligent technique to model the system [108]. Many researchers have worked in an application area where the fusion of ANN and fuzzy logic approach has been effectively implemented.

For real-time applications, a comprehensive survey has been carried out based on neuro-fuzzy rule generation algorithm for delivering maximum power to the load based on Maximum Power Point Tracking (MPPT) conditions as it gives a faster response with precision and accuracy. Many grid-connected solar PV plants are based on photovoltaic technology, but varying sky-conditions makes the output of the system non-deterministic and stochastic [109-115]. So, accurate forecasting is essential as the uncertainty of sky-conditions greatly affects the power of solar PV systems. Lot of research has been done for forecasting global solar energy by employing ANFIS modelling; however, literature based on ANFIS modelling for forecasting global solar energy in different sky-conditions and for distinct climatic conditions is less reported.

This chapter proposes hybrid intelligent model i.e. ANFIS-based model for forecasting global solar energy based on sky-conditions using meteorological parameters. Simulations have been carried out for different climatic conditions across India with aid of statistical performance indicators.

The obtained results have been implemented to forecast power in solar PV system at Maximum Power Point (MPP) conditions. Lastly, the comparison of the ANFIS-based model has been made with variants of ANN model and the fuzzy logic based model for validation of the results.

6.2 DEVELOPMENT OF ANFIS BASED MODEL FOR FORECASTING SOLAR ENERGY

The ANFIS involves hybrid learning rule for system optimization. It is a graphical analysis of Fuzzy-Sugeno system which lies within the framework of adaptive networks and is surrounded by neural learning capabilities. The main factor influencing the hybrid method is that the convergence rate is faster as search space dimensions have been reduced for the back-propagation neural network method. Neuro-fuzzy systems combine artificial neural network with fuzzy inference systems, which allows transformation of the system into if-then rules set, and the fuzzy inference system becomes a neural network structure with distributed connection strengths. Hybrid intelligent model is advantageous for research and applications based on an artificial neural network algorithms and adaptation of fuzzy linguistic rules. An adaptive network is basically a network structure comprising nodes and directional links with overall input-output behaviour defined with a set of modifiable parameters and makes use of hybrid learning algorithm for identifying parameters of the fuzzy inference system. It combines least-squares and back-propagation gradient descent method to train the parameters of the membership function. In the forward phase of the network algorithm, identification of the least squares estimates has been done by the consequent parameters. In the backward phase, the derivatives of the squared error propagate backwards from the output layer to

the input layer wherein the premise parameters are updated by the gradient descent algorithm. ANFIS training uses algorithms for reducing the error. ANFIS is the fuzzy model put in the framework of the adaptive system for model building and validation to facilitate training and adaptation [116-120].

6.2.1 The ANFIS Architecture

The ANFIS network is a multilayer feed-forward network comprising nodes wherein each node is connected by directed links and is performing the function for generating single node output from incoming signals. In an ANFIS network, each link specifies signal direction from one node to another node. The adaptive network configuration perform a node function in signals coming from previous nodes for generating a single output at the node and each node function is parameterized and by changing the modifiable parameters, the overall functioning of the node and behaviour of the network are changed. The architecture of ANFIS has been shown in Fig. 6.1 which comprises five layers i.e. fuzzy layer, product layer, normalized layer, de-fuzzy layer and the output layer.

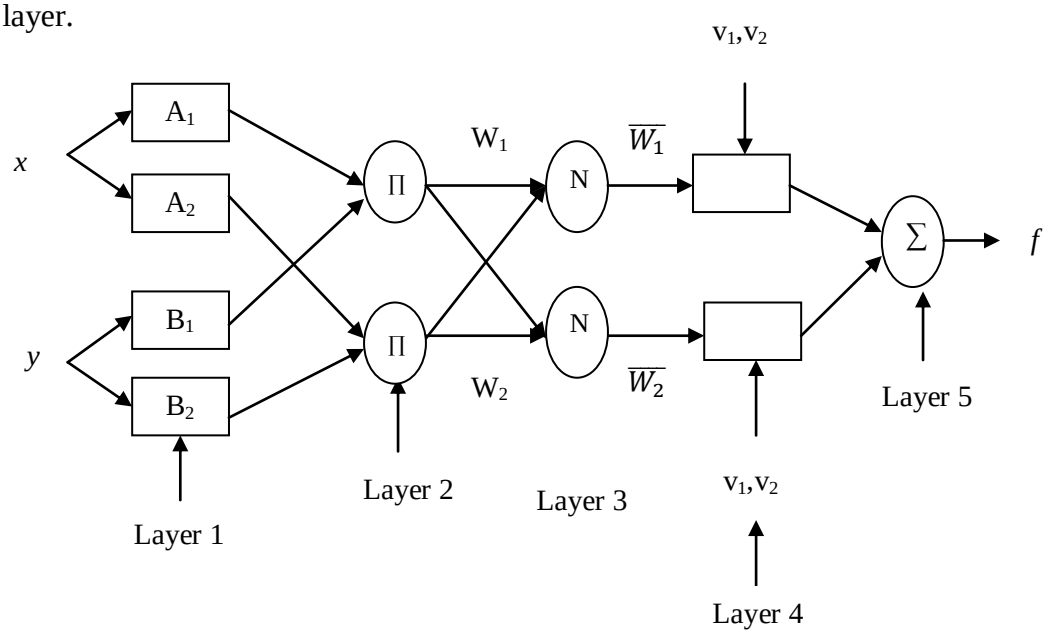

Fig. 6.1 Architecture of ANFIS for forecasting global solar energy

The ANFIS architecture comprises a fuzzy inference system (FIS) and membership functions are tuned with the back-propagation algorithm and least squares method. The aim is to determine the optimum values of FIS with aid of algorithm. Optimization has been done during the training session wherein the error between the measured and targeted output is minimized. A hybrid algorithm which combines least squares estimates and gradient descent method has been used for optimization [121]. Consider that the ANFIS architecture has two inputs namely *x* and *y* and one output *f*.

A first-order Takagi, Sugeno and Kang (TSK) fuzzy inference system has been implemented comprising two rules:

Rule 1: If (x is A_1) and (y is B_1) then $f_1 = p_1x + q_1y + r_1$

Rule 2: If (x is A_2) and (y is B_2) then $f_2 = p_2x + q_2y + r_2$

where p_1, p_2, q_1, q_2, r_1 and r_2 represent the linear parameters; and A_1, A_2, B_1 and B_2 are non-linear parameters.

While defining ANFIS architecture, one of the important considerations is that tuning of the number of training epochs, the number of fuzzy rules and the number of membership functions should be made accurately. A better and more accurate system can be well defined if the difference between desired output and measured data output is less.

The integration of artificial neural network and fuzzy logic i.e. fuzzy neural network has been established; generally, the arrangements of fuzzy logic and the neural network are called as ANFIS.

6.2.2 Layers of ANFIS

A concise outline of five layers of ANFIS architecture with inputs *x*, *y* and one output *f* has been shown in Fig. 6.1 which comprises five layers as:

(a) Layer 1

For this layer, input node i comprises an adaptive node producing membership of the linguistic label. In this layer, A_1, A_2, B_1 and B_2 are the input of the system and $O_{1,i}$ defines the output of the i^{th} node of layer 1. Each adaptive node is a square node with square function represented by using Eq. (6.1) - Eq. (6.2).

$$O_{1,i} = \mu_{A,i}(x) \text{ for } i = 1,2 \quad (6.1)$$

$$O_{1,j} = \mu_{B,j}(y) \text{ for } j = 1,2 \quad 6.2)$$

where $\mu_{A,i}$ and $\mu_{B,j}$ are the membership function degree, $O_{1,i}$ and $O_{1,j}$ represents the output function, for fuzzy sets A_i and B_i respectively.

(b) Layer 2

In layer 2, membership function weights are checked, which receives input A_i from the previous layer and acts as a membership function to represent fuzzy sets of respective input variables. Each node represents the fixed node labeled with '$\prod$' where the output is the product of all incoming signals which can be shown by using Eq. (6.3) as:

$$O_{2,i} = \mu_{A,i}(x) * \mu_{B,j}(y) \text{ for } i = 1,2 \quad (6.3)$$

which are the firing strengths of the rules. In general, any T-norm operator that performs fuzzy AND can be used as a node function in this layer.

(c) Layer 3

This layer is marked with a circle labeled as 'N', which indicates the normalization to the firing strength from the previous layer. It does pre-condition matching of fuzzy rules which otherwise compute activation level of each rule. In this layer, the i^{th} node computes the ratio of i^{th} rule's strength to

the sum of all rules firing strength and the output can be expressed as $O_{3,i}$ using Eq. (6.4) as:

$$O_{3,i} = \frac{w_i}{w_1+w_2} \text{ for } i = 1,2 \quad (6.4)$$

For convenience, outputs of this layer will be called as normalized firing strengths.

(d) Layer 4

In this, the output values are resulted from the rules inference and represent the product of the normalized firing rule strength and first-order polynomial which can be expressed by Eq. (6.5) as:

$$O_{4,i} = \overline{w_i} f_i = \overline{w_i}(p_i x + q_i y + r_i) \text{ for } i = 1,2 \quad (6.5)$$

where $O_{4,i}$ represents layer 4 output. In this layer, p_i, q_i and r_i are linear parameters or consequent parameters.

(e) Layer 5

This layer basically does the summation of all incoming signals coming from its previous layer i.e. layer 4 and does the transformation of fuzzy classification results into crisp values which comprise single fixed node labeled as 'Σ'. This layer does the summing of all the incoming signals calculated using Eq. (6.6) as:

$$O_{5,i} = \sum \overline{w_i} f_i = \frac{\sum w_i f_i}{w_1+w_2} \text{ for } i = 1, 2 \quad (6.6)$$

Hence, when the premise parameters are fixed, the adaptive network output can be expressed as a combination of a consequent parameter and the behaviour of the network is considered to be the same as that of the Sugeno fuzzy model.

6.3 RESULTS AND DISCUSSIONS

In this chapter, ANFIS-based model has been employed for forecasting global solar energy with aid of meteorological parameters. For training and testing of the data, MATLAB software has been used with function "anfisedit" in the command window and evaluating the output by using the function "evalfis (input, tra)" where the term "input" contains the input data and "tra" represents the training data as shown in Fig. 6.2 respectively.

Fig. 6.2 ANFIS training data simulated in MATLAB with five inputs and one output

Further, the ANFIS model structure simulated in MATLAB with five meteorological parameters as inputs namely wind speed, dew-point, sunshine hours, relative humidity, ambient temperature and global solar energy as the output have been shown in Fig. 6.3. Here, ground data of five meteorological stations have been considered using statistical performance indicators and are illustrated in Table 6.1.

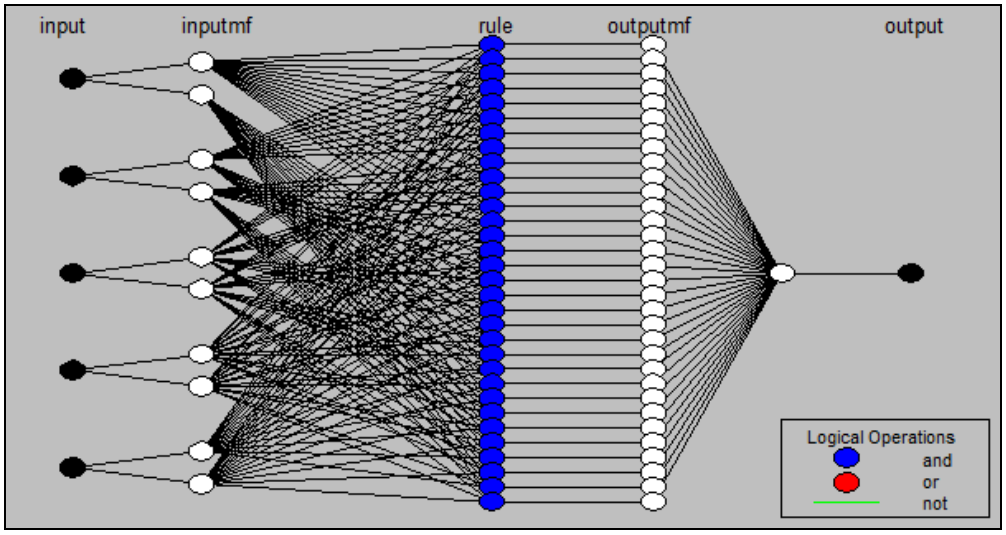

Fig. 6.3 ANFIS model structure with five inputs and one output simulated in MATLAB

From Table 6.1, following can be briefly summarized:-

6.3.1 Clear/Sunny Sky (Type-a)

In sunny/clear sky-condition, the computed error is observed to be minimum for Jodhpur station in comparison to other station with averaged mean absolute percentage error of $1x10^{-4}$%. The reason behind is that Jodhpur enjoys hot and dry climatic conditions wherein sunny weather prevails all throughout the year.

6.3.2 Hazy Sky (Type-b)

In hazy sky-condition, the computed error is observed to be minimum for the composite climate in comparison to other climatic conditions with averaged mean absolute percentage error of $5x10^{-5}$%. This is due to the presence of high value of relative humidity which varies about 25-35% during dry periods to 60-90% during wet periods.

Table 6.1 ANFIS based model for forecasting global solar energy along with statistical performance indicators for distinct climate zone

Climate Zone	**Sky-Conditions**	**Global Solar Energy H_g (MJ/m^2)**		**MAPE (%)**	**NMAE (%)**	**nRMSE (%)**
		Measured	**Fuzzy**			
New Delhi (Composite)	Clear/Sunny Sky	20.60	20.60	0.00013	0.00012	0.13798
	Hazy Sky	18.10	18.10	0.00005	0.00008	0.13700
	Partially Foggy/Cloudy Sky	12.52	12.52	0.00089	0.00006	0.19377
	Fully Foggy/Cloudy Sky	7.48	7.48	0.00004	0.00000	0.00000
Chennai (Warm and Humid)	Clear/Sunny Sky	23.60	23.60	0.00012	0.00012	0.11429
	Hazy Sky	21.11	21.11	0.00924	0.00852	0.19315
	Partially Foggy/Cloudy Sky	17.58	17.58	0.00750	0.00610	0.19967
	Fully Foggy/Cloudy Sky	12.30	12.20	0.00008	0.41493	0.49918
Jodhpur (Hot and Dry)	Clear/Sunny Sky	21.758	21.758	0.00010	0.00013	0.12458
	Hazy Sky	19.986	19.986	0.00006	0.00005	0.11210
	Partially Foggy/Cloudy Sky	18.075	18.075	0.00905	0.00007	0.13261
	Fully Foggy/Cloudy Sky	16.628	16.752	0.00544	0.00442	0.09626
Shillong (Cold and Cloudy)	Clear/Sunny Sky	22.83	22.83	0.00966	0.00889	0.14512
	Hazy Sky	19.25	19.25	0.00662	0.00509	0.20678
	Partially Foggy/Cloudy Sky	16.09	16.09	0.00421	0.00267	0.24032
	Fully Foggy/Cloudy Sky	11.22	11.22	0.00001	0.00054	0.20333
Pune (Moderate)	Clear/Sunny Sky	21.49	21.52	0.10504	0.09868	0.28673
	Hazy Sky	20.42	20.43	0.03890	0.03146	0.21360
	Partially Foggy/Cloudy Sky	18.71	18.71	0.00180	0.00013	0.10925
	Fully Foggy/Cloudy Sky	13.73	13.83	0.00012	0.00006	0.13132

6.3.3 Partially Foggy/Cloudy Sky (Type-c)

For this sky-condition, the error is observed to be minimum for warm and humid climate in comparison to other climate zone with mean absolute percentage error of $7.5x10^{-3}$%. This condition is apparently due to high diffused radiations owing to the cloudy conditions, which also results in the marginal dissipation of heat during the night.

6.3.4 Fully Foggy/Cloudy Sky (Type-d)

In this sky-condition, the computed error is observed to be minimum for Shillong station in comparison to other station with mean absolute percentage error of $1x10^{-5}$%.

The main contributing factor is that during winter the solar radiation intensity is comparatively lower with a high percentage of diffused solar radiation, which makes extremely cold winters.

Further, the comparison of the measured and forecasted data obtained by using ANFIS based model for varying sky-conditions have been presented in Fig. 6.4 – Fig. 6.8 and further simulated for distinct climate zone across India.

It has been observed from Fig. 6.4 - Fig. 6.8 that the forecasted data attained by employing the ANFIS-based model in varying sky-conditions is same as that of the measured data and the performance of the model is satisfying.

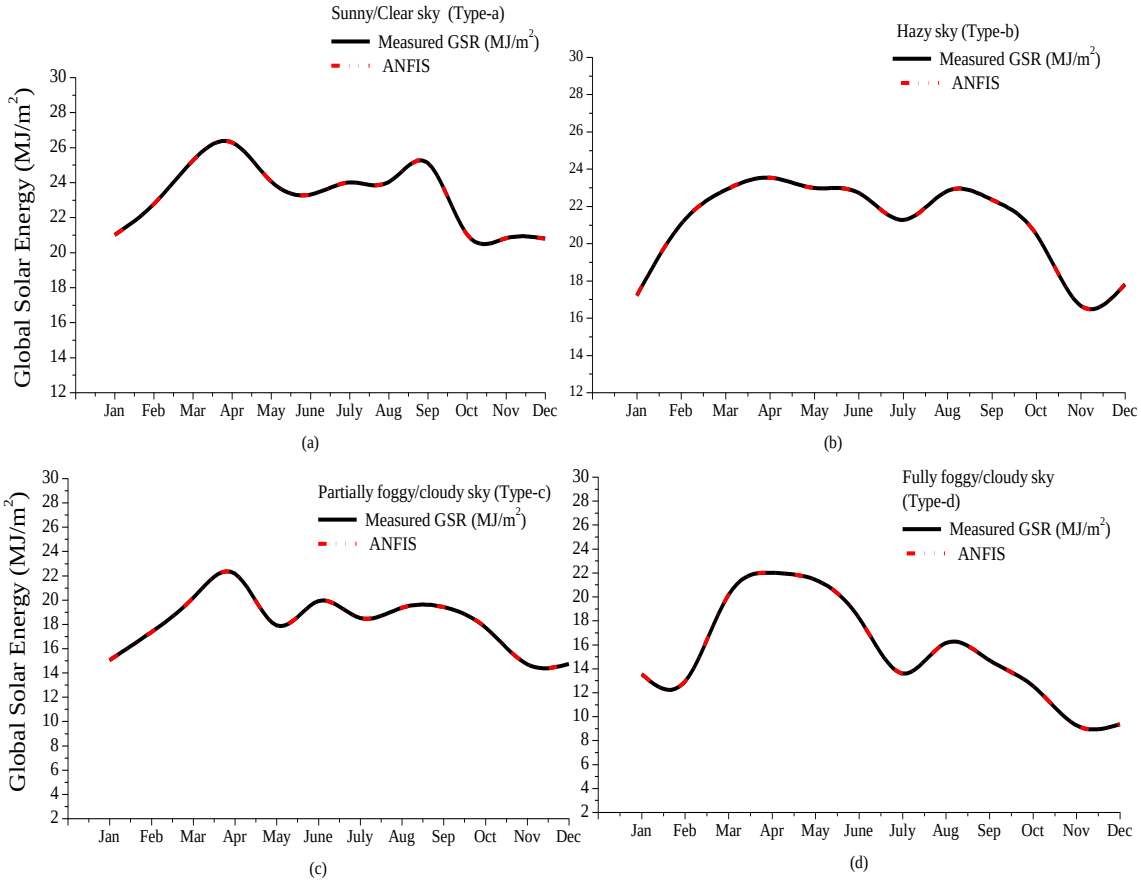

Fig. 6.4 Graphical representation of measured and forecasted global solar energy using ANFIS methodology for warm and humid climate zone

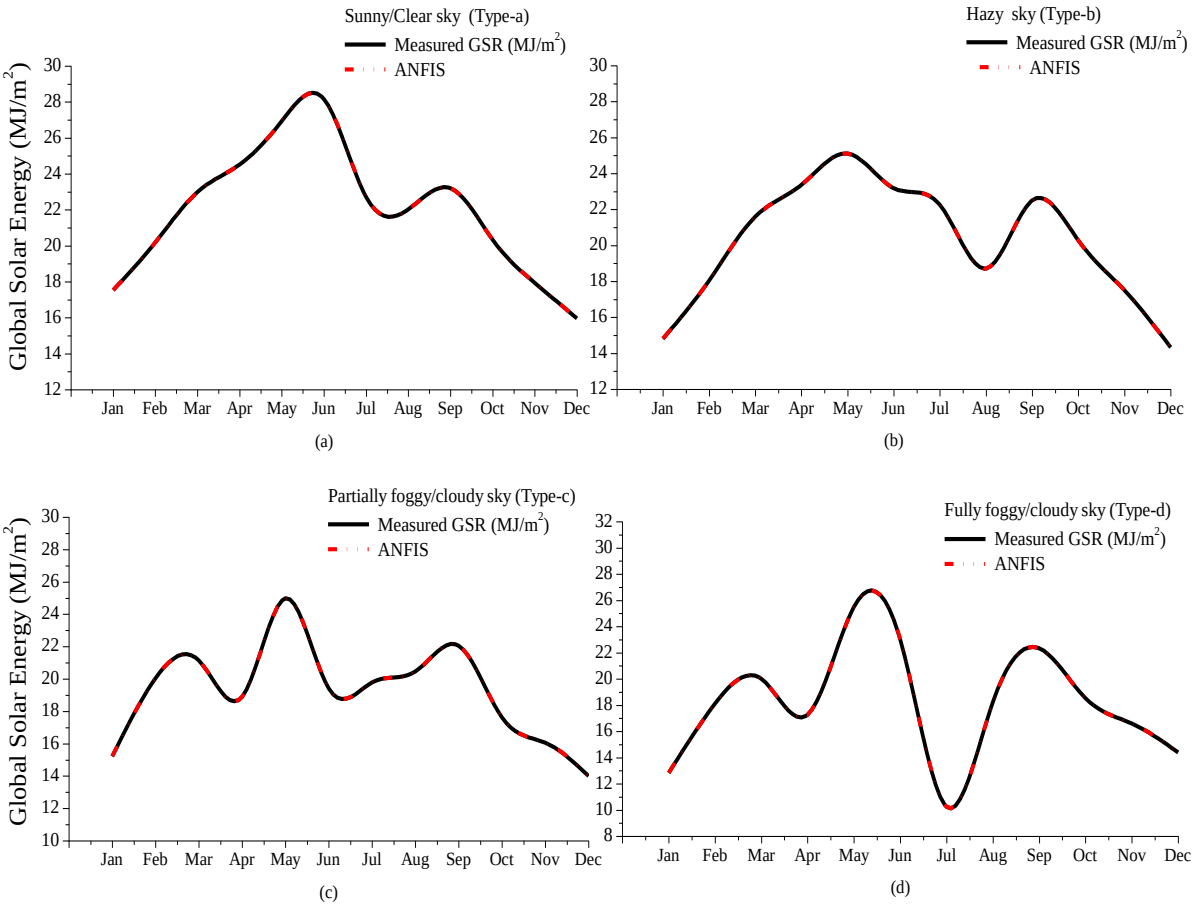

Fig. 6.5 Graphical representation of measured and forecasted global solar energy using ANFIS methodology for hot and dry climate zone

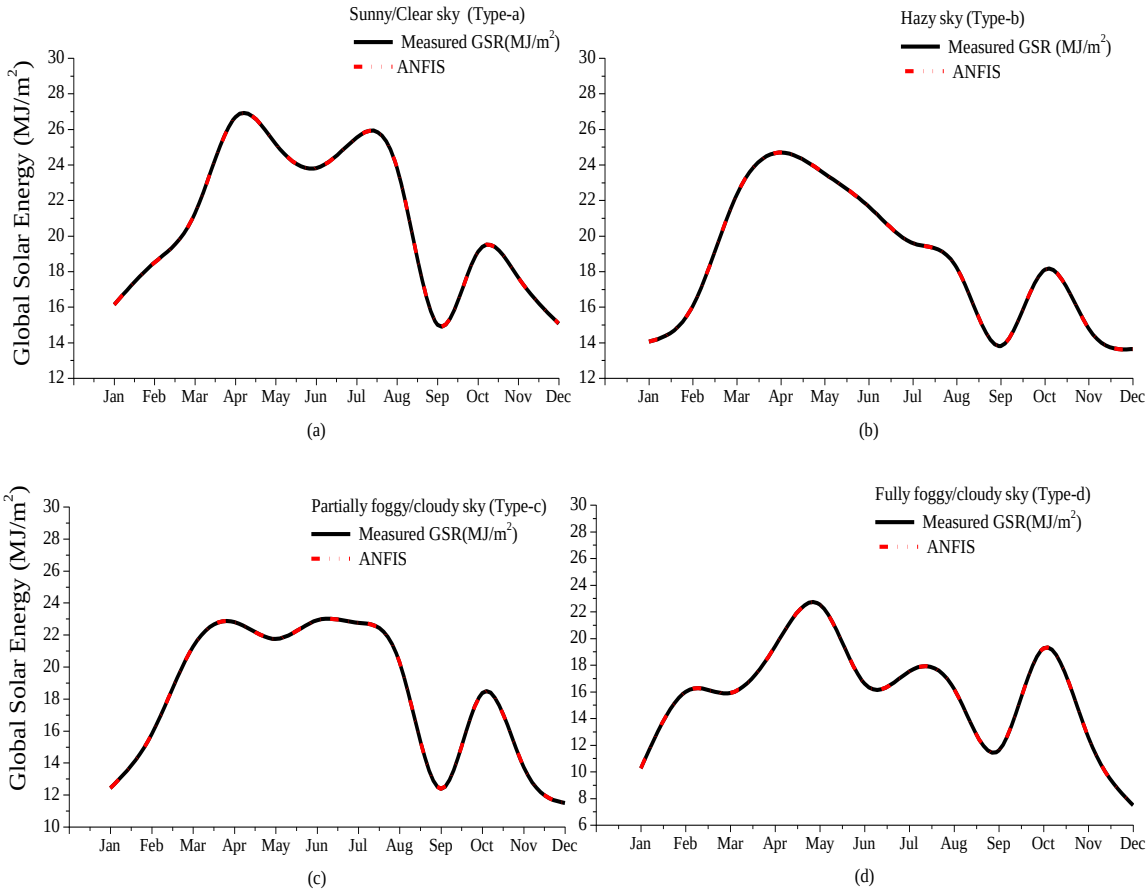

Fig. 6.6 Graphical representation of measured and forecasted global solar energy using ANFIS methodology for composite climate zone

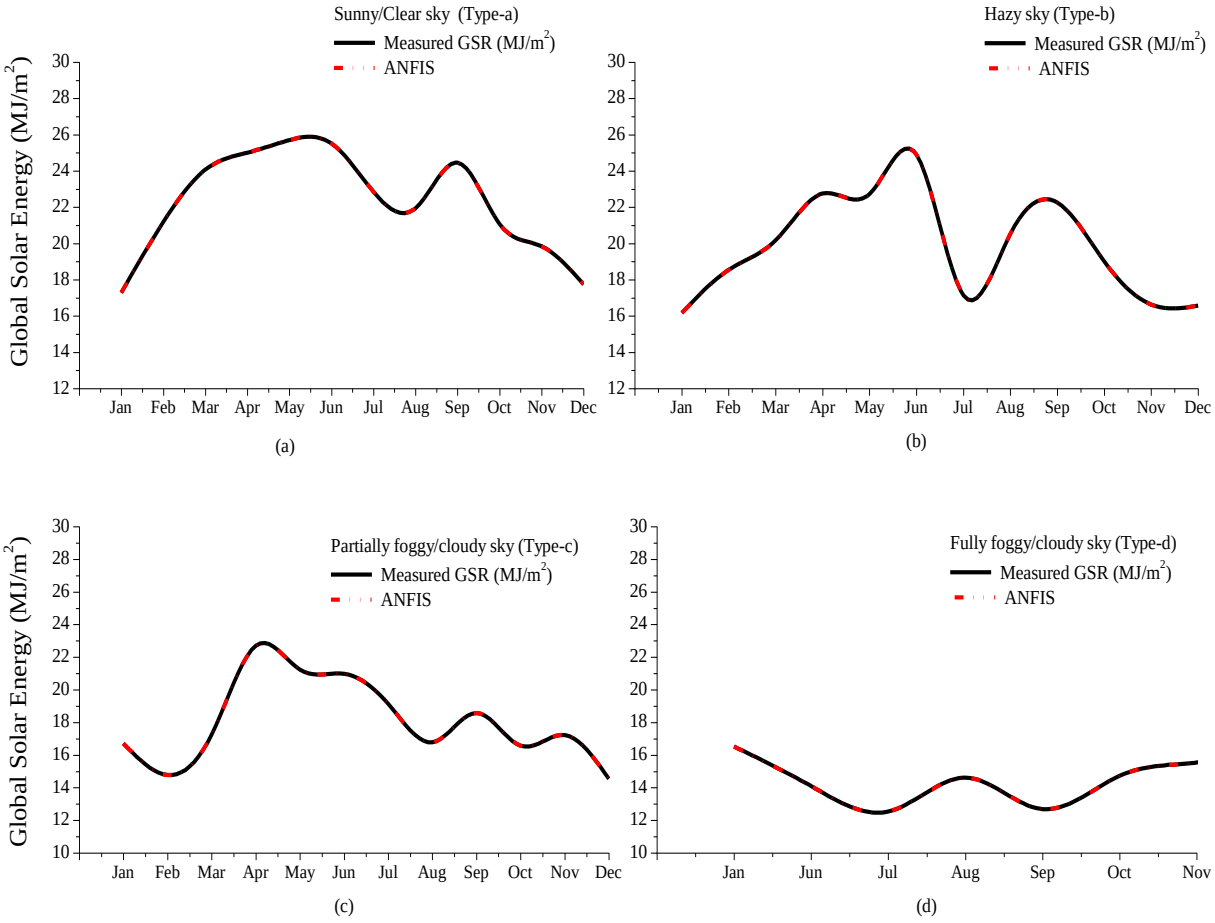

Fig. 6.7 Graphical representation of measured and forecasted global solar energy using ANFIS methodology for moderate climate zone

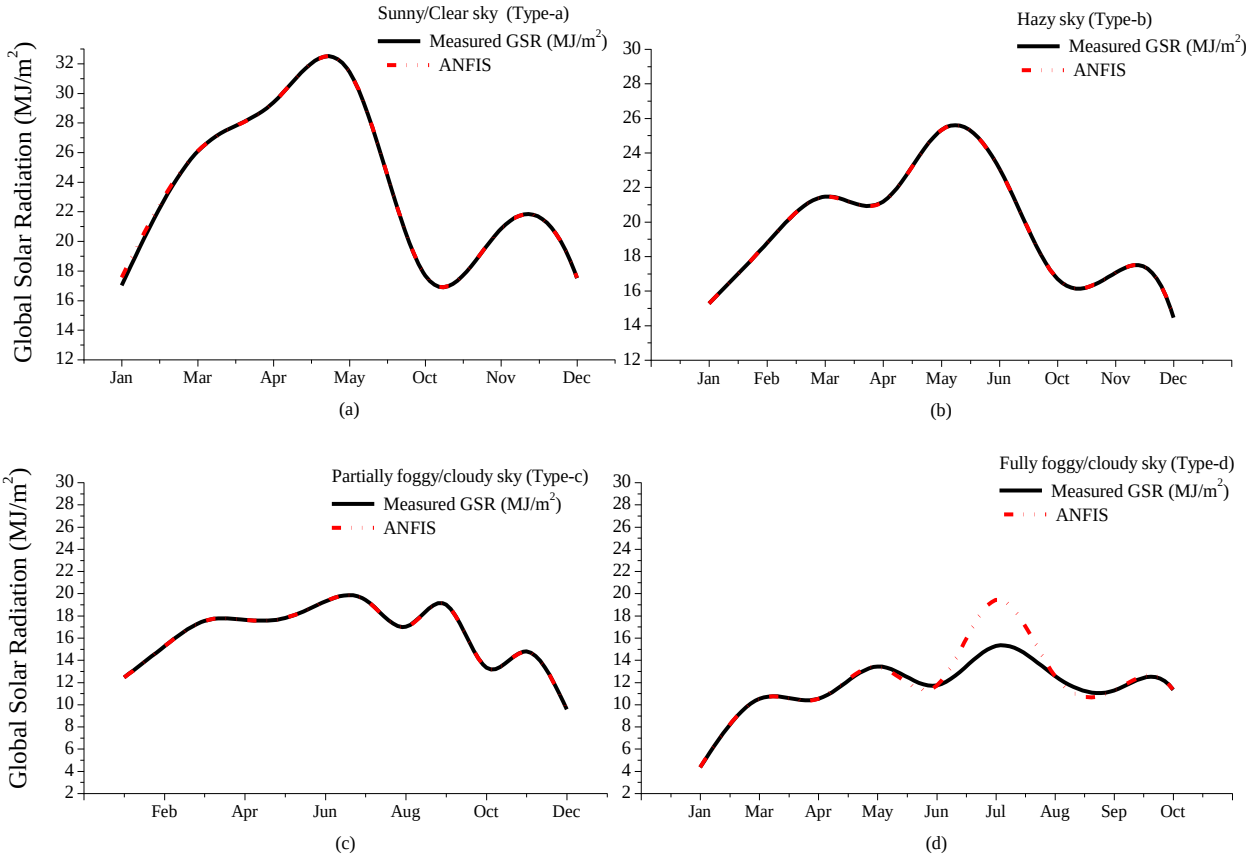

Fig. 6.8 Graphical representation of measured and forecasted global solar energy using ANFIS methodology for cold and cloudy climate zone

6.4 IMPLEMENTATION OF ANFIS-BASED MODEL FOR SOLAR PV APPLICATIONS

Attributing to meteorological factor, the solar PV power output fluctuates along with the solar insolation intensity, which shows random behaviour based on the topographical location and seasonal variation and is difficult to control. In the present work, 250 W_p multi-crystalline solar PV modules have been used whose performance specification are listed in table A.1 of Appendix. The ANFIS based model has been employed to forecast the behaviour of power generation in a solar photovoltaic system and shown in Table 6.2 for composite climate zone.

From Table 6.2, it is evident that the mean absolute percentage error of a solar photovoltaic system is 0.0077% by employing ANFIS based model, which is accurate and within the permissible error limit. Further, it is to be noted that for the winter season (January), the mean absolute percentage error is 0.0057%; for the summer season (May), the mean absolute percentage error obtained is 0.0027% respectively. The value of mean absolute percentage error is comparatively large for the rainy season (July) of the value of 0.0220%, due to large uncertainties associated with the data.

The ANFIS methodology integrates the features of fuzzy logic and artificial neural network which increases the system accuracy, robustness and adaptability with the non-linearity associated with the data.

6.5 SHORT-TERM PV POWER FORECASTING USING ANFIS BASED MODEL

The daily power generation in a solar photovoltaic system based on the performance characterization is presented in Fig. 6.9.

Table 6.2 Forecasted power of a solar PV system employing ANFIS modelling under composite climate zone

Month	**V_{pmax} (V)**	**I_{pmax} (A)**	**Solar Irradiance (W/m^2)**	**V_{oc} (V)**	**I_{sc} (A)**	**Cell Temp. (^oC)**	**Power (W)**		**MAPE (%)**	**NMAE (%)**	**nRMSE (%)**
							Measured	**Forecasted**			
Jan	60.48	1.05	341.98	69.5	1.1	20.80	64.15	64.12	0.0057	0.0027	0.0031
Feb	59.95	1.49	450.78	69.6	1.5	28.19	89.61	89.57	0.0022	0.0017	0.0020
Mar	-	-	-	-	-	-	-	-	-	-	-
April	-	-	-	-	-	-	-	-	-	-	-
May	56.93	1.38	557.92	66.4	1.4	44.53	79.08	79.06	0.0027	0.0020	0.0023
June	57.57	1.20	528.54	66.2	1.2	42.32	68.28	70.19	0.0346	0.0262	0.0460
July	57.03	1.02	532.32	66.3	1.0	39.15	59.03	59.03	0.0220	0.0156	0.0354
Aug	57.07	1.03	411.69	66.7	1.1	38.15	59.52	59.52	0.0036	0.0022	0.0027
Sep	57.36	1.11	418.73	66.9	1.2	35.56	64.35	64.28	0.0052	0.0024	0.0029
Oct	57.78	1.52	464.71	68.1	1.6	37.75	88.08	88.09	0.0003	0.0002	0.0002
Nov	58.90	1.15	346.12	68.6	1.2	29.33	68.21	68.21	0.0005	0.0003	0.0003
Dec	60.09	1.26	359.34	69.8	1.3	23.94	76.30	76.30	0.0006	0.0004	0.0006
Avg.	58.32	1.22	441.21	67.8	1.3	33.97	71.66	71.84	0.0077	0.0054	0.0096

*Data could not be arranged for these months

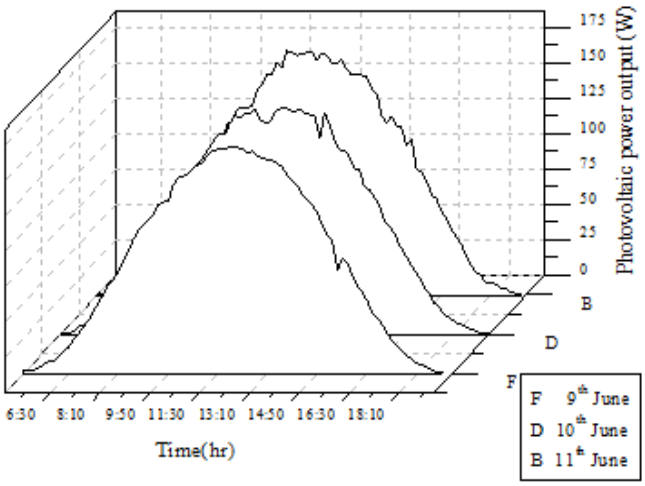

Fig 6.9 Photovoltaic system power generation on daily basis for 3 days

Fig. 6.9 presents the generation of power for 3 days i.e. 9th, 10th and 11th June and the days considered represent sunny days so solar radiation remains almost the same. Thus, it has been concluded that a high correlation prevails for generated power on a daily basis. The power output is available during the entire day and causes fluctuation to the grid when integrating unsteady photovoltaic power into the grid. Since many factors are involved which affects the solar photovoltaic system power output but the main factor is the variation in sky-condition, which makes it difficult to examine the performance characteristics with a single model.

In this, the power in a solar PV system is classified based on different sky-condition such as sunny sky, hazy sky, partially and fully foggy/cloudy sky respectively. The data has been collected on a daily basis and arranged within 1 hour for short-term PV power forecasting. The ANFIS-based model has been implemented to forecast the behaviour of a solar PV system under composite climatic conditions. The architecture of ANFIS simulated in MATLAB with two inputs namely cell temperature, solar irradiance and power output are shown in Fig. 6.10.

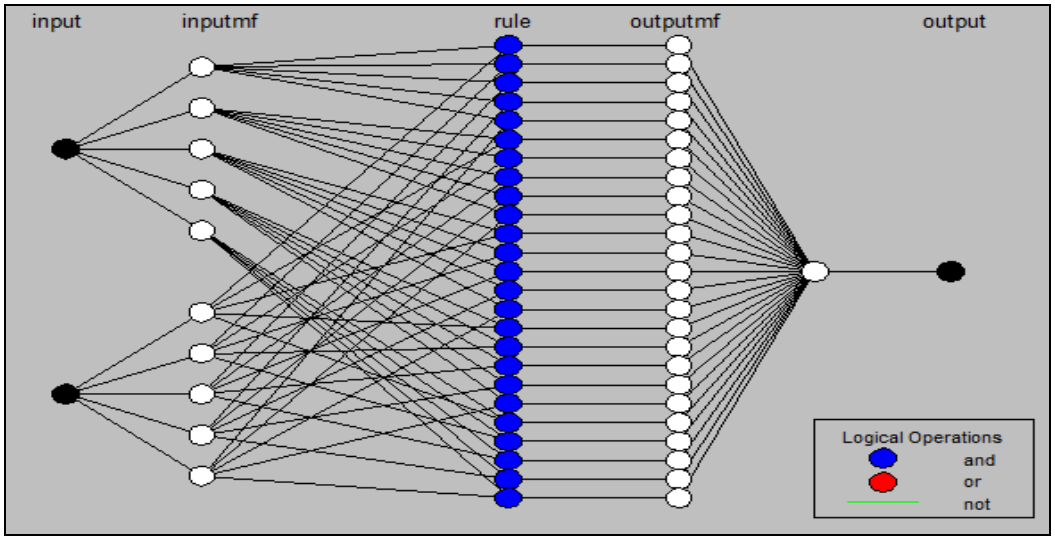

Fig. 6.10 ANFIS model structure with two inputs and one output simulated in MATLAB

Further, the graphical representation between the measured and forecasted power employing ANFIS modelling technique under four weather types is shown in Fig. 6.11.

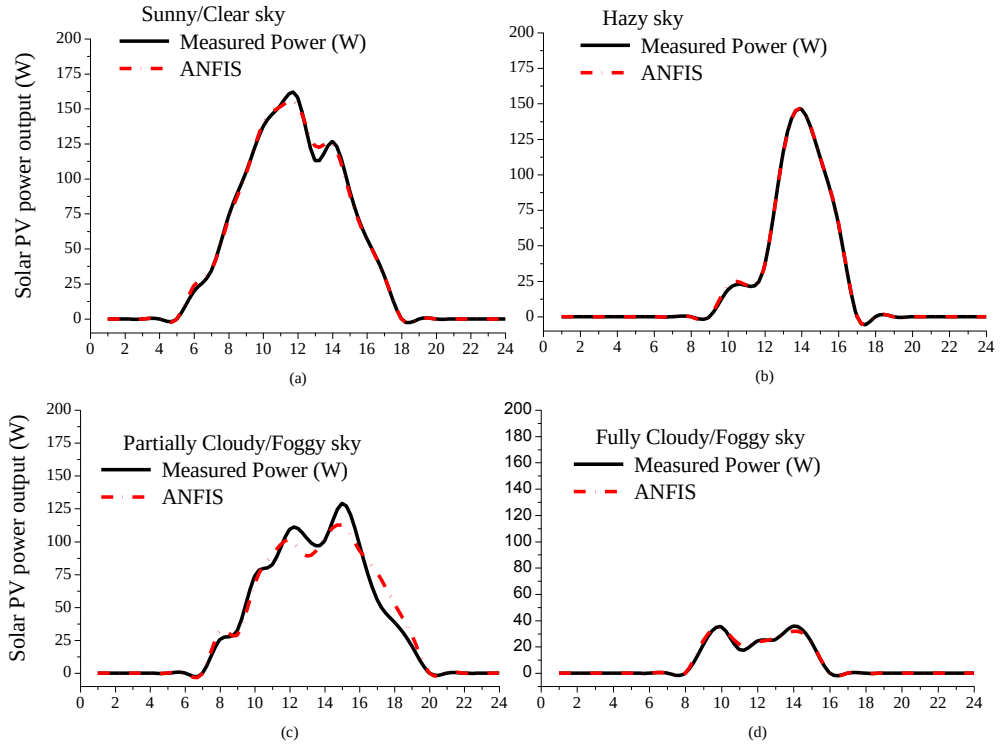

Fig 6.11 Graphical analysis of PV power output in a solar photovoltaic system

From Fig. 6.11, it is evident that the generation of power in a solar PV system varies significantly with sky-conditions. It has been observed that the hazy sky model performs well in power forecasting of solar PV system. This observation reveals that the forecasting model should be based on sky classifications.

6.6 COMPARISON OF ANFIS-BASED MODEL WITH ANN MODELS

The proposed ANFIS-based model is compared with the ANN model trained with the feed-forward neural network, linear layer network in forecasting global solar energy. Also, the comparison has been made with generalized regression neural network and the performance is measured using statistical performance tests and shown in Table 6.3.

It has been observed from Table 6.3, that the ANFIS-based model provides accurate results with MAPE of 2.1×10^{-7}% as compared to ANN model. The value of MAPE obtained by employing feed-forward neural network is 0.0020%, with generalized regression neural network, the mean absolute percentage error obtained is 0.30%, and with linear layer neural network, the mean absolute percentage error obtained is 0.016%.

6.7 COMPARISON OF INTELLIGENT MODELS WITH EMPIRICAL MODELS

Further, the comparative analysis of ANFIS based models have been made with fuzzy logic, ANN and with empirical models using multiple regression analysis. The performance has been evaluated using statistical validation test for composite climate of India and are presented in Table 6.4.

It has been observed from Table 6.4 that the hybrid intelligent models perform best in comparison to other models for forecasting global solar energy. The average mean percentage error obtained by using regression models is 1.67% for composite climatic conditions. However, the obtained result is far better by using intelligent models for global solar energy forecasting. With fuzzy logic methodology, the average mean percentage error reduced to 0.41% which is comparatively lesser than the empirical model using multiple regression analysis.

The mean percentage error further reduced to 0.12% by using the ANN model trained with feedforward back-propagation neural network. Lastly, by using hybrid intelligent model i.e. ANFIS methodology, the averaged mean percentage error further reduced to 3.84×10^{-5}% which provides accurate results as compared to other models.

It is, therefore, revealed from the results that by employing hybrid intelligent models, the obtained error is less. This is due to the reason that the ANFIS-based model presents a specified mathematical structure and makes it a good adaptive approximator. Further, for a network of similar complexity, the ANFIS model provides better learning ability and reduces convergence error. The ANFIS model achieves non-linear mapping and shows supremacy to the neural network and other methods of similar complexity.

Table 6.3 Comparison of ANFIS-based model with ANN model

Month	Measured H_g (MJ/m^2)	ANFIS		FFNN		GRNN		LNN	
		Forecasted H_g (MJ/m^2)	MAPE (%)	Forecasted H_g (MJ/m^2)	MAPE (%)	Forecasted H_g (MJ/m^2)	MAPE (%)	Forecasted H_g (MJ/m^2)	MAPE (%)
Jan	13.985	13.98	0.00000016	13.969	0.0018	13.91	0.26	13.951	0.021
Feb	16.788	16.79	0.00000017	16.903	0.0047	16.76	0.31	16.788	0.000
Mar	21.118	21.12	0.00000020	21.131	0.0019	21.30	0.27	21.123	0.044
Apr	25.214	25.21	0.00000010	25.166	0.0008	25.26	0.20	25.215	0.004
May	24.227	24.23	0.00000020	24.251	0.0009	24.28	0.18	24.230	0.013
Jun	20.912	20.91	0.00000025	20.931	0.0009	21.17	0.36	20.912	0.000
Jul	19.381	19.38	0.00000014	19.339	0.0019	19.31	0.47	19.381	0.036
Aug	18.802	18.80	0.00000021	18.837	0.0015	18.95	0.54	18.804	0.008
Sep	13.851	13.85	0.00000019	13.854	0.0008	13.83	0.24	13.853	0.004
Oct	18.334	18.33	0.00000027	18.339	0.0011	18.36	0.21	18.335	0.012
Nov	14.562	14.56	0.00000011	14.568	0.0004	14.59	0.21	14.564	0.024
Dec	12.124	12.12	0.00000051	12.151	0.0071	12.21	0.37	12.127	0.027
Avg.	18.275	18.27	0.00000021	18.287	0.0020	18.33	0.30	18.273	0.016

Table 6.4 Comparative analysis of intelligent models with empirical models under composite climate zone

Month	Measured H_g (MJ/m^2)	Regression			Fuzzy			ANN			ANFIS		
		Forecasted H_g (MJ/m^2)	MPE (%)	RMSE (%)	Forecasted H_g (MJ/m^2)	MPE (%)	RMSE (%)	Forecasted H_g (MJ/m^2)	MPE (%)	RMSE (%)	Forecasted H_g (MJ/m^2)	MPE (%)	RMSE (%)
Jan	13.98	14.02	1.21	1.24	13.85	-0.79	0.574	13.97	-0.12	0.05	13.98	-0.00002964	0.000000000
Feb	16.79	16.79	0.96	1.90	16.62	-0.82	0.838	16.90	0.82	0.21	16.79	-0.00004093	0.000000000
Mar	21.12	21.11	1.53	1.95	21.12	0.19	0.973	21.13	0.12	0.09	21.12	-0.00004902	0.000000002
Apr	25.21	25.25	0.89	1.58	25.16	-0.13	1.393	25.07	-0.18	0.13	25.12	-0.00003183	0.000000001
May	24.23	24.22	0.31	1.96	23.58	-2.5	1.405	24.25	0.07	0.05	24.23	-0.00002040	0.000000002
Jun	20.91	20.93	2.58	1.90	21.23	1.7	1.361	20.93	0.06	0.04	20.91	-0.00007744	0.000000002
Jul	19.38	19.38	3.23	1.69	19.53	2.07	3.629	19.34	-0.28	0.11	19.38	-0.00002974	0.000000000
Aug	18.80	18.85	3.51	1.78	18.98	0.69	2.582	18.84	0.25	0.05	18.80	-0.00005338	0.000000001
Sep	13.85	13.90	1.37	1.87	13.89	0.85	0.905	13.85	0.04	0.00	13.85	-0.00002834	0.000000000
Oct	18.33	18.36	0.39	1.45	18.72	2.24	0.728	18.34	0.04	0.02	18.33	-0.00002741	0.000000001
Nov	14.56	14.58	0.76	1.79	14.48	-0.51	0.444	14.57	0.05	0.00	14.56	-0.00002199	0.000000000
Dec	12.12	12.12	3.27	1.97	12.3	1.92	0.559	12.15	0.54	0.14	12.12	-0.00005155	0.0000000009
Avg.	18.27	18.29	1.67	1.76	18.29	0.41	1.28	18.28	0.12	0.08	18.27	-0.00003847	0.000000001

6.8 CONCLUSION

In this chapter, a model underlying the principle of ANFIS architecture has been established in forecasting global solar energy with aid of meteorological parameters namely sunshine hours, global solar energy, wind speed, relative humidity, ambient temperature and dew-point. Three criteria namely mean absolute percentage error, normalized mean absolute error and normalized root mean square error have been used for verifying the forecasting errors of proposed ANFIS based models. Simulations have been carried out for varying sky-conditions i.e. sunny sky (type-a), hazy sky (type-b), partially foggy/cloudy sky (type-c) and fully foggy/cloudy sky (type-d) conditions and successfully applied for distinct climate zone across India.

It has been concluded from the overall statistical analysis that by employing hybrid intelligent model, the error has been reduced significantly for each of the climate zone across the entire country. Also, the obtained results reveals that the sunny/clear sky (type-a) model performs better for hot and dry climate zone as compared to other climate zone. Similarly, the hazy sky (type-b) model provides favourable results for composite climate zone, partially foggy/cloudy sky (type-c) model favours warm and humid climate zone and lastly, fully foggy/cloudy sky (type-d) model achieves favourable results for cold and cloudy climate zone, respectively.

Obtained results are further exploited to forecast solar PV system power based on sky-conditions which employ 250 W_p Multi-crystalline solar PV modules operated at MPPT conditions for composite climatic conditions. It

has been concluded that the hazy sky model perform better than other sky model for composite climate zone.

Further, the proposed model has been compared with the variants of ANN models i.e. feed-forward neural network, generalized regression neural network and linear layer neural network. It has been observed that the proposed model underlying the principle of ANFIS methodology reveals precise and accurate results.

Also, a comparison of the proposed model has been made with the fuzzy logic based model and traditional regression models. It has been concluded from the obtained results that the hybrid intelligent models provides convenience and supremacy to other model.

CHAPTER 7

SOLAR ENERGY FORECASTING APPLICATIONS FOR SOLAR PV SYSTEMS

7.1 INTRODUCTION

In the previous chapter, the solar energy forecasting is performed using hybrid intelligent model consisting of fuzzy inference systems and artificial neural network. This chapter is based on the application of solar energy forecasting in solar photovoltaic systems. As the power from solar energy sources is fluctuating and nonlinear in nature, therefore, the power variation in a solar photovoltaic system can lead to the unstable operation of the power system. Therefore, intelligent approaches based on fuzzy logic, Artificial Neural Network (ANN) and Adaptive Neuro-Fuzzy Inference Systems (ANFIS) have been used for 10 minutes ahead solar energy forecasting fluctuations in solar PV systems. Using the above model, faster convergence rate and stronger training and learning ability may be achieved. The proposed work would be useful for power engineers in proper operation and control of the power plants. The short-term PV power forecasting may be implemented for many applications such as providing appropriate control for PV system integration, optimization, power smoothening, real-time power dispatch which may mitigate the issues of power fluctuations obtained from solar PV systems.

This chapter is partially based on the following published papers:

1. **Gulnar Perveen**, M. Rizwan and Nidhi Goel, "Performance mapping of solar thermal technologies," Proceedings of **International Conference on Renewable Energy and Sustainable Climate (Solaris 2019)**, Feb 07-09, 2019, Jamia Millia Islamia, Delhi, India.

7.2 COLLECTION OF DATA

The data for solar irradiance, ambient temperature, cell temperature, relative humidity have been collected from National Institute of Solar Energy (NISE) for Delhi location at 10 minutes time interval and used as input for very short-term power forecasting in a solar PV system.

7.3 INTELLIGENT APPROACH FOR SHORT-TERM SOLAR ENERGY FORECASTING

The power output from renewable energy sources is seeking attention due to advancement in the field of solar PV systems including enhanced efficiency of solar cells. In the current situation, bidding on power has been done on 10 minutes timescale by most of the distribution companies. Further, the uncertainty and the variability associated with the solar PV power plant lead to the inappropriate operation. Hence, this mandates the short-term power forecasting for successfully and efficiently integrating the power plants into the utility grid.

In this chapter, an intelligent modelling technique such as fuzzy logic, artificial neural network and hybrid intelligent model have been presented for very short-term power forecasting of a solar photovoltaic system under composite climatic conditions. The input includes the parameters such as solar irradiance, cell temperature and solar photovoltaic generation at a time scale of 10 minutes for the day [122-129].

The power generation has been affected by many parameters such as climatic variations, solar insolation, solar panel temperature, ambient temperature and the topographical position. So, it becomes difficult to define the output with single model; therefore, the output is modelled based on

different weather conditions such as sunny, hazy, partially foggy/cloudy and fully foggy/cloudy sky-conditions using meteorological parameters as these factors make a significant impact on solar PV system power output. Solar irradiance is the factor by which the PV power is most significantly gets affected. The PV power output estimation can be expressed by Eq. (7.1) as:

$$P_{PV} = \left[P_{PV,STC} * \frac{G_T}{1000} * \ [1 - \gamma * (T_j - \ 25)]\right] * N_{PVs} \ * \ N_{PVp} \tag{7.1}$$

$$\text{and } T_j = \ T_{amb} + \frac{G_T}{800} * (N_{OCT} - 20) \tag{7.2}$$

where $P_{PV,STC}$ represents the rated power output of solar PV system of single array at maximum power point, P_{PV} is the solar PV array power output at MPP, G_T is solar irradiance at STC in W/m^2, N_{PVS} represents the series PV arrays, γ is temperature parameter at Maximum Power Point (MPP), N_{PVP} represents the parallel PV arrays, T_{amb} is ambient temperature in ^{o}C, T_j is the temperature of the solar panel in ^{o}C and N_{OCT} is a constant.

Further, weather conditions such as cloudy, dusts have large influence on solar irradiance reaching to the PV panels by scattering and reflecting, thereby reducing the direct radiation to the ground. Therefore, a good and accurate forecasting model for solar energy requires an intelligent approach which uses historical PV power and meteorological parameters.

7.4 EVALUATION INDEXES

The effect of the different methods of training is investigated by means of some evaluation indexes. These indexes aim at assessing the accuracy of the forecasts and the related error, it is therefore necessary to define the indexes.

7.4.1 Mean Absolute Percentage Error (MAPE)

The hourly error e_h is the staring definition given as the difference between the hourly mean values of the power measured in the h-th hour $P_{m,h}$ and the forecast $P_{p,h}$ provided by the adopted model.

$e_h = P_{m,h} - P_{p,h}$ (W)

From the hourly error expression and its absolute value, other definitions can be inferred; i.e., the well-known mean absolute percentage error (MAPE):

$$\text{MAPE}_{\%} = \frac{1}{n}\sum_{i=1}^{n}\left|\frac{eh}{\text{P}m,h}\right| * 100 \tag{7.3}$$

where n is the number of sample (hours) considered, usually it is calculated for a single day, month, or year.

7.4.2 Normalized Mean Absolute Error (NMAE)

Since the hourly measured power $P_{m,h}$ significantly changes during the same day (i.e., sunrise, noon, and sunset), for the sake of a fair comparison, in this chapter normalized mean absolute error have been preferred.

$$\text{NMAE}_{\%} = \frac{1}{n}\sum_{i=1}^{n}\left|\frac{eh}{\text{C}}\right| * 100 \tag{7.4}$$

where n is the number of sample (hours) considered and the percentage of the absolute error is referred to the rated power C of the plant, in place of the hourly measured power $P_{m,h}$. It is largely used to evaluate the accuracy of predictions and trend estimations.

7.4.3 Normalized Root Mean Square Error (nRMSE)

It is based on the maximum hourly power output $P_{m,h}$ described by the Eq. (7.5) and expressed as:

$$\text{nRMSE}_{\%} = \frac{\sqrt{\frac{1}{n}\sum_{i=1}^{n}|eh|^2}}{\max(\text{P}m,h)} * 100 \tag{7.5}$$

This definition of error is the well-known root mean square error (RMSE) which has been normalized over the maximum hourly power output $P_{m,h}$ measured in the considered time range, for the sake of a fair comparison.

7.5 RESULTS AND DISCUSSIONS

The solar PV power forecasting is an important element for smart grid approach which helps in optimization of the smart energy management system and has the ability to integrate the renewable power generation in an efficient manner.

Considering different weather conditions, various seasons are chosen accordingly for covering wider aspects of the developed model. Since the power generating from solar energy resource is fluctuating in nature, so, it becomes difficult to estimate power output with mathematical models; therefore, intelligent approaches based on fuzzy logic, ANN and ANFIS models have been presented for power forecasting of solar PV system.

In this research, 250 W_p Multi-crystalline and 210 W_p Heterojunction with Intrinsic Thin Layer (HIT) solar PV modules have been considered whose performance characteristics have been shown in Table A.1 - Table A.2 of Appendix A respectively.

7.5.1 Intelligent Modelling for Short-Term Power Forecasting in Solar PV System Employing 210 W_p HIT PV Modules

Intelligent modelling techniques i.e. fuzzy logic, ANN and ANFIS modelling have been applied in forecasting power of a solar PV system and are presented in Table 7.1.

It has been observed from Table 7.1 that the month-wise average mean absolute percentage error using fuzzy logic methodology is 0.10%; for ANN methodology, the mean absolute percentage error reduced to 0.04%; and for ANFIS methodology the mean absolute percentage error further reduced to 0.01% which reveals that the obtained results are precise and far accurate as the computed error is less.

This is due to the reason that ANFIS based model integrates the features of both fuzzy logic approach and artificial neural network. Further, the graphical representation between the measured and forecasted power employing different methodologies have been presented in Fig. 7.1.

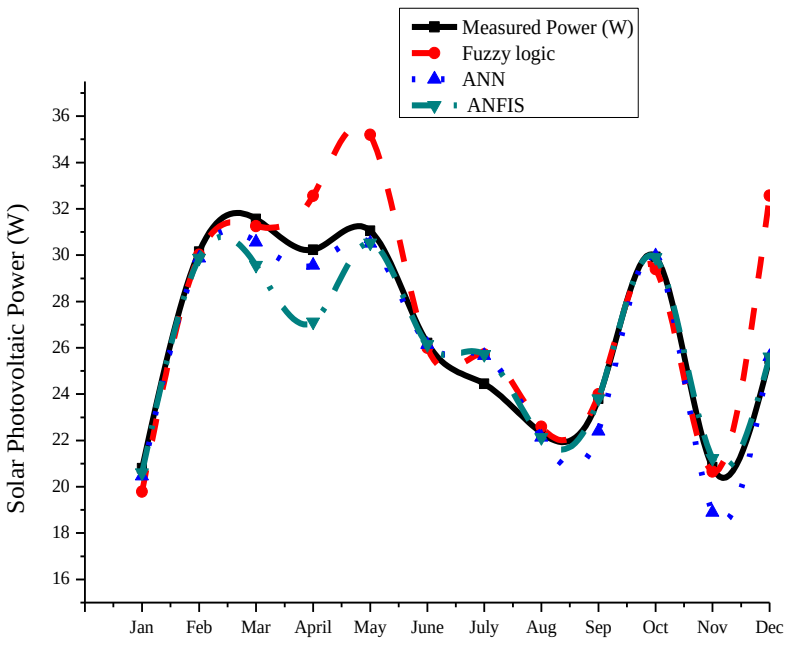

Fig. 7.1 Graphical analysis of measured and forecasted PV power employing fuzzy logic, ANN and ANFIS methodologies

Table 7.1 Intelligent methodologies for forecasting power in a solar PV system employing HIT solar PV modules under composite climate zone

Month	Solar Irradiance (W/m^2)	V_{oc} (V)	I_{sc} (A)	Cell Temp (^oC)	Measured Power (W)	Fuzzy				ANN				ANFIS			
						Forecasted Power (W)	MAPE (%)	NMAE (%)	nRMSE (%)	Forecasted Power (W)	MAPE (%)	NMAE (%)	nRMSE (%)	Forecasted Power (W)	MAPE (%)	NMAE (%)	nRMSE (%)
Jan	361.15	81.47	0.42	28.14	20.80	19.79	0.18	0.09	0.11	20.46	0.01	0.01	0.02	20.61	0.00	0.00	0.00
Feb	461.52	82.03	0.61	35.69	30.15	30.02	0.07	0.05	0.07	29.87	0.00	0.00	0.01	29.87	0.00	0.00	0.00
Mar	548.24	83.64	0.62	40.12	31.56	31.25	0.01	0.03	0.03	30.56	0.01	0.02	0.00	29.56	0.00	0.00	0.00
April	575.12	79.62	0.60	42.53	30.23	32.56	0.15	0.06	0.04	29.56	0.00	0.02	0.00	27.12	0.00	0.00	0.00
May	559.67	77.35	0.59	46.22	31.05	35.19	0.12	0.05	0.06	30.52	0.00	0.00	0.00	30.53	0.00	0.00	0.00
June	537.17	76.92	0.55	45.24	26.20	26.00	0.07	0.06	0.07	26.14	0.00	0.00	0.00	26.14	0.01	0.00	0.01
July	537.81	76.66	0.05	48.28	24.45	25.72	0.05	0.04	0.05	25.67	0.02	0.02	0.03	25.71	0.00	0.00	0.00
Aug	428.80	76.90	0.47	53.27	22.33	22.59	0.06	0.04	0.05	22.14	0.03	0.01	0.04	22.13	0.00	0.00	0.00
Sep	437.51	77.78	0.50	51.62	23.80	23.99	0.13	0.07	0.09	22.40	0.27	0.12	0.19	23.80	0.07	0.03	0.04
Oct	466.57	78.74	0.63	53.21	29.92	29.40	0.07	0.06	0.07	29.97	0.01	0.00	0.01	29.90	0.00	0.00	0.00
Nov	369.82	78.48	0.44	45.08	20.85	20.65	0.13	0.05	0.06	18.90	0.03	0.01	0.02	21.23	0.00	0.00	0.00
Dec	370.84	80.66	0.47	43.36	25.53	32.57	0.12	0.01	0.09	25.62	0.10	0.08	0.43	25.61	0.00	0.00	0.01
Avg.	471.19	79.19	0.50	44.40	26.41	27.48	0.10	0.05	0.07	25.98	0.04	0.03	0.06	26.02	0.01	0.00	0.01

From Fig. 7.1, it has been observed that the forecasted power employing ANFIS methodology closely follows the measured power as compared to others methodologies such as fuzzy logic and artificial neural network.

Further, the power generation in a solar PV system with 210 W_p HIT solar PV modules for different sky-conditions has been shown in Table 7.2. Following inferences can be drawn from Table 7.2 shown as:

(a) Sunny/clear sky

1st June 2015 is considered as a sunny day based on the annual analysis of solar radiation data and availability of sunshine hours. Further, the graphical representation between measured and forecasted power for sunny sky condition have been shown in Fig. 7.2 from which it has been observed that the forecasted power employing ANFIS methodology on hour basis closely follows the measured power, whereas some deviation can be seen in terms of fuzzy logic approach and ANN approach.

The maximum power output is observed to be 62 W during the day with averaged mean absolute percentage error of 0.0610% using the fuzzy logic methodology, by employing ANN methodology the error is 0.0014% and by employing ANFIS methodology the mean absolute percentage error has been further reduced to 0.0010%.

Table 7.2 Short-term PV power forecasting employing HIT solar PV module under composite climatic conditions

Sky - conditions	Time (hr)	Cell Temp (^oC)	Solar Irradiance (W/m^2)	Measured Power (W)	Fuzzy		ANN		ANFIS	
					Forecasted Power (W)	MAPE (%)	Forecasted Power (W)	MAPE (%)	Forecasted Power (W)	MAPE (%)
Sunny sky	7:00	34.11	140.93	7.00	7.02	0.0900	7.02	0.0027	7.03	0.0036
	8:00	40.55	273.76	13.83	15.00	0.0840	13.84	0.0015	12.85	0.0001
	9:00	48.14	486.12	28.00	30.34	0.0830	28.02	0.0009	28.01	0.0004
	10:00	52.23	625.25	39.83	41.66	0.0460	39.82	0.0002	39.83	0.0002
	11:00	57.79	783.13	52.33	54.17	0.0350	52.31	0.0005	52.34	0.0002
	12:00	62.86	875.34	59.33	60.50	0.0200	59.35	0.0003	59.06	0.0040
	13:00	64.69	888.95	62.00	61.17	0.0900	61.88	0.0018	61.99	0.0005
	14:00	63.91	744.96	43.17	42.00	0.0270	43.16	0.0000	43.46	0.0052
	15:00	61.55	726.73	48.33	46.32	0.0420	48.32	0.0001	48.33	0.0007
	16:00	58.04	549.15	34.33	31.51	0.0820	34.34	0.0004	34.35	0.0006
	17:00	52.72	361.6	20.83	19.32	0.0720	20.79	0.0024	20.82	0.0004
	Avg.	**54.24**	**586.90**	**37.18**	**37.18**	**0.0610**	**37.17**	**0.0014**	**37.10**	**0.0010**
Hazy sky	10:00	40.83	123.1	8.00	7.12	0.0100	8.39	0.0492	8.03	0.0031
	11:00	44.49	146.12	8.50	9.70	0.0020	9.45	0.1408	8.49	0.0011
	12:00	43.56	307.56	19.67	24.20	0.2300	20.25	0.0123	19.66	0.0004
	13:00	52.55	519.54	45.00	45.46	0.0100	44.82	0.0031	44.98	0.0003
	14:00	42.4	467.65	39.00	37.40	0.0410	39.25	0.0060	39.01	0.0001
	15:00	49.36	313.06	24.50	21.50	0.0170	24.54	0.0012	24.51	0.0004
	16:00	41.05	185.35	11.00	10.09	0.0830	11.68	0.0828	11.00	0.0001
	Avg.	**44.89**	**294.63**	**22.24**	**22.21**	**0.0561**	**22.63**	**0.0422**	**22.24**	**0.0008**
Partially foggy /cloudy sky	8:00	45.79	134.08	9.67	10.26	0.0610	9.72	0.0045	9.66	0.0008
	9:00	47.49	179.69	27.33	12.99	0.5250	27.32	0.0038	12.36	0.0670
	10:00	52.07	355.98	32.50	30.14	0.0730	33.33	0.0125	27.53	0.0031
	11:00	55.57	463.45	44.00	40.78	0.0730	44.01	0.0010	32.56	0.0108
	12:00	58.38	547.32	39.50	44.39	0.1240	39.24	0.0013	43.92	0.0005
	13:00	59.96	519.74	39.83	31.40	0.2120	39.95	0.0130	39.49	0.0026
	14:00	55.52	492.69	50.17	40.93	0.1840	50.28	0.0024	39.78	0.0009
	15:00	61.3	647.1	37.33	51.69	0.3850	37.60	0.0178	50.22	0.0010
	16:00	59.64	562.02	21.17	35.16	0.6610	21.20	0.0114	37.59	0.0139
	17:00	50.88	299.99	15.33	18.22	0.1880	15.39	0.0034	20.88	0.0096
	18:00	50.73	235.3	7.33	12.65	0.7250	7.53	0.0473	15.30	0.0076
	19:00	47.99	156.43	7.33	7.23	0.0130	7.75	0.0858	8.81	0.2480
	Avg.	**53.78**	**382.82**	**27.62**	**27.99**	**0.2687**	**27.78**	**0.0305**	**28.18**	**0.0170**
Fully foggy /cloudy sky	9:00	19.08	170.77	12.50	10.75	0.1400	12.60	0.0066	12.48	0.0011
	10:00	19.02	74.87	8.33	10.62	0.2750	8.35	0.0030	8.40	0.0099
	11:00	23.29	96.49	11.17	8.72	0.2190	12.78	0.1733	10.98	0.0442
	12:00	18.5	41.2	7.83	8.10	0.0340	7.82	0.0018	7.81	0.0036
	13:00	18.57	140.77	10.67	10.46	0.0200	10.66	0.0002	10.63	0.0056
	14:00	18.59	87.31	9.83	11.14	0.1330	10.11	0.0243	10.01	0.0735
	15:00	17.86	164.25	12.00	10.83	0.0970	12.01	0.0016	12.00	0.0004
	Avg.	**19.27**	**110.81**	**10.33**	**10.09**	**0.1311**	**10.62**	**0.0301**	**10.33**	**0.0198**

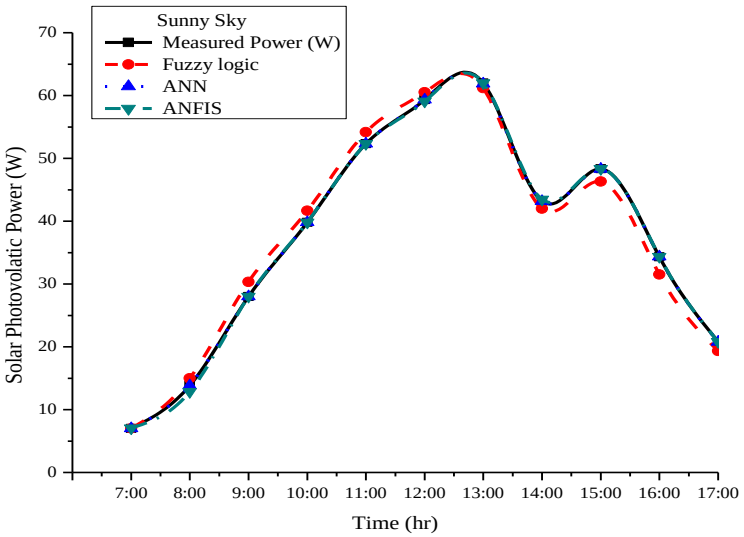

Fig. 7.2 Graphical analysis of measured and forecasted PV power employing intelligent methodologies for sunny sky-condition

(b) Hazy sky

26th December 2015 is considered as a hazy day based on the annual analysis of solar radiation data and availability of sunshine hours. Further, the graphical representation between measured and forecasted power for hazy sky condition have been shown in Fig. 7.3 from which it has been observed that the forecasted power employing ANFIS methodology on hour basis closely follows the measured power, whereas some deviation can be seen in terms of fuzzy logic approach and ANN.

The maximum power output is observed to be 50 W during the day with averaged mean absolute percentage error by employing fuzzy logic methodology is 0.0561%, by employing artificial neural network methodology the mean absolute percentage error reduced to 0.0422% and by employing ANFIS methodology the error have been further reduced to 0.0008%.

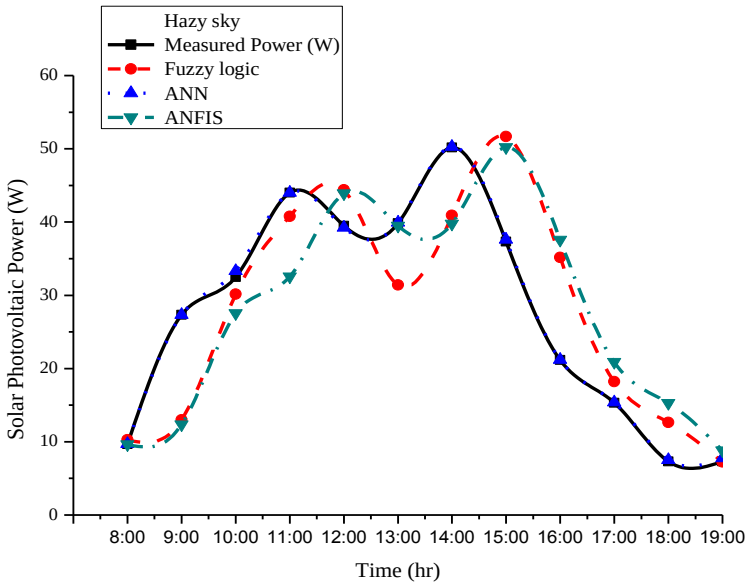

Fig. 7.3 Graphical analysis of measured and forecasted PV power employing intelligent methodologies for hazy sky-condition

(c) Partially foggy/cloudy sky

3rd August 2015 is considered as partially foggy/cloudy day based on the annual analysis of solar radiation data and availability of sunshine hours. Further, the graphical representation between measured and forecasted power for partially foggy/cloudy sky condition have been shown in Fig. 7.4 from which it has been observed that the forecasted power employing ANFIS methodology on hour basis closely follows the measured power, whereas some deviation can be seen in terms of fuzzy logic approach and ANN.

The maximum power output is observed to be 44 W during the day with averaged mean percentage error by employing fuzzy logic methodology is 0.2687%, by employing ANN methodology the mean absolute percentage error reduced to 0.0305%, and by employing ANFIS methodology the error further reduced to 0.0170%.

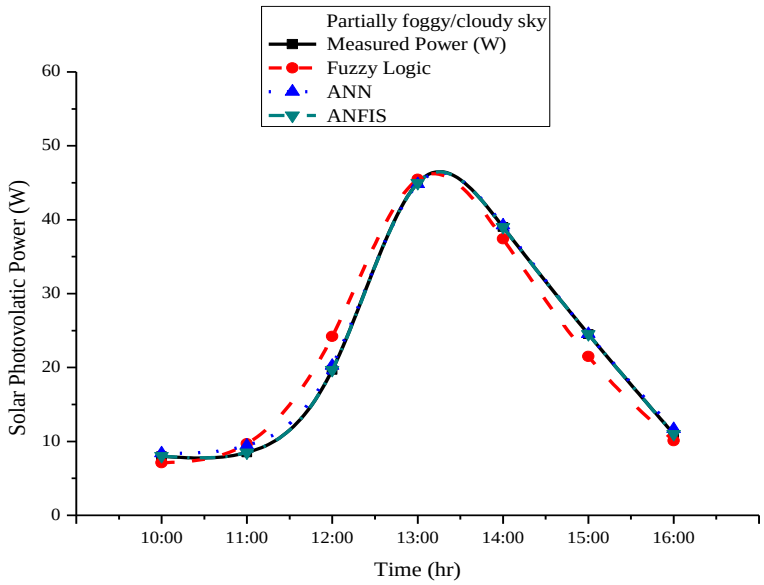

Fig. 7.4 Graphical analysis of measured and forecasted PV power employing intelligent methodologies for partially foggy/cloudy sky-condition

(d) Fully foggy/cloudy sky

3rd January 2015 is considered as a fully foggy/cloudy day based on the annual analysis of solar radiation data and availability of sunshine hours. Further, the graphical representation between measured and forecasted power for fully foggy/cloudy sky condition have been shown in Fig. 7.5 from which it is evident that the forecasted power employing ANFIS methodology on hour basis closely follows the measured power, whereas some deviation can be seen in terms of fuzzy logic approach and ANN.

The maximum power output is observed to be 12 W during the day with averaged mean absolute percentage error by employing fuzzy logic methodology is 0.1311%, by using ANN methodology the error reduced to 0.0301% and by employing ANFIS methodology the mean absolute percentage error further reduced to 0.0198%.

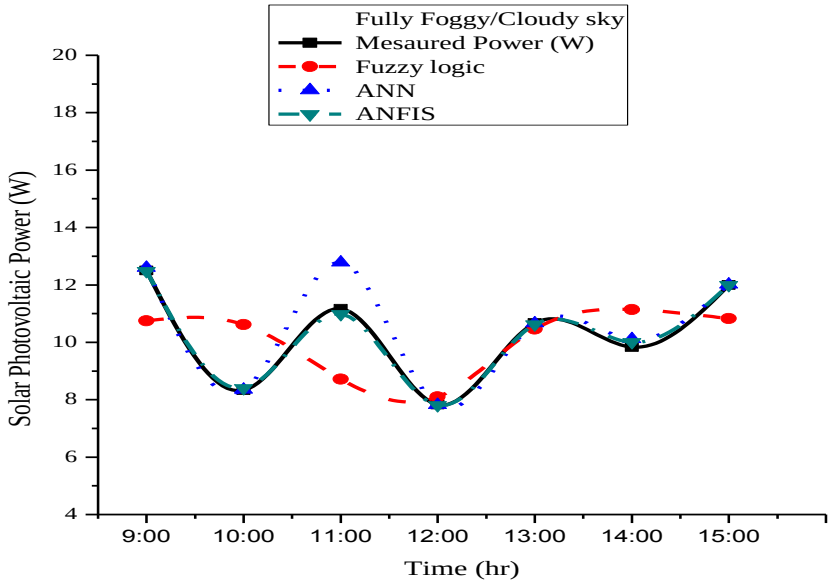

Fig. 7.5 Graphical analysis of measured and forecasted power employing intelligent methodologies for fully foggy/cloudy sky-condition

From Table 7.2, it has been observed that out of the four models, especially the hazy sky model perform well with mean absolute mean percentage error of 0.0008% in forecasting the power of a solar photovoltaic system followed by sunny sky model with mean absolute percentage error of 0.0010%, partially foggy/cloudy sky model with mean absolute percentage error of 0.0170% and fully foggy/cloudy sky model with mean absolute percentage error of 0.0198% by using ANFIS methodology.

7.5.2 Intelligent Modelling for Short-Term Power Forecasting in Solar PV System Employing 250 W_p Multi-crystalline PV Modules

Similarly, intellgent modelling techniques have been presented for power forecasting of solar PV system employing Multi-crystalline 250 W_p solar PV modules operating at Maximum Power Point Tracking (MPPT) conditions and are presented in Table 7.3.

From Table 7.3, it has been observed that by employing the ANFIS-based model, the average MPE obtained is 0.0001% which is far less as compared to

other models. By employing fuzzy logic, the MPE obtained is 0.01% and with ANN model mean percentage error of 0.0021% is achieved. Hence, the hybrid modelling approach is far accurate and precise as compared to other models.

Further, it has been concluded from the obtained results that for all months of the year, error is less in case of the ANFIS model.

For winter season (January), the averaged MPE by employing fuzzy logic approach is 0.09%, using ANN the error reduced to 0.004% and with ANFIS model the error further reduced to 0.0003%.

Similarly, for the summer season (June) the averaged MPE by employing fuzzy logic is 0.07%, by using ANN the error reduced to 0.0033% and with ANFIS model the error further reduced to 0.0001%.

It has been observed that error is large for the rainy season (August) because of large uncertainties associated with the data. The average mean percentage error by employing fuzzy logic is 0.28%, using ANN the error reduced to 0.0304% and with ANFIS model the error further reduced to 0.0003%.

In view of aforesaid, it has been observed that the ANFIS-based model performs better than other models in terms of faster convergence rate with learning and training ability. The ANFIS methodology makes use of training pattern as compared to other methods and hence reduces the computational time complexity. It has certain advantages such as the ease of design, robustness and adaptability with the non-linearity associated with the data. The ANFIS methodology integrates the features of both fuzzy logic and ANN which increases the system accuracy and makes the system response much faster.

Table 7.3 Intelligent methodologies for forecasting power in a solar PV system employing Multi-crystalline solar PV modules under composite climate zone

Month	Solar Irradiance (W/m^2)	V_{pmax} (V)	I_{pmax} (A)	Cell Temp. (^oC)	Measured Power (W)	Fuzzy			ANN			ANFIS		
						Forecasted Power (W)	MPE (%)	RMSE (%)	Forecasted Power (W)	MPE (%)	RMSE (%)	Forecasted Power (W)	MPE (%)	RMSE (%)
Jan	341.98	60.48	1.05	20.80	64.15	64.37	-0.09	0.10	63.82	0.0040	0.01	64.12	-0.0003	0.00
Feb	450.78	59.95	1.49	28.19	89.61	88.66	-0.02	0.08	86.93	0.0161	0.05	89.57	0.0005	0.00
Mar*	-	-	-	-	-	-	-	-	-	-	-	-	-	-
April*	-	-	-	-	-	-	-	-	-	-	-	-	-	-
May	557.92	56.93	1.38	44.53	79.08	78.12	0.00	0.07	79.03	0.0007	0.00	79.06	0.0003	0.00
June	528.54	57.57	1.20	42.32	68.28	44.66	-0.07	0.07	70.19	0.0033	0.01	70.19	-0.0001	0.00
July	532.32	57.03	1.02	39.15	59.03	56.59	-0.04	0.13	59.22	-0.0049	0.01	59.03	-0.0024	0.04
Aug	411.69	57.07	1.03	38.15	59.52	61.77	0.28	0.50	59.29	-0.0304	0.05	59.52	-0.0003	0.05
Sep	418.73	57.36	1.11	35.56	64.35	52.35	0.13	0.14	64.40	-0.0009	0.01	64.28	0.0011	0.00
Oct	464.71	57.78	1.52	37.75	88.08	90.44	-0.04	0.06	88.24	-0.0027	0.01	88.09	-0.0001	0.00
Nov	346.12	58.90	1.15	29.33	68.21	64.64	-0.01	0.12	68.29	-0.0050	0.01	68.21	0.0000	0.00
Dec	359.34	60.09	1.26	23.94	76.30	70.93	-0.05	0.17	76.20	-0.0009	0.01	76.30	0.0000	0.00
Avg.	441.21	58.32	1.22	33.97	71.66	67.25	0.01	0.14	71.56	-0.0021	0.02	71.84	-0.0001	0.01

*Data could not be arranged for these months

Further, the uncertainty associated with the solar PV power plant leads to the inappropriate operation of the system. Therefore, short-term power forecasting is essential for successful and efficient integration of solar power generating plants into the utility grid. In this chapter, an intelligent modelling technique such as fuzzy logic, artificial neural network and a hybrid modelling approach has been presented for very short-term power forecasting of a solar photovoltaic system under composite climatic conditions and is shown in Fig. 7.6.

The input includes the measurements of solar irradiance, cell temperature, and PV generation for the day at a timescale of 10 minutes and used as input for short-term PV power output forecasting which varies according to different weather conditions and is illustrated in Table 7.4 – Table 7.7 respectively.

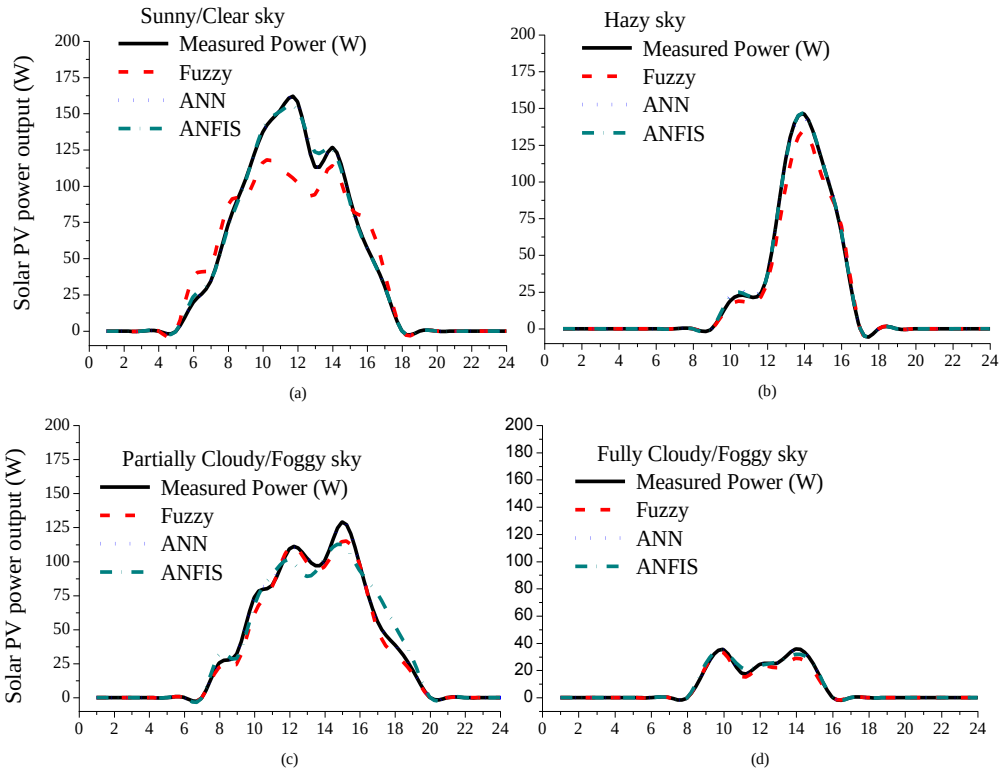

Fig. 7.6 Graphical analysis of short-term PV power forecasting for (a) sunny sky; (b) hazy sky; (c) partially foggy/cloudy sky; and (d) fully foggy/cloudy sky

Further, parallel computation is allowed in ANFIS structure which presents a well-structured representation with a hybrid platform for solving complex problems and is a feasible alternative to the conventional model-based control schemes. This hybrid approach deals with the issues associated with variations and uncertainty in the power plant parameters and structure, thereby improving the system robustness. Further, it allows better integration with other control design methods.

(a) Sunny sky

From Table 7.4, it has been observed that the performance of the sunny sky model is better in power forecasting of a solar PV system. The average measured power during a sunny sky day is 98 W. However, the MPE obtained is 0.077% by employing fuzzy logic methodology, the error reduces to 0.0079% by using ANN, and it further reduces to 0.0054% with ANFIS methodology.

(b) Hazy sky

It has been observed from Table 7.5 that the mean percentage error obtained by using the fuzzy logic methodology for this sky condition is 0.049%, the error reduced to 0.022% by using the artificial neural network; however, with ANFIS model the mean percentage error is less and further reduced to 0.004%. The averaged measured power during a hazy sky day is 82 W.

(c) Partially foggy/cloudy sky

It has been observed from Table 7.6 that the mean percentage error obtained by using fuzzy logic methodology for this sky-condition is 1.20%, this error reduced to 0.20% by using ANN; however, with ANFIS model the mean percentage error is less and further reduced to 0.03%.

Table 7.4 Intelligent models for very short-term PV power forecasting for sunny sky-condition under composite climate

Time (hr)	Cell Temperature (^oC)	Solar Irradiance (W/m^2)	Measured Power (W)	Fuzzy		ANN		ANFIS	
				Forecasted Power (W)	MPE (%)	Forecasted Power (W)	MPE (%)	Forecasted Power (W)	MPE (%)
7:00	172.30	32.74	24.00	40.03	-0.67	24.07	0.01	24.34	-0.003
7:10	203.49	33.82	28.00	39.12	-0.65	28.03	-0.08	25.74	-0.001
7:20	237.48	35.78	34.00	38.39	-0.13	32.82	-0.11	30.25	0.035
7:30	273.82	36.38	39.00	38.21	0.02	38.93	0.02	39.70	0.002
7:40	309.60	37.18	46.00	52.53	-0.14	46.00	0.06	48.73	0.000
7:50	344.42	38.67	52.00	69.39	-0.33	51.97	0.01	52.28	0.001
8:00	375.21	38.52	58.00	76.46	-0.58	57.95	-0.04	55.48	0.001
8:10	416.11	40.17	65.00	86.79	-0.35	65.10	-0.04	62.59	-0.002
8:20	449.55	41.67	71.00	89.33	-0.29	71.03	0.01	71.81	0.000
8:30	473.28	41.37	76.00	90.41	-0.44	75.92	0.01	76.98	0.001
8:40	498.73	42.48	84.00	91.14	-0.74	84.03	-0.04	80.65	0.000
8:50	526.30	44.24	90.00	91.50	-0.02	90.06	-0.07	84.07	-0.001
9:00	552.73	43.69	91.00	91.68	-0.01	90.94	-0.01	89.66	0.001
9:10	572.15	43.29	95.00	91.50	0.04	94.93	0.01	95.71	0.001
9:20	577.01	44.16	103.00	91.86	0.11	102.91	-0.06	97.15	0.001
9:30	608.90	42.08	111.00	91.50	0.18	110.95	-0.01	110.15	0.000
9:40	643.27	43.88	112.00	91.68	0.18	112.02	0.02	114.78	0.000
9:50	660.41	44.97	118.00	96.39	0.18	117.98	-0.01	116.86	0.000
10:00	689.73	46.23	122.00	104.55	0.14	121.97	0.00	121.52	0.000
10:10	721.67	47.69	134.00	111.26	0.17	133.90	-0.03	130.12	0.001
10:20	757.03	46.45	136.00	119.05	0.12	136.08	0.04	141.86	-0.001
10:30	776.57	46.66	140.00	120.86	0.14	140.07	0.04	146.16	0.000
10:40	798.90	47.27	144.00	120.32	0.16	144.06	0.03	148.99	0.000
10:50	804.94	49.59	148.00	121.95	0.18	148.16	0.01	149.45	-0.001
11:00	839.69	50.09	153.00	121.41	0.21	152.98	-0.01	150.93	0.000
11:10	852.43	50.22	152.00	121.23	0.20	152.09	-0.01	151.16	-0.001
11:20	869.61	51.26	151.00	117.78	0.22	150.96	0.00	151.49	0.000
11:30	871.66	52.55	155.00	109.08	0.30	154.88	-0.02	151.89	0.001
11:40	876.80	53.20	148.00	105.09	0.29	148.08	0.03	152.20	-0.001
11:50	881.92	54.57	157.00	98.57	0.37	156.55	-0.03	152.62	0.003
12:00	899.63	54.18	164.00	99.84	0.39	163.75	-0.07	152.69	0.002
12:10	908.85	52.84	158.00	107.27	0.32	159.77	-0.04	152.26	-0.011
12:20	897.87	53.69	155.00	102.19	0.34	154.92	-0.02	152.54	0.001
12:30	887.53	53.28	158.00	103.83	0.34	158.22	-0.04	152.33	-0.001
12:40	891.21	54.17	162.00	99.66	0.38	162.12	-0.06	152.64	-0.001
12:50	887.54	53.98	149.00	100.38	0.33	148.96	0.02	152.56	0.000
13:00	860.72	54.87	152.00	97.12	0.36	152.03	0.00	152.27	0.000
13:10	878.20	54.84	150.00	97.12	0.35	150.05	0.02	152.61	0.000
13:20	831.79	55.48	142.00	95.31	0.33	142.08	0.06	150.83	-0.001
13:30	820.42	54.47	130.00	99.48	0.23	129.95	0.15	149.67	0.000
13:40	663.15	54.04	52.00	102.01	-0.96	52.41	0.04	54.15	-0.008
13:50	544.29	49.97	53.00	74.83	-0.41	53.06	0.52	80.33	-0.001
14:00	731.88	51.01	137.00	115.97	0.15	137.02	-0.06	128.69	0.000
14:10	735.79	52.71	128.00	111.44	0.13	127.81	-0.08	117.28	0.001
14:20	749.46	52.35	125.00	113.43	0.09	125.01	0.03	129.11	0.000
14:30	753.09	52.34	137.00	113.61	0.17	136.99	-0.04	131.53	0.000
14:40	747.67	51.80	117.00	116.69	0.00	117.16	0.12	131.58	-0.001
14:50	711.90	51.56	116.00	112.16	0.03	115.99	-0.01	114.97	0.000
15:00	662.45	51.18	106.00	101.83	0.04	106.01	-0.01	104.95	0.000
15:10	638.30	51.41	107.00	95.49	0.11	107.05	-0.09	96.93	0.000
15:20	595.64	50.84	89.00	84.61	0.05	88.97	0.03	91.43	0.000
15:30	577.80	50.35	99.00	80.44	0.19	98.95	-0.10	89.09	0.001
15:40	540.84	49.93	76.00	75.19	0.01	75.91	0.05	80.03	0.001
15:50	485.17	49.64	69.00	75.91	-0.85	69.04	-0.01	68.35	-0.001
16:00	457.16	48.68	63.00	79.90	-0.27	63.05	0.07	67.18	-0.001
16:10	425.11	47.84	66.00	83.16	-0.26	65.91	-0.08	60.73	0.001
16:20	423.65	47.33	61.00	85.52	-0.40	60.99	0.02	62.31	0.000
16:30	365.12	46.93	53.00	77.91	-0.47	53.05	-0.03	51.48	-0.001
16:40	340.34	46.94	54.00	71.02	-0.32	53.97	-0.09	48.91	0.001
Avg.	593.61	47.26	98.26	87.89	**-0.077**	98.27	**0.007**	98.19	**0.0054**

Table 7.5 Intelligent models for very short-term PV power forecasting for hazy sky-condition under composite climate zone

Time (hr)	Cell Temperature (^oC)	Solar Irradiance (W/m^2)	Measured Power (W)	Fuzzy		ANN		ANFIS	
				Forecasted Power (W)	MPE (%)	Forecasted Power (W)	MPE (%)	Forecasted Power (W)	MPE (%)
10:00	125.45	10.63	18	16.54	0.08	22.14	-0.23	22.36	0.24
10:10	126.52	10.21	22	16.61	0.25	23.09	-0.05	22.27	0.01
10:20	127.23	9.10	24	16.66	0.10	23.97	0.00	22.14	-0.08
10:30	125.81	5.45	24	16.57	0.31	27.09	-0.13	22.08	-0.08
10:40	150.74	12.43	25	27.34	0.00	24.77	0.01	23.55	-0.06
10:50	171.66	8.37	25	15.51	0.38	25.64	-0.03	22.95	-0.08
11:00	174.73	10.67	25	14.93	0.28	25.95	-0.04	23.40	-0.06
11:10	208.48	11.50	33	18.35	0.08	32.50	0.02	34.07	0.03
11:20	227.30	18.44	33	37.04	0.08	34.03	-0.03	31.93	-0.03
11:30	247.76	17.34	39	37.92	0.03	40.48	-0.04	41.64	0.07
11:40	276.06	19.01	37	41.09	-0.11	36.31	0.02	37.05	0.00
11:50	406.26	16.92	57	44.44	0.22	56.81	0.00	55.45	-0.03
12:00	479.51	17.24	49	71.58	-0.46	49.41	-0.01	51.99	0.06
12:10	498.50	17.48	69	80.75	-0.17	69.22	0.00	66.41	-0.04
12:20	527.75	22.37	139	89.56	0.02	138.21	0.01	136.34	-0.02
12:30	527.66	25.23	135	95.02	0.30	135.15	0.00	142.69	0.06
12:40	525.47	27.16	153	107.18	0.30	150.98	0.01	146.73	-0.04
12:50	525.18	31.56	150	138.91	0.07	147.60	0.02	147.44	-0.02
13:00	512.66	32.20	150	138.03	0.08	147.86	0.01	147.44	-0.02
13:10	500.73	30.07	159	137.15	0.14	152.83	0.04	147.39	-0.07
13:20	489.57	31.91	145	136.26	0.06	146.45	-0.01	147.38	0.02
13:30	494.87	35.14	143	138.73	0.03	141.03	0.01	147.41	0.03
13:40	491.77	35.69	134	139.08	-0.04	132.80	0.01	147.39	0.10
13:50	427.95	32.66	143	118.99	0.17	143.22	0.00	141.34	-0.01
14:00	401.02	33.05	125	114.41	0.08	130.69	-0.05	125.52	0.00
14:10	400.24	34.07	127	116.17	0.09	130.40	-0.03	124.92	-0.02
14:20	357.63	34.09	114	112.65	0.01	114.40	0.00	114.48	0.00
14:30	331.88	31.96	114	110.88	0.03	114.50	0.00	113.55	0.00
14:40	285.04	32.76	99	87.80	-0.25	96.29	0.03	104.56	0.06
14:50	261.53	29.54	95	66.29	0.03	96.04	-0.01	89.16	-0.06
15:00	242.06	31.93	77	76.52	0.01	77.87	-0.01	75.63	-0.02
15:10	230.01	31.82	69	75.46	0.11	70.38	-0.02	69.24	0.00
15:20	221.92	29.72	63	66.47	-0.13	63.89	-0.01	66.01	0.05
15:30	188.42	27.89	58	65.41	-0.13	59.83	-0.03	60.77	0.05
15:40	155.54	26.57	60	63.65	-0.18	61.30	-0.02	57.50	-0.04
Avg.	321.27	23.41	82	74.06	**0.049**	82.37	**-0.022**	82.01	**0.004**

(d) Fully foggy/cloudy sky

From Table 7.7, it is evident that the photovoltaic power output is less during fully foggy/cloudy sky condition with averaged measured power of only 27 W. The mean percentage error is 0.21% by employing fuzzy logic methodology, the error reduces to 0.091% by using ANN and with ANFIS the error obtained is 0.04% respectively.

Table 7.6 Intelligent models for very short-term PV power forecasting for partially foggy/cloudy sky-condition under composite climate zone

Time (hr)	Cell Temperature (^oC)	Solar Irradiance (W/m^2)	Measured Power (W)	Fuzzy		ANN		ANFIS	
				Forecasted Power (W)	MPE (%)	Forecasted Power (W)	MPE (%)	Forecasted Power (W)	MPE (%)
7:30	27.78	126.72	21.00	17.00	0.19	20.77	0.05	21.97	0.01
7:40	27.32	200.00	22.00	19.43	-3.88	22.11	0.53	33.70	0.00
7:50	30.58	213.53	34.00	31.55	-2.06	34.07	0.20	40.90	0.00
8:00	30.38	196.07	29.00	21.85	0.01	28.85	0.12	32.41	0.01
8:10	32.13	155.48	21.00	18.46	-4.05	20.78	0.15	24.05	0.01
8:20	30.11	145.30	32.00	29.13	-2.21	32.24	-0.28	22.96	-0.01
8:30	30.71	189.78	43.00	19.43	-1.43	42.97	-0.30	30.21	0.00
8:40	31.05	194.45	24.00	21.85	-3.35	23.84	0.32	31.63	0.01
8:50	31.60	198.55	48.00	41.25	-1.17	47.89	-0.31	33.25	0.00
9:00	32.83	194.56	28.00	26.70	-2.74	27.88	0.13	31.75	0.00
9:10	32.52	171.08	25.00	21.85	-3.22	24.76	0.05	26.34	0.01
9:20	36.07	428.21	145.00	101.88	0.21	145.06	-0.41	85.45	0.00
9:30	39.29	556.78	137.00	124.91	0.09	136.80	-0.09	125.07	0.00
9:40	39.48	364.60	58.00	58.23	-0.76	57.93	0.36	78.99	0.00
9:50	36.55	291.87	50.00	38.83	-1.17	49.82	0.24	61.90	0.00
10:00	36.52	323.32	70.00	70.35	-0.56	70.08	0.04	72.69	0.00
10:10	40.46	647.12	56.00	52.65	-1.20	55.77	1.45	137.36	0.00
10:20	42.29	471.39	60.00	62.83	-1.01	59.75	0.58	94.76	0.00
10:30	40.12	422.82	69.00	67.93	-0.64	68.91	0.22	83.88	0.00
10:40	39.86	355.46	52.00	53.38	-0.95	51.76	0.50	78.08	0.00
10:50	37.21	335.57	190.00	181.90	0.45	207.69	-0.60	75.13	-0.09
11:00	40.62	548.37	205.00	205.91	0.39	204.92	-0.40	123.47	0.00
11:10	43.14	614.47	35.00	34.95	-2.33	34.80	2.75	131.26	0.01
11:20	41.61	559.81	182.00	184.08	0.33	181.87	-0.31	125.65	0.00
11:30	47.08	685.34	165.00	168.56	0.36	164.86	-0.18	135.74	0.00
11:40	47.73	536.57	46.00	46.10	-1.25	45.61	0.28	59.10	0.01
11:50	39.88	190.67	24.00	26.70	-2.92	23.74	0.34	32.13	0.01
12:00	38.71	697.05	205.00	197.66	0.40	204.93	-0.02	199.91	0.00
12:10	48.17	691.84	44.00	41.25	-1.40	43.67	1.22	97.48	0.01
12:20	39.87	357.89	211.00	208.58	0.52	210.61	-0.63	78.33	0.00
12:30	49.96	999.30	95.00	89.75	-0.20	96.63	0.22	116.09	-0.02
12:40	47.13	314.66	17.00	17.00	-2.45	18.48	-0.17	14.12	-0.09
12:50	33.73	159.05	42.00	41.25	-1.56	42.14	-0.34	27.91	0.00
13:00	35.99	595.71	96.00	92.18	-0.27	95.76	0.37	131.61	0.00
13:10	45.39	494.68	116.00	114.00	0.09	115.71	-0.12	102.64	0.00
13:20	44.69	611.38	171.00	162.50	0.37	170.10	-0.24	130.79	0.01
13:30	48.66	771.60	47.00	46.10	-1.38	46.97	1.54	119.16	0.00
13:40	38.09	197.20	47.00	43.68	-1.15	46.78	-0.30	32.74	0.00
13:50	32.41	269.89	129.00	121.28	0.20	129.09	-0.21	101.86	0.00
14:00	40.22	611.36	120.00	101.88	-0.04	119.94	0.09	131.00	0.00
14:10	44.97	622.18	131.00	118.85	0.18	130.80	0.00	131.64	0.00
14:20	45.83	564.36	160.00	143.10	0.35	159.66	-0.23	123.50	0.00
14:30	50.30	816.62	140.00	121.28	0.19	139.92	-0.17	115.93	0.00
14:40	52.02	732.09	154.00	135.83	0.25	154.48	-0.27	112.02	0.00
14:50	51.68	601.10	69.00	67.93	-0.50	70.33	-0.13	59.79	-0.02
15:00	46.00	546.27	152.00	157.17	0.31	151.95	-0.22	118.74	0.00
15:10	49.51	730.86	132.00	132.92	0.17	131.75	-0.15	112.26	0.00
15:20	49.95	708.75	141.00	138.74	0.24	140.92	-0.27	102.79	0.00
15:30	49.20	559.45	53.00	46.10	-0.96	52.72	0.00	52.82	0.01
15:40	44.75	318.37	46.00	43.68	-0.82	45.90	0.54	70.84	0.00
15:50	42.11	492.21	61.00	65.02	-0.98	60.62	0.69	102.92	0.01
16:00	44.46	562.50	114.00	109.15	0.04	114.49	0.11	126.08	0.00
16:10	45.29	498.01	77.00	70.35	-0.38	77.39	0.35	104.30	-0.01
16:20	43.82	376.77	33.00	21.85	-2.17	33.13	1.42	79.96	0.00
16:30	36.07	141.85	18.00	14.72	-5.19	18.63	0.67	30.00	-0.03
16:40	29.57	142.20	25.00	21.85	-3.07	24.70	-0.09	22.73	0.01
16:50	32.19	264.58	68.00	61.86	-0.52	67.81	0.39	94.71	0.00
Avg.	39.53	407.10	76.95	71.80	**-1.20**	77.22	**0.20**	76.94	**0.03**

Table 7.7 Intelligent models for very short-term PV power forecasting for fully foggy/cloudy sky-condition under composite climate zone

Time (hr)	Cell Temperature (^oC)	Solar Irradiance (W/m^2)	Measured Power (W)	Fuzzy		ANN		ANFIS	
				Forecasted Power (W)	MPE (%)	Forecasted Power (W)	MPE (%)	Forecasted Power (W)	MPE (%)
8:40	14.86	168.07	19	20.94	-0.33	18.95	0.32	25.00	0.00
8:50	13.76	161.85	25	24.25	-0.06	25.15	0.00	25.01	-0.01
9:00	14.97	182.38	21	20.94	0.00	21.05	0.19	24.99	0.00
9:10	15.45	101.30	23	20.94	-0.60	22.89	0.27	29.26	0.00
9:20	15.35	135.45	15	12.99	-0.76	15.00	0.64	24.57	0.00
9:30	15.08	132.03	28	26.30	0.06	28.10	-0.12	24.77	0.00
9:40	15.75	101.30	60	56.05	0.37	60.07	-0.37	37.96	0.00
9:50	19.77	101.30	64	60.03	0.40	63.69	0.00	64.01	0.00
10:00	19.73	181.75	27	20.94	0.22	26.90	0.01	27.16	0.00
10:10	17.71	261.96	11	10.63	0.03	11.03	0.00	11.00	0.00
10:20	16.14	187.71	16	14.31	-0.06	15.99	0.42	22.69	0.00
10:30	15.76	129.26	14	12.33	-1.00	14.19	0.77	24.80	-0.01
10:40	15.14	101.30	21	17.63	-0.73	20.87	0.09	22.89	0.01
10:50	14.45	101.30	18	16.30	-1.00	18.10	0.24	22.25	-0.01
11:00	14.77	101.30	24	20.28	-0.50	24.06	-0.07	22.28	0.00
11:10	15.13	101.30	22	20.28	-0.64	21.91	0.04	22.81	0.00
11:20	15.32	120.11	23	20.94	-0.33	22.92	0.08	24.85	0.00
11:30	15.28	101.30	19	17.63	-0.92	18.80	0.28	24.29	0.01
11:40	14.93	127.09	22	20.94	-0.26	21.91	0.11	24.52	0.00
11:50	15.10	101.30	37	36.18	0.02	36.78	-0.39	22.68	0.01
12:00	16.76	101.30	26	20.94	-0.39	26.03	0.51	39.27	0.00
12:10	17.05	134.24	33	27.96	0.15	33.14	-0.28	23.63	0.00
12:20	17.61	123.50	30	28.89	-0.02	30.14	-0.08	27.67	0.00
12:30	17.46	148.36	33	27.56	0.16	32.98	-0.31	22.83	0.00
12:40	17.42	142.59	17	14.31	-0.63	17.06	0.35	22.95	0.00
12:50	16.14	150.40	15	14.31	-0.84	14.93	0.52	22.76	0.00
13:00	15.43	145.55	33	32.20	0.20	33.05	-0.27	24.21	0.00
13:10	16.44	101.30	50	36.51	0.27	50.06	-0.21	39.26	0.00
13:20	16.17	101.30	23	20.28	-0.61	22.83	0.71	39.22	0.01
13:30	14.61	217.00	24	20.94	0.13	23.93	0.00	23.98	0.00
13:40	14.99	155.18	44	26.97	0.39	44.16	-0.43	24.98	0.00
13:50	16.19	101.30	41	37.04	0.10	41.00	-0.04	39.23	0.00
14:00	16.00	151.67	29	27.43	0.05	29.14	-0.22	22.76	0.00
14:10	15.87	187.44	29	18.62	0.36	28.39	-0.22	22.74	0.02
14:20	15.65	176.43	18	16.30	-0.23	17.74	0.28	23.09	0.01
14:30	15.27	128.87	17	12.33	-0.61	16.80	0.45	24.67	0.01
Avg.	15.93	137.94	27	23.70	**-0.21**	26.94	**0.091**	26.97	**0.04**

It has been concluded from the obtained results that by employing ANFIS methodology for composite climatic conditions, the hazy-sky model (type-b) with mean percentage error of 0.004% outperforms other models as the measured data matches the forecasted data followed by the sunny-sky model (type-a) with mean percentage error of 0.0054%, partially foggy/cloudy sky model (type-c) with mean percentage error of 0.03% and fully foggy/cloudy sky model (type-d) with mean percentage error of 0.04% respectively. The result reveals that the proposed model may be implemented for a broad series of applications.

7.6 CONCLUSION

In this chapter, different models based on intelligent approaches such as fuzzy logic, artificial neural network and adaptive neural-fuzzy inference system have been developed and presented for short-term PV power forecasting using meteorological parameters. Further, the simulations have been carried out based on sky-conditions such as sunny sky, hazy sky, partially foggy/cloudy sky and fully foggy/cloudy sky under composite climate zone. It has been observed from the overall analysis that for composite climate zone, hazy sky model performs better than other sky-based model. A comparison of proposed ANFIS methodology has been made with fuzzy logic and ANN methodologies. It has been concluded that the performance of ANFIS based model provides accurate results as compared to other intelligent models.

CHAPTER 8

CONCLUSIONS AND FUTURE SCOPE

8.1 CONCLUSIONS OF THE CURRENT RESEARCH

For the effective and accurate utilization of solar energy devices, data based on solar radiation resource plays an important role. Unfortunately, the devices for the measurement of such data are rarely available because of instrument high cost, limited spatial coverage and limited length of the record. Due to unavailability of the measured data, global solar energy forecasting is of prime importance at the earth's surface. For this purpose, it is essential to develop models based on more readily available meteorological data for forecasting global solar energy for such locations where measurements have not been done with reasonable accuracy. The mathematical and regression models of solar energy forecasting were found satisfactorily but for clear sky conditions. Due to high uncertainty in weather conditions, intelligent approaches based models such as fuzzy logic, artificial neural network and other hybrid models are being proposed by researchers for forecasting global solar energy using meteorological parameters.

Further, the variation in the power output of the solar PV system is dependent on external environmental factors such as ambient temperature, sky-condition etc. which can make system unstable. The variations and fluctuations in the power output subsequently reduces the PV power generation capacity. Short-term solar energy forecasting models such as

hourly and weekly are available in the literature but 10 minutes ahead solar energy forecasting are less reported in the literature.

In this research, an attempt has been made to establish intelligent models such as fuzzy logic approach, Artificial Neural Network (ANN) and hybrid intelligent models i.e. Adaptive Neural-Fuzzy Inference System (ANFIS) model for forecasting global solar energy based on sky-conditions defined as clear sky (type-a), hazy sky (type-b), partially foggy/cloudy sky (type-c) and fully foggy/cloudy (type-d) sky-conditions and for five weather stations across India covering widely changing climatic conditions thereof, such as warm and humid, hot and dry, cold and cloudy, composite and moderate climatic conditions.

Firstly, sunshine-based models with linear and non-linear correlations have been developed and presented using sunshine duration as a meteorological parameter. Secondly, empirical models have been established based on multiple regression analysis which correlates global solar energy with other meteorological parameter namely sunshine hours, ambient temperature, relative humidity, wind speed, amount of rainfall, atmospheric pressure and cloudiness index and applied for five weather stations across India. The regression and correlation coefficients for each model is calculated and presented. Principle component analysis have been performed based on statistical error-tests. After the statistical analysis, it has been observed that the correlation which incorporates seven variables has emerged to provide accurate results for estimating global solar energy for each of the climate zone across the entire country. Good agreement has been noticed between measured and estimated data based on seven variables correlations, which

makes it useful in estimating global solar energy. The models presented have reasonable estimation errors. Based on the overall analysis, it has been concluded that the considered parameters have strong influence on estimating global solar energy. Therefore, the proposed models can be successfully used to estimate global solar energy in distinct climate zone across India or elsewhere with similar climatic conditions.

The mathematical models available in the literature shows relative large errors and not suitable to estimate global solar energy in varying sky-conditions. Therefore, an intelligent approach based on fuzzy logic modelling have been devloped and presented to forecast global solar energy using dew-point as meteorological parameter along with other known available parameters namely sunshine duration, global solar energy, wind speed, ambient temperature and relative humidity for varying sky-conditions namely clear sky (type-a), hazy sky (type-b), partially foggy/cloudy sky (type-c) and fully foggy/cloudy sky (type-d) conditions. Three criteria namely mean percentage error, mean bias error and root mean square error are used to verify the forecasting errors of the proposed modelling approach. The obtained results concludes that the fuzzy logic based models achieves better accuracy and is convenient than the traditional regression methods.

Further, it has been observed that for complex systems with large data sets, maintaining accuracy for such data sets using fuzzy logic modelling would be a tedious task. Therefore, ANN based models are introduced, employing artificial intelligent techniques which can subsequently perform the structure simulation. In this research, the variants of ANN architecture have been discussed for modelling the system in forecasting global solar energy. Cascade-

forward, feed-forward, elman back-propagation, generalized regression, layered recurrent, linear layer, and radial basis function neural network architecture has been developed under composite climate zone using MATLAB. Simulations have been carried out by selecting the most suitable model based on evaluation indexes. Among the several discussed ANN architectures, the Radial Basis Function Neural network (RBFNN) model has emerged to provide a better prediction with minimum error based on evaluation indexes. Further, a close comparison of radial basis function neural network model has been made with Feed-Forward Neural Network (FFNN) model and successfully applied for five meteorological stations i.e. warm and humid (Chennai), hot and dry (Jodhpur), cold and cloudy (Shillong), moderate (Pune) and composite (Delhi) climate zone across India. It has been observed from the obtained results, that the radial basis function neural network model provides more accurate results in comparison to other ANN models i.e. feed-forward neural network model for each of the climate zones across the entire country.

Using ANN, an accurate analysis of a number of neurons and hidden layers becomes a difficult task since they are large in number which involves large training time that subsequently slows down the response of the system. Therefore, hybrid intelligent models i.e. Adaptive Neural-Fuzzy Inference System (ANFIS) are introduced for forecasting solar energy which is a fusion of artificial neural network and fuzzy logic approach for forecasting global solar energy. In this research, a model underlying the principle of ANFIS architecture has been employed for forecasting global solar energy using meteorological parameters. Three criteria namely mean absolute percentage error, normalized root mean square error and normalized mean absolute error and have been used

for verifying the forecasting errors of proposed ANFIS based models. Simulations have been carried out for varying sky-conditions and successfully applied for distinct climate zone. Further, comparison of ANFIS-based model has been fuzzy logic based model and ANN models. It has been concluded from the obtained results that the ANFIS-based model are far accurate and precise than other existing neural network and fuzzy logic based models.

Further, in this thesis, a very short-term solar energy forecasting based on 10-minutes timescale has been presented to forecast the power output of a solar PV system. It has been concluded from the obtained results that for composite climatic conditions, the hazy sky (type-b) model outperforms other models as the measured data matches the forecasted data followed by the sunny sky model (type-a), partially foggy/cloudy sky model(type-c) and fully foggy/cloudy sky (typed) model. The result reveals that the short-term PV power forecasting may be implemented for for a broad series of applications.

This research would be practically useful in providing appropriate control, optimization, power smoothening, real-time dispatch, the requirement of additional generating stations and the selection of appropriate energy storage system which may mitigate the issues of power fluctuations obtained from solar photovoltaic systems.

Such forecasts would be helpful for managing supply and demand for energy building in a smart grid environment. This research will help the stakeholders such as power engineer, technocrats, utility, designer, service provider and operation engineer for developing the smart energy management

system wherein the photovoltaic based power forecasting is one of the key components for this new paradigm.

8.2 SCOPE OF FUTURE WORK

In the present research, all efforts have been made to present different intelligent techniques such as fuzzy logic, ANN and ANFIS for global solar energy forecasting. The results obtained from these models have been applied for solar photovoltaic power forecasting. Presented intelligent model may be improved by using some other optimization techniques such as Grey Wolf Optimization (GWO) and Genetic Algorithm (GA) for solar energy forecasting problem. In addition, few more parameters such as aerosol index, dust accumulation etc. may be added as input parameters in the aforesaid models.

Solar PV forecasting is a paradigm for smart-grid environment. Some issues related to the grid like reliability and stability resulting from unpredictable events may be addressed. Further, an appropriate energy storage system may be proposed in the distributed generating systems using forecasting models.

REFERENCES

[1] N. Mahmud and A. Zahedi, "Review of control strategies for voltage regulation of the smart distribution network with high penetration of renewable distributed generation," Renewable and Sustainable Energy Reviews, vol. 64, pp. 1170-1184, 2016.

[2] M. Rizwan, M. Jamil and D. P. Kothari, "Generalized neural network approach for global solar energy estimation in India," IEEE Transactions on Sustainable Energy, vol. 3, no. 3, pp. 576-584, July 2012.

[3] P. Chaudhary and M. Rizwan, "Energy management supporting high penetration of solar photovoltaic generation for smart grid using solar forecasts and pumped hydro storage system," Renewable Energy, vol.118, pp.928-946, 2018.

[4] Ministry of New and Renewable Energy Source (MNRE), https://www.mnre.gov.in/achievements.htm [online].

[5] Ministry of Power, https://powermin.nic.in/en/content/power-sector-glance-all-india [online].

[6] The Electricity (Amendment) Act, 2003 by Ministry of Law and Justice, Government of India, published in The Gazette of India Extraordinary Part II Section I, at New Delhi on 2nd June, 2003.

[7] The Electricity (Amendment) Act, 2003 by Ministry of Law and Justice, Government of India, published in The Gazette of India Extraordinary Part II Section I, at New Delhi on 2nd May, 2007.

[8] Government of India. National Electricity Policy 2005, Available: http://www.powermin.nic.in [online].

[9] Government of India. Annual Report 2009-10, New Delhi: Ministry of New and Renewable Energy, Government of India; 2010 [Online].

[10] Government of India, "Tariff policy," 6th January, 2006, Available: http://www.powermin.nic.in [Online].

[11] Government of India, "National Electricity Policy and Plan," Available: http://www.powermin.nic.in [Online].

[12] Electricity, Electricity Feed Laws, Feed-in Tariffs and Advanced Renewable Tariffs, Available: http://www.wind-works.org [Online].

[13] Government of India National Knowledge Commission Science and environment, "Policies for renewable energies/biomass in India".

[14] Ministry of New and Renewable Energy source (MNRES), "Policy support for grid interactive renewable power," Available: http://mnres.nic.in [Online].

[15] MNRE, "Jawaharlal Nehru National Solar Mission," towards building SOLAR INDIA, (2010).

[16] Renewables global status report. REN21; 2016.

[17] N. K. Bansal and G. Minke, Climatic Zones and Rural Housing in India, vol. 35, Scientific Series of the International Bureau, Forschungszentrum Julich GmbH, Zentralbibliothek, 1995.

[18] M. Rizwan, M. Jamil and D. P. Kothari, "Solar energy estimation using REST model for PV-ECS based distributed power generating system," Solar Energy, vol. 94, no. 8, pp. 1324-1328, 2010.

[19] C. A. Gueymard, "REST2: Hi performance solar radiation model for cloudless-sky irradiance, illumination, and photosynthetically active radiation – validation with a benchmark dataset," Solar Energy, vol. 82, no. 3, pp. 272-285, 2008.

[20] C. A. Gueymard, "Direct solar transmittance and irradiance predictions with broadband models. Part I: detailed theoretical performance assessment," Solar Energy, vol. 74, no. 5, pp. 355-379, 2003.

[21] C. A. Gueymard, "Direct solar transmittance and irradiance predictions with broadband models. Part II: validation with high-quality measurements," Solar Energy, vol. 74, no. 5, pp. 381-395, 2003.

[22] A. Angstrom, "Solar and terrestrial radiation," Quarterly Journal of Royal Meteorological Society, vol. 50, no. 4, pp. 121-126, 1924.

[23] J. K. Page, "The estimation of monthly mean values of daily total short wave radiation on vertical and inclined surfaces from sunshine records for latitudes 40^{o}N–40^{o}S," Proceedings of UN Conference on New Sources of Energy, Rome, Italy, vol. 4, pp. 378-90, 1961.

[24] J. A. Prescott, "Evaporation from the water surface in relation to solar radiation," Transaction of the Royal Society of South Australia, vol. 64, pp. 114-118, 1940.

[25] S. Kirmani, M. Jamil and M. Rizwan, "Empirical correlation of estimating global solar radiation using meteorological parameters," International Journal of Sustainable Energy, vol. 34, no. 5, pp. 327-339, 2013.

[26] B. H. Cenk, D. Cihan and K. Ali, "The development of empirical models for estimating global solar radiation on a horizontal surface: A case study," Renewable and Sustainable Energy Reviews, vol. 81, no. P2, pp. 2771-2782, 2018.

[27] S. A. Khalil and H. A. S. Aly, "Comparative and evaluate of empirical models for estimation of global solar radiation in Al-Baha, KSA," Journal of Earth Science and Climate Change, vol. 9, no. 9, pp. 1-10, 2018.

[28] A. B. Awan, M. Zubair, R. P. Praveen and A. G. Abokhalil, "Solar energy resource analysis and evaluation of photovoltaic system performance in various regions of Saudi Arabia," Sustainability, vol. 10, no. 4, pp. 1-27, 2018.

[29] A. Teke and H. B. Yildirim, "Estimating the monthly global solar radiation for the Eastern Mediterranean Region," Energy Conversion and Management, vol. 87, pp. 628-635, 2014.

[30] J. Liu, T. Pan, D. Chen, X. Zhou, Q. Yu, G. N. Flerchinger, D. L. Liu, X. Zou, H. W. Linderholm, J. Du, D. Wu and Y. Shen, "An improved Angstrom type-model for estimating solar radiation over the Tibetan Plateau," Energies, vol. 10, pp. 1-28, 2017.

[31] R. Ihaddadene, N. Ihaddadene, M. Salemi and A. Beghidja, "New model to estimate monthly global solar radiation from air temperature in Algeria," 9th International Renewable Energy Congress (IREC), Hammamet, Tunisia, pp. 1-6, 2018.

[32] V. Bahel, H. Baksh and R. Srinivasan, "A correlation for estimation of global solar radiation," Energy, vol. 12, pp. 131-135, 1987.

[33] Y. A. G. Abdalla, "New correlation of global solar radiation with meteorological parameters for Bahrain," International Journal of Solar Energy, vol. 16, pp. 111-120, 1994.

[34] B. G. Akinoglu and A. Ecevit, "Construction of a quadratic model using modified Angstrom coefficients to estimate global solar radiation," Solar Energy, vol. 45, no. 2, pp. 85-92, 1990.

[35] Z. Sen, "Fuzzy algorithm for estimation of solar irradiation from sunshine duration," Solar Energy, vol. 63, pp. 39 - 49, 1998.

[36] L. Suganthi, S. Iniyan and A. A. Samuel, "Applications of fuzzy logic in renewable energy systems – A review," Renewable and Sustainable Energy Reviews, vol. 48, pp. 585-607, 2015.

[37] D. Saez, F. Avila, D. Olivares, C. Canizares and L. Marin, "Fuzzy prediction interval models for forecasting renewable resources and loads in Micro-grids," IEEE Transaction on Smart Grid, vol. 6, pp. 548-556, 2015.

[38] G. Perveen, M. Rizwan and N. Goel, "Intelligent model for solar energy forecasting and its implementation for solar photovoltaic applications," Journal of Renewable and Sustainable Energy, vol. 10, no. 6, Article ID. 063702, pp. 1-23, 2018.

[39] N. D. Kaushika, R. K. Tomar and S. C. Kaushik, "Artificial neural network model based on the interrelationship of direct, diffuse and global solar radiation," Solar Energy, vol. 103, pp. 327-342, 2014.

[40] A. K. Yadav and S. S. Chandel, "Solar radiation prediction using artificial neural network techniques: A review," Renewable and Sustainable Energy Reviews, vol. 33, pp. 772-781, 2014.

[41] G. W. Chang, H. J. Lu, Y. R. Chang and Y. D. Lee, "An improved neural network-based approach for short-term wind speed and power forecast," Renewable Energy, vol. 105, pp. 301-311, 2017.

[42] M. Jamil and M. Zeeshan, "A comparative analysis of ANN and chaotic approach-based wind speed prediction in India," Neural Computing and Applications, vol. 31, pp. 1-13, 2018.

[43] A. Khosravi, R. N. N. Koury, L. Machado and J. J. G. Pabon, "Prediction of wind speed and wind direction using artificial neural network, support vector regression, and adaptive neuro-fuzzy

inference system," Sustainable Energy Technologies and Assessments, vol. 25, pp. 146-160, 2018.

[44] K. R. Kumar and M. S. Kalavathi, "Artificial intelligence based forecast models for predicting solar power generation," Proceedings on Materials Today, vol. 5, no. 1, pp. 796-802, 2018.

[45] N. Walia, H. Singh and A. Sharma, "ANFIS: Adaptive neuro-fuzzy inference system - A survey," International Journal of Computer Applications, vol. 123, no. 13, pp. 32-38, 2015.

[46] J. R. Jang, "ANFIS: Adaptive-Network-Based Fuzzy Inference System," IEEE Transactions on Systems, MAN and Cybernetics, vol. 23, no. 3, pp. 665-685, 1993.

[47] D. Zheng, A. T. Eseye, J. Zhang and H. Li, "Short-term wind power forecasting using a double-stage hierarchical ANFIS approach for energy management in micro-grids," Protection and Control of Modern Power Systems, vol. 2, no. 13, pp. 1-10, 2017.

[48] J. Liu, X. Wang and Y. Lu, "A novel hybrid methodology for short-term wind power forecasting based on adaptive neuro-fuzzy inference system," Renewable Energy, vol. 103, pp. 620-629, 2017.

[49] M. Mosa, M. B. Shadmand, R. S. Balog and H. A. Rub, "Efficient maximum power point tracking using model predictive control for photovoltaic systems under dynamic weather condition," IET Renewable Power Generation, vol. 11, no. 11, pp. 1401-1409, 2017.

[50] M. Mehrabankhomartash, M. Rayati, A. Sheikhi and A. M. Ranjbar, "Practical battery size optimization of a PV system by considering individual customer damage function," Renewable and Sustainable Energy Reviews, vol. 67, pp. 36-50, 2017.

[51] C. Chen, S. Duan, T. Cai and B. Liu, "Online 24-h solar power forecasting based on weather type classification using artificial neural network," Solar Energy, vol. 85, no. 11, pp. 574-632, 2011.

[52] H. Mahmoudi, P. Moamaei, M. Aleenejad and R. Ahmadi, "A new maximum power point tracking method for photovoltaic applications based on finite control set model predictive control," IEEE Applied Power Electronics Conference and Exposition (APEC), Tampa, USA, pp. 1111-1115, March 2017.

[53] J. Shi, W. J. Lee, Y. Liu, Y. Yang and P. Wang, "Forecasting power output of photovoltaic systems based on weather classification and support vector machines," IEEE Transactions on Industry Applications, vol. 48, no. 3, pp. 1064-1069, 2012.

[54] A. A. Abushaiba, S. M. M. Eshtaiwi and R. Ahmadi, "Comparative analysis of dynamic performance of four prominent maximum power point tracking algorithms in photovoltaic systems using realistic experimental implementation," Proceedings of IEEE International Conference on Electro Information Technology (EIT), Grand Forks, USA, pp. 0576-0579, 2016.

[55] D. Yang, J. Kleissl, C. Gueymard, H. T. C. Pedro and C. F. M. Coimbra, "History and trends in solar irradiance and PV power forecasting: A preliminary assessment and review using text mining," Solar Energy, vol. 168, pp. 60-101, 2018.

[56] Y. Riffonneau, B. Seddik, F. Barruel and S. Ploix, "Optimal power flow management for grid-connected PV systems with batteries," IEEE Transaction of Sustainable Energy, vol. 2, no. 3, pp. 309-320, 2011.

[57] P. Chaudhary and M. Rizwan, "Short-term PV power forecasting using generalized neural network and weather-type classification," Chapter in Lecture Notes in Electrical Engineering, Advances in Energy and Power Systems, pp. 13-20, 2018.

[58] P. T. Ajit, Solar Radiant Energy over India, Ministry of New and Renewable Energy and India Meteorological Department, India, 2009.

[59] F. J. Newland, "A study of solar radiation models for the coastal region of South China," Solar Energy, vol. 43, no. 4, pp. 227-235, 1989.

[60] D. B. Ampratwum and A. S. S. Dorvlo, "Estimation of solar radiation from the number of sunshine hours," Applied Energy, vol. 63, pp. 161-7, 1991.

[61] K. Bakirci, "Correlations for estimation of global solar radiation with hours of bright sunshine in Turkey," Energy, vol. 34, pp. 485-501, 2009.

[62] J. Almorox, C. Hontoria and M. Benito, "Models for obtaining daily global solar radiation with measured air temperature data in Madrid (Spain)," Applied Energy, vol. 88, pp. 1703-1709, 2011.

[63] J. A. Duffie and W. A. Beckman, Solar Engineering of Thermal Processes, Second edition, John Wiley & Sons Inc., June 1980.

[64] K. Ulgen and A. Hepbasli, "Diffuse solar radiation estimation models for Turkey's big cities," Energy Conversion and Management, vol. 50, no. 1, pp. 149-156, 2009.

[65] W. Yao, Z. Li, Y. Wang, F. Jiang and L. Hu, "Evaluation of global solar radiation models for Shanghai, China," Energy Conversion and Management, vol. 84, pp. 597-612, 2014.

[66] X. Sun, Z. Ouyang and D. Yue, "Short-term load forecasting based on multivariate linear regression," IEEE Conference on Energy Internet and Energy System Integration (EI2), Beijing, China, pp. 1-5, 2017.

[67] S. C. Nwokolo, "A comprehensive review of empirical models for estimating global solar radiation in Africa," Renewable and Sustainable Energy Reviews, vol. 78, no. (c), pp. 955-995, 2017.

[68] Z. A. Al-Mostafa, A. H. Maghrabi and S. M. Al-Shehri, "Sunshine-based global radiation models: A review and case study," Energy Conversion and Management, vol. 84, pp. 209-216, 2014.

[69] M. J. Yau, M. A. Gele, Y. Y. Ali and A. M. Alhaji, "Global solar radiation models: A review," Journal of Photonic Materials and Technology, vol. 4, no. 1, pp. 26-32, 2018.

[70] S. A. Al-Ghamdi, A. M. Abdel-Latif, A. S. Nada, E. F. Mohamed, A. S. Emam and Emam, "Global Solar Radiation over Al-Baha City, KSA: Comparison of predicted models and measured data," International Journal of Innovative Research in Computer and Communication Engineering, vol. 5, no. 1, pp. 132-145, 2016.

[71] A. Samy, A. Khalil and M. Shaffie, "Evaluation of transposition models of solar irradiance over Egypt," Renewable and Sustainable Energy Reviews, vol. 66, pp.105-119, 2016.

[72] M. Y. Sulaiman and A. B. Umar, "A comparative analysis of empirical models for the estimations of monthly mean daily global solar radiation using different climate parameters in Sokoto, Nigeria,"

International Journal of Marine, Atmospheric and Earth Sciences, vol. 5, no. 1, pp.1-19, 2017.

[73] A. Alkasim, A. A. Suberu and M. T. Baba, "Empirical model for the estimation of global and diffuse solar radiation in Nigeria, based on sunshine hours," International Journal of Scientific and Engineering Research, vol. 8, no. 2, pp. 360-366, 2017.

[74] M. J. Yau, M. A. Gele, Y. Y. Ali and A. M. Alhaji, "Global solar radiation models: A review," Journal of Photonic Materials and Technology, vol. 4, no. 1, pp. 26-32, 2018.

[75] A. A. G. Saeed, M. A. L. Ahmed, S. N. Adel, F. M. El-Shahat and S. E. Ashraf, "Wind data analysis for Albaha city, Saudi Arabia," Journal of Basic and Applied Sciences, vol. 1, pp. 1-9, 2017.

[76] M. Chelbi, Y. Gagnon and J. Waewsak, "Solar radiation mapping using sunshine duration-based models and interpolation techniques: Application to Tunisia," Energy Conversion and Management, vol. 101, pp. 203-215, 2015.

[77] M. Rizwan, M. Jamil, S. Kirmani and D. P. Kothari, "Fuzzy logic based modelling and estimation of global solar energy using meteorological parameters," Energy, vol. 70, pp. 685-691, 2014.

[78] A. Bardossy, L. Duckstein and I. Bogardi, "Fuzzy rule-based classification of atmospheric circulation patterns," International Journal of Climatology, vol. 15, no.10, pp. 1087-1097, 1995.

[79] R. Morales, D. Saez, L. G. Marin and N. V. Alfredo, "Micro-grid planning based on fuzzy interval models of renewable resources," Proceedings in IEEE International Conference on Fuzzy Systems, pp. 336-343, 2016.

[80] A. Yona, T. Senjyu, T. Funabashi and C. Kim, "Determination method of insolation prediction with fuzzy and applying neural network for long-term ahead PV power output correction," IEEE Transactions on Sustainable Energy, vol. 4, no. 2, pp. 527-533, April 2013.

[81] M. Colak and I. Kaya, "Prioritization of renewable energy alternatives by using an integrated fuzzy MCDM model: A real case application

for Turkey," Renewable and Sustainable Energy Reviews, vol. 80, pp. 840-853, 2017.

[82] B. Meghni, D. Dib and A. T. Azar, "A second-order sliding mode and fuzzy logic control to optimal energy management in wind turbine with battery storage," Neural Computing and Applications, vol. 28, no. 6, pp. 1417-1434, 2017.

[83] C. Murat and K. Ihsan, "Prioritization of renewable energy alternatives by using an integrated fuzzy MCDM model: A real case application for Turkey," Renewable and Sustainable Energy Reviews, vol. 80, pp. 840-853, 2017.

[84] E. Lotfi, A. Khosravi and S. Nahavandi, "Prediction granules for uncertainty modelling," IEEE International Conference on Fuzzy Systems (FUZZ-IEEE), Vancouver, Canada, pp. 961-968, 2016.

[85] B. A. Baum, V. Tovinkere, J. Titlow and R. M. Welch, "Automated cloud classification of global AVHRR data using a fuzzy logic approach," Journal of Applied Meteorology, vol. 36, pp. 1519-1540, 1997.

[86] E. T. Paulescu and M. Paulescu, "Fuzzy modelling of solar irradiation using air temperature data," Theoretical and Applied Climatology, vol. 91, pp. 181-92, 2008.

[87] V. Gomez and A. Casanovas, "Fuzzy logic and meteorological variables: a case study of solar irradiance," Fuzzy Sets and Systems, vol. 126, pp. 121-8, 2002.

[88] www.niwe.res.in

[89] A. Chel and G. N. Tiwari, "A case study of a typical 2.32 kW_p stand-alone photovoltaic (SAPV) in a composite climate of New Delhi (India)," Applied Energy, vol. 88, pp. 1415-1426, 2011.

[90] M. Ozgoren, M. Bilgili and B. Sahin, "Estimation of global solar radiation using ANN over Turkey," Expert Systems with Applications, vol. 39, no. 5, pp. 5043-5051, 2012.

[91] A. K. Yadav and S. S. Chandel, "Solar radiation prediction using artificial neural network techniques: A review," Renewable and Sustainable Energy Reviews, vol. 33, pp. 772-781, 2014.

[92] J. C. Lam, K. K. W. Wan and L. Yang, "Solar radiation modelling using ANNs for different climates in China," Energy Conversion and Management, vol. 49, no. 5, pp. 1080-1090, 2008.

[93] A. K. Yadav, H. Malik and S. S. Chandel, "Selection of most relevant input parameters using WEKA for artificial neural network based solar radiation prediction models," Renewable and Sustainable Energy Reviews, vol. 31, pp. 509-519, 2014.

[94] R. Azimi, M. Ghayekhloo and M. Ghofrani, "A hybrid method based on a new clustering technique and multilayer perceptron neural network for hourly solar radiation forecasting," Energy Conversion and Management, vol. 118, pp. 331-344, 2016.

[95] P. F. Jimenez-Perez and L. Mora-Lopez, "Modeling and forecasting hourly global solar radiation using clustering and classification techniques," Solar Energy, vol. 135, pp. 682-669, 2016.

[96] C. Voyant, G. Notton, S. Kalogirou, M. Nivet, C. Paoli, F. Motte and A. Fouilloy, "Machine learning methods for solar radiation forecasting: A review," Renewable and Sustainable Energy Reviews, vol. 105, pp. 569-582, 2017.

[97] E. Izgi, A. Oztopal, B. Yerli, K. K. Mustafa and A. D.Sahin, "Short-mid-term solar power prediction by using artificial neural network," Solar Energy, vol. 86, no. 2, pp. 725-733, 2012.

[98] I. P. Panapakidis and A. S. Dagoumas, "Day-ahead electricity price forecasting via the application of artificial neural network based models," Applied Energy, vol. 172, pp. 132-151, 2016.

[99] Y. N. Noorollahi, M. A. Jokar and A. Kalhor, "Using artificial neural networks for temporal and spatial wind speed forecasting in Iran," Energy Conversion and Management, vol. 115, pp.17-25, 2016.

[100] M. K. Yadav, K. G. Singh and A. Chaturvedi, "Short-term wind speed forecasting of knock airport based on ANN algorithms," Proceedings of International Conference on Information, Communication, Instrumentation and Control (ICICIC), Indore, India, pp. 1-8, Feb 2018.

[101] A. T. Eseye, J. H. Zhang, D. H. Zheng and D. Shiferaw, "Short-term wind power forecasting using an artificial neural network for resource

scheduling in micro-grids," International Journal of Science and Engineering Applications, vol. 5, no. 3, pp. 144-151, 2016.

[102] F. Fazelpour, N. Tarashkar and M. A. Rosen, "Short-term wind speed forecasting using artificial neural networks for Tehran, Iran," International Journal of Energy and Environmental Engineering, vol. 7, no. 4, pp. 377-390, 2016.

[103] G. Kacem, K. Abdallah, M. Youcef and C. Farouk, "Estimation of the daily global solar radiation based on Box–Jenkins and ANN models: A combined approach," Renewable and Sustainable Energy Reviews, vol. 57, pp. 238-249, 2016.

[104] R. Y. Mukh, G. S. Kumar and C. Anurag, "Short-term wind speed forecasting of knock airport based on ANN algorithms," Proceedings of International Conference on Information, Communication, Instrumentation and Control (ICICIC), Indore, India, Feb 2018, pp. 1-8, 2018.

[105] G. W. Chang, H. J. Lu, Y. R. Chang and Y. D. Lee, "An improved neural network-based approach for short-term wind speed and power forecast," Renewable Energy, vol. 105, pp. 301-311, 2017.

[106] A. Rasit, "RETRACTED: Artificial neural networks applications in wind energy systems: a review," Renewable and Sustainable Energy Reviews, vol. 49, pp. 534-562, 2015.

[107] A. Dolara, F. Grimaccia, S. Leva, M. Mussetta and E. Ogliari, "Comparison of training approaches for photovoltaic forecasts by means of machine learning," Applied Sciences, vol. 8, no. 228, pp. 1-16, 2018.

[108] N. Younes, A. J. Mohammad and K. Ahmad, "Using artificial neural networks for temporal and spatial wind speed forecasting in Iran," Energy Conversion and Management, vol. 115, pp. 17-25, 2016.

[109] K. Kampouropoulos, "A combined methodology of adaptive neuro-fuzzy inference system and genetic algorithm for short-term energy forecasting," Advances in Electrical and Computer Engineering, vol. 14, no. 1, pp. 9-14, 2014.

[110] S. Mitra, Y. Hayashi and S. Member, "Neuro-Fuzzy Rule Generation: Survey in soft computing framework," IEEE Transactions on Neural Networks, vol. 11, no. 3, pp. 748-768, 2011.

[111] H. Abu-rub, A. Iqbal, M. Ahmed, Z. Peng, Y. Li and G. Baoming, "Quasi-Z-Source inverter-based photovoltaic generation system with maximum power tracking control using ANFIS," IEEE Transactions on Sustainable Energy, vol. 4, no. 1, pp. 11-20, 2013.

[112] Y. Yang, Y. Chen, Y. Wang, C. Li and L. Li, "Modelling a combined method based on ANFIS and neural network improved by DE algorithm: A case study for short-term electricity demand forecasting," Applied Soft Computing, vol. 49, pp. 663-675, 2016.

[113] S. Barak and S. S. Sadegh, "Forecasting energy consumption using ensemble ARIMA–ANFIS hybrid algorithm," International Journal of Electrical Power and Energy Systems, vol. 82, pp. 92-104, 2016.

[114] R. K. Mavi, N. K. Mavi and M. Goh, "Modeling corporate entrepreneurship success with ANFIS," Operational Research, vol. 17, no. 1, pp. 213-238, 2017.

[115] L. Olatomiwa, S. Mekhilef, S. Shamshirband and D. Petkovic, "Adaptive neuro-fuzzy approach for solar radiation prediction in Nigeria," Renewable and Sustainable Energy Reviews, vol. 51, pp. 1784-1791, 2015.

[116] G. J. Osorio, J. C. O. Matias and J. P. S. Catalao, "Short-term wind power forecasting using adaptive neuro-fuzzy inference system combined with evolutionary particle swarm optimization, wavelet transform and mutual information," Renewable Energy, vol. 75, pp. 301-307, 2015.

[117] Y. Kassa, J. H. Zhang, D. H. Zheng and D. Wei, "Short-term wind power prediction using ANFIS," Proceedings of IEEE International Conference on Power and Renewable Energy (ICPRE), Shanghai, China, pp. 388-393, 2016.

[118] G. D. Santika, W. F. Mahmudy and A. Naba, "Electrical load forecasting using adaptive neuro-fuzzy inference system," International Journal of Advance Soft Computing Applications, vol. 9, no. 1, pp. 50-69, 2017.

[119] H. H. Cevik and M. Cunkas, "Short-term load forecasting using fuzzy logic and ANFIS," Neural Computing and Application, vol. 26, no. 6, pp. 1355-67, 2015.

[120] G. Perveen, M. Rizwan and N. Goel, "Comparison of intelligent modelling techniques for solar energy forecasting and its application in solar PV systems," IET Energy Systems Integration, Vol. 1, No.1, pp. 34-51, 2019.

[121] R. Jang, "ANFIS: Adaptive-network-based fuzzy inference system," IEEE Transactions on Systems, MAN and Cybernetics, vol. 23, no. 3, pp. 665-685, 1993.

[122] J. Antonanzas, N. Osorio, R. Escobar, R. Urraca, F. J. Martinez-de-Pison and F. Antonanzas-Torres, "Review of photovoltaic power forecasting," Solar Energy, vol.136, pp. 78-111, 2016.

[123] E. B. Ssekulima, M. B. Anwar, A. A. Hinai and M. S. El-Moursi, "Wind speed and solar irradiance forecasting techniques for enhanced renewable energy integration with the grid: a review," IET Renewable Power Generation, vol. 10, no. 7, pp. 885- 989, 2016.

[124] R. Singh, Y. R. Sood and N. P. Padhy, "Development of renewable energy sources for Indian power sector moving towards competitive electricity market," IEEE Power and Energy Society General Meeting, Calgary, pp. 1-6, 2009.

[125] S. N. Fallah, R. C. Deo, M.Shojafar, M. Conti and S. Shamshirband, "Computational intelligence approaches for energy load forecasting in smart energy management grids: State of the art, future challenges, and research directions," Energies, vol. 11, pp. 1-31, 2018.

[126] A. A. Abushaiba, S. M. M. Eshtaiwi and R. Ahmadi, "A new model predictive based maximum power point Tracking method for photovoltaic applications," IEEE International Conference on Electro Information Technology (EIT), Grand Forks, USA, pp. 0571-0575, 2016.

[127] H. Yang, C. Huang, Y. Huang and Y. Pai, "A weather-based hybrid method for 1-day ahead hourly forecasting of PV power output," IEEE Transaction on Sustainable Energy, vol. 5, no. 3, pp. 917-926, 2014.

[128] Y. Wu, C. Chen and H. A. Rahman, “A novel hybrid model for short-term forecasting in PV power generation,” International Journal of Photoenergy, vol. 2014, Article ID 569249, pp. 1-9, 2014.

[129] S. Kalogirou, “Solar thermal collectors and applications,” Progress in Energy and Combustion Science, vol. 30, no. 3, pp. 231-295, 2004.

APPENDIX-A

Table A.1 Performance specifications of 250 W_p multi-crystalline solar PV modules

Multi-crystalline solar PV module	**Specifications**
The efficiency of module η_o	15.30%
maximum power point voltageV_{pmax}	34.92 V
maximum power point current I_{pmax}	8.59 A
Open circuit voltage V_{oc}	44.83 V
NOCT	45^oC to $\pm 2^oC$

Table A.2 Performance specifications of 210 W_p HIT solar PV modules

HIT solar PV module	**Specifications**
The efficiency of module η_o	16.70%
The efficiency of the cell	18.9%
Short circuit current I_{sc}	5.57 A
Open circuit voltage V_{oc}	50.9 V
Ambient temperature	-4^oF to 115^oF

APPENDIX-B

Fig. A.1 Experimental demonstration of Heterojunction with Intrinsic Thin Layer (HIT) solar PV module at National Institute of Solar Energy (NISE), India

Fig. A.2 Experimental demonstration of multi-crystalline solar PV module at National Institute of Solar Energy (NISE), India

List of Research Publications

Following are the publications in journals and conference proceedings out of this research work.

- **List of paper(s) published in Peer Reviewed International Journals:**

1. **Gulnar Perveen**, M. Rizwan and Nidhi Goel, "Intelligent model for solar energy forecasting and its implementation for solar photovoltaic applications," **Journal of Renewable and Sustainable Energy**, **AIP**, Vol. 10, No. 6, Article ID. 063702, pp. 1-23, 2018. ISSN No.1941-7012, Impact factor: 1.337, SCI Expanded.
2. **Gulnar Perveen**, M. Rizwan, and Nidhi Goel, "Comparison of intelligent modelling techniques for solar energy forecasting and its application in solar PV systems," **IET Energy Systems Integration**, Vol. 1, No. 1, pp. 34-51, 2019. ISSN No. 2516-8401 (Online).

- **List of paper(s) published in Peer Reviewed International/National Conference Proceedings/Presented in the Conference:**

1. **Gulnar Perveen**, M. Rizwan and Nidhi Goel, "Correlations for forecasting global solar radiation using meteorological parameters," Proceedings of **IEEE 41st National Systems Conference (NSC) 2017 on Super-Intelligent Machines and Man**, December 1-3, pp. 49-57, 2017, Dayalbagh Educational Institute, Agra, India.
2. **Gulnar Perveen**, M. Rizwan and Nidhi Goel, "Fuzzy logic modelling and its solar thermal applications," Proceedings of **2nd IEEE International Conference on Power Electronics, Intelligent Control, and Energy Systems (ICPEICES-2018)**, October 22-24, 2018, Delhi Technological University, Delhi, India.
3. **Gulnar Perveen**, M. Rizwan, and Nidhi Goel, "Development of Empirical models for forecasting global solar energy," Proceedings of **2nd IEEE International Conference on Power Electronics, Intelligent Control, and Energy Systems (ICPEICES-2018)**, October 22-24, 2018, Delhi Technological University, Delhi, India.
4. **Gulnar Perveen**, M. Rizwan and Nidhi Goel, "Performance mapping of solar thermal technologies," Proceedings of **International Conference on Renewable Energy and Sustainable Climate**

(Solaris 2019), February 07-09, 2019, Jamia Millia Islamia, Delhi, India.

5. **Gulnar Perveen**, M. Rizwan and Nidhi Goel, "ANN modelling for estimating global solar energy and its implementation in Solar Thermal Systems," Proceedings of **International Conference on Renewable Energy and Sustainable Climate (Solaris 2019)**, February 07-09, 2019, Jamia Millia Islamia, Delhi, India.

- **List of paper(s) communicated in Peer Reviewed International Journals:**

1. **Gulnar Perveen**, M. Rizwan and Nidhi Goel, "Global solar energy forecasting using ANN intelligent technique and its application in solar photovoltaic systems," **Journal of Green Energy**, **Taylor and Francis online**, 2018. ISSN No. 1543-5075 (Print), ISSN No. 1543-5083 (Online), Impact factor: 1.171, SCI Expanded (Manuscript ID - IJGE-2018-0791).
2. **Gulnar Perveen**, M. Rizwan and Nidhi Goel, "Hybrid intelligent model for forecasting global solar energy forecasting and its solar photovoltaic applications," **International Journal of Global Energy Issues, Inderscience,** 2018. ISSN No. 0954-7118 (Print), ISSN No. 1741-5128 (Online), Emerging SCI, H-Index-22, (Manuscript ID - IJGEI-239966).
3. **Gulnar Perveen**, M. Rizwan and Nidhi Goel, "Short-term PV power forecasting based on sky-condition using intelligent modelling techniques," **International Journal of Energy and Environment Engineering, Springer**, 2019. ISSN No. 2008-9163 (Print), ISSN No. 2251-6832 (Online), Scopus, (Manuscript ID IJEE-D-19-00168).